LESIONS AND MICROSCOPIC STRUCTURE OF CLAW HORN IN DAIRY CATTLE

Volume 2

KATHARINE A. LEACH

Thesis presented for the Degree of

Doctor of Philosophy

The University of Edinburgh

March 1996

TABLE OF CONTENTS

VOLUME 2 : FIGURES

FIGURES

CHAPTER 2

Figure 2.1
Lateral view of the right fore foot to illustrate the gross appearance

The region of the junction between the hairy skin (sk) and the claw capsule is called the coronary border (cb). The perioplic horn (ph) forms a band at the coronary border at the transition between skin and claw horn. The perioplic horn increases in depth towards the bulb of the heel (b). The abaxial groove (ab) is clearly visible at the junction between the bulb and the dorsal wall (w) of the claw capsule of the lateral claw (L) (digit 4). The dorsal border of the medial claw (M) (digit 3) is visible. The lateral accessory claw (ac) (digit 5) can also be seen.

Figure 2.2
View of the interior of the horny capsule of the left front outer claw

The claw capsule is formed by the *stratum corneum* of the claw epidermis. The most caudal bulb horn (b) has been cut away to give a clearer view into the claw capsule and an indication of the thickness of the horn in this region.
The narrow layer of perioplic horn (ph) has curled slightly on removal of the underlying tissues. Distal to this is the light coloured band of coronary horn (ch). The individual laminar horn leaflets which interdigitate with the dermal laminae can be seen in the laminar horn (lh). On the interior surface of the sole (s) are depressions which receive the dermal papillae of the sole corium. Ridges are present on the exterior surface of the axial wall (w). The axial region of the sole is concave and the distal border of the axial wall does not normally bear weight.

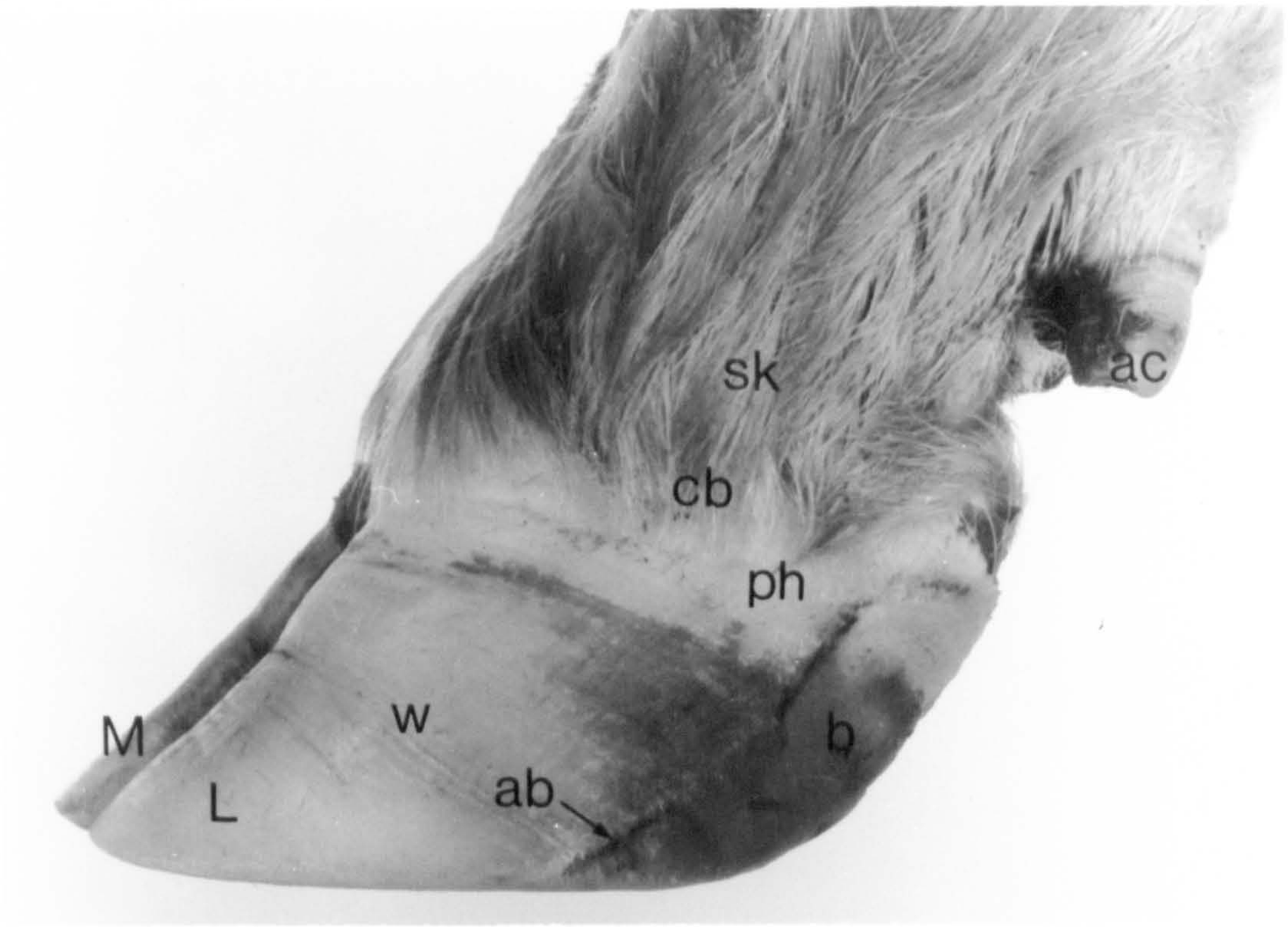
sk
ac
cb
ph
M
w
b
L
ab

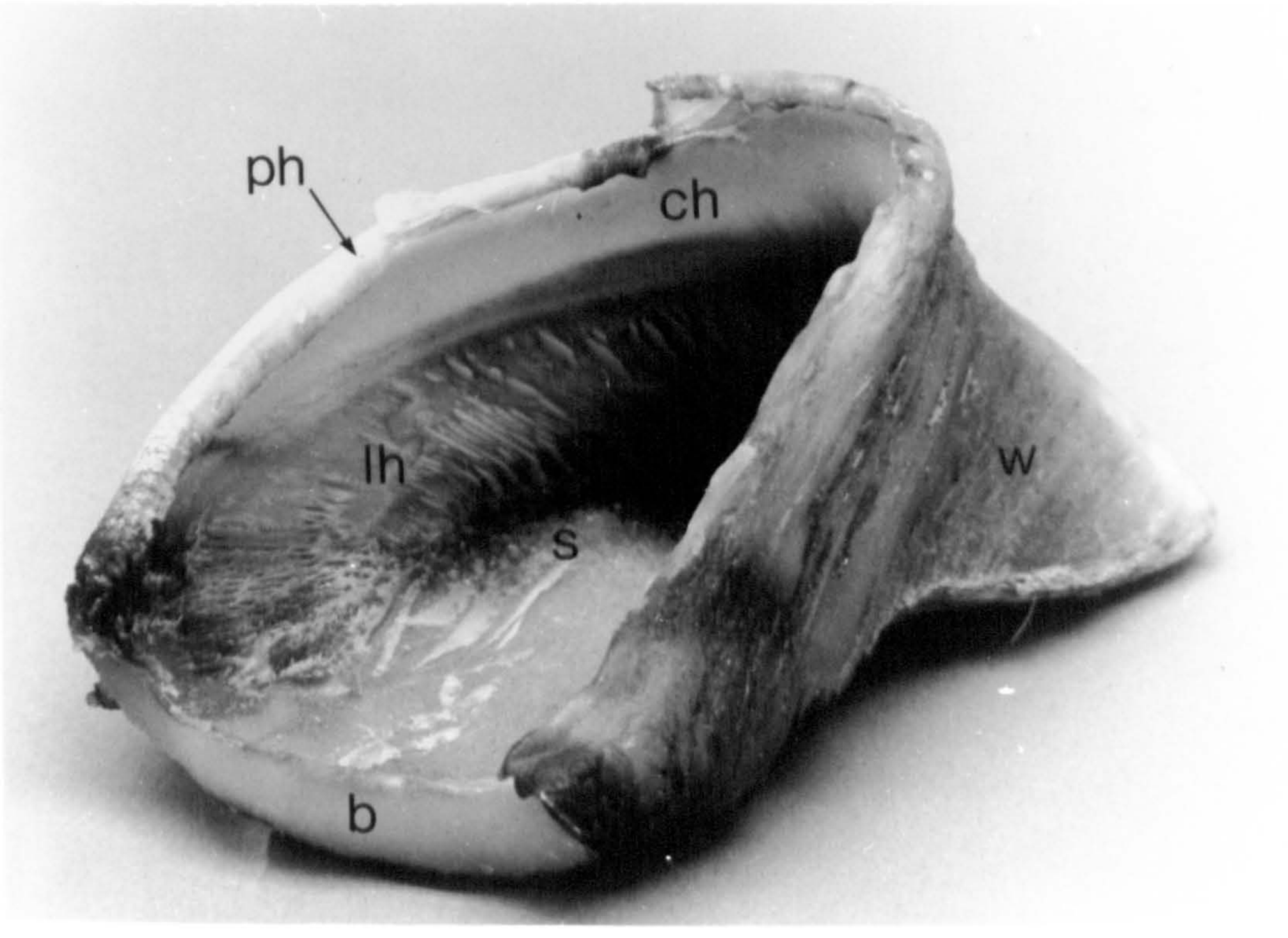
ph
ch
lh
w
s
b

Figure 2.3
Sagittal section throught the lateral claw of the right hind foot.

The proximal (PI), middle (PII) and distal (PIII) phalanges and the distal sesamoid or navicular bone (n) form the skeleton of the digital region. The distal part of the middle phalanx, the distal sesamoid bone and the whole of the distal phalanx lie within the claw capsule. The joint capsule of the distal interphalangeal joint (di) is extensive. The terminal arch of the digital artery (ta) is visible within the distal phalanx. The tendon (et) of the long extensor muscle has insertions on both the middle phalanx and the extensor process (ex) of the distal phalanx. The tendon (sf) of the superficial digital flexor muscle inserts on the proximal plantar surface of the middle phalanx. The tendon (df) of the deep digital flexor muscle has one smaller branch which inserts on the plantar surface of the middle phalanx and a larger branch which inserts on the flexor tubercle (ft) of the distal phalanx. A narrow layer of perioplic horn (ph) overlies the coronary horn which forms the wall (w) of the claw capsule. Distal to and continuous with the coronary corium (cc) is the laminar corium (lc). The white line (wl) lies at the junction between the wall (w) and the sole (s). The sole corium (sc) lies between the horn of the sole and the plantar border of the distal phalanx. The bulb horn (b) covers the caudal aspect of the digit. The corium of the bulb (bc) lies between the bulb horn and the digital torus (dt). The digital torus (dt) is a fatty fibrous pad which is thicker towards the heel and thins towards the toe. The accessory claw (ac) contains a rudimentary bone which does not articulate with the rest of the digital skeleton, and is enclosed in its own horny capsule.

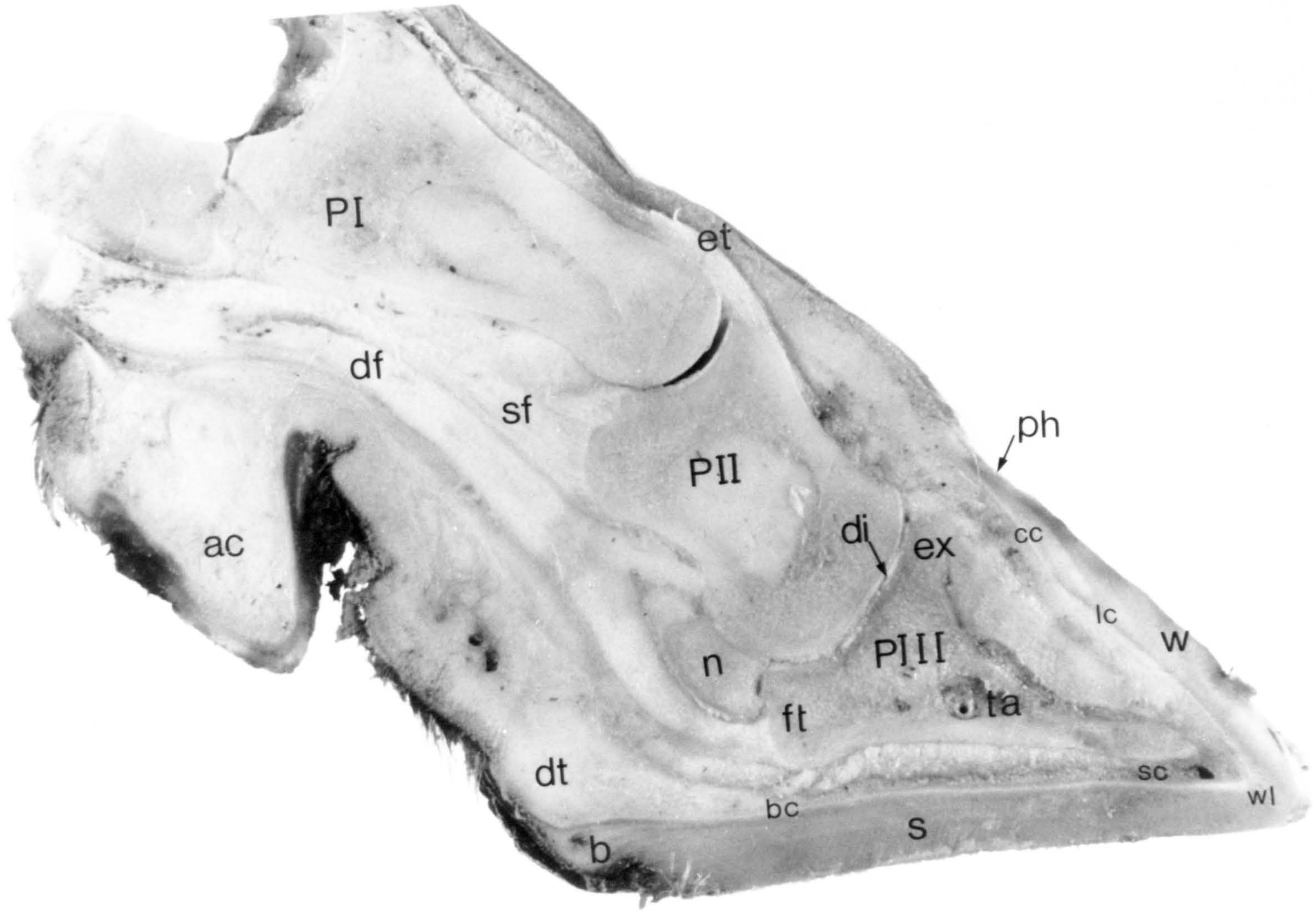
PI
et
df
sf
ph
PII
ac
di
ex
cc
lc
w
PIII
n
ta
ft
dt
sc
wl
bc
s
b

Figure 2.4
Palmar view of right forefoot

The medial claw (M) is broader than the lateral claw (L). The distal end of the abaxial groove (ab) marks the junction between the wall (w) and the bulb of the heel (b) The position of the distal end of the axial groove is indicated (↑ ax). A slight ridge is visible at the sole-bulb junction (j). The white line (wl) forms the junction between wall and sole (s).

Figure 2.5
Diagram to show the zones of the distal surface of the claw established at the Sixth International Symposium on Disorders of the Ruminant Digit, 1990, in order to unify description and recording of the position of lesions

1. White line at toe
2. Abaxial white line
3. Abaxial wall-bulb junction
4. Sole-bulb junction
5. Apex of sole (true sole)
6. Bulb

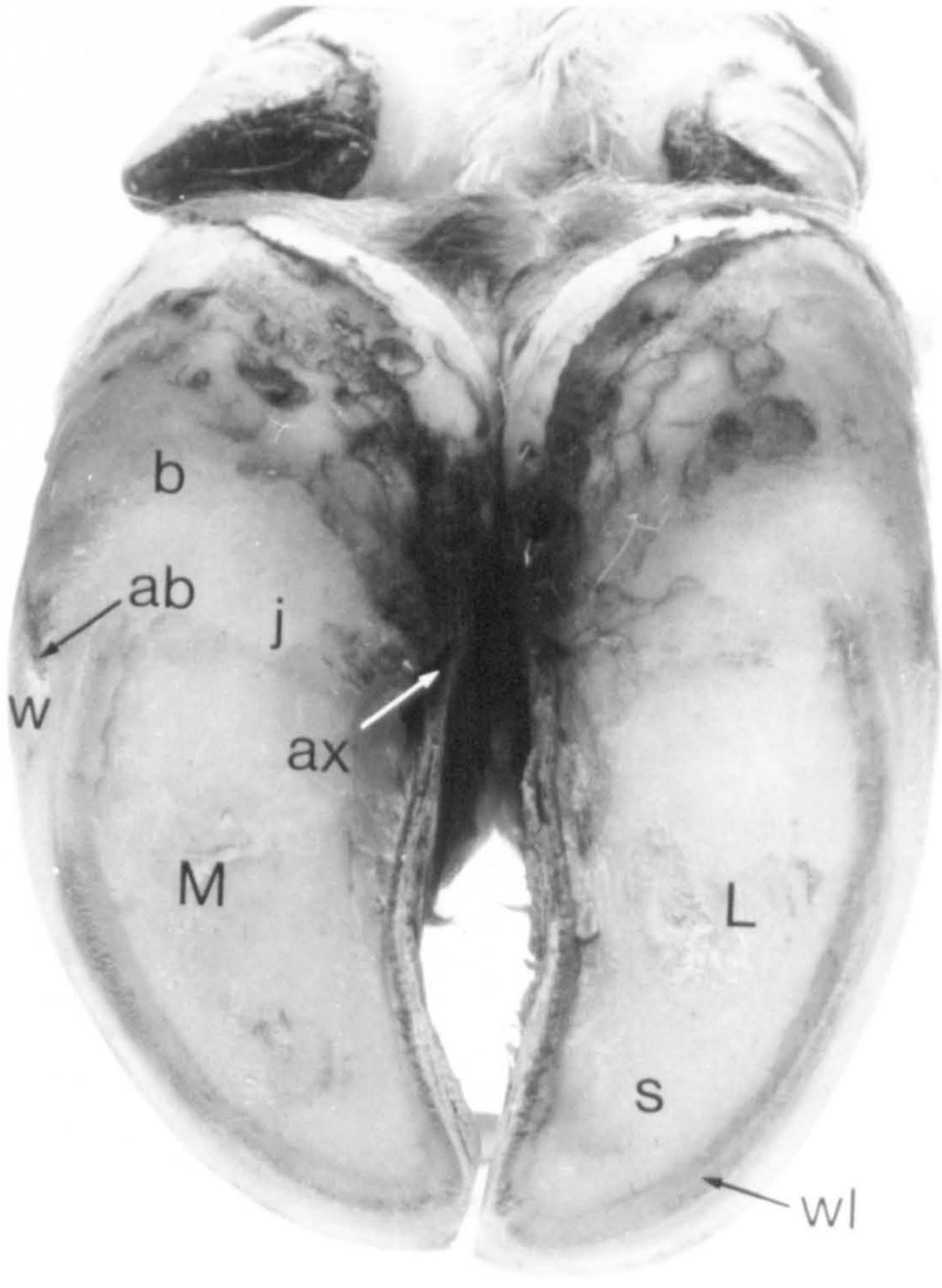
b
ab
j
w
ax
M
L
s
wl

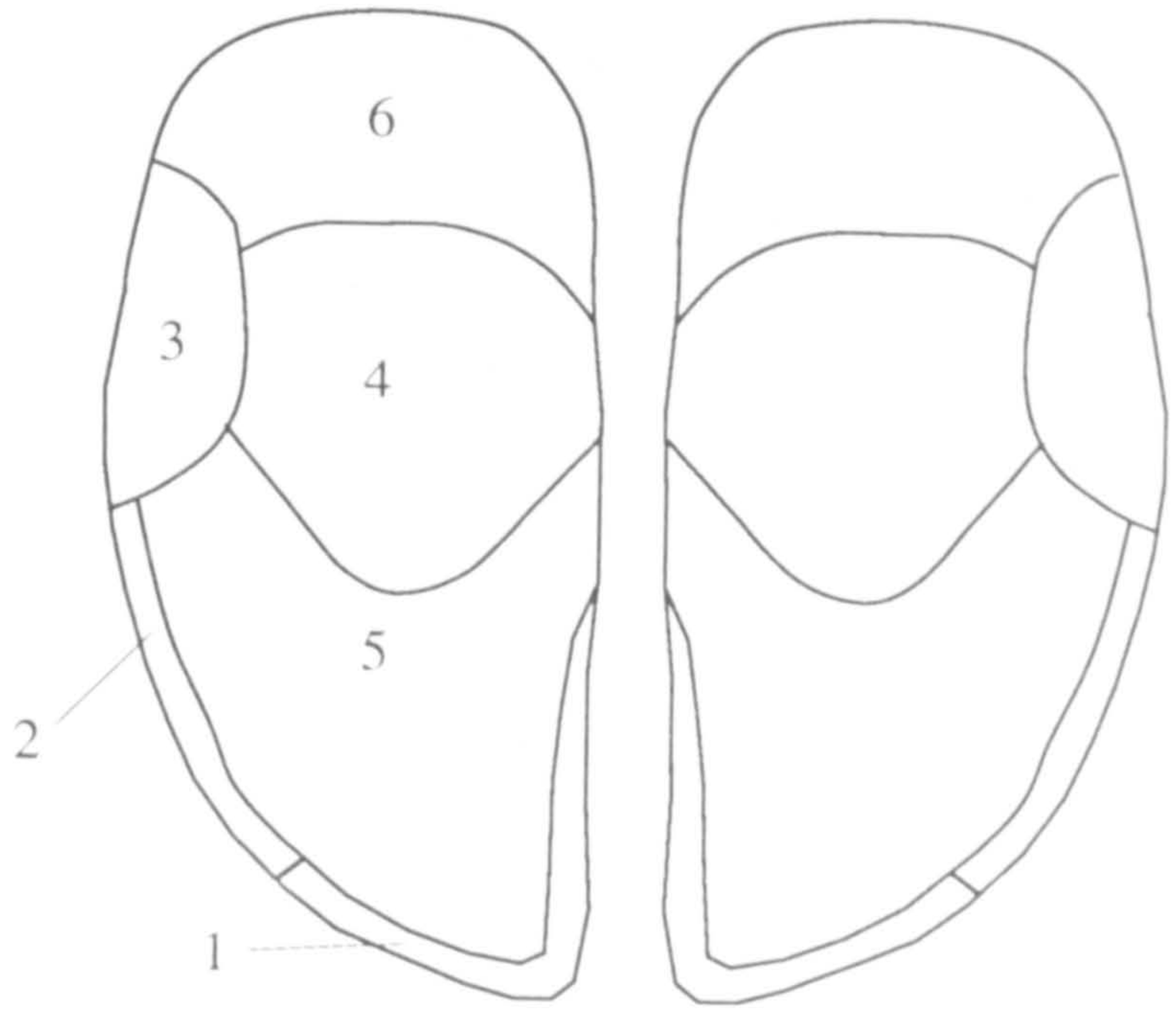
6
3
4
5
2
1

Figure 2.6
Sliver of horn from the distal surface of the abaxial border of the claw, photographed in a dissection microscope

The white line (wl) is found at the junction between the wall (w) and the sole (s). The striated appearance of the white line arises because it is composed of two types of horn. The laminar horn leaflets (lh), which appear lighter in this illustration, are continuous with the horn of the wall while the darker interdigitating horn (idh) is continuous with the sole. Three regions of haemorrhage (ha) are visible in the interdigitating horn.

x 7

Figure 2.7
Light micrograph of the horn of the white line

At this magnification the interdigitation between the laminar horn leaflets (lh) and the interdigitating horn (idh) can be seen more clearly. The boundary between the white line and the wall (w) is quite marked but that between the white line and the sole (s) is less distinct.

x 45

Stain : Martius Scarlet-Blue

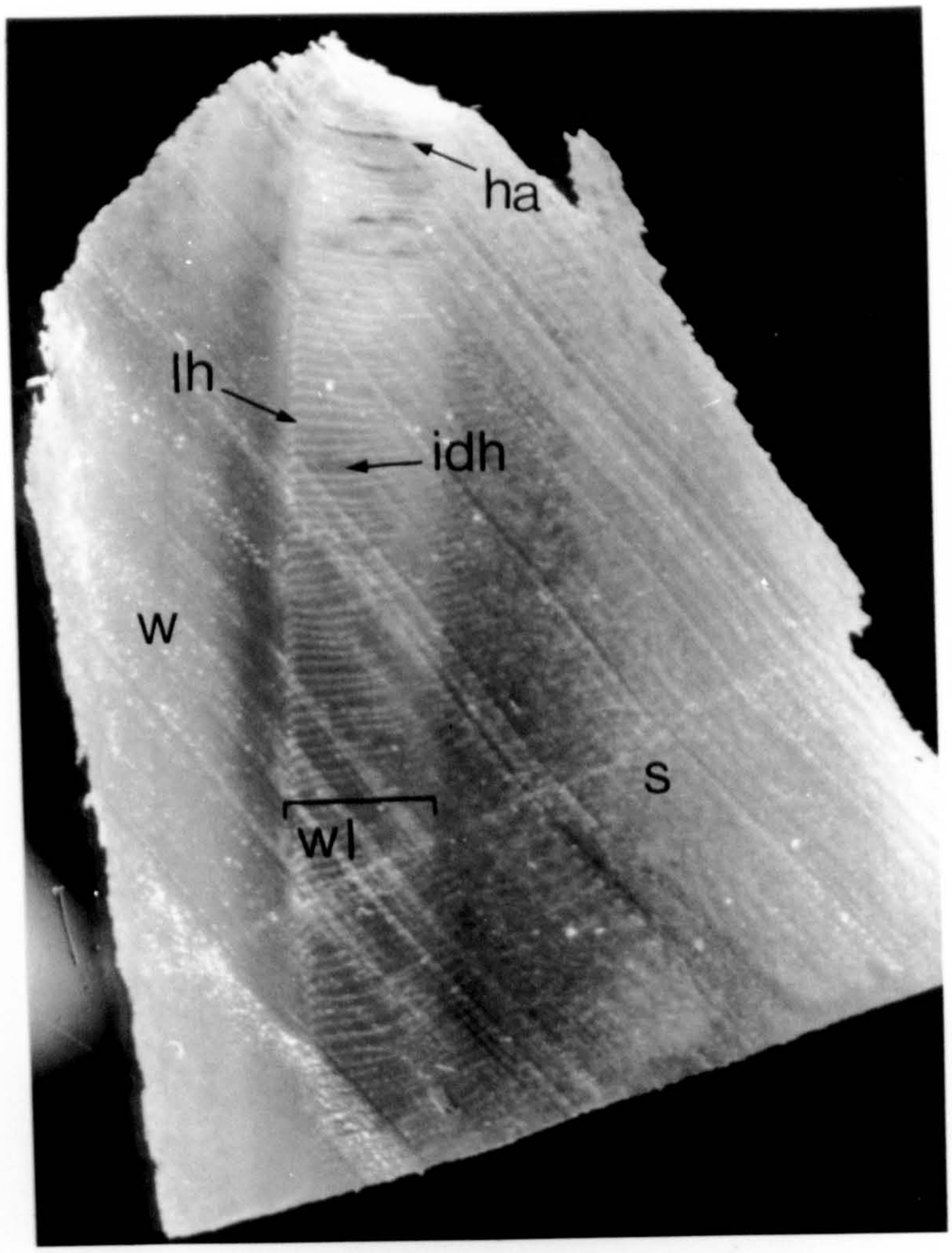
ha
lh
idh
w
s
wl

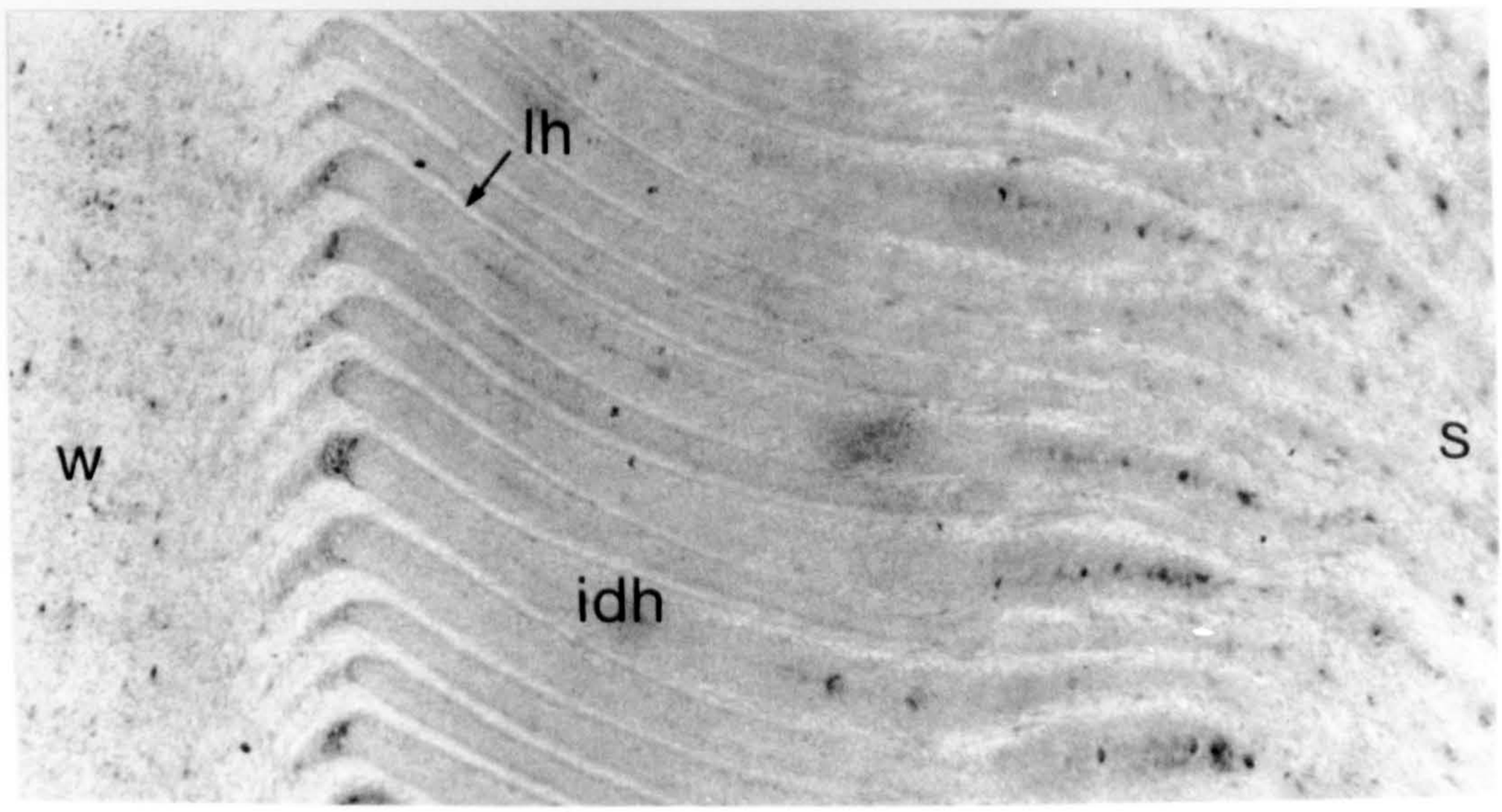
lh
w
s
idh

Figure 2.8
Outlines of the palmar/plantar surfaces of the eight claws, traced from photographs of the feet of a cow aged two and a half years

Left front foot

Lateral Medial

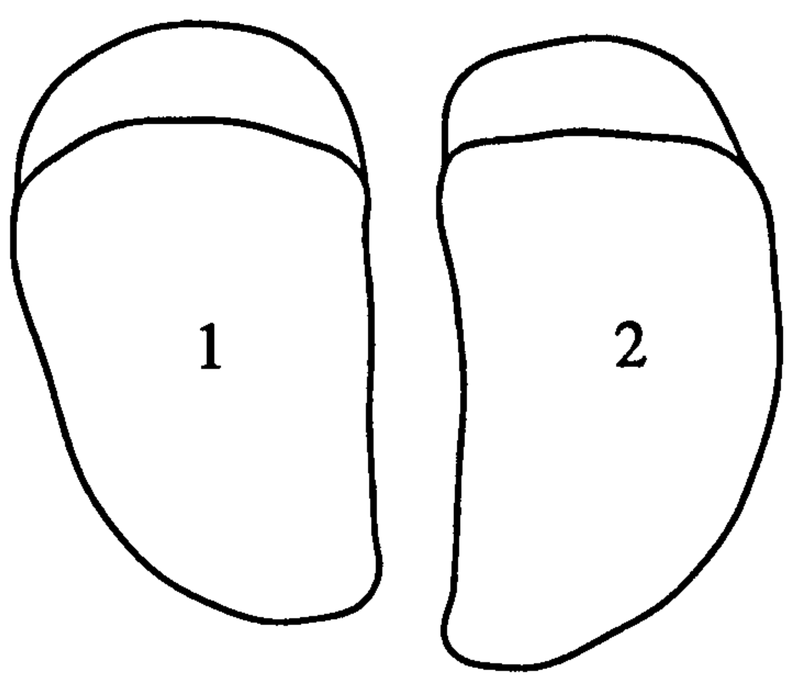

Right front foot

Medial Lateral

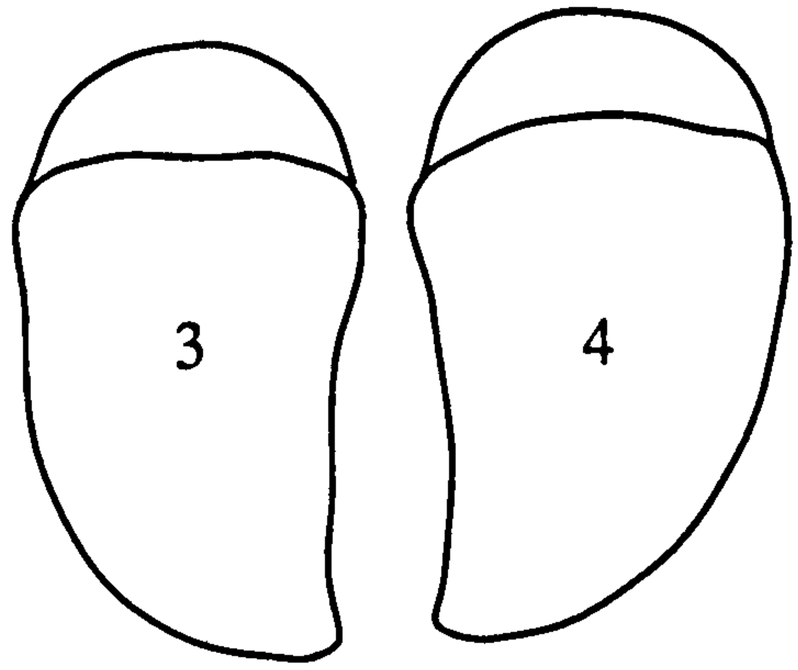

Left hind foot

Lateral Medial

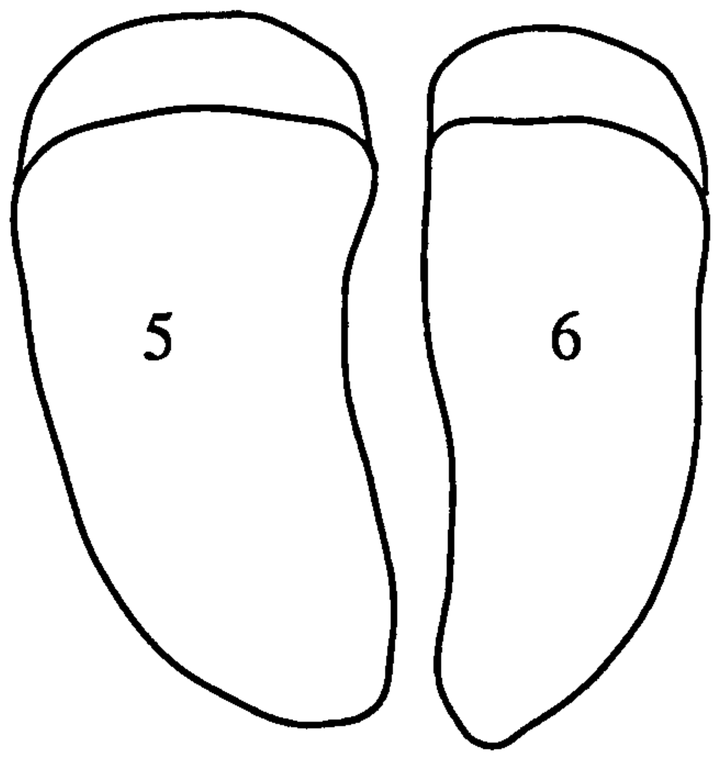

Right hind foot

Medial Lateral

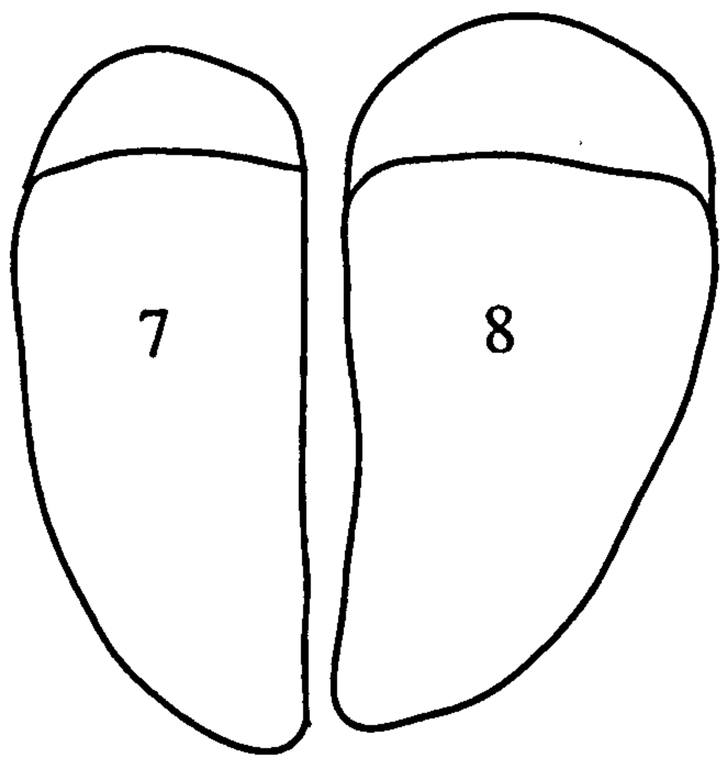

Figure 2.9
Lateral view of the right front foot with claw capsules removed to reveal the coria.

The perioplic corium (pc), which underlies the junction between skin and horn-producing epidermis, is almost entirely hidden by the hair. The coronary corium (cc) extends over approximately half of the lateral and dorsal surfaces of the foot. The surfaces of the coronary corium, the corium of the bulb (bc) and the sole corium (sc) bear dermal papillae. The surface of the laminar corium (lc) is formed into thin dermal laminae which interdigitate with the epidermal laminae visible in Figure 2.2.

Figure 2.10
Palmar view of the right front foot with claw capsules removed to reveal the coria.

The bulb corium (bc) covers the caudal aspect of the digit. The surface of this and the sole corium (sc) bear dermal papillae. Blood vessels (bv) are prominent at the junction between the bulb corium and the sole corium. The caudal limits of the coronary corium (cc) and laminar corium (lc) can be seen on the lateral claw.

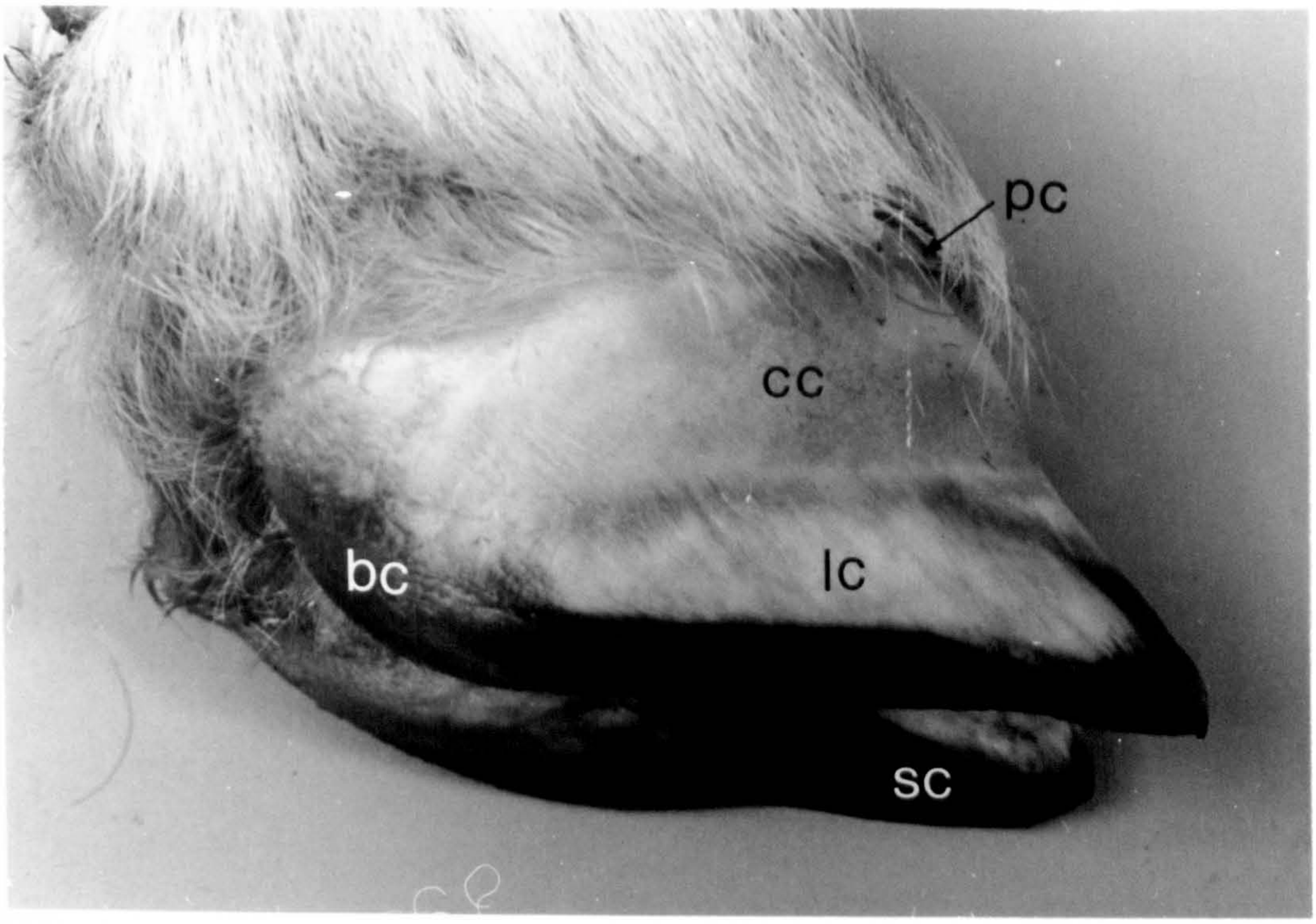
pc
cc
bc
lc
sc

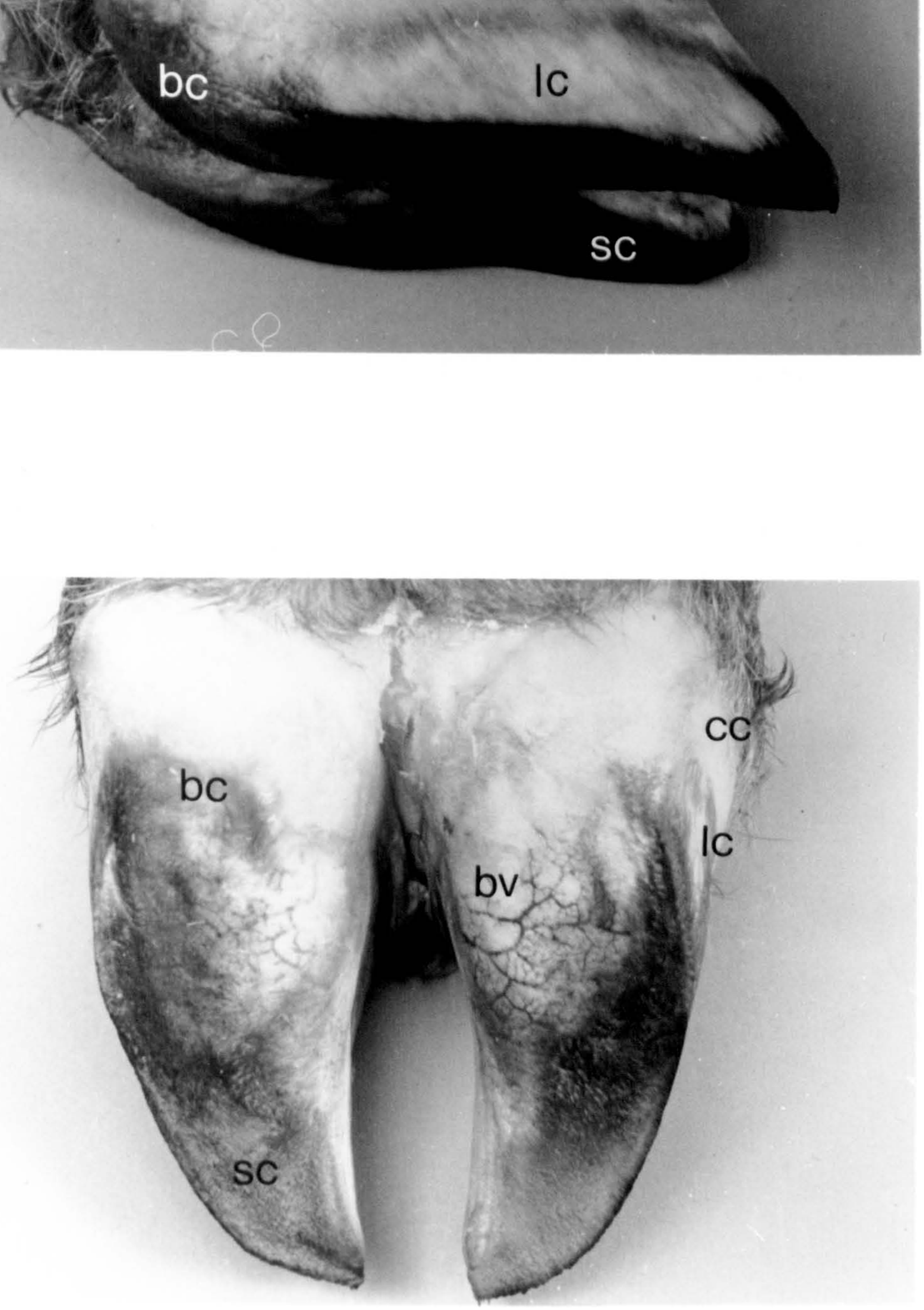
bc
cc
lc
bv
sc

Figure 2.11
Diagram of a sagittal section through the bovine claw and an enlargement of the section through the region of the sole-bulb junction.

PII	Middle phalanx	sc	Sole corium
PIII	Distal phalanx	bc	Bulbar corium
ex	Extensor process of distal phalanx	ph	Perioplic horn
ft	Flexor tubercle of distal phalanx	ch	Coronary horn
di	Joint capsule of distal inter-phalangeal joint	lh	Laminar horn
s	Distal sesamoid bone	wl	White line
nb	Navicular bursa	sh	Sole horn
et	Extensor tendon	bh	Bulb horn
df	Deep digital flexor tendon		
dt	Digital torus	dp	Dermal papilla
cu	Coronary cushion	tm	Tubule medulla
pc	Perioplic corium	tc	Tubule cortex
cc	Coronary corium	it	Intertubular horn
lc	Laminar corium	h	Horn

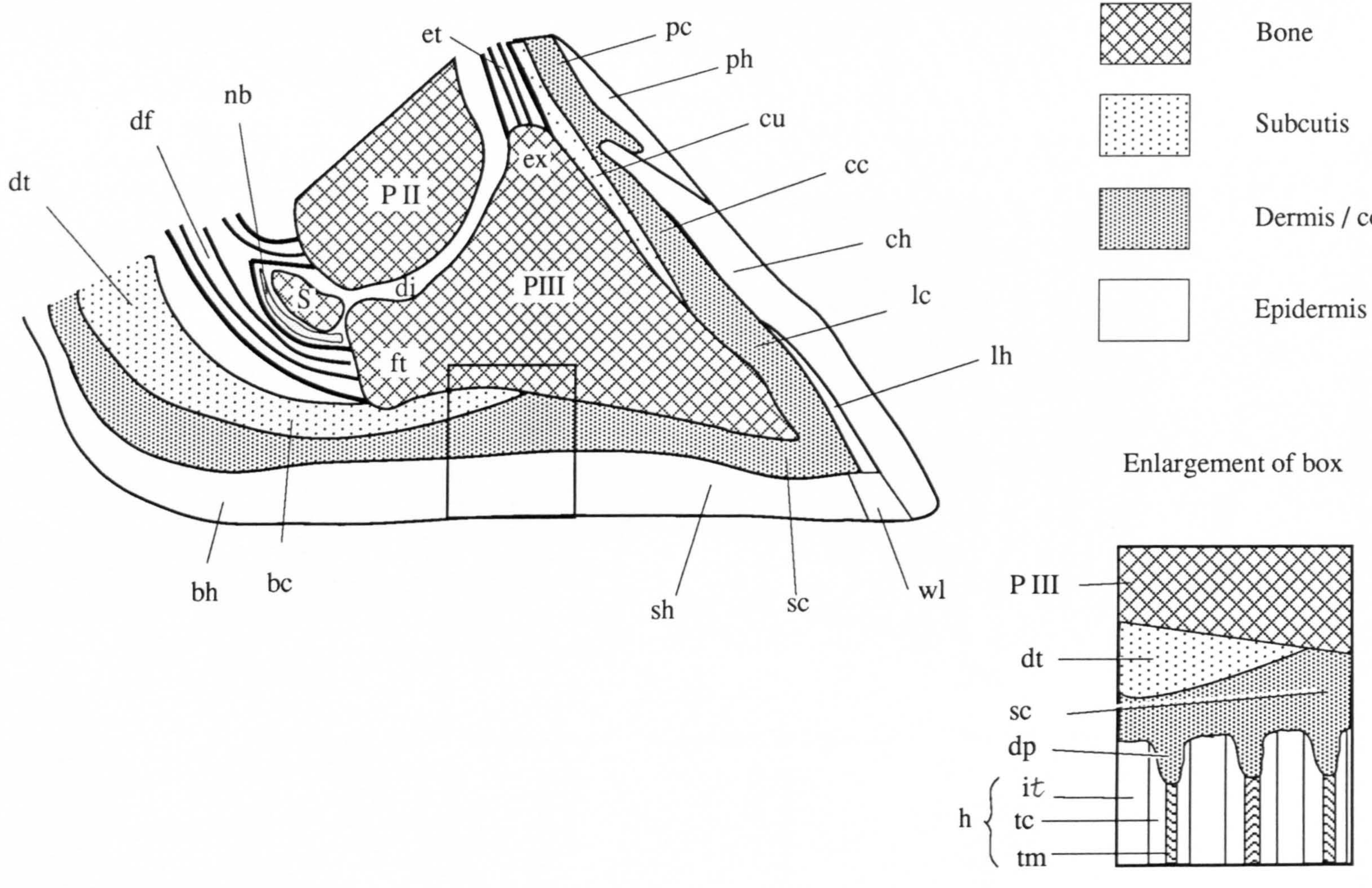
et
pc
ph
nb
df
cu
ex
cc
dt
P II
ch
dj
PIII
S
lc
ft
lh
bh
bc
sh
sc
wl
Bone
Subcutis
Dermis / corium
Epidermis
Enlargement of box
P III
dt
sc
dp
it
h
tc
tm

Figure 2.12
Schematic diagram of the dermis and epidermis in the bovine claw

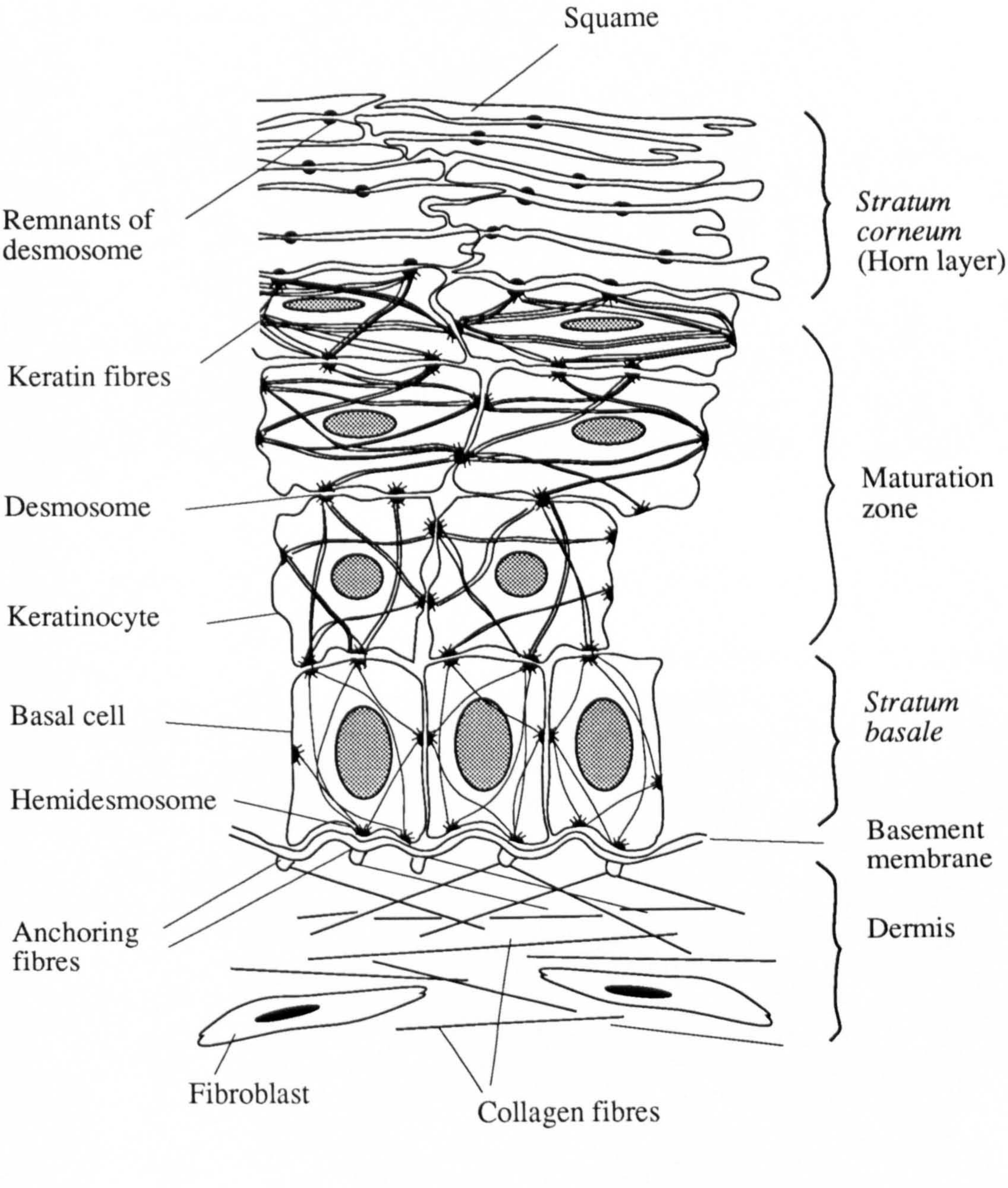
Squame
Remnants of desmosome
Keratin fibres
Desmosome
Keratinocyte
Basal cell
Hemidesmosome
Anchoring fibres
Fibroblast
Collagen fibres
Stratum corneum (Horn layer)
Maturation zone
Stratum basale
Basement membrane
Dermis

Figure 2.13
Light micrographs of the dermis and epidermis of the coronary region of the bovine claw (transverse section)

Figure 2.13a Low power micrograph

The dermis (d), maturation zone (mz) and *stratum corneum* or horn (h) are clearly distinguished by histological staining. The surface of the dermis bears papillae (dp) which project into the epidermis. Due to the plane of section many papillae have been cut in cross section and appear as pale circular areas within the dark maturation zone. Keratinocytes undergo progressive changes as they migrate through the maturation zone (mz). Their staining properties alter abruptly when they enter the *stratum corneum* or horn (h) as fully keratinized squames.

x 32

Stain : Phloxine-Tartrazine

Figure 2.13b High power micrograph

At higher magnification the single layer of basal cells (ba) can be distinguished, lying adjacent to the dermal papillae (dp). These columnar cells have prominent nuclei. They undergo mitosis and one of the daughter cells migrates into the maturation zone (mz). Keratinocytes in the maturation zone become increasingly flattened as they move towards the surface of the epidermis. They undergo the final stages of keratinization as they move from the maturation zone (mz) into the *stratum corneum* or horn layer (h).

x 100

Stain : Phloxine-Tartrazine

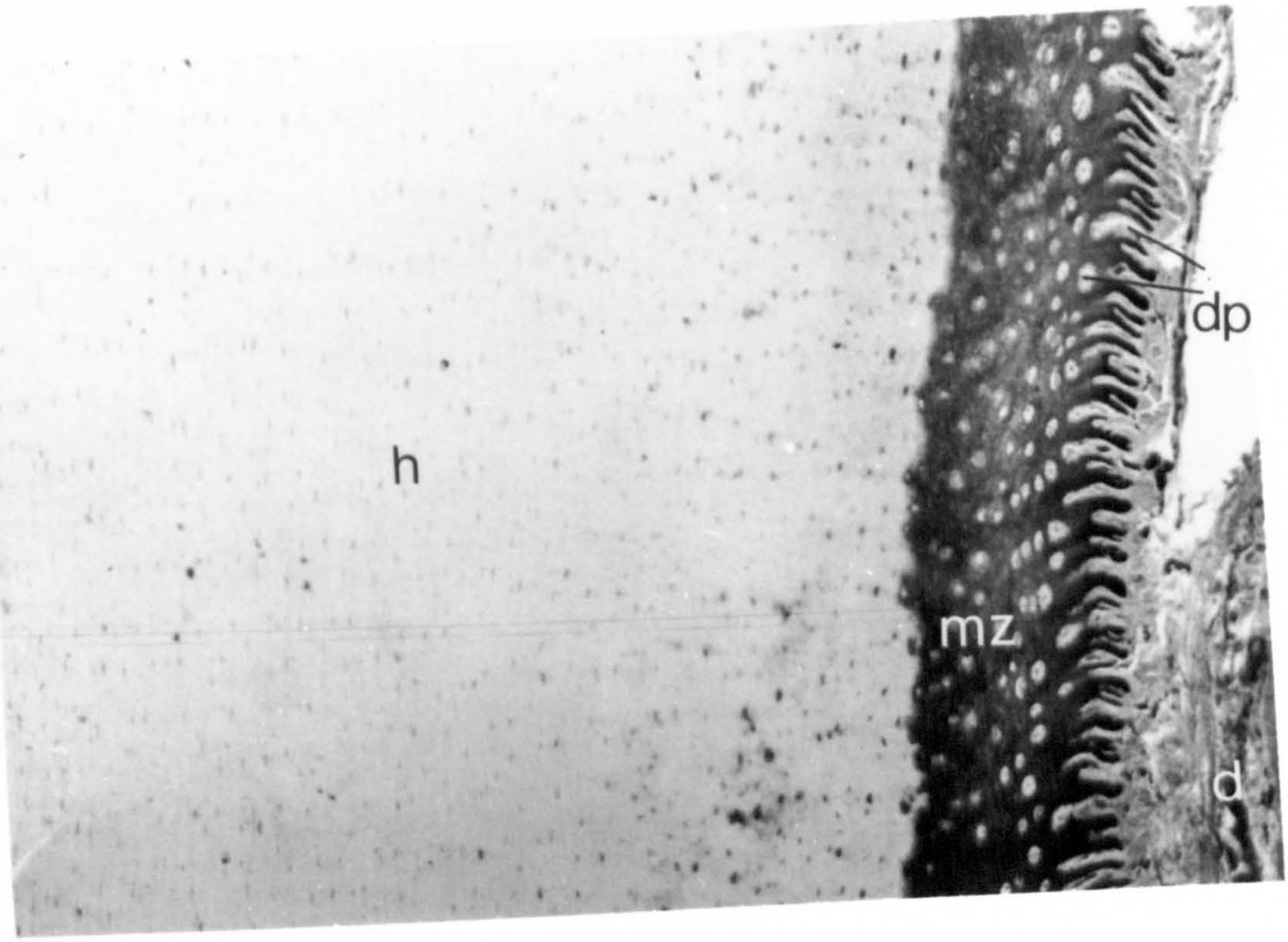
h
dp
mz
d

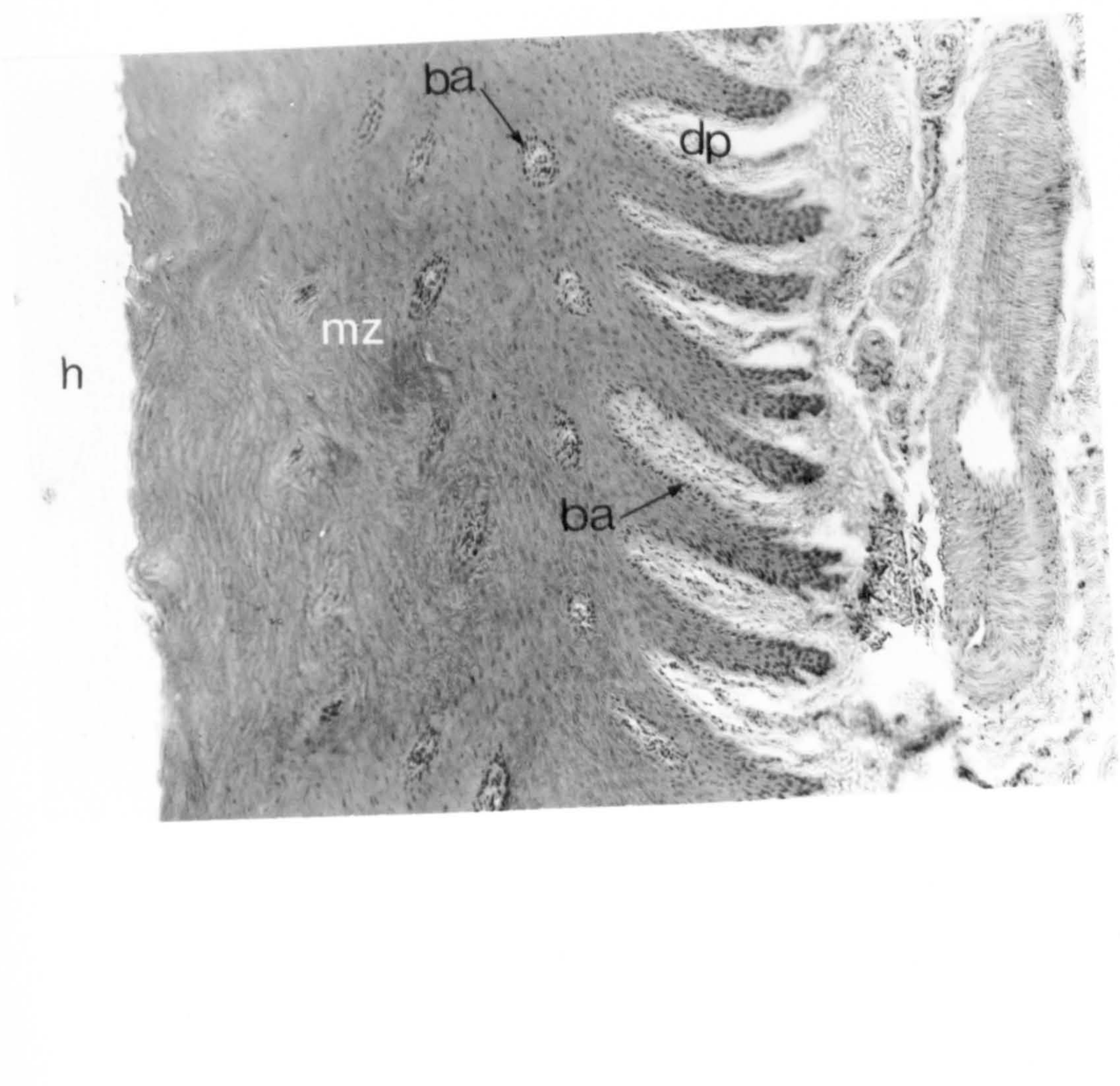
ba
dp
mz
h
ba

Figure 2.14
Light micrograph of basal cells in the laminar region of the bovine claw

Adjacent to the dermis (d) and separated from it by the basal lamina (↑) lies the *stratum basale* (sb_1, sb_2). This is a single layer of columnar basal cells (ba) with large nucleii. Cell division occurs in the *stratum basale*. The cells produced migrate into the maturation zone (mz). Basal cells can be distinguished from the adjacent keratinocytes of the maturation zone (mz) by their shape. Cells in the maturation zone are flattened parallel to the dermal-epidermal junction. In this micrograph two layers of *stratum basale* overlying adjacent dermal laminae (sb1 and sb2) are visible. These two layers contribute cells to the same horny lamina (hl).

x 720

Stain : Phloxine-Tartrazine

Figure 2.15
Transition electron micrograph of basal cells in the epidermis of the laminar region of the bovine claw

The basement membrane (bm↑) lies at the junction of the dermis (d) and epidermis (e). Finger-like cytoplasmic processes (↑) extend from the dermal aspect of the basal cells (ba) into the dermis, greatly increasing the surface area of the basement membrane. The keratin fibres (kf ↑) in the basal cells are loosely scattered in the cytoplasm. The flattened cells of the maturation zone (mz) contain more densely packed keratin filaments which are orientated parallel to the long axis of the cells, The fully keratinized squames of the stratum corneum (sc) packed with keratin filaments are electron dense. The intercellular spaces of the basal cell layer are relatively large compared to those of the maturation zone and *stratum corneum*.

x 7,000

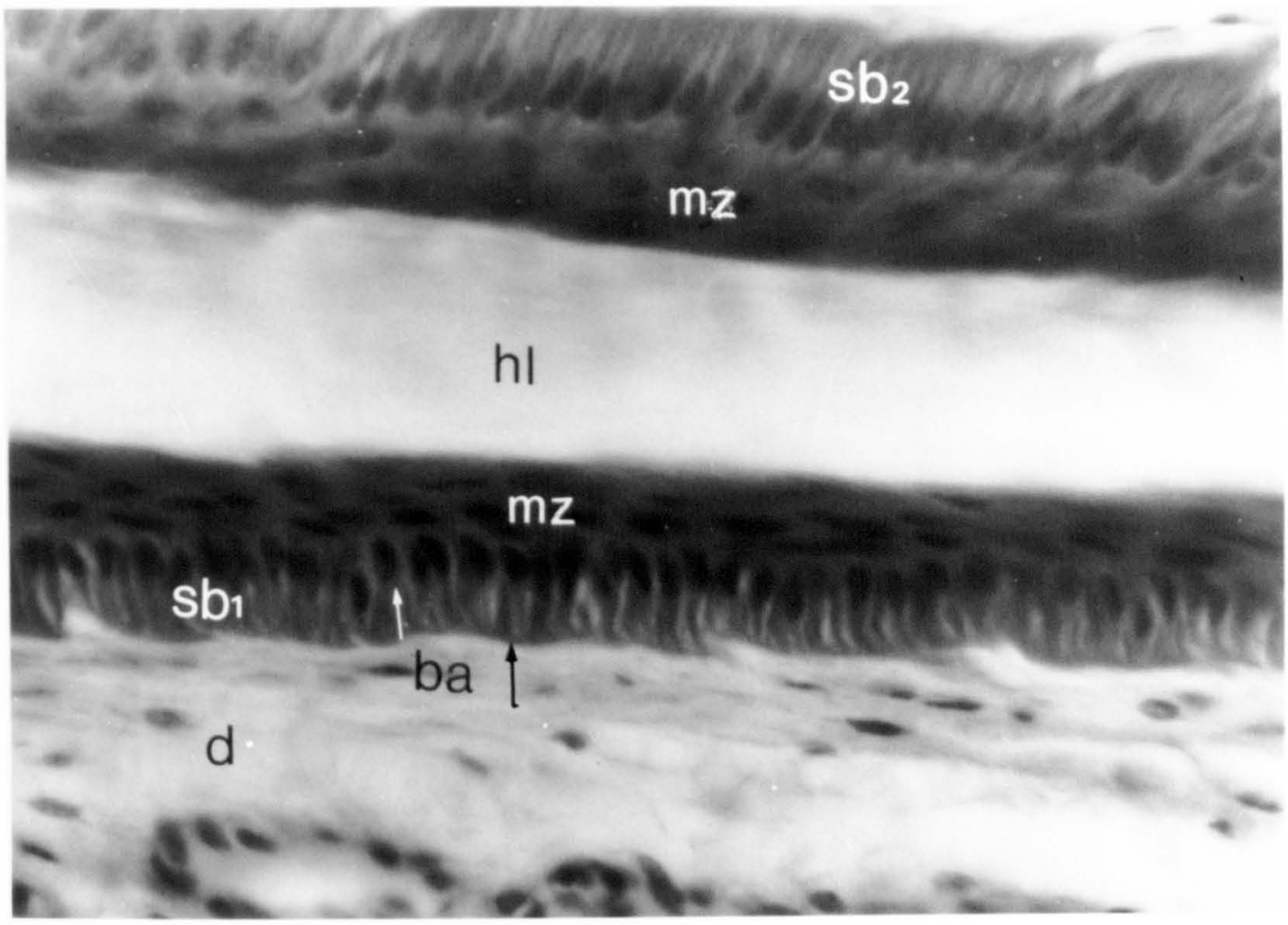
sb2
mz
hl
mz
sb1
ba
d

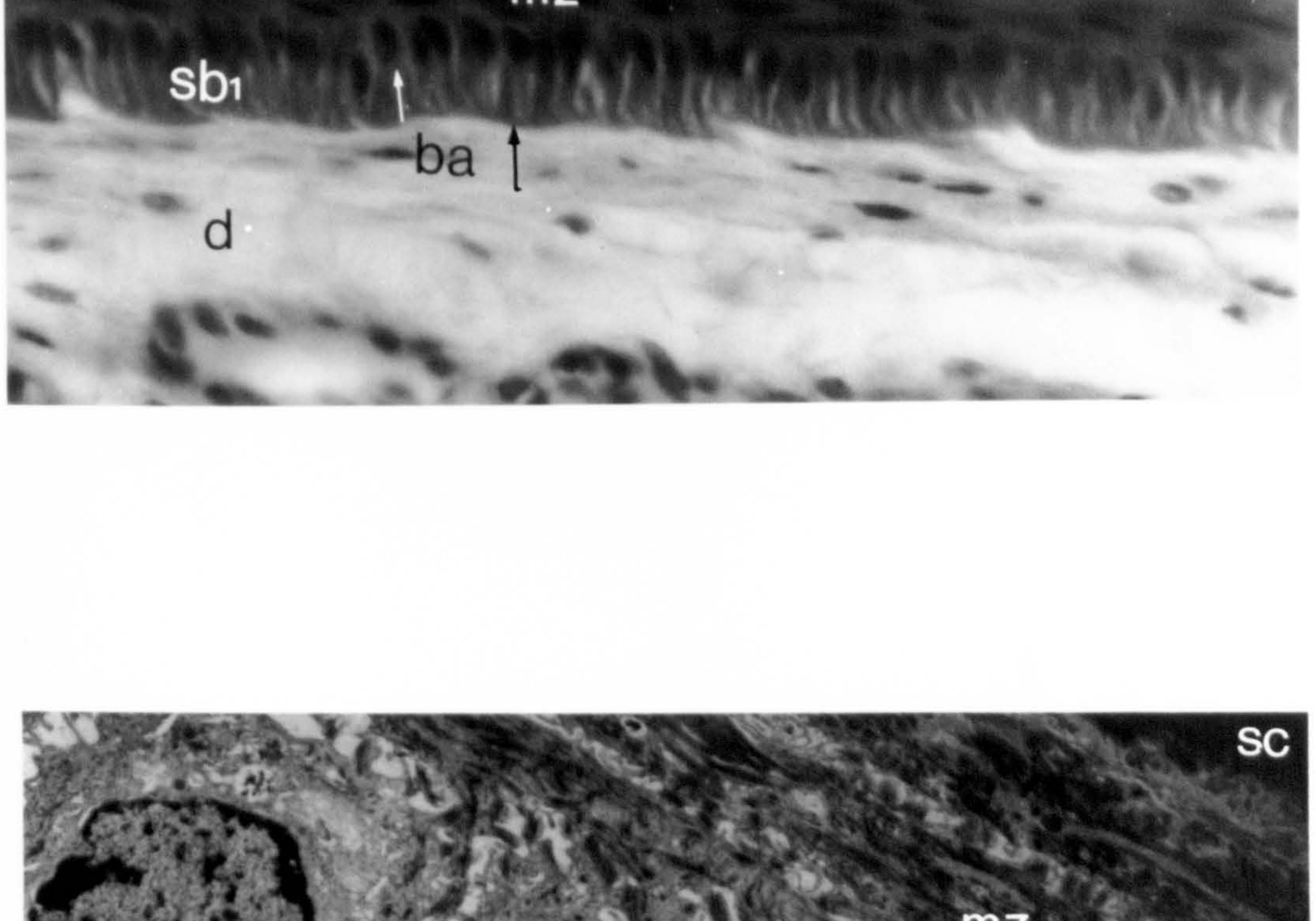
sc
mz
kf
ba
e
d
bm

Figure 2.16a
Transmission electron micrograph of the squames of the stratum corneum in the laminar horn of the white line of the bovine claw

The flattened cells or squames (sq) of the stratum corneum are orientated with their long axes parallel to the axis of the lamina. In this section the sqames have been sectioned parallel to their long axes. Each squame is composed of keratin filaments embedded in interfilamentous matrix, surrounded by a cell membrane (cm). The cell membranes of adjacent squames are closely apposed to one another. In some regions, particularly at the narrow ends of the squames, the cell membranes are thrown into numerous folds (↑).

x 4,300

Figure 2.16b
Transmission electron micrograph of the squames of the stratum corneum in the interdigitating horn of the white line of the bovine claw

This micrograph shows squames which have been sectioned at right angles to their long axes. Bundles of keratin fibres (kf ↑) are visible in transverse section, embedded in interfilamentous matrix (m).

x 9,200

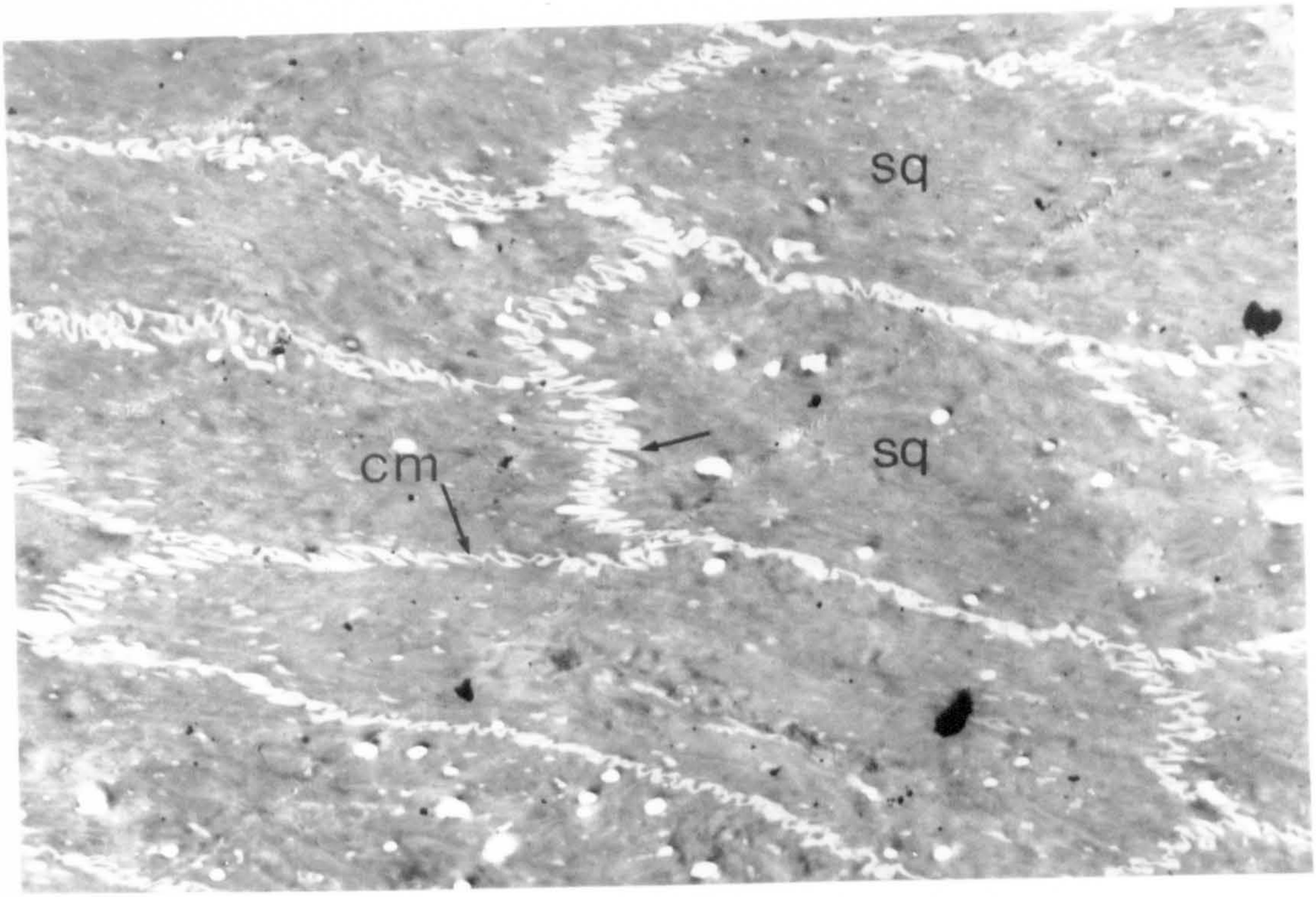
sq
cm
sq

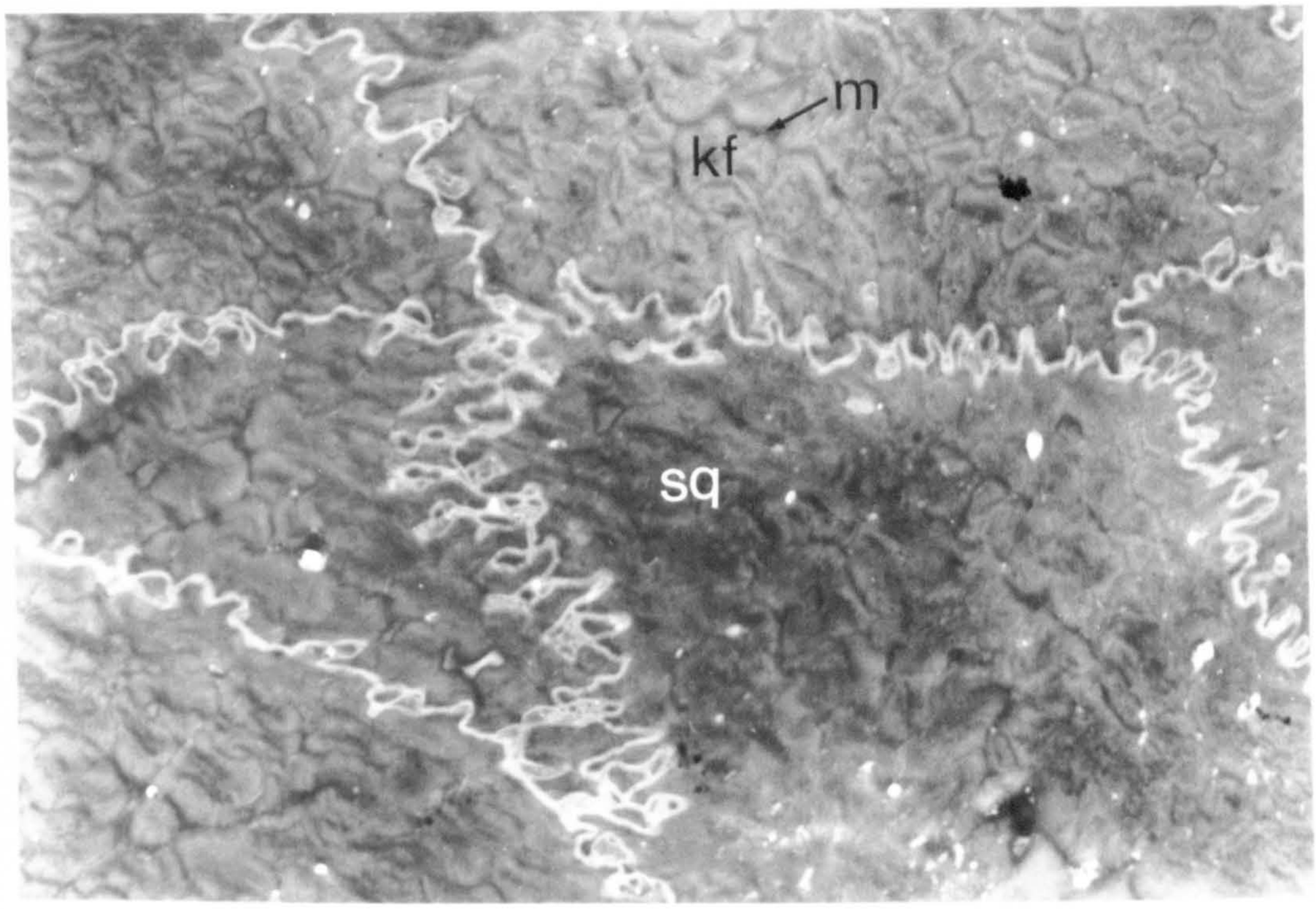
m
kf
sq

Figure 2.17
Transmission electron micrograph of the region of the basement membrane in the bovine claw

The basement membrane is found at the junction between dermis (d) and epidermis (e). The *lamina lucida* (ll) and *lamina densa* (ld) of the basement membrane can be distinguished. Anchoring fibrils (af) on the dermal side of the membrane are looped around dermal collagen fibres (cf) and insert into the *lamina densa*. Hemidesmosomes (hd) attach the basal cells (ba) to the basement membrane.

x 120,000

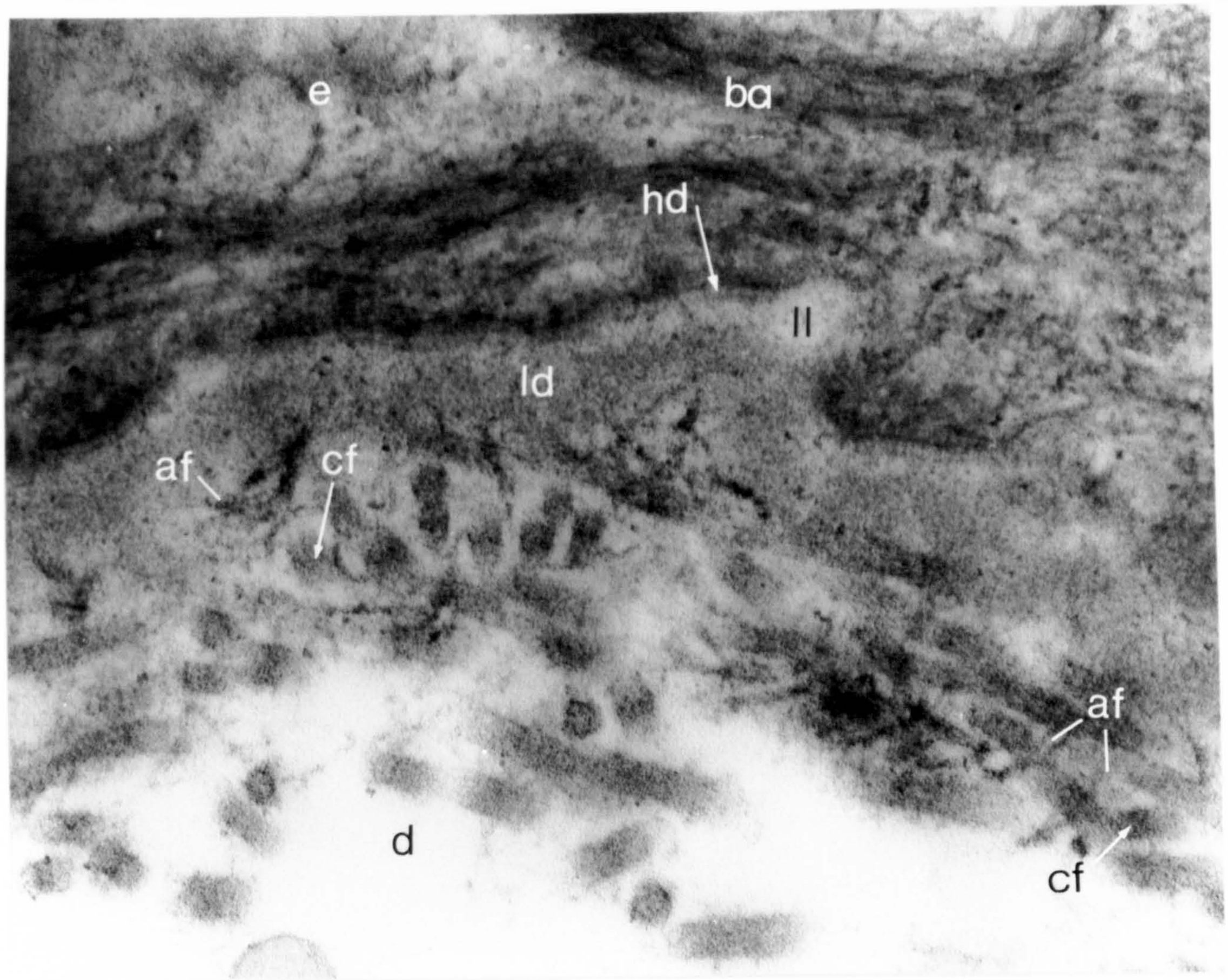
e
ba
hd
ll
ld
af
cf
d
af
cf

Figure 2.18
Light micrograph of sole corium of the bovine claw (longitudinal section)

The dermis (d) contains bundles of collagen fibres (cf ↑) and the blood vessels (bv ↑) are concentrated near the dermal-epidermal junction. The primary cells of the dermis are fibroblasts (f ↑). The surface of the dermis bears numerous papillae (dp).

x 75

Stain : Phloxine-Tartrazine

Figure 2.19
Transmission electron micrograph of a fibroblast in the laminar corium of the bovine claw

The electron dense nucleus (n) of the fibroblast (f) is surrounded by a thin layer of cytoplasm (cy). The fibroblast is surrounded by extracellular bundles of collagen fibres (cf).

x 17,000

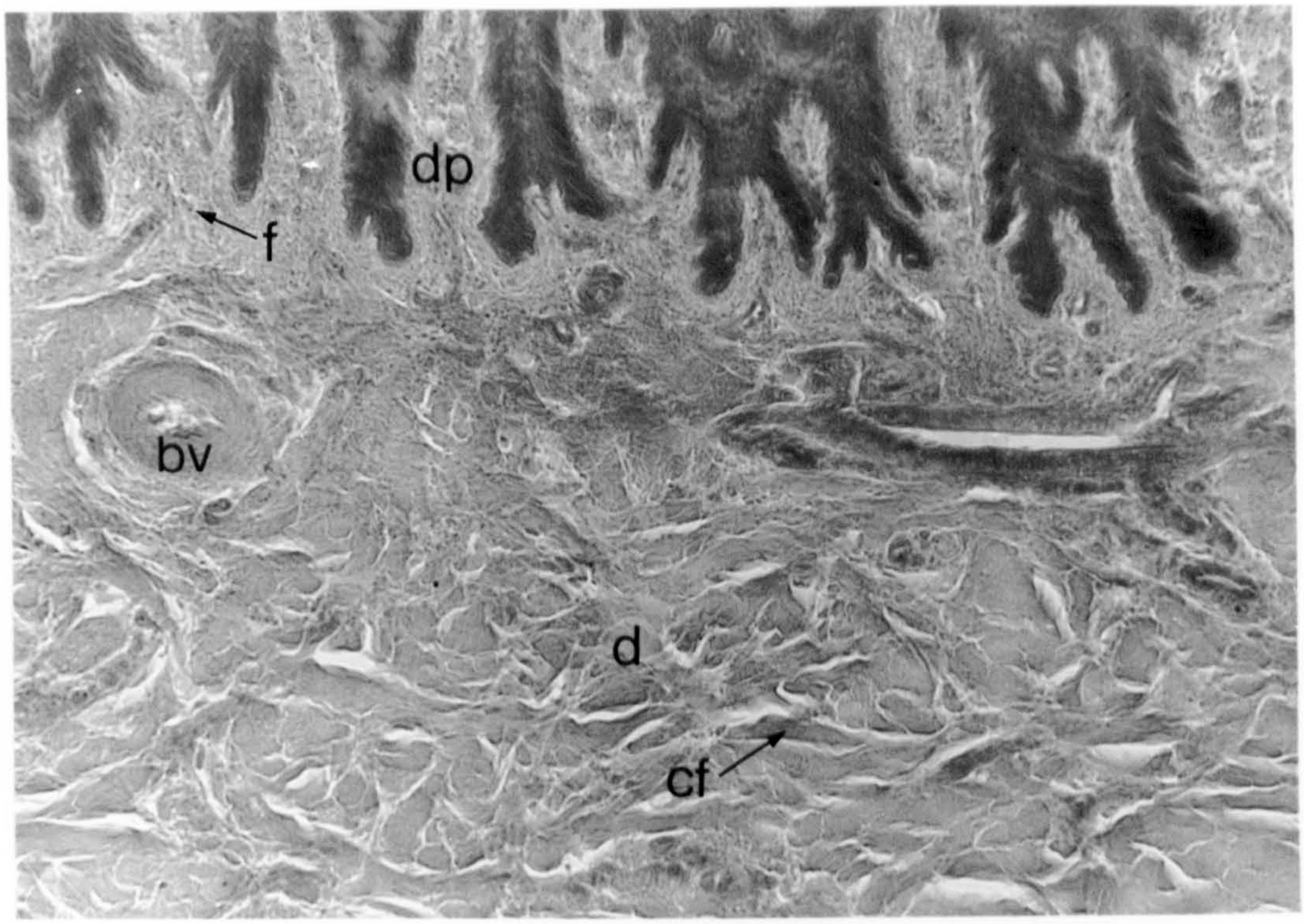
dp
f
bv
d
cf

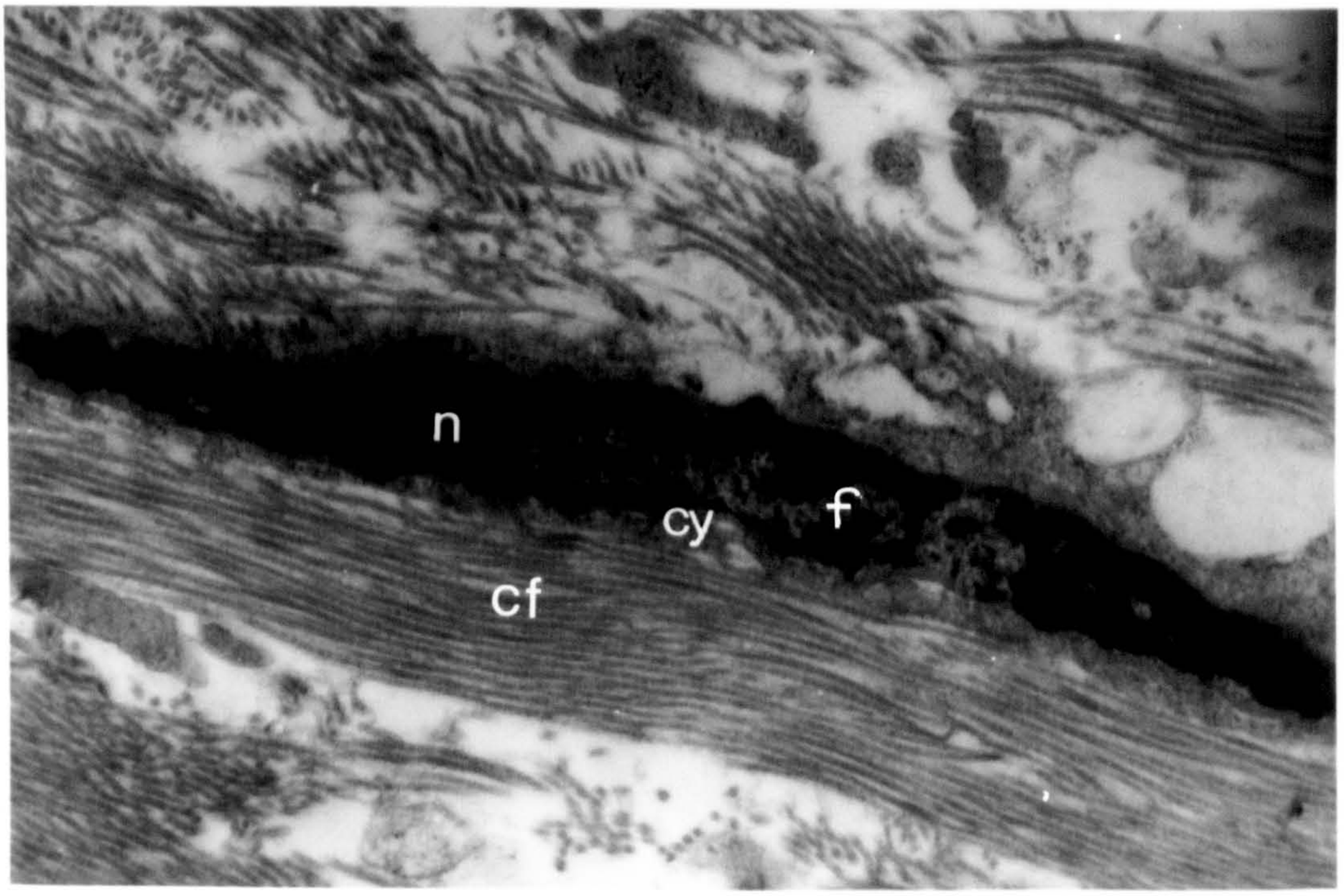
n
cy
f
cf

Figure 2.20
Scanning electron micrograph of the papillae of the sole corium of the bovine foot after removal of the claw capsule

The sample has been mounted on its proximal surface. The surface of each individual dermal papilla (dp) bears ridges running parallel to the axis of the papilla. These may reflect the pattern of underlying blood capillaries, or be caused by regional differences in the level of tissue separation during sample preparation.

x 27

Figure 2.21
Longitudinal section through the heel bulb of the bovine claw, after removal of the claw capsule

The majority of the sample is composed of the tissues of the digital torus (dt). A network of highly organised bundles of collagen fibres (cf) encloses regions of adipose tissue (at). Distally the thin layer of the bulb corium (bc) shows numerous dermal papillae (dp).

x 6

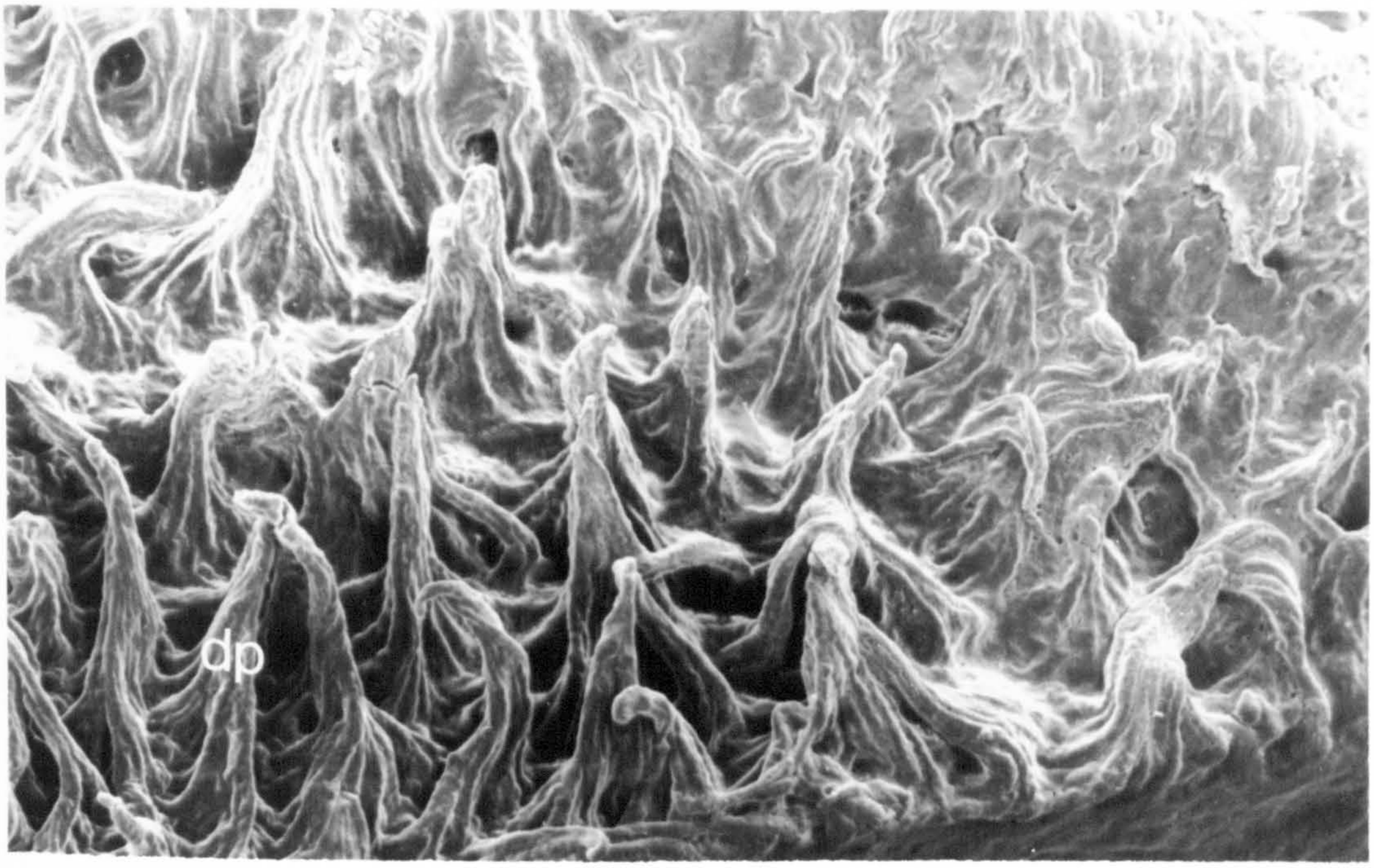
dp

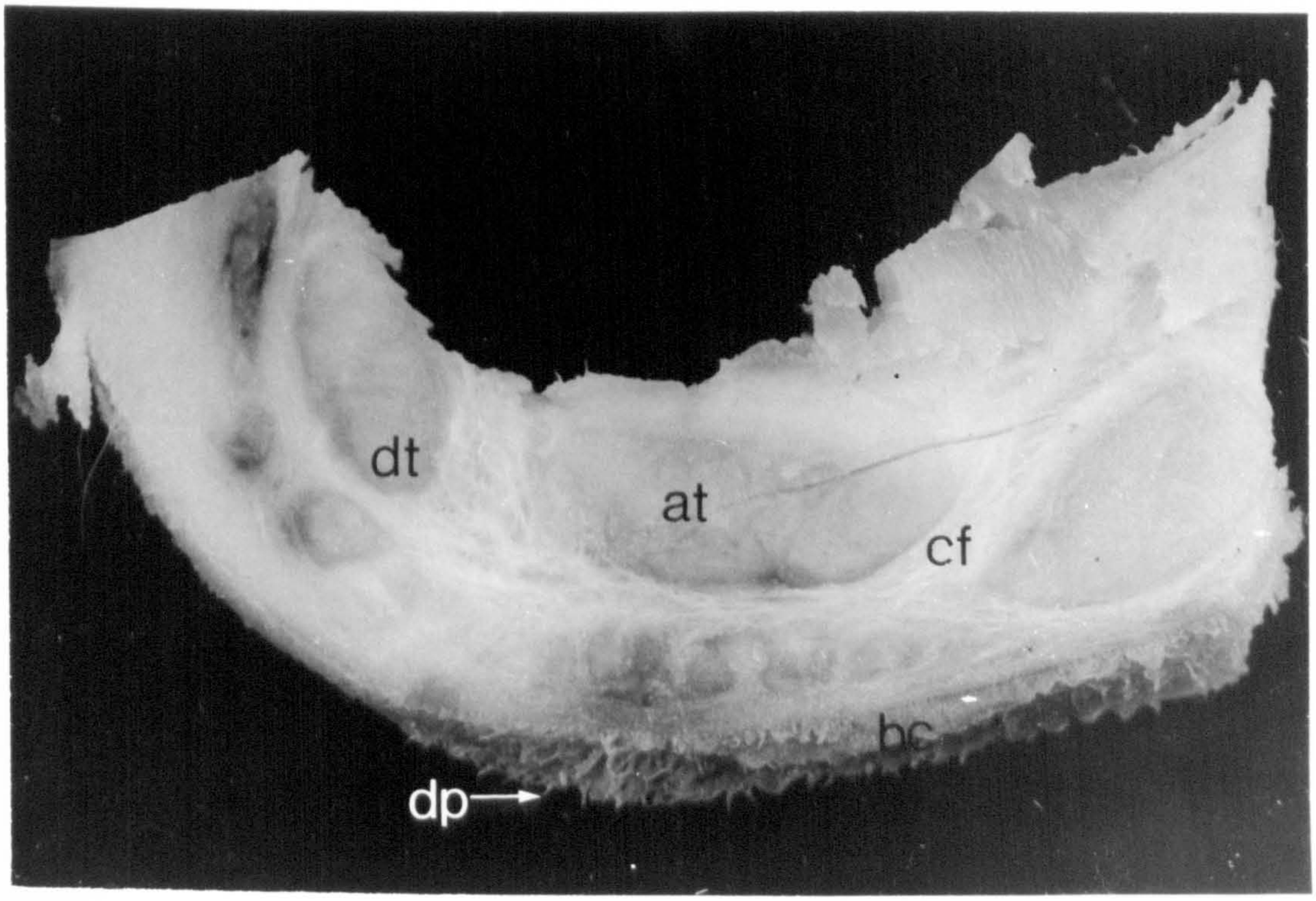
dt
at
cf
bc
dp

Figure 2.22
Transmission electron micrograph of a keratinocyte in the maturation zone of the epidermis in the laminar region of the bovine claw

The nucleus (n) is flattened but maintains its internal structure. A nucleolus (nu) is clearly visible. Bundles of keratin filaments (kf) run parallel to the long axis of the cell, surrounded by ribosome-rich cytoplasm. The proportion of cytoplasm to nucleus is higher in cells of the maturation zone than in the basal cells. Desmosomes (de↑) are visible on the cell membranes.

x 7,100

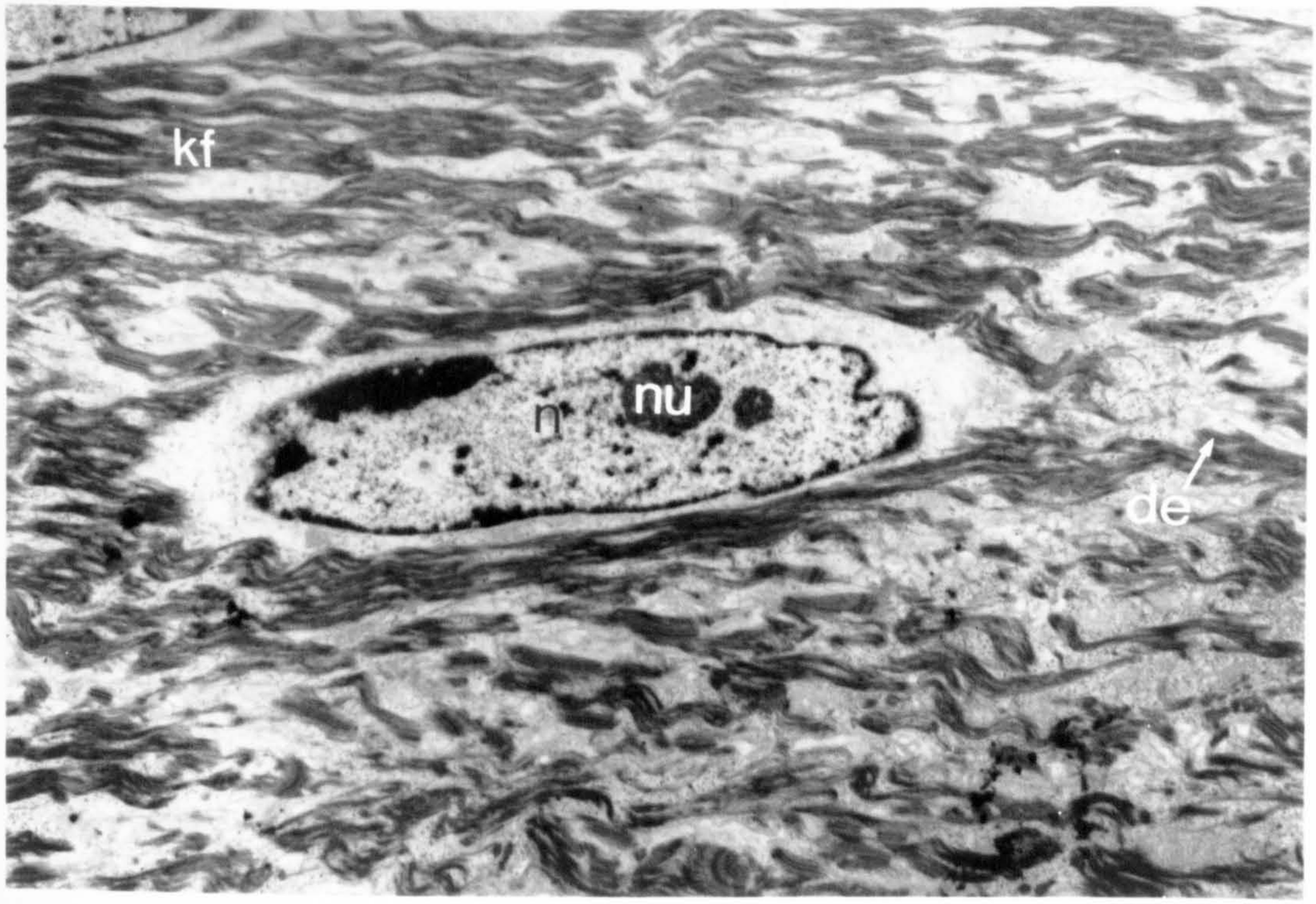
kf
nu
de

Figure 2.23
Transmission electron micrograph of fully keratinized squames of the *stratum corneum* from the laminar horn in the white line of the bovine claw

Squames (sq) are completely filled with keratin fibres (kf ↑) embedded in matrix. The bundles of keratin fibres run parallel to the long axis of the squames. The membranes (cm) of adjacent squames are closely apposed. Small amounts of intercellular material (i) are present in widened intercellular spaces between remnants of desmosomes (d ↑). Juxtaposed cell membranes (cm) form deep folds, particularly at the narrow ends of the squames (↑).

x 22,500

Figure 2.24
Transmission electron micrograph of the remnants of a desmosome between two adjacent squames of the *stratum corneum*

The desmosome (d) is the specialised area of attachment between two adjacent cell membranes (cm). Desmosomal placques (↑) can be distinguished on the intracellular aspect of the adjoining cell membranes (cm).

x 72,000

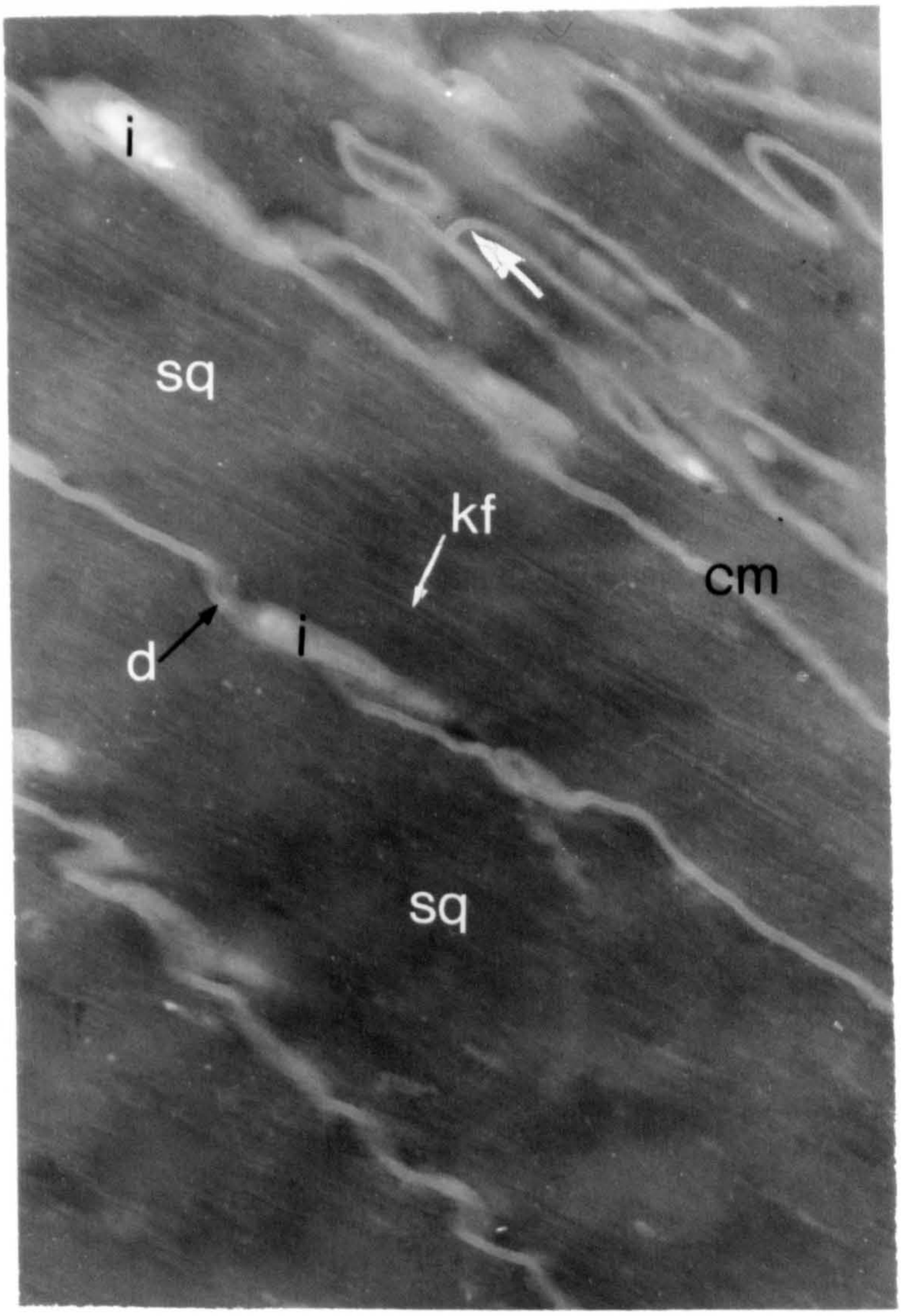
i
sq
kf
cm
d
i
sq

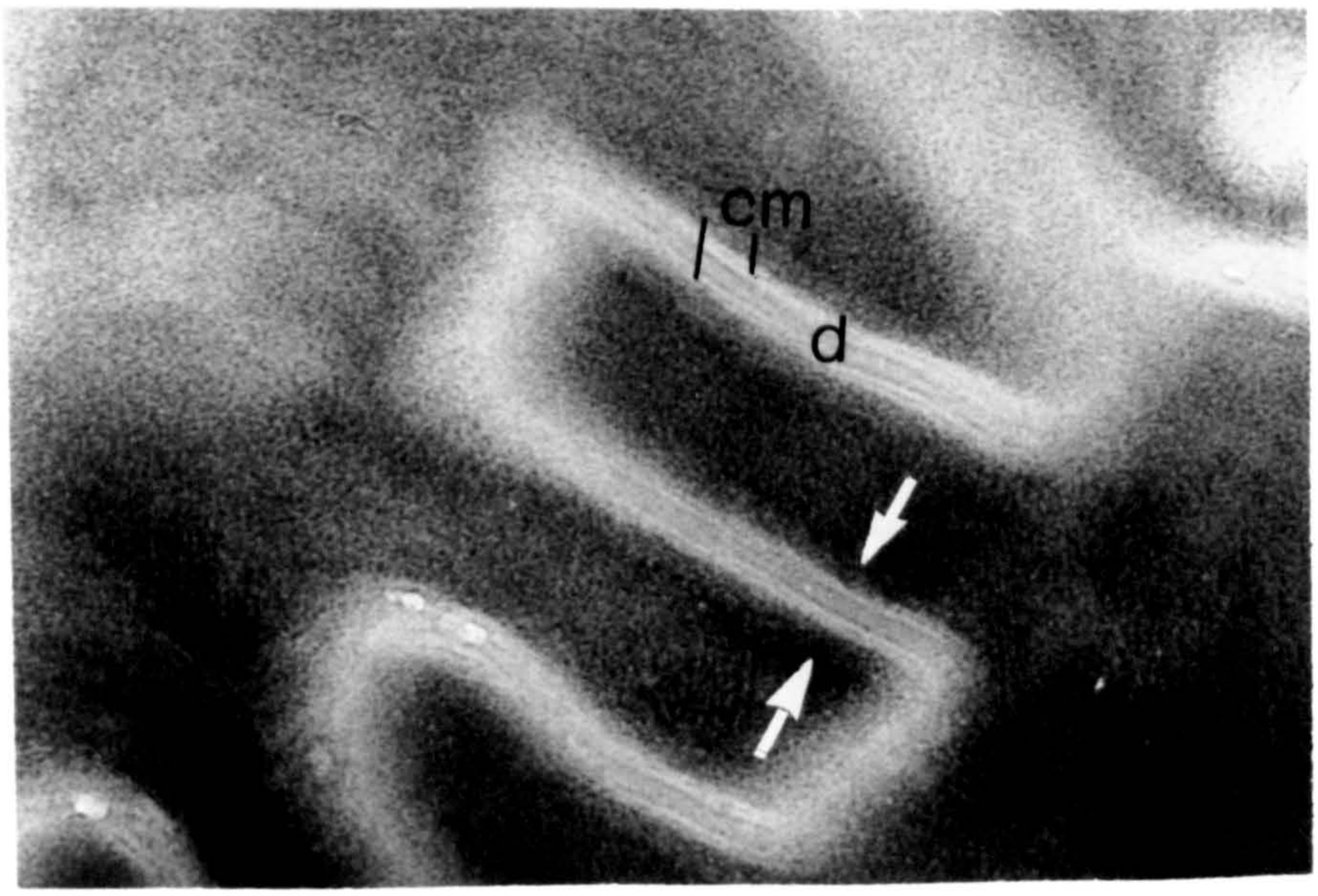
cm
d

Figure 2.25
Low power light micrograph of a transverse section through the dermis and epidermis in the laminar region of the dorsal wall of the bovine claw

In the laminar region of the foot the surface of the dermis (d) is formed into numerous narrow folds, the dermal laminae (dl). These specialised dermal structures interdigitate with epidermal laminae (el) giving a large surface area of attachment between dermis and epidermis. The region of the interdigitating dermal and epidermal laminae is referred to as the *stratum internum* (si). A narrow region of horn without tubules (*) separates the *stratum internum* from the tubular coronary horn of the wall (ch). The position of tubules in the coronary horn is marked by densely stained tubule medullae (tm↑). The distribution, density and size of horn tubules varies across the width of the wall. Tubules are most prominent and their distribution is most dense in the middle region of the wall (mi).

x 18

Stain : Phloxine-Tartrazine

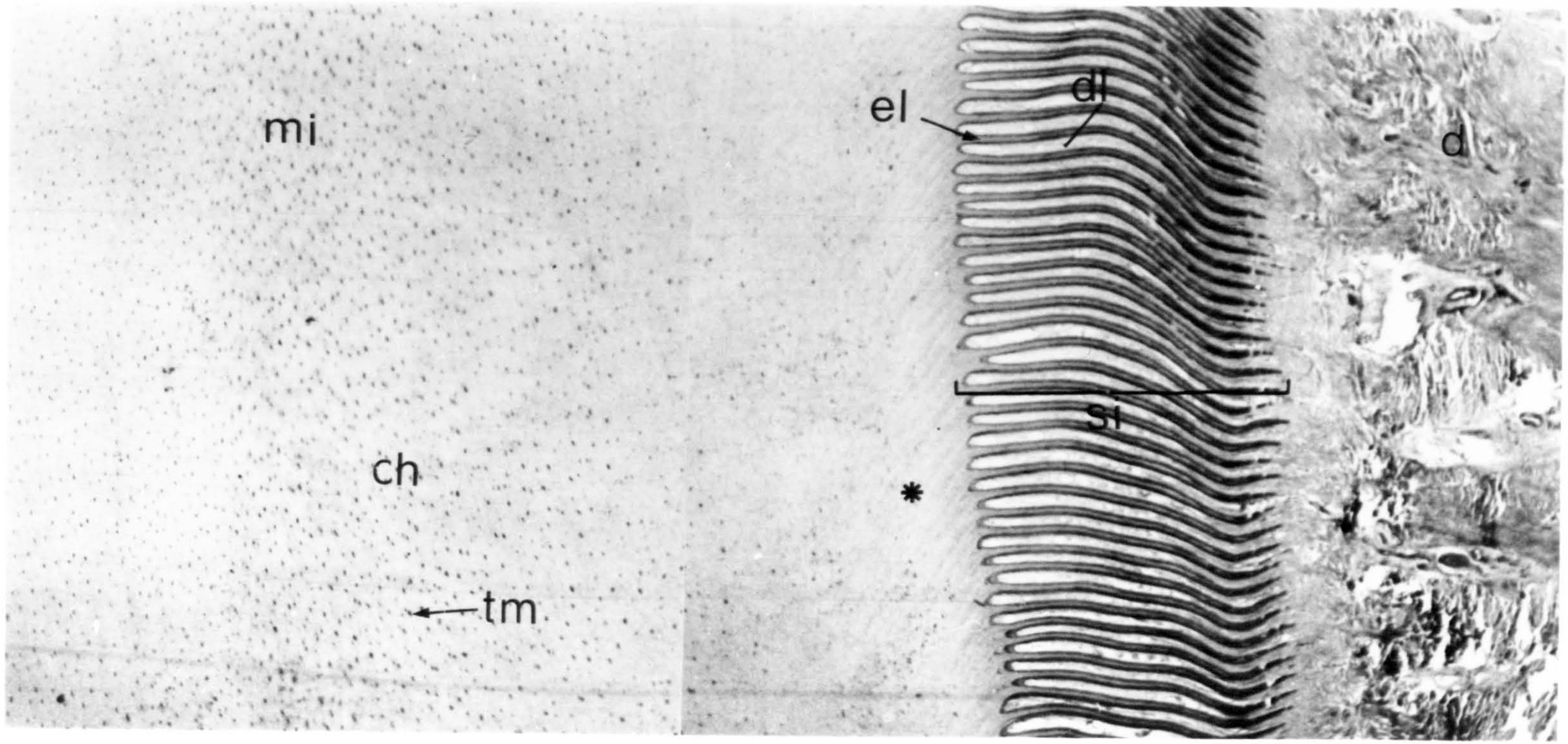
mi
el
dl
d
sl
ch
tm
*

Figure 2.26
High power micrograph of the dermal and epidermal laminae in transverse section

The dermal laminae (dl) contain a large number of conspicuous blood capillaries (ca). The epidermal laminae are composed of the *stratum basale* (sb), the maturation zone (mz ↑) and the laminar horn leaflets (lh). Squames developing from the epidermis over the peripheral tips or "crests" of the dermal laminae are arranged in arched formations (↑) referred to as the cap horn.

x 180

Stain : Phloxine-Tartrazine

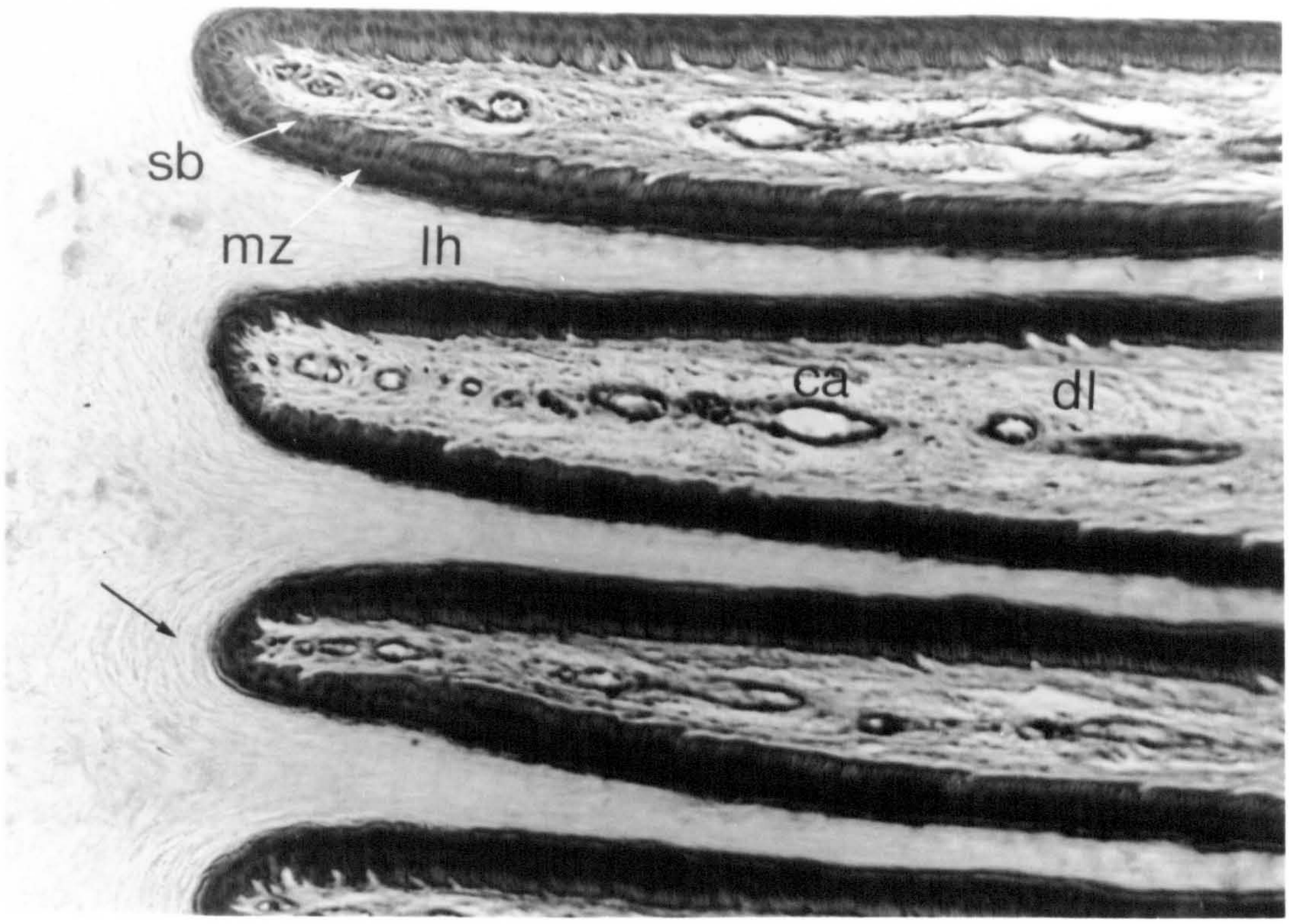
sb
mz
lh
ca
dl

Figure 2.27
Light micrograph of a longitudinal section through the coronary corium of the bovine claw illustrating the production of a horn tubule over a dermal papilla

The tips of three dermal papillae (dp) are visible projecting into the maturation zone (mz). The epidermis overlying dermal papillae produces tubular horn. The horn of the tubule medulla (tm↑) is produced over the tip of the papilla. It is more densely stained than the horn forming the cortex (tc↑) which is produced by epidermis surrounding the papilla. The intertubular horn (it) is the end product of keratinization of the epidermis overlying the inter-papillary regions of the dermis.

x 27

Stain : Phloxine-Tartrazine

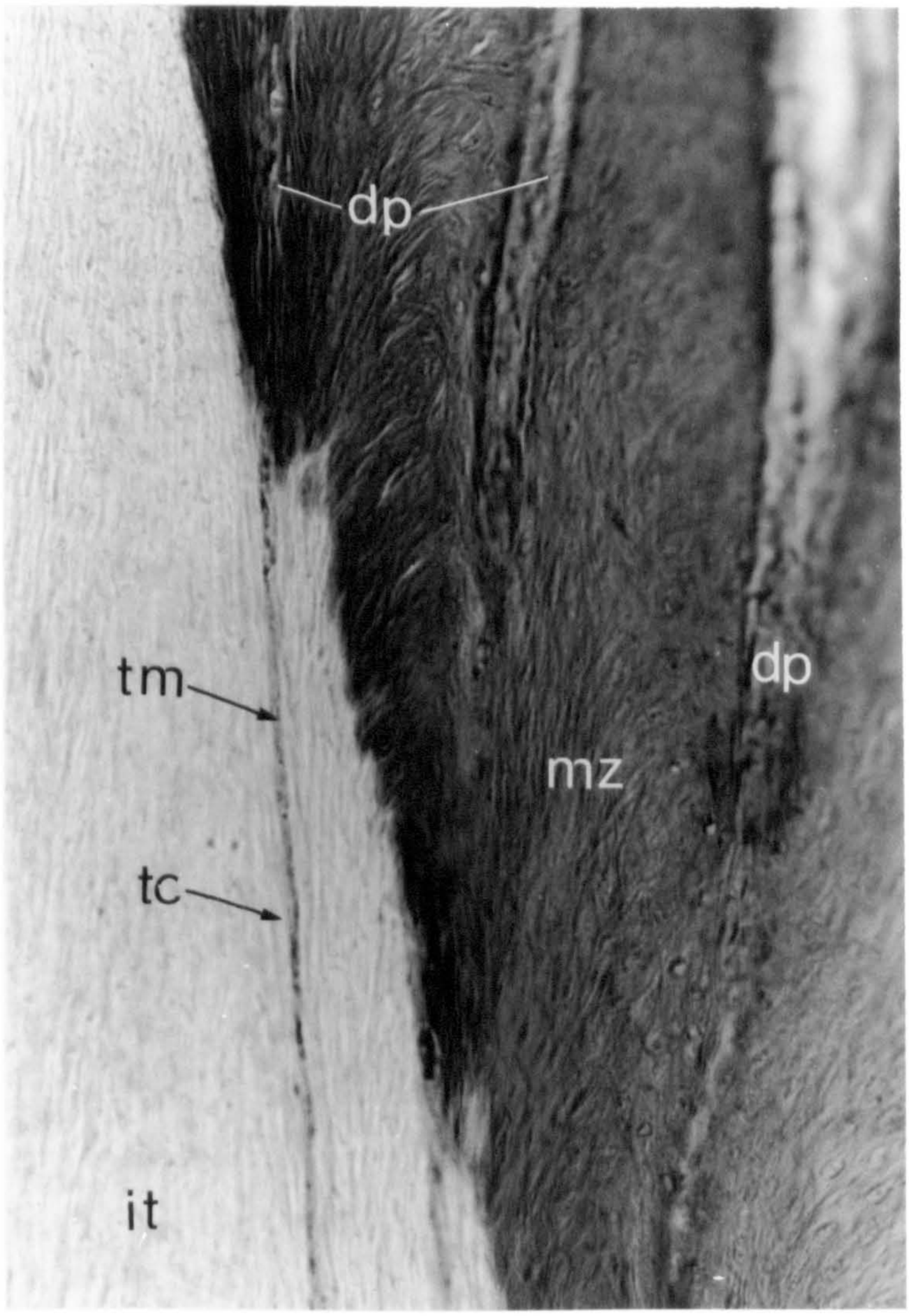
dp
tm
mz
dp
tc
it

Figure 2.28
Transmission electron micrograph of a horn tubule from the wall of the bovine claw in transverse section

Many of the squames of the medulla of the tubule (tm) are degenerate or incompletely keratinized. Lipid droplets (lp) are found within many medullary squames. These are thought to be the product of organelle breakdown. Scattered keratin filaments (kf) are visible. The flattened dense squames of the tubule cortex (tc) are arranged concentrically around the medulla.

x 5,500

Figure 2.29
Scanning electron micrograph of a tubule from the sole of the bovine claw in transverse section

The difference in structure and physical characteristics of the horn of the medulla and the cortex is clearly evident. Squames of the tubule medulla (tm) have separated and in places disintegrated during dehydration, leaving holes. This indicates that they had a high moisture content. Squames of the cortex (tc) are arranged around the medulla in concentric layers and are densely packed together. The tubule is surrounded by intertubular horn (it). This tubule is more circular in outline than the wall tubule shown in Figure 2.28. Tubule outline varies characteristically between different regions of the claw.

x 520

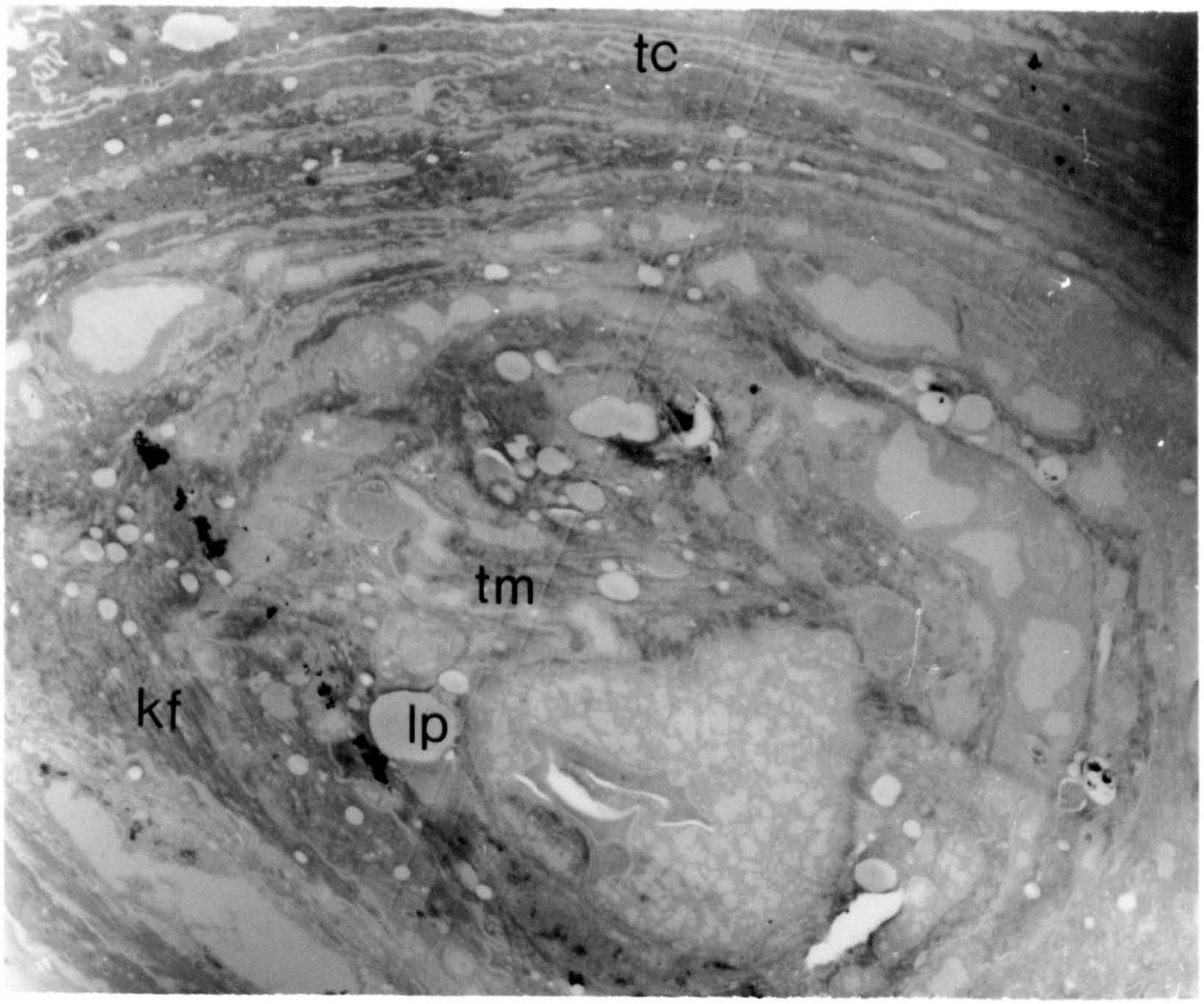
tc
tm
kf
lp

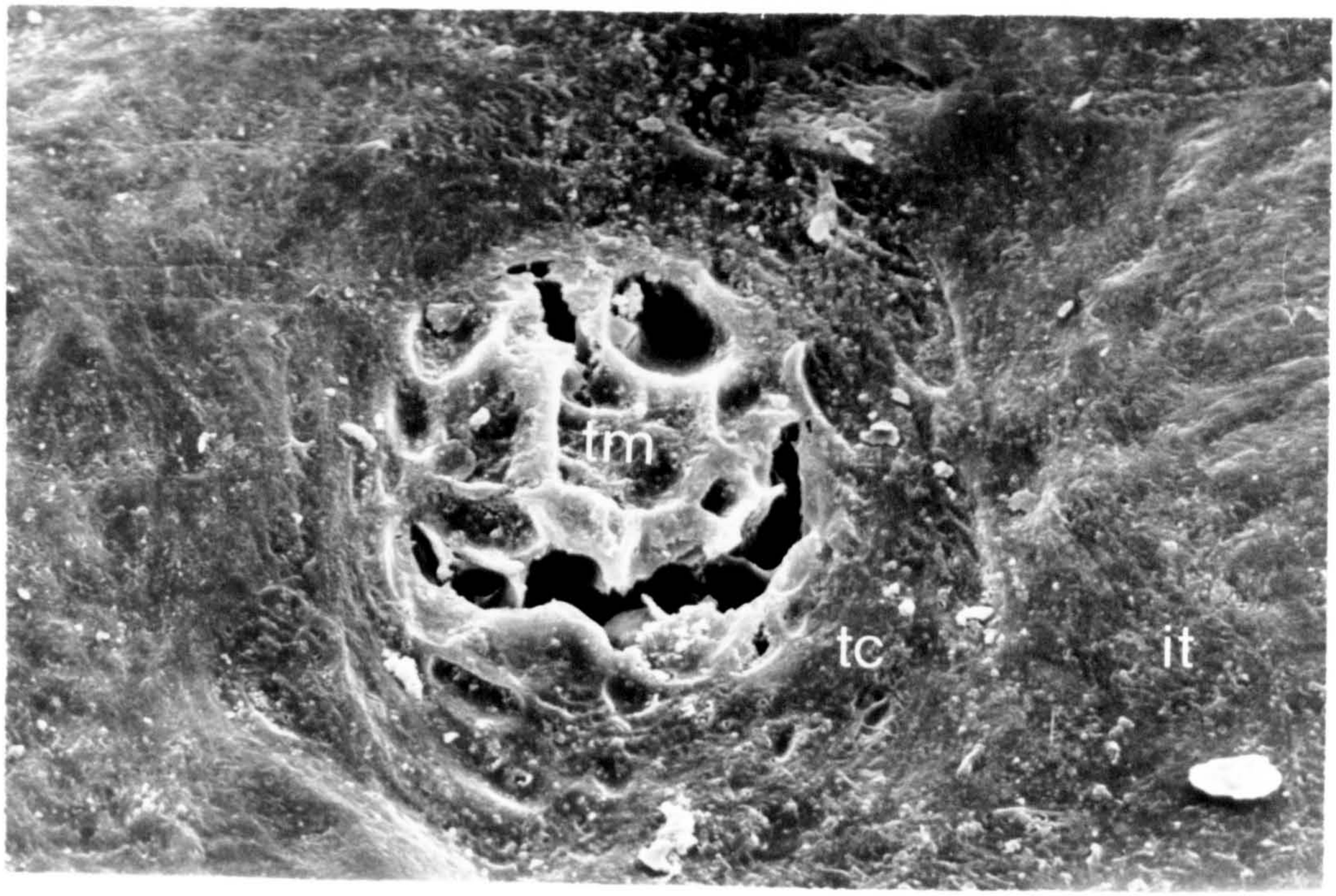
tm
tc
it

Figure 2.30
Low power light micrograph of the coronary horn of the wall in transverse section

At low power the position of the tubules is marked by the densely stained tubule medullae (tm↑).The tubules in the outer zone of the wall (o) are flattened in transverse section, compared with those of the middle zone of the wall (mi), whose medullae are circular in cross-section.

x 23

Stain : Phloxine-Tartrazine

Figure 2.31
High power light micrograph of the transition between the outer and middle zones of the wall

The difference in shape of tubules is more clearly visible at higher power. The medullae (tm↑) of tubules of the outer zone (ot) are oval or slightly eliptical in outline while those of the middle zone (mt) are almost circular. The dotted lines outline tubule cortices, which are not distinguishable from the intertubular horn (it) by this staining proceedure.

x 144

Stain : Phloxine-Tartrazine

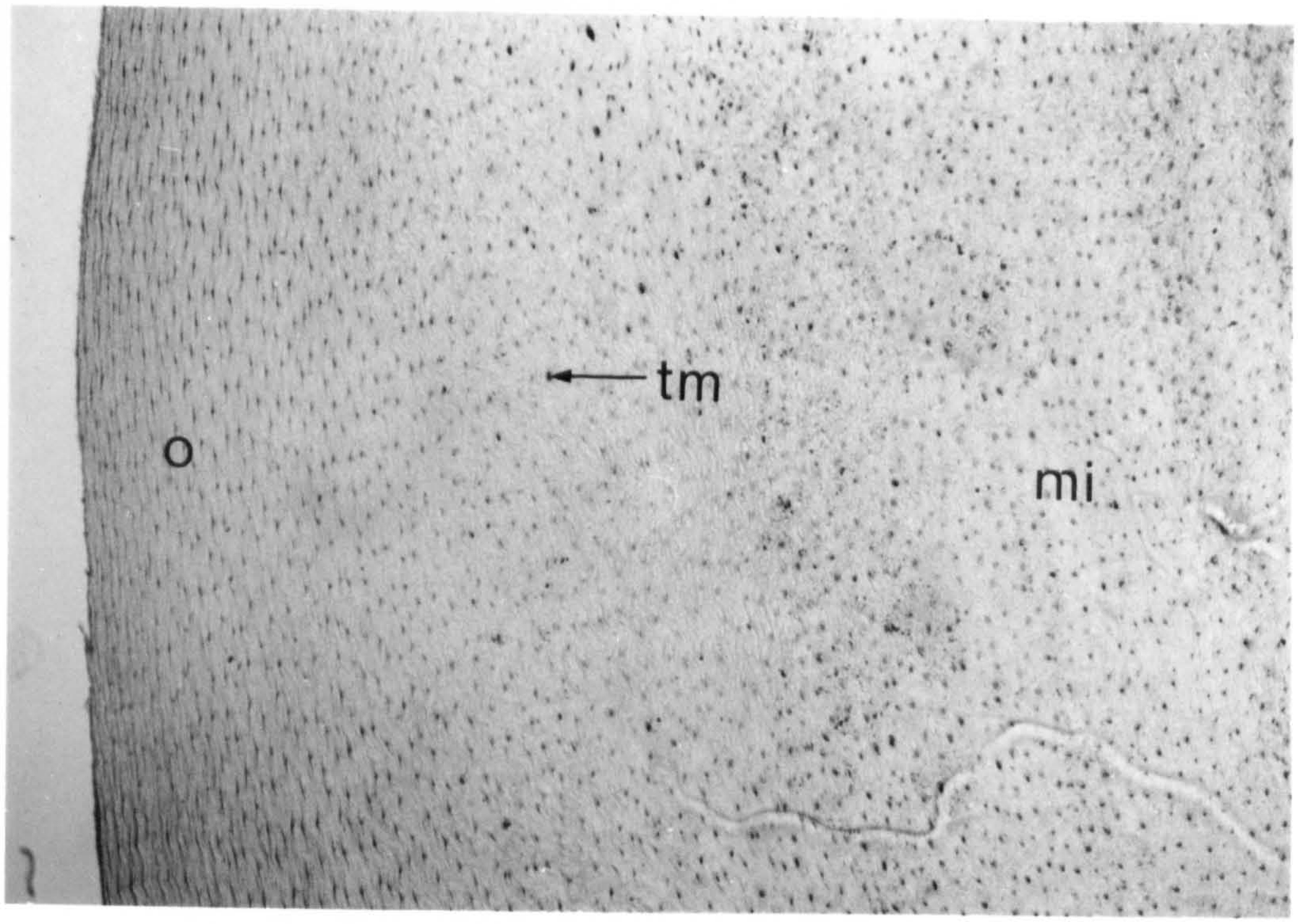
tm
o
mi

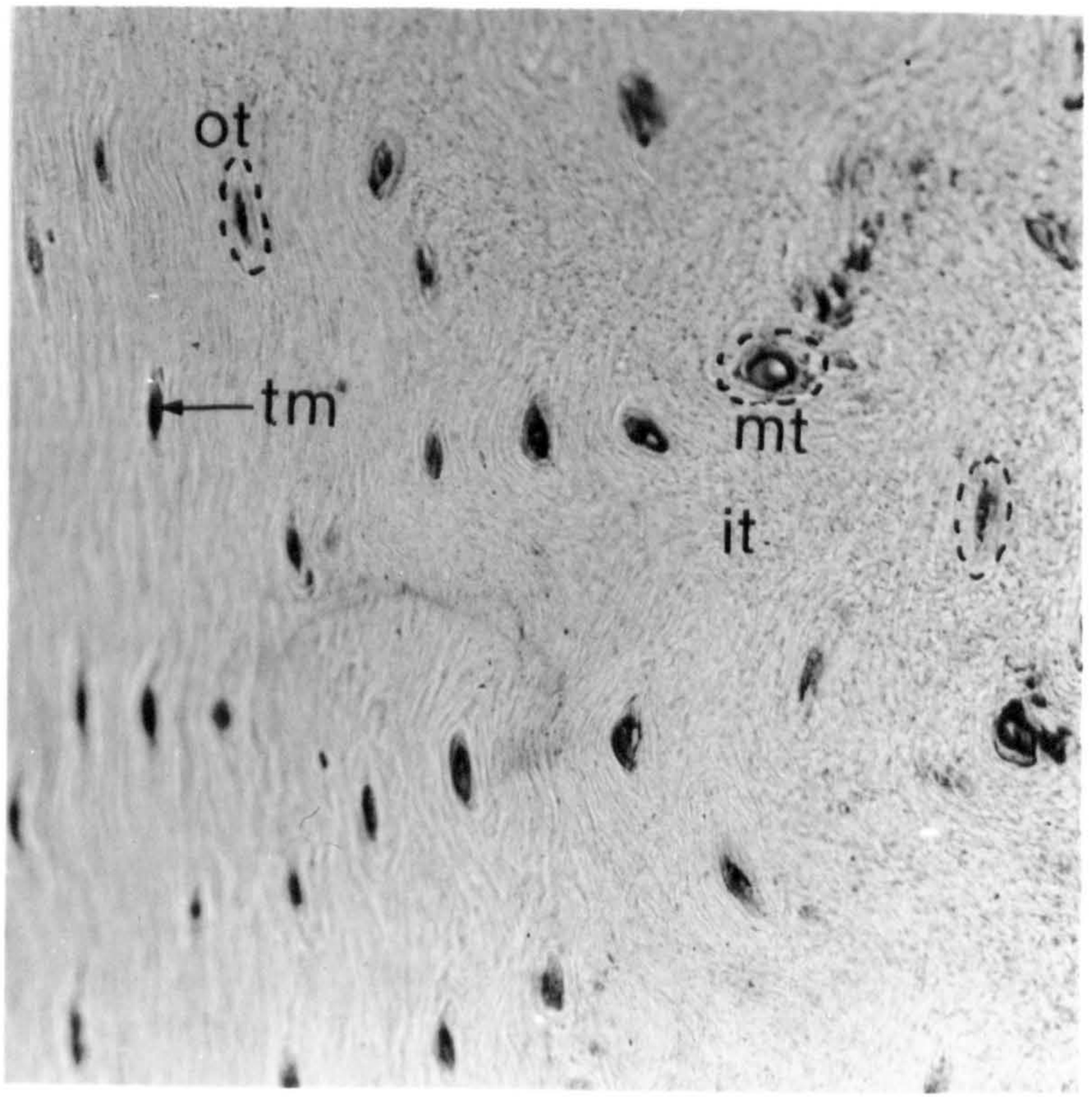
ot
tm
mt
it

Figure 2.32
Schematic diagram showing longitudinal and transverse sections through the dorsal wall of the bovine claw

ha	Hair
e	Skin epidermis
d	Dermis of skin
pc	Perioplic corium
ph	Perioplic horn
cc	Coronary corium
ch	Coronary horn
lc	Laminar corium
lh	Laminar horn
el	Epidermal lamina
dl	Dermal lamina
si	*Stratum internum* of the wall
sc	Sole corium
sp	Sole papilla
sh	Sole horn
ht	Horn tubule
wl	White line

Section A	T.S. skin
Section B	L.S. perioplic and coronary regions
Section C	T.S. perioplic and coronary regions
Section D	L.S. coronary region
Section E	L.S. laminar region, sectioned through laminar horn leaflet
Section F	T.S. laminar region
Section G	L.S. distal laminar region, sole and white line, sectioned through a dermal lamina

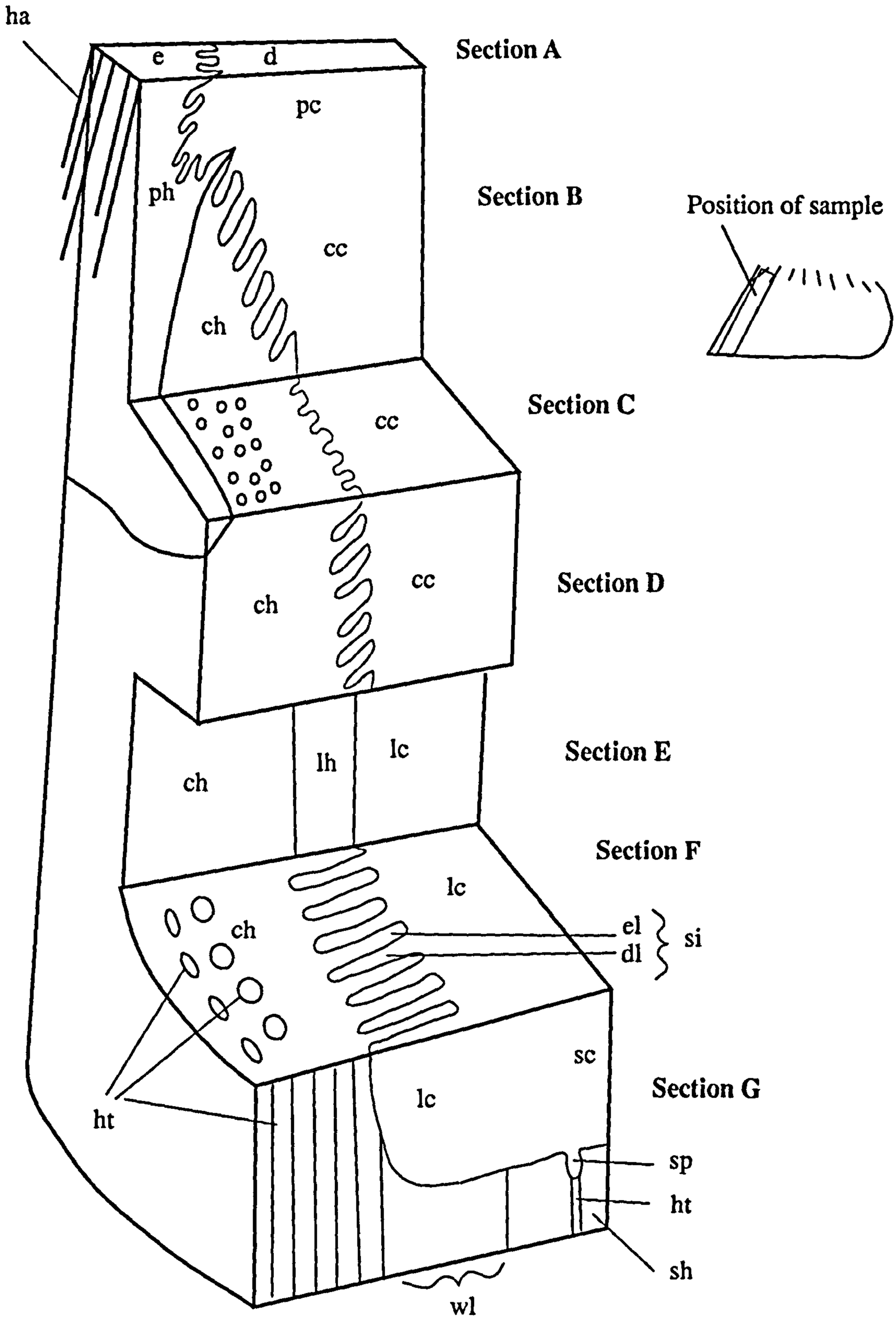
ha
e
d
pc
ph
cc
ch
Section A
Section B
Position of sample
Section C
cc
Section D
ch
cc
Section E
ch
lh
lc
Section F
lc
ch
el
dl
si
sc
lc
Section G
ht
sp
ht
sh
wl

Figure 2.33
Light micrograph of a longitudinal section through the perioplic and coronary regions of the dorsal wall of the bovine claw
(corresponding to Section B in Figure 2.32)

The surfaces of both perioplic (pc) and coronary coria (cc) bear papillae (dp). Those of the perioplic corium are much longer than those of the coronary corium. There is a distinct fold in the corium at the junction between perioplic and coronary coria (↑). The maturation zone (mz) is much thicker in the perioplic epidermis than in the coronary region. Proximally the perioplic horn (ph) is very thin but it increases in thickness distally where it overlies the coronary horn (ch). The perioplic and coronary horn show different reactions to the histological stain. Densely stained tubule medullae (tm↑) are visible in the perioplic horn.

x 20

Stain : Phloxine-Tartrazine

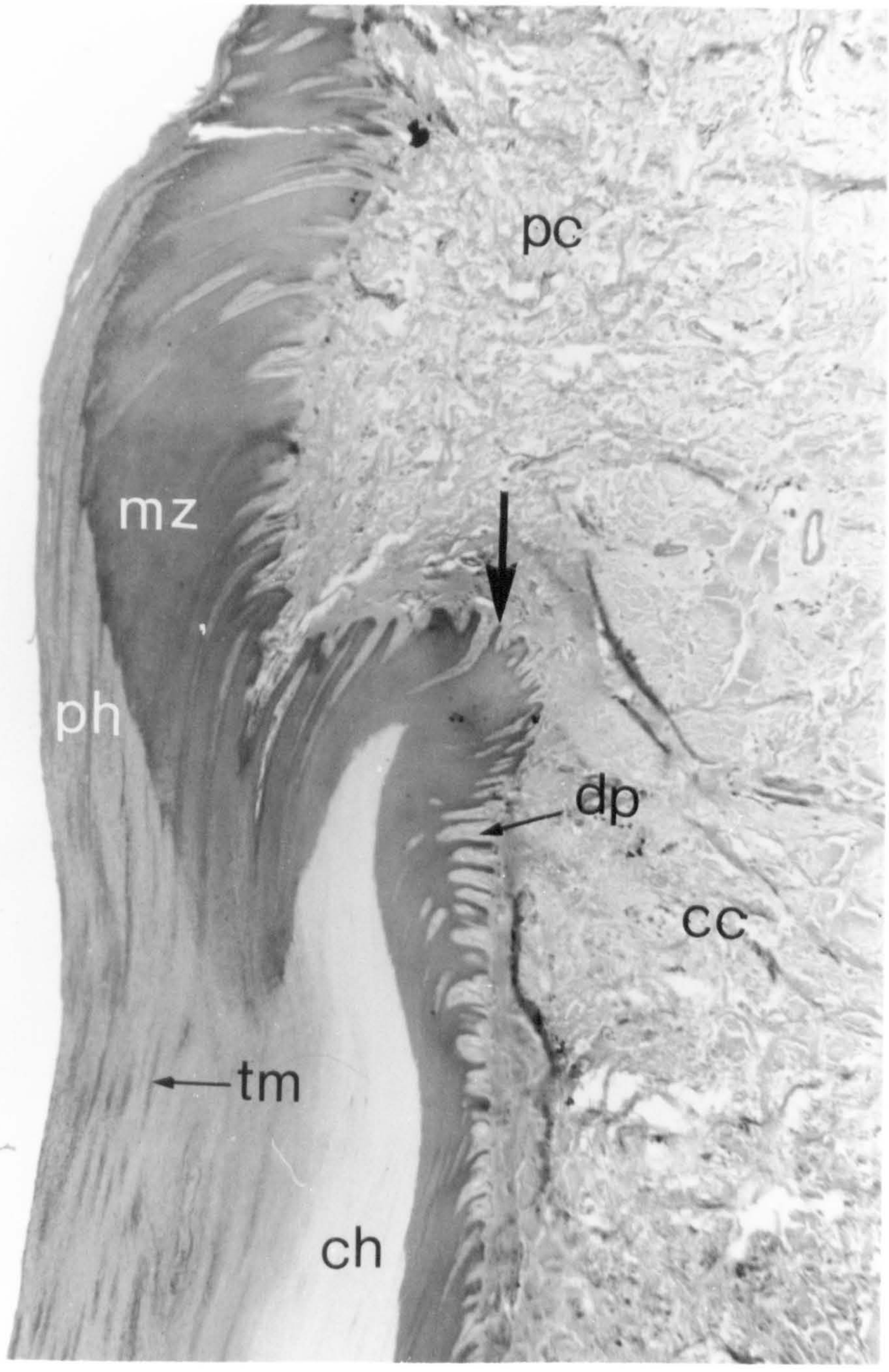
pc
mz
ph
dp
cc
tm
ch

Figure 2.34
Diagram of longitudinal (LS) and transverse (TS) sections through the coronary and laminar regions to illustrate the directions of growth and movement of coronary horn and laminar horn.

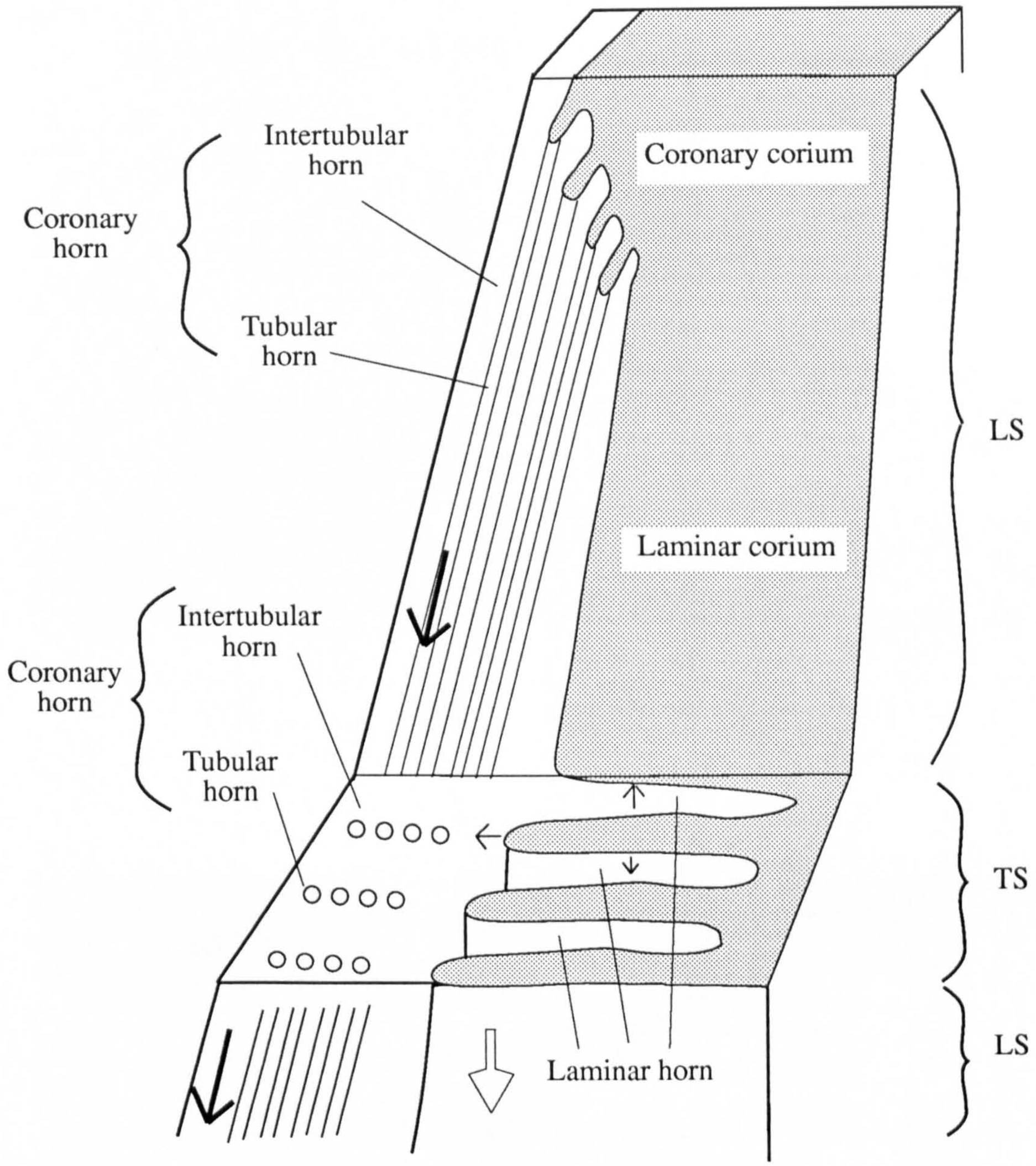

← Direction of growth of laminar horn in the horizontal plane

↓ Direction of growth of coronary horn in the vertical plane

⇩ Direction of movement of laminar horn in the vertical plane

Figure 2.35
Scanning electron micrograph of a longitudinal section through the proximal region of the heel bulb of the bovine claw

The junction between the hairy skin (sk) and the horn producing epidermis is visible (↑). The digital torus (dt) underlies the bulb corium (bc). The surface of the bulb corium bears papillae (dp ↑). Tubules (t) are visible in longitudinal section in the inner layers of the bulb horn (bh). In the outer layers of bulb horn (o) structure is lost and the surface horn is flaking away.

x 15

Figure 2.36
Scanning electron micrograph of a transverse section through the bulb of the bovine claw

The digital torus (dt) is composed of adipose tissue (at) and a network of collagen fibres (cf ↑). Dermal papillae (dp↑) are visible on the surface of the bulb corium (bc). The maturation zone (mz) can be distinguished from the bulb horn (bh).

x 20

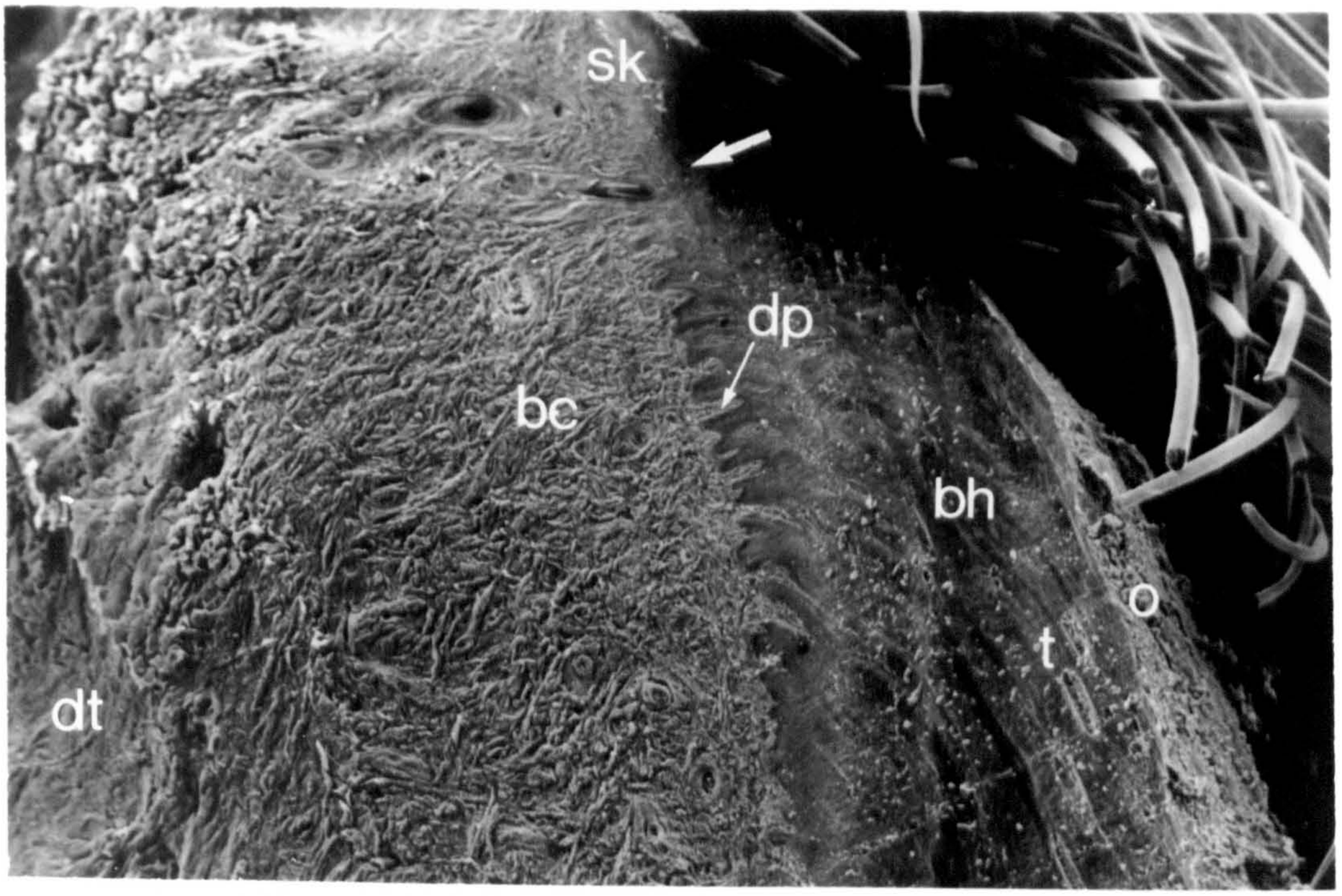
sk
dp
bc
bh
o
t
dt

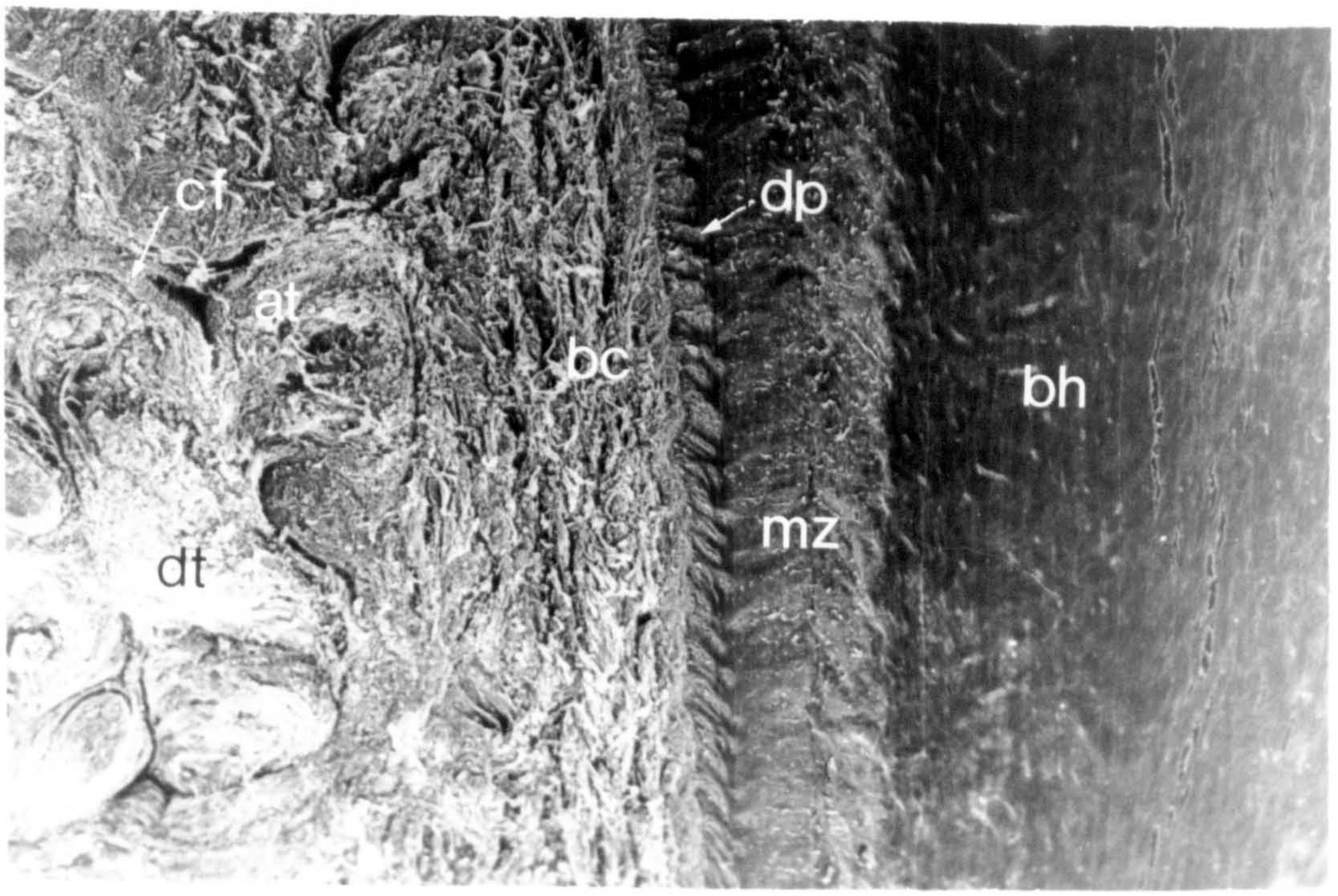
cf
dp
at
bc
bh
mz
dt

FIGURES

CHAPTER 3

Figure 3.1
Diagram to illustrate the typical site of sole ulceration on the plantar surface of the outer hind claws

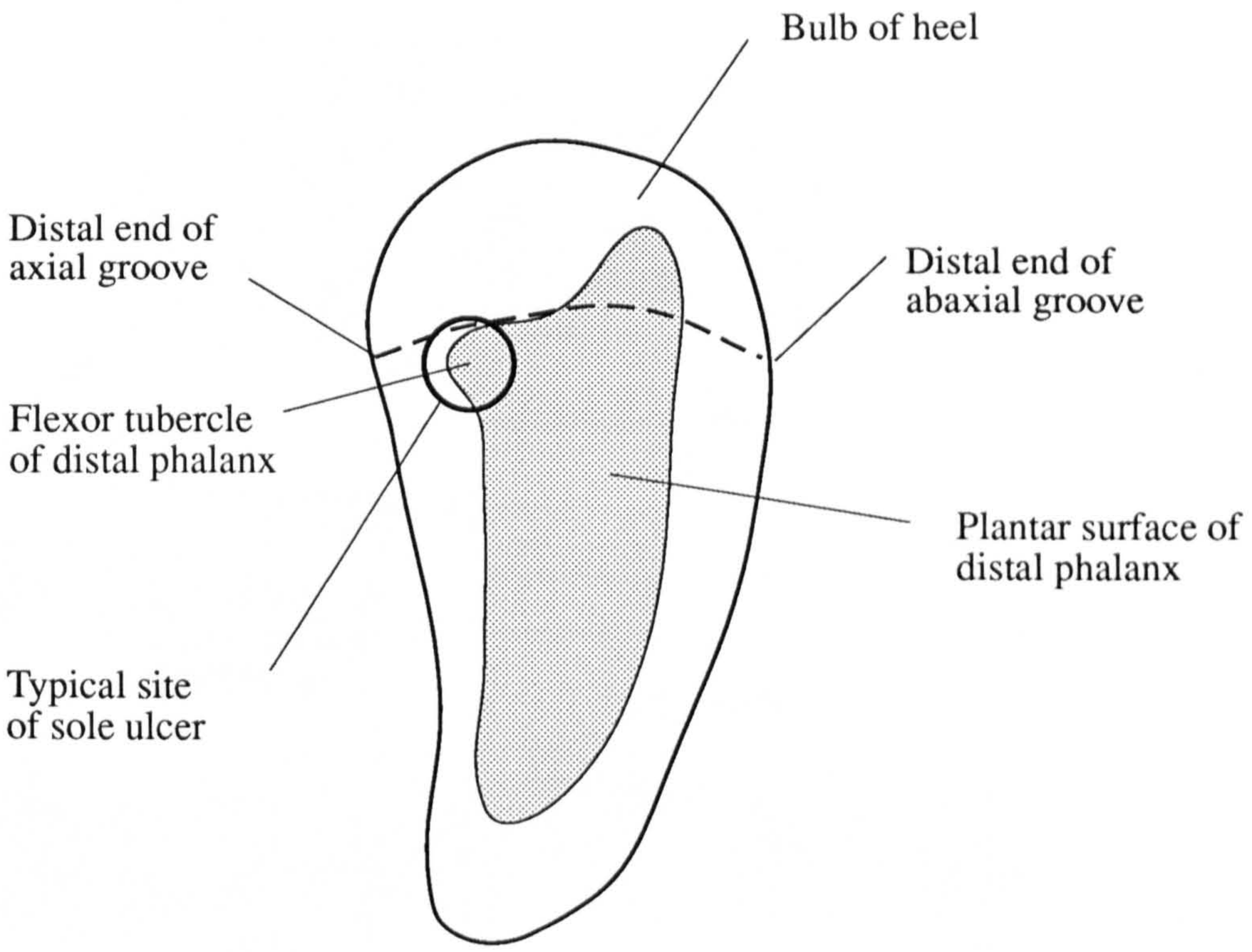
Bulb of heel
Distal end of axial groove
Distal end of abaxial groove
Flexor tubercle of distal phalanx
Plantar surface of distal phalanx
Typical site of sole ulcer

Figure 3.2
Diagram to illustrate the proposed relationship between elongation of the toe and ulceration of the sole (after Rusterholz 1920)

Figure 3.3
Anatomical features of the outer hind claw proposed as factors of predilection to sole ulceration

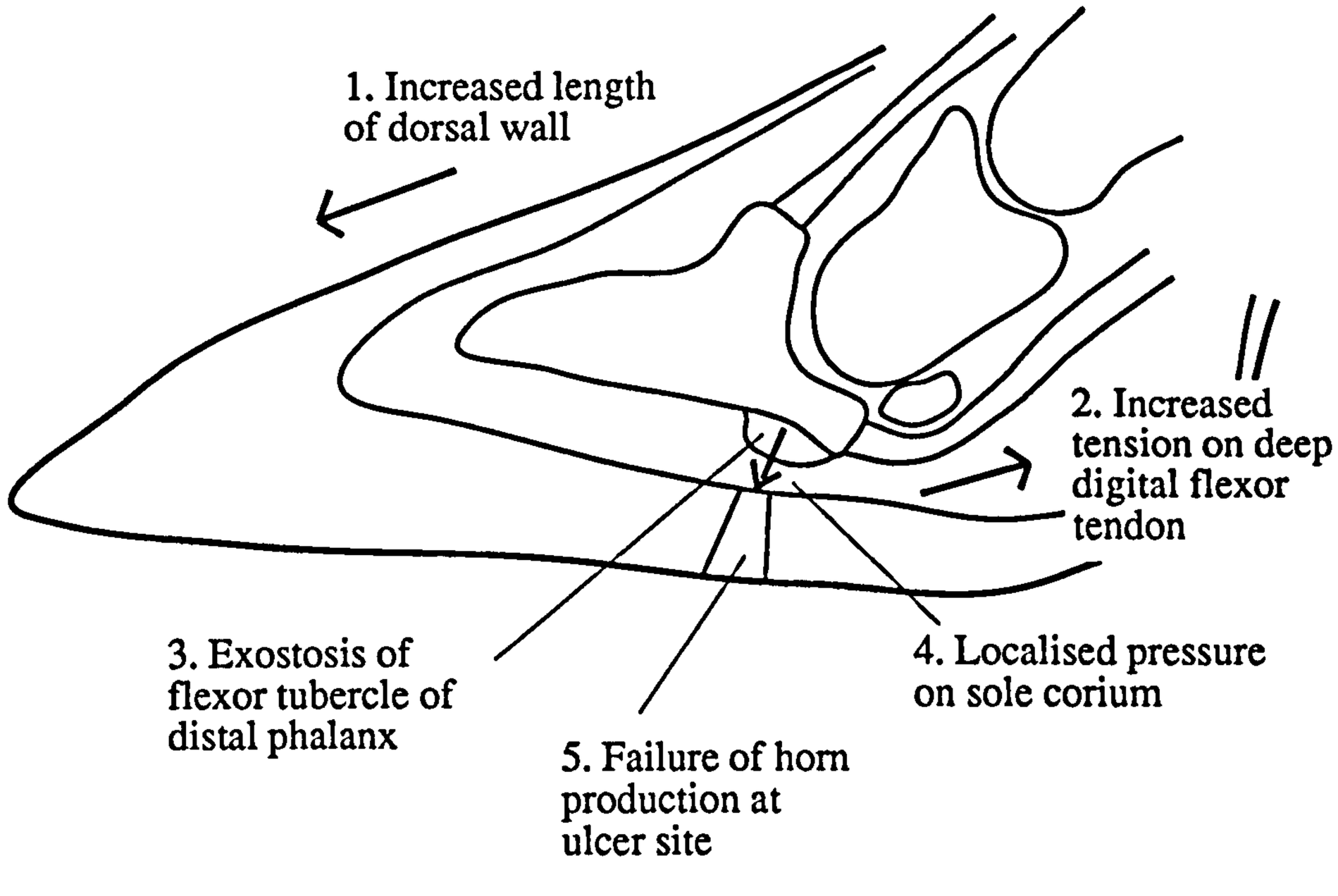

Medial distal phalanx firmly attached to wall (Zantinga 1973)

Lateral distal phalanx more able to tilt and cause pressure on sole corium at the typical site (Zantinga 1973)

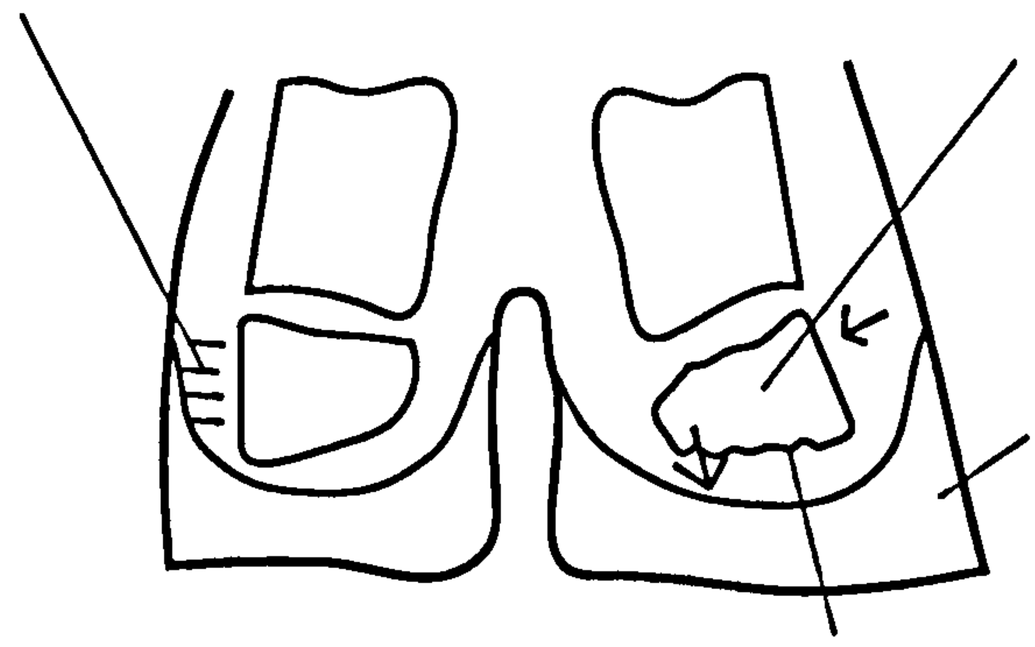

Lateral claw overgrown causing imbalance of weight-bearing between medial and lateral claws (Toussaint-Raven 1973b)

Plantar surface of lateral distal phalanx roughened as a result of variations in weight-bearing (Toussaint-Raven 1985)

FIGURES

CHAPTER 4

Figure 4.1
Zones of the distal surface of the claw, adapted from recommendations of the 6th International Symposium on Diseases of the Ruminant Digit, Liverpool 1990

1. White line at toe
2. Abaxial white line

3s. Abaxial sole/bulb junction

3l. Abaxial white line adjacent to abaxial groove

4. Sole/bulb junction
5. Apex of sole
6. Bulb of heel

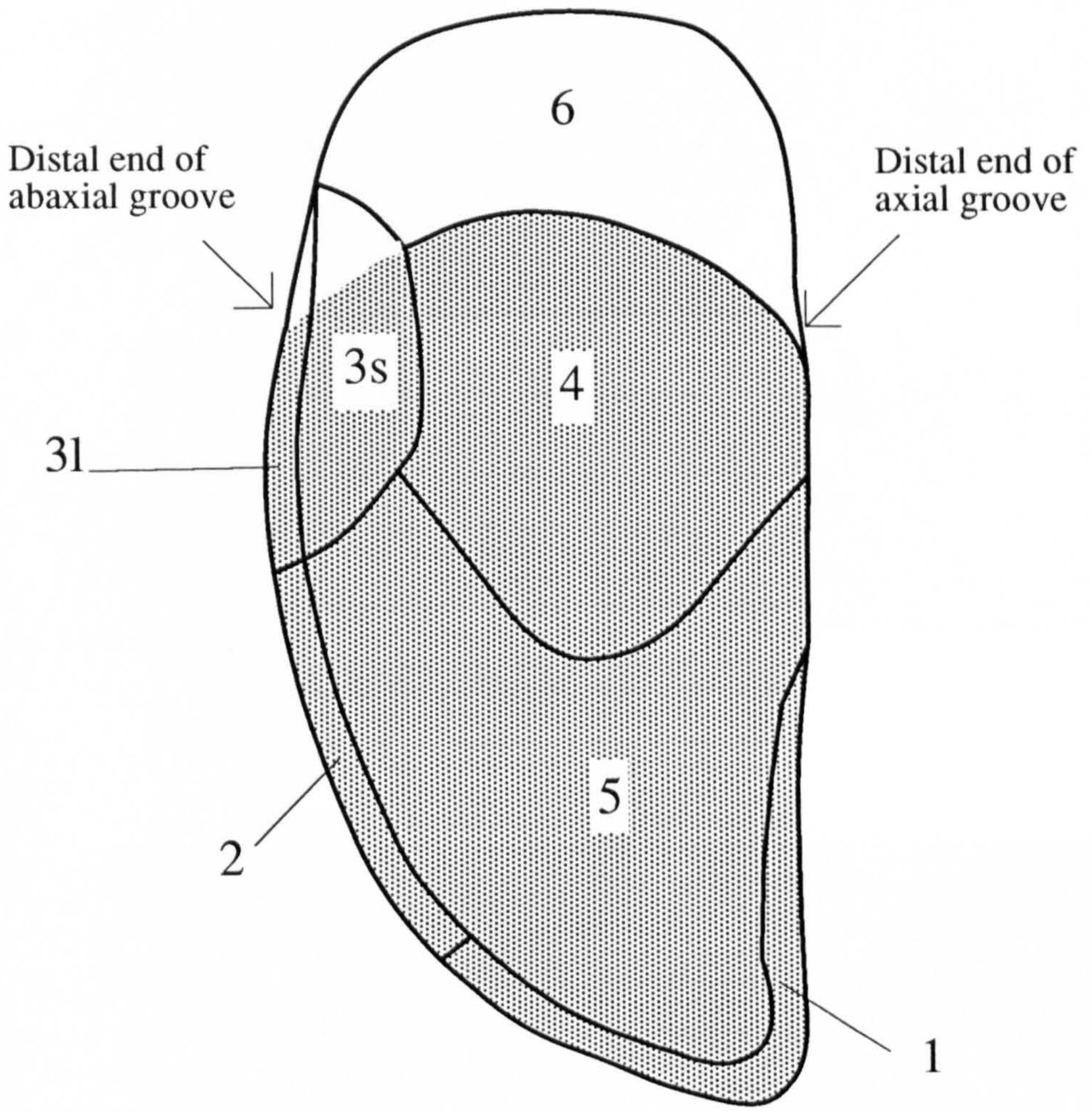
6
Distal end of abaxial groove
Distal end of axial groove
3s
4
3l
5
2
1
Measured area of claw

Figures 4.2 to 4.8 are examples of photographs of the plantar surface of the claw used in analyses, which illustrate lesions of different types and severities. The severities of the lesions are indicated on the outlines opposite the photographs. This type of outline was obtained using the image analysis programme.

Figure 4.2 Cow 30 Right hind 14 weeks post-calving

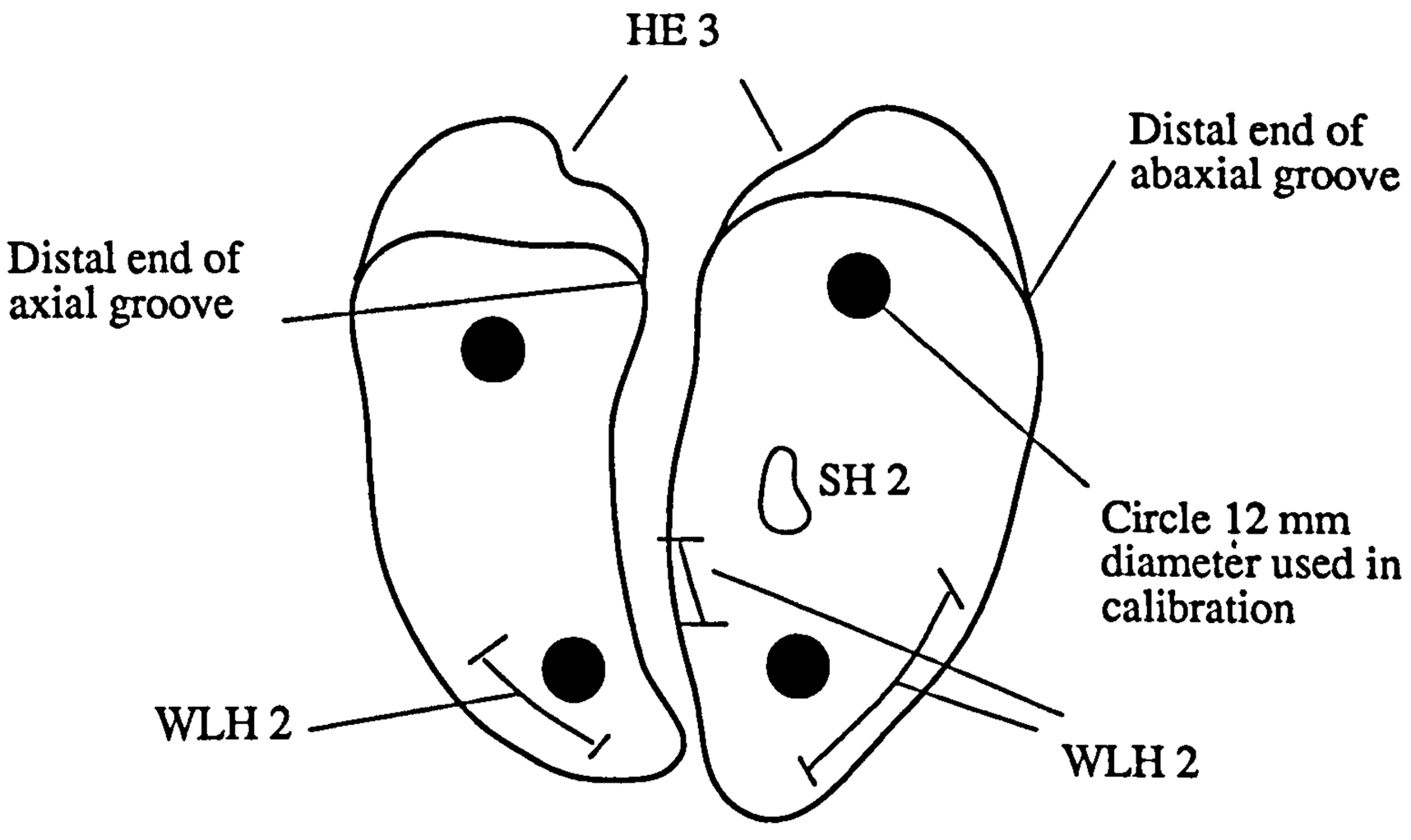

Figure 4.3 Cow 65 Left hind 14 weeks post-calving

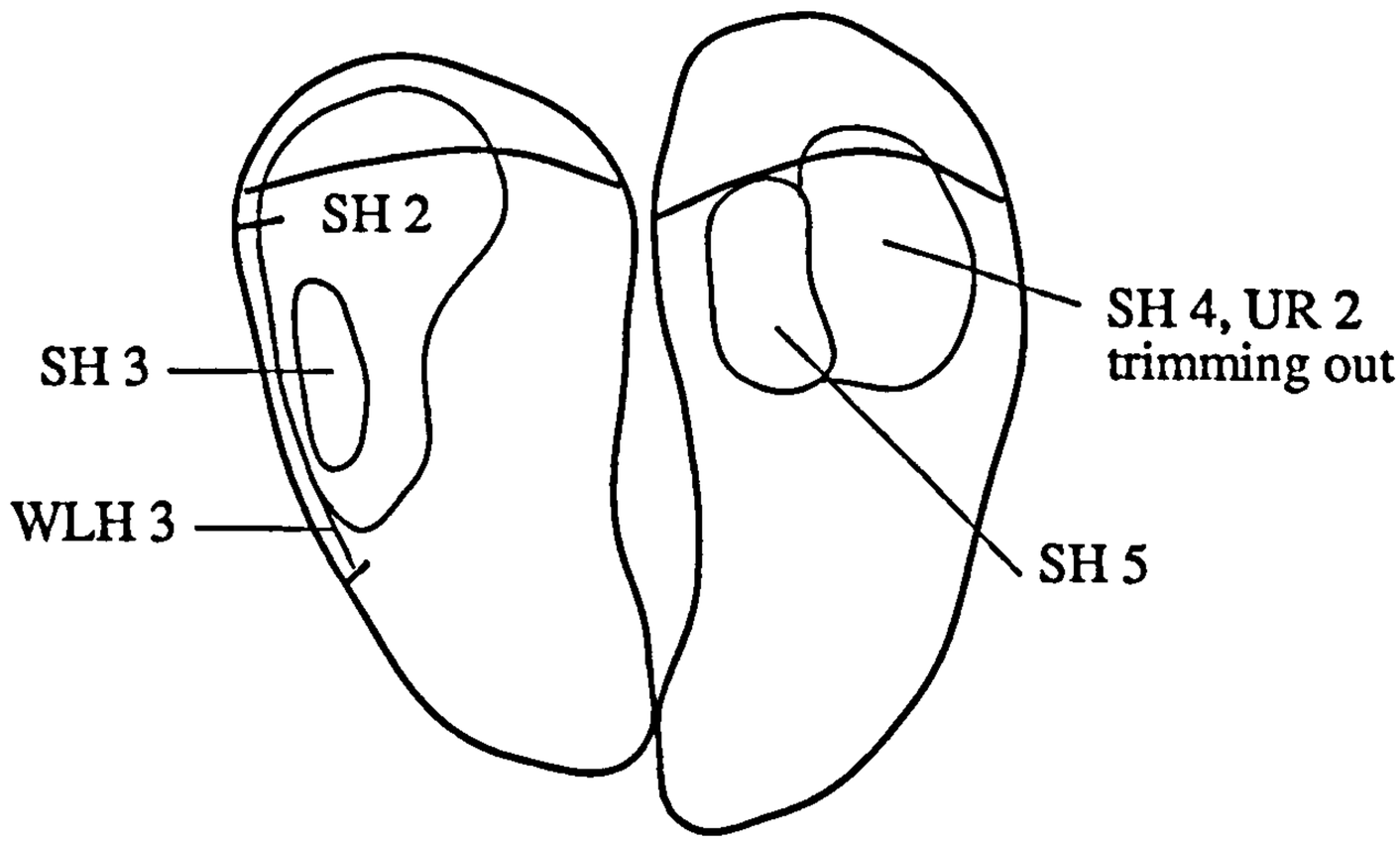

HE - heel erosion; SH - sole haemorrhage; UR - under-running;
WLH - white line haemorrhage.
Numbers indicate severity of lesions (see Table 4.2)

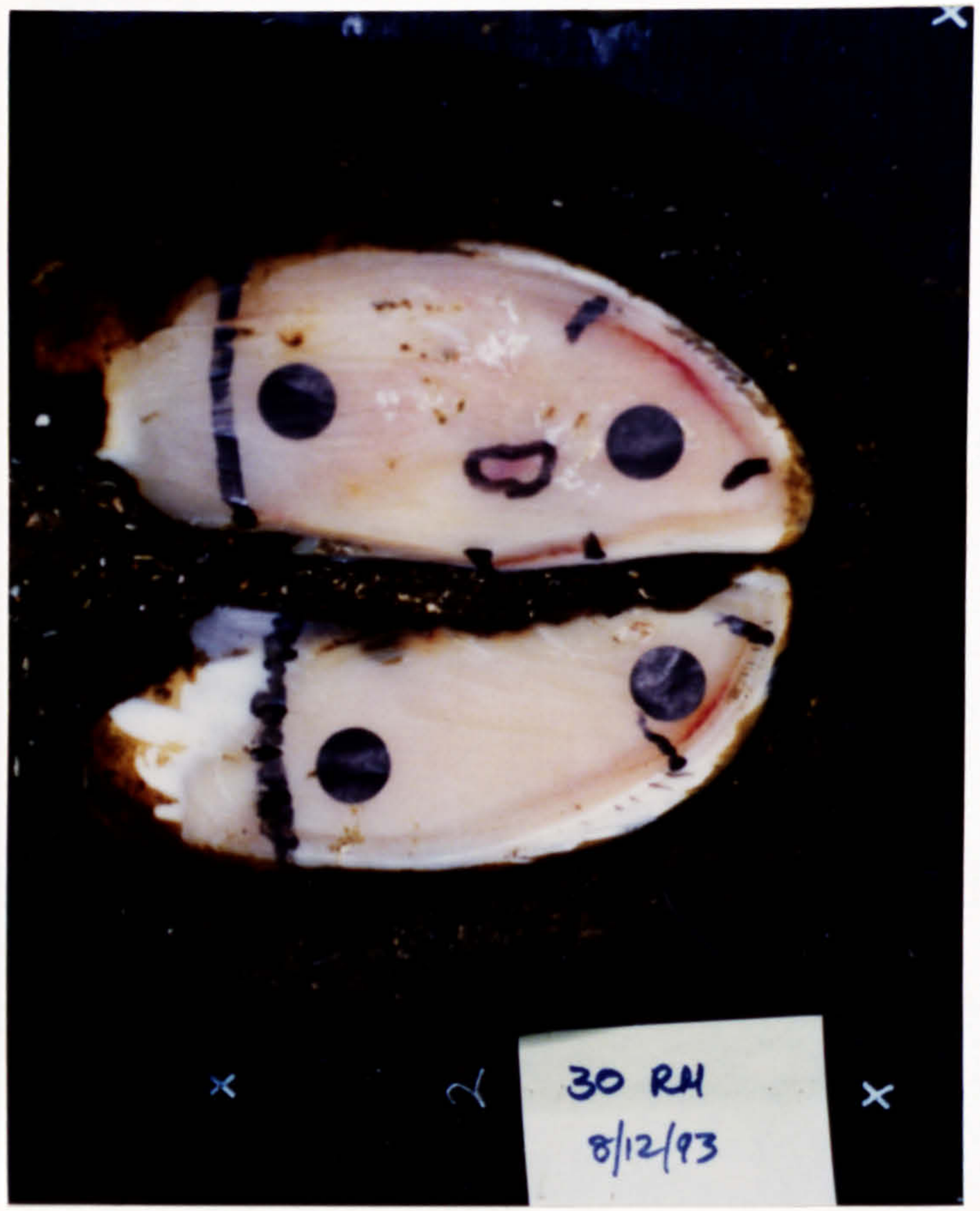
30 RH
8/12/93

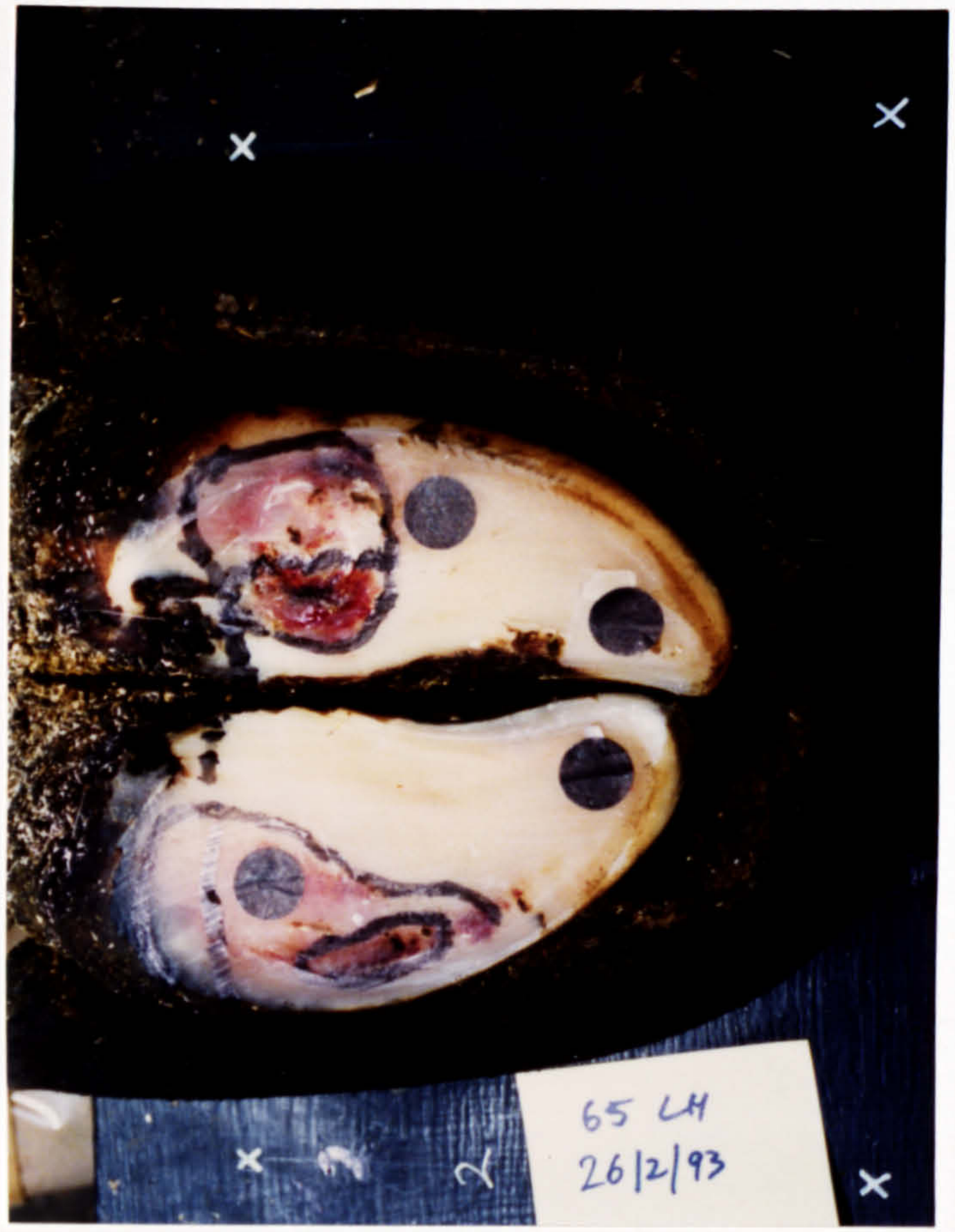
65 LH
26/2/93

Figure 4.4 Cow 32 Left hind 14 weeks post-calving

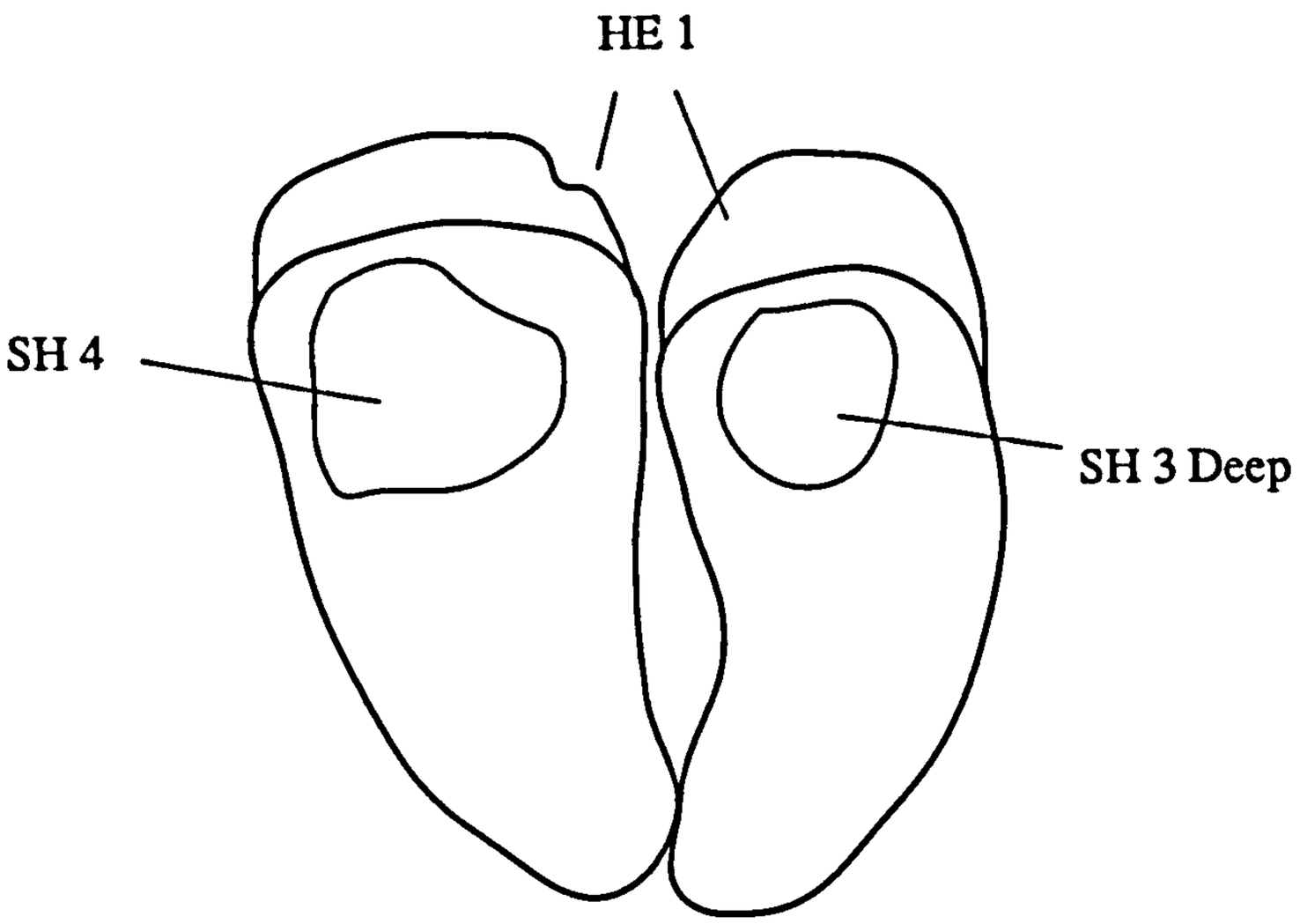

Figure 4.5 Cow 68 Left hind 14 weeks post-calving

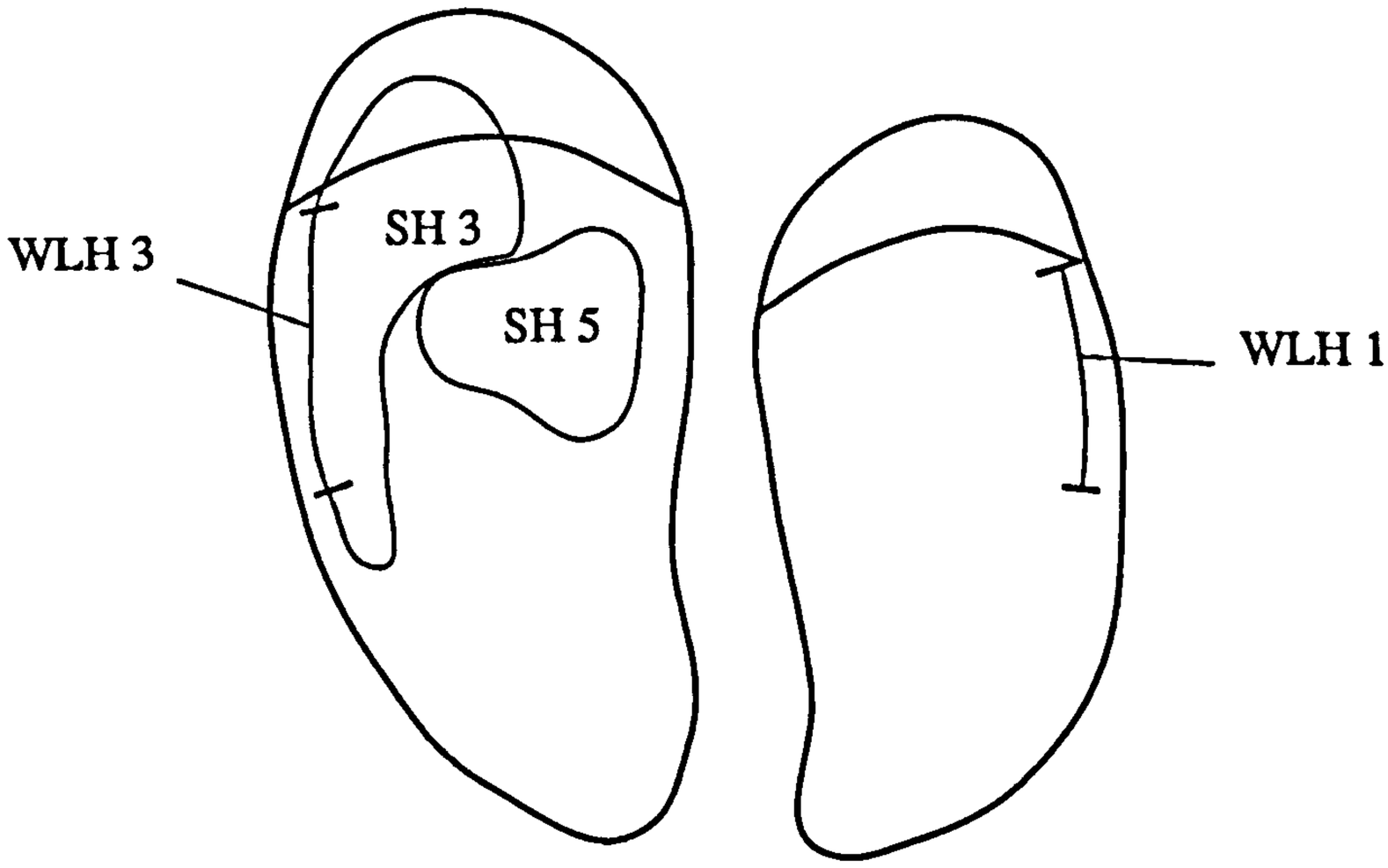

HE - heel erosion; SH - sole haemorrhage;
WLH - white line haemorrhage.
Numbers indicate severity of lesions (see Table 4.2)


2
24/1/93
32 LH

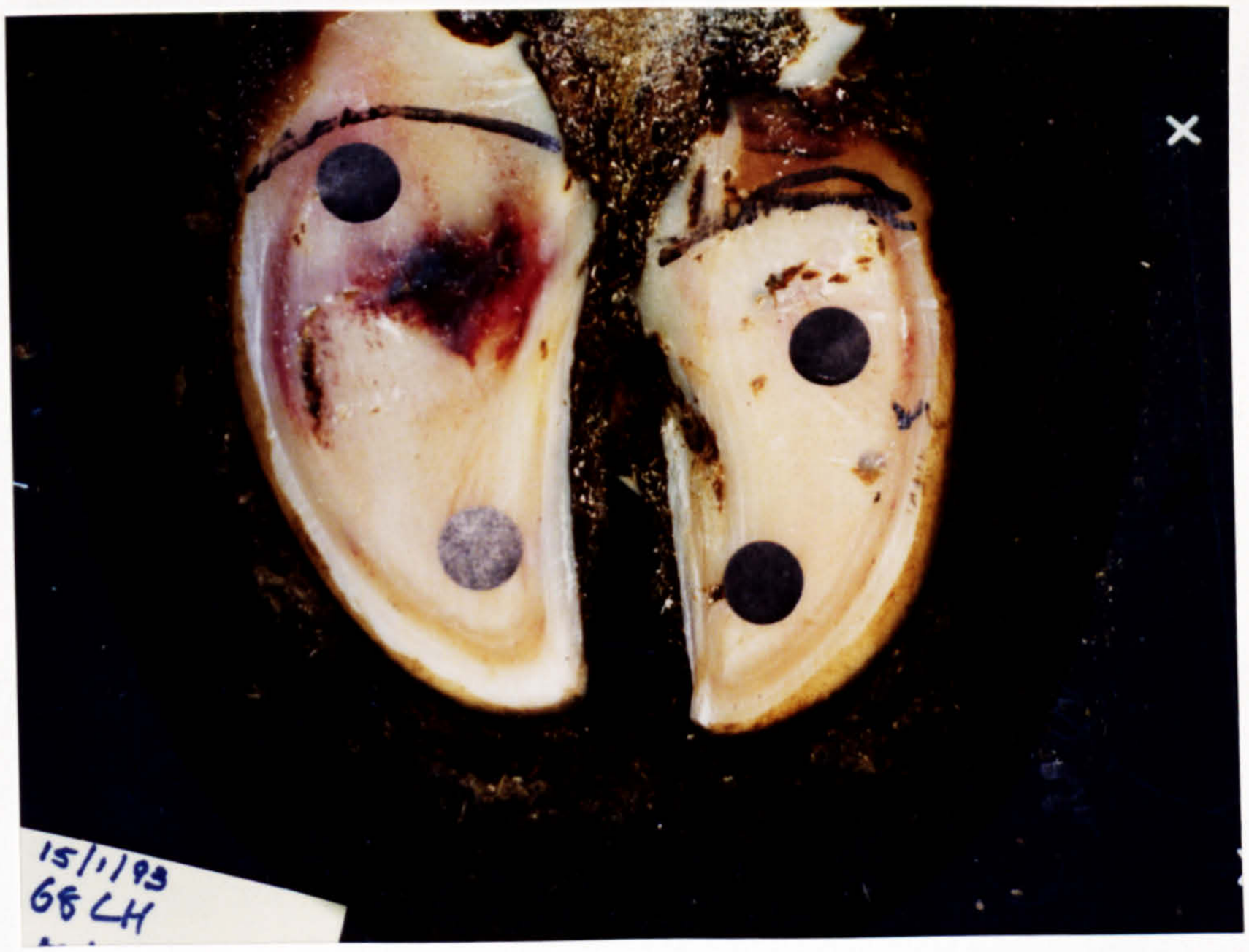
15/1/93
66 LH

Figure 4.6 Cow 53 Left hind 14 weeks post-calving

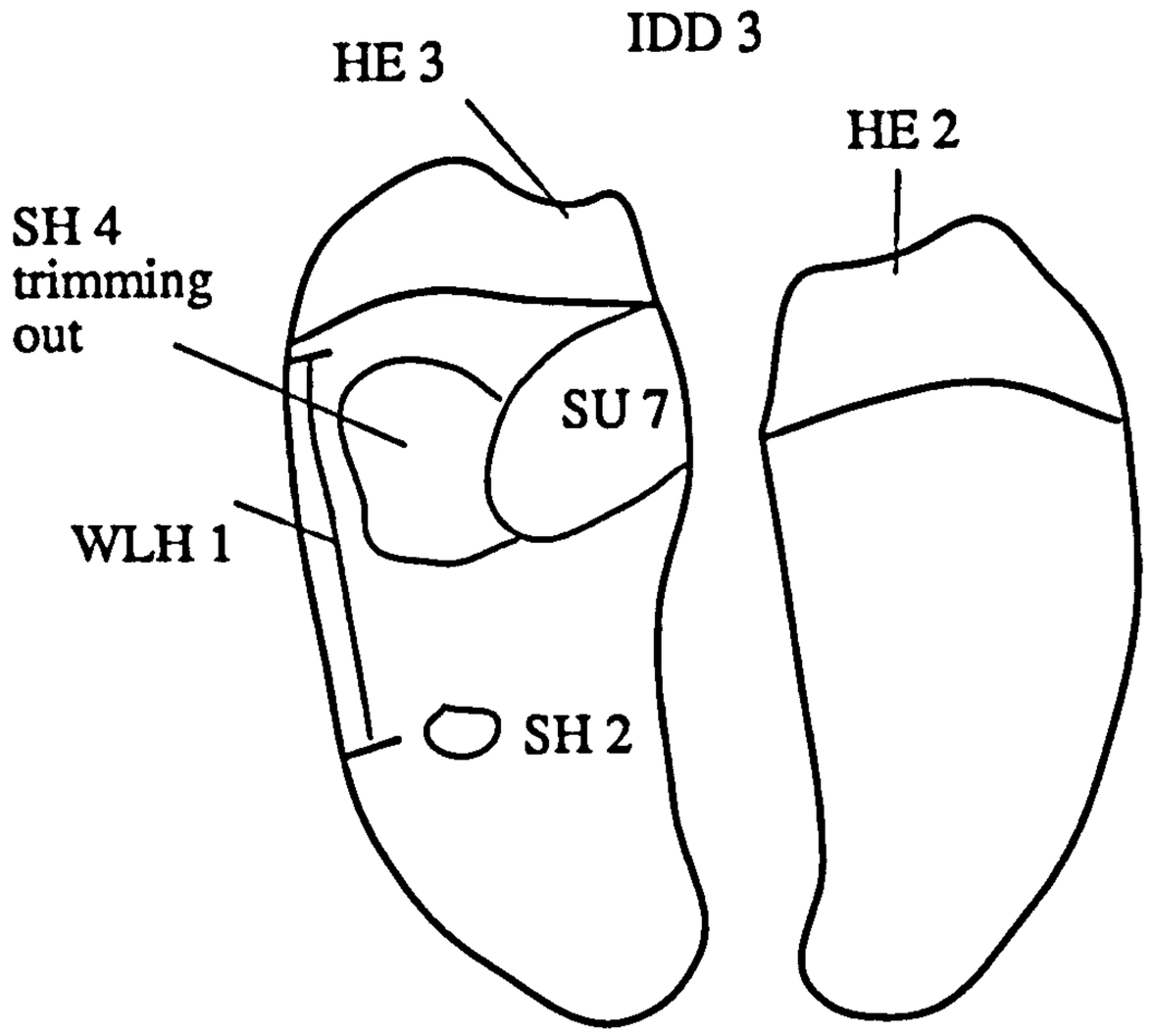

Figure 4.7 Cow 53 Right hind 14 weeks post-calving

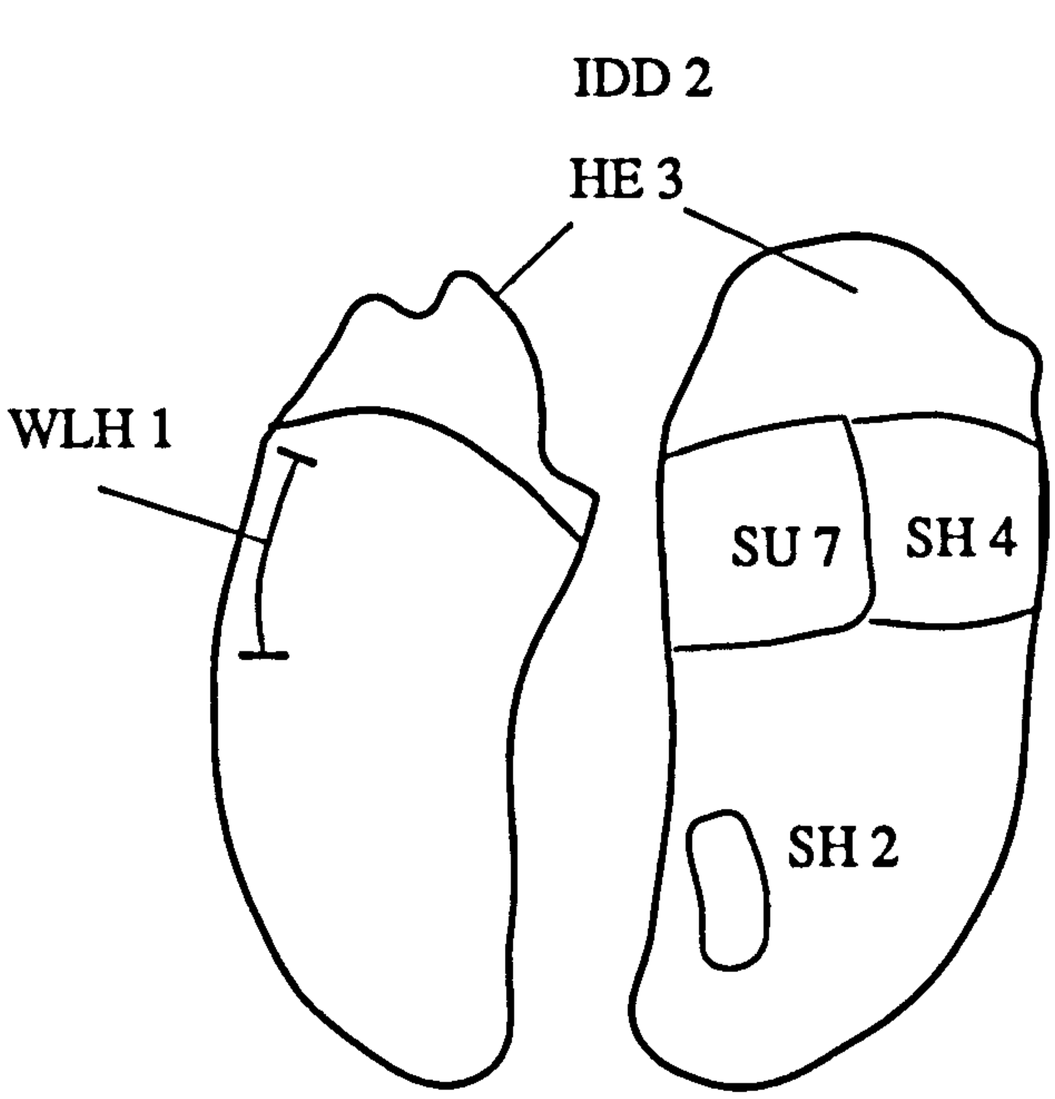

HE - heel erosion; IDD - interdigital dermatitis; SH - sole haemorrhage;
SU - sole ulcer; WLH - white line haemorrhage.
Numbers indicate severity of lesions (see Table 4.2)


53 LH
22/1/93


53 RH
22/1/93

Figure 4.8 Cow 84 right hind 20 weeks post-calving

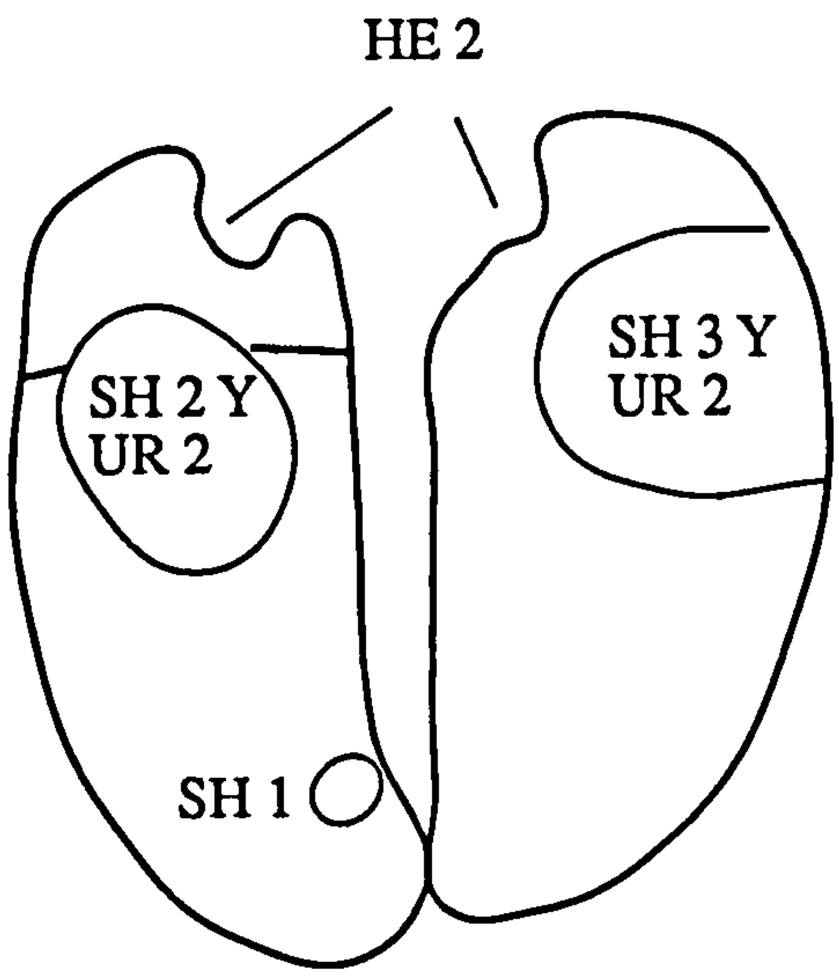

HE - heel erosion; SH - sole haemorrhage; UR - under-running.
Numbers indicate severity of lesions (see Table 4.2)


2
84 RH
25/2/93

Figure 4.9
Number of sole lesions in each claw position in Groups AC1 and AC2 throughout the lactation

Group AC1 : "Clover" herd

Group AC2 : "Nitrogen" herd

Inner front claws

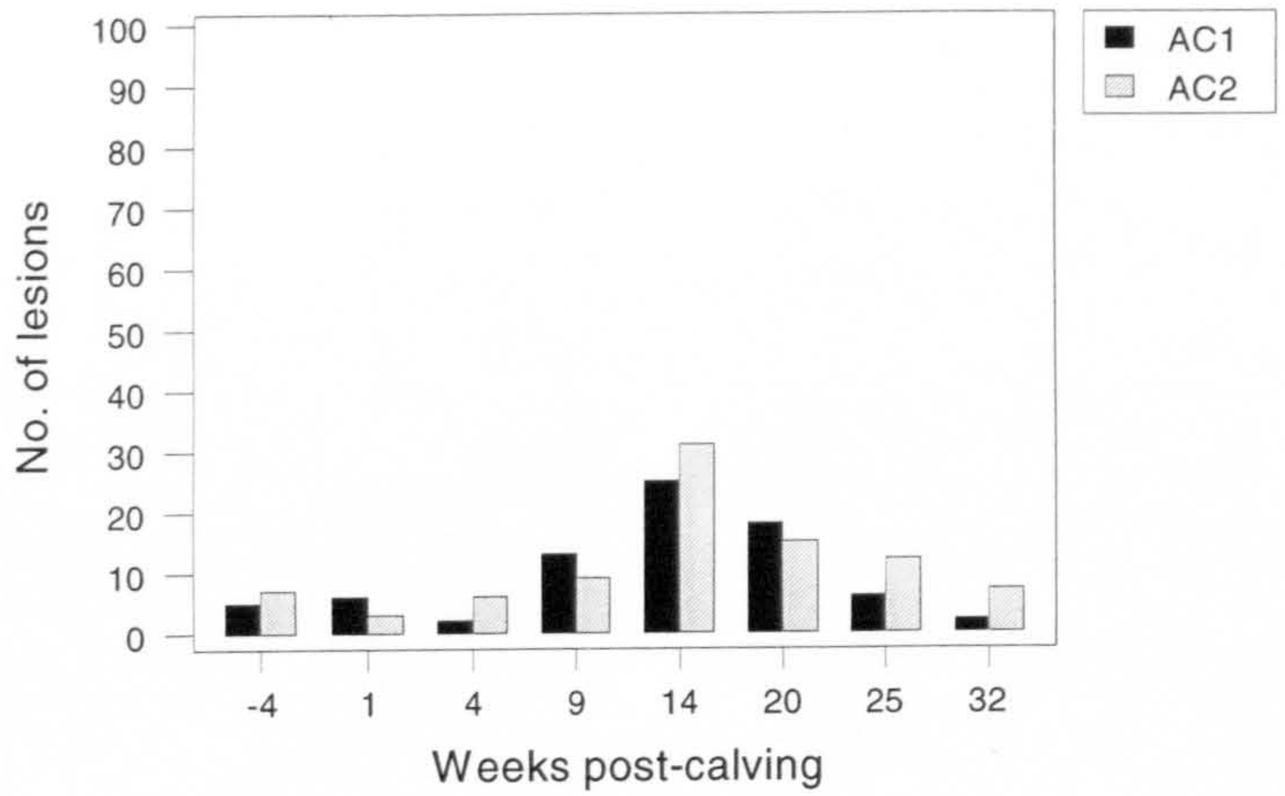

Outer front claws

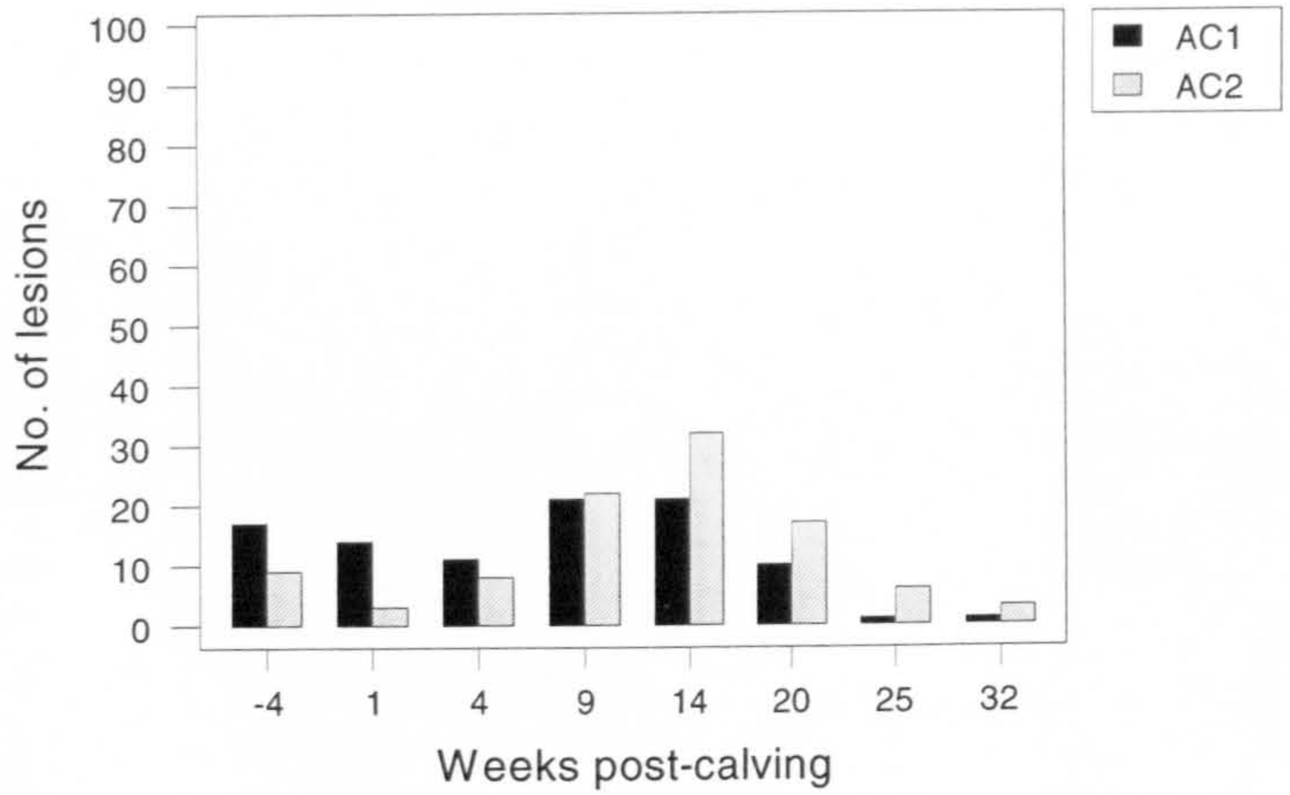

Inner hind claws

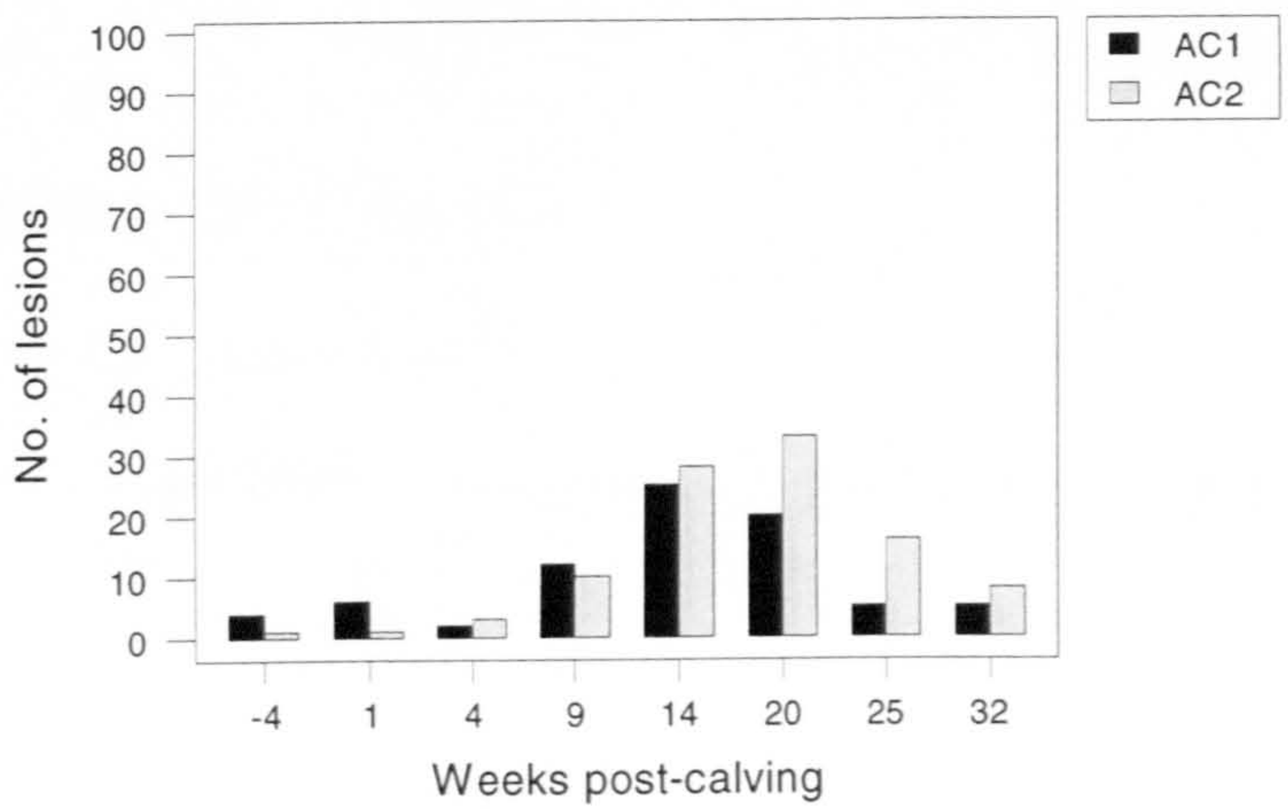

Outer hind claws

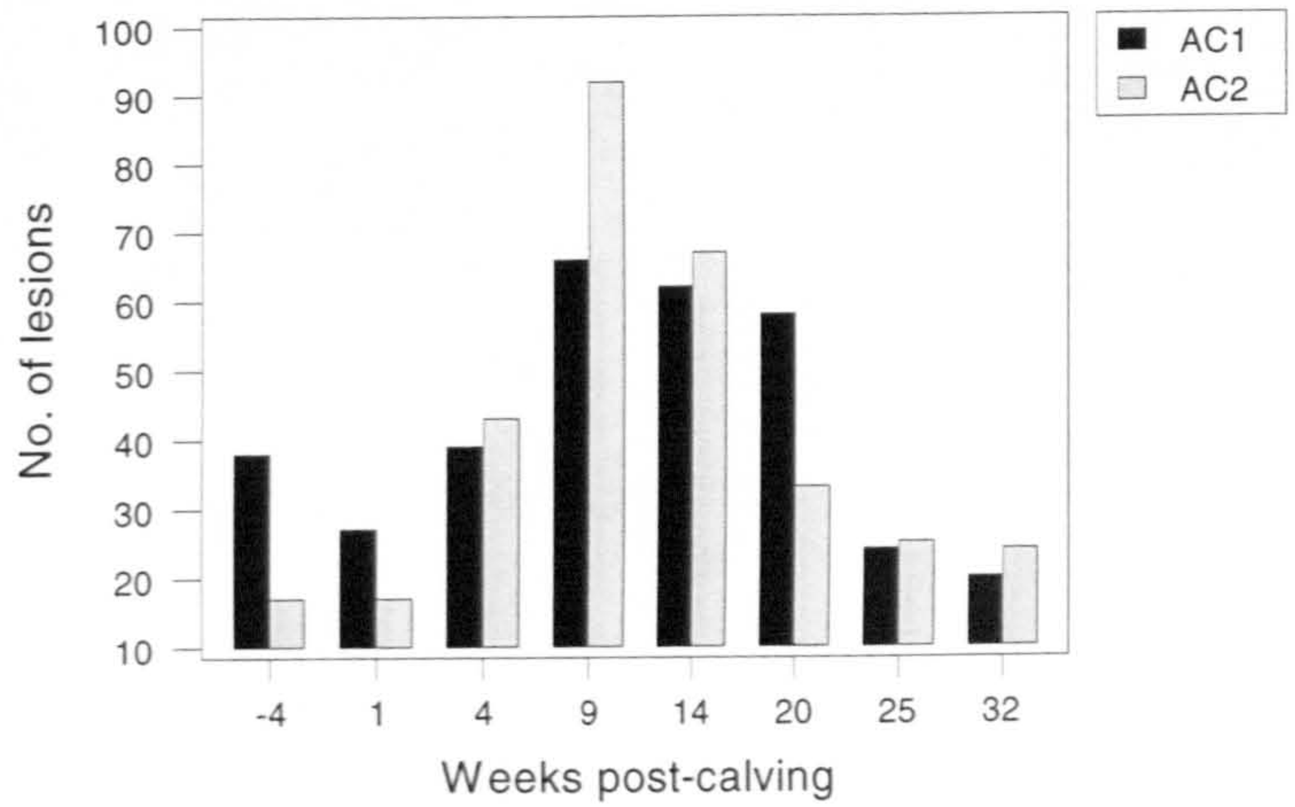

Figure 4.10
Number of white line lesions in each claw position in Groups AC1 and AC2 throughout the lactation

Group AC1 : "Clover" herd

Group AC2 : "Nitrogen" herd

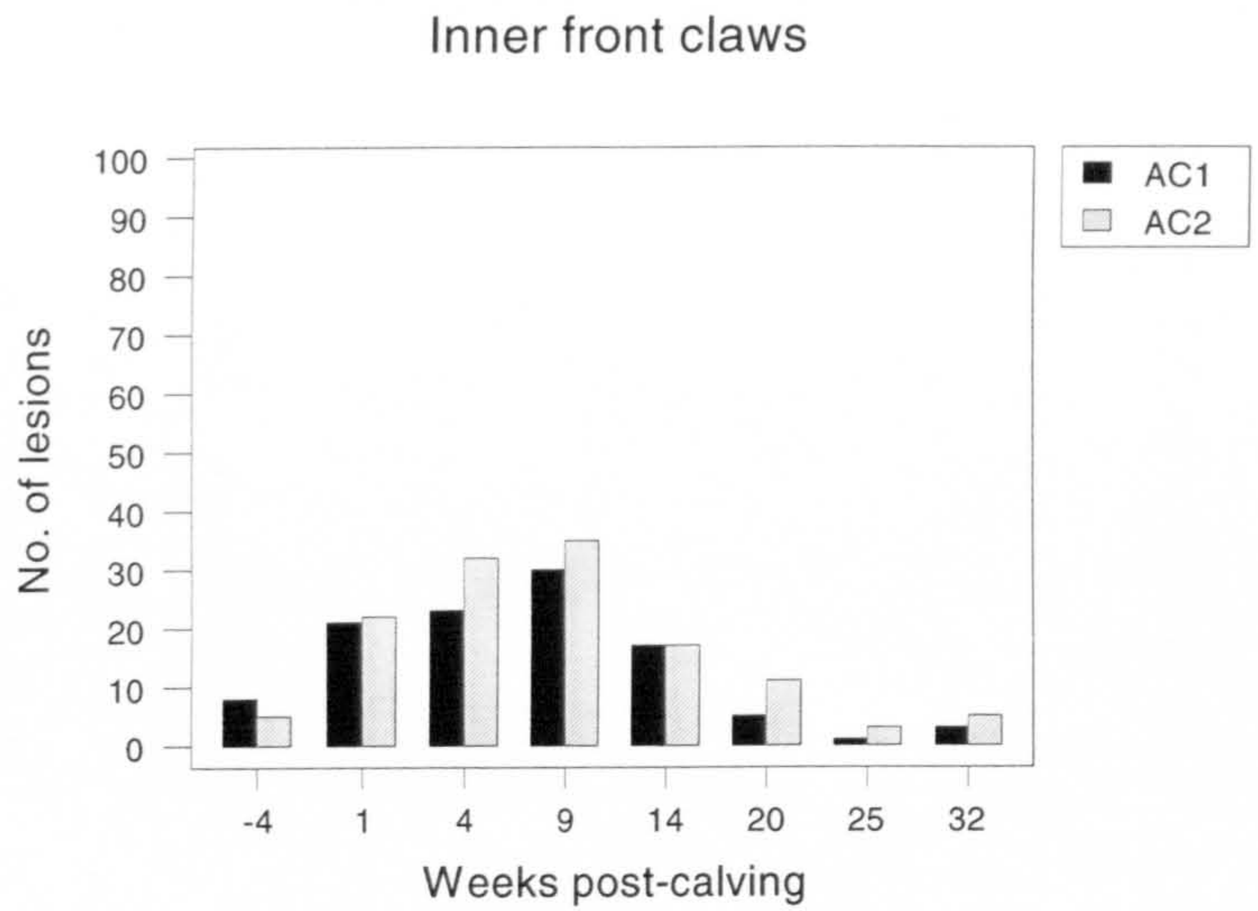
Inner front claws
No. of lesions
100
90
80
70
60
50
40
30
20
10
0
-4
1
4
9
14
20
25
32
Weeks post-calving
AC1
AC2

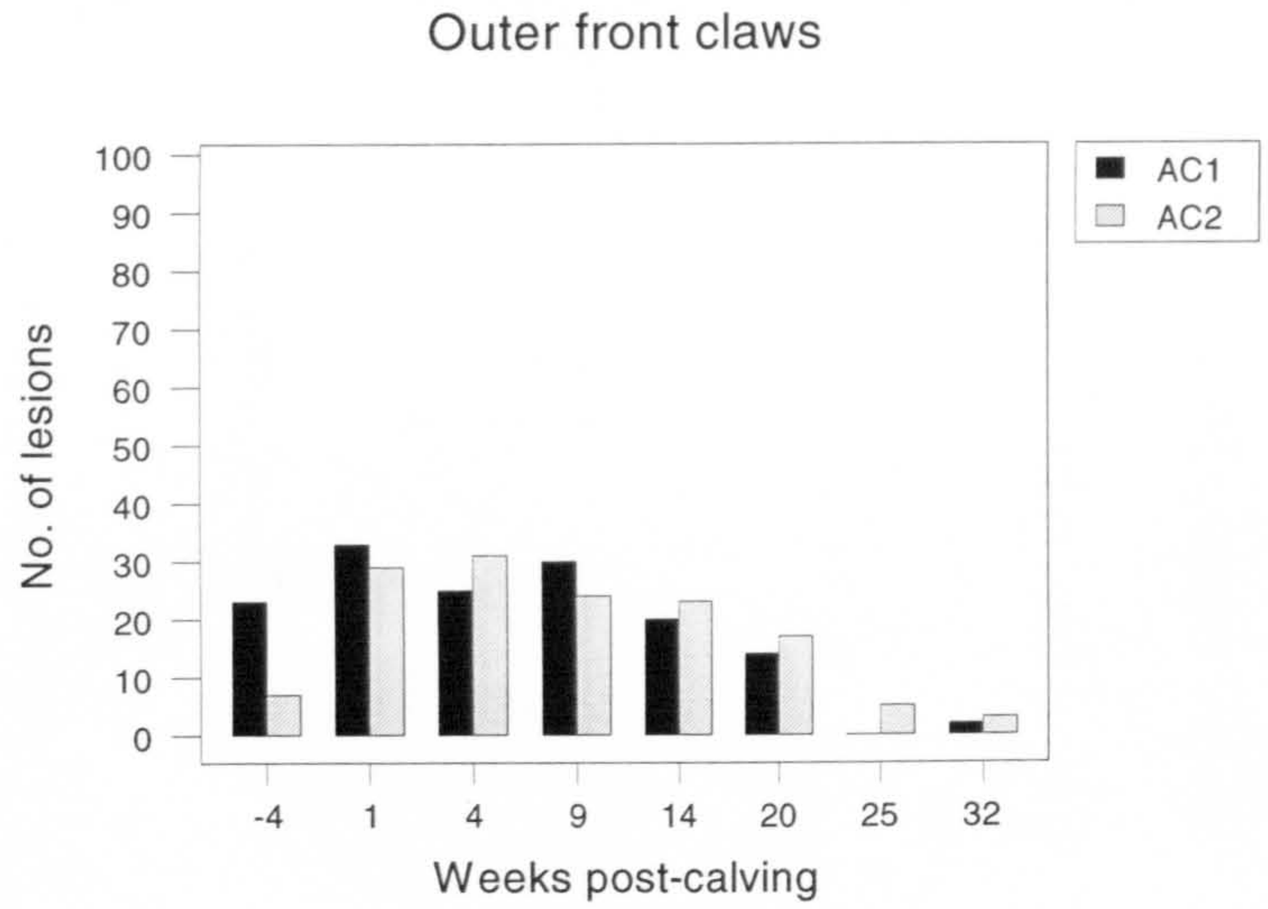
Outer front claws
No. of lesions
100
90
80
70
60
50
40
30
20
10
0
-4
1
4
9
14
20
25
32
Weeks post-calving
AC1
AC2

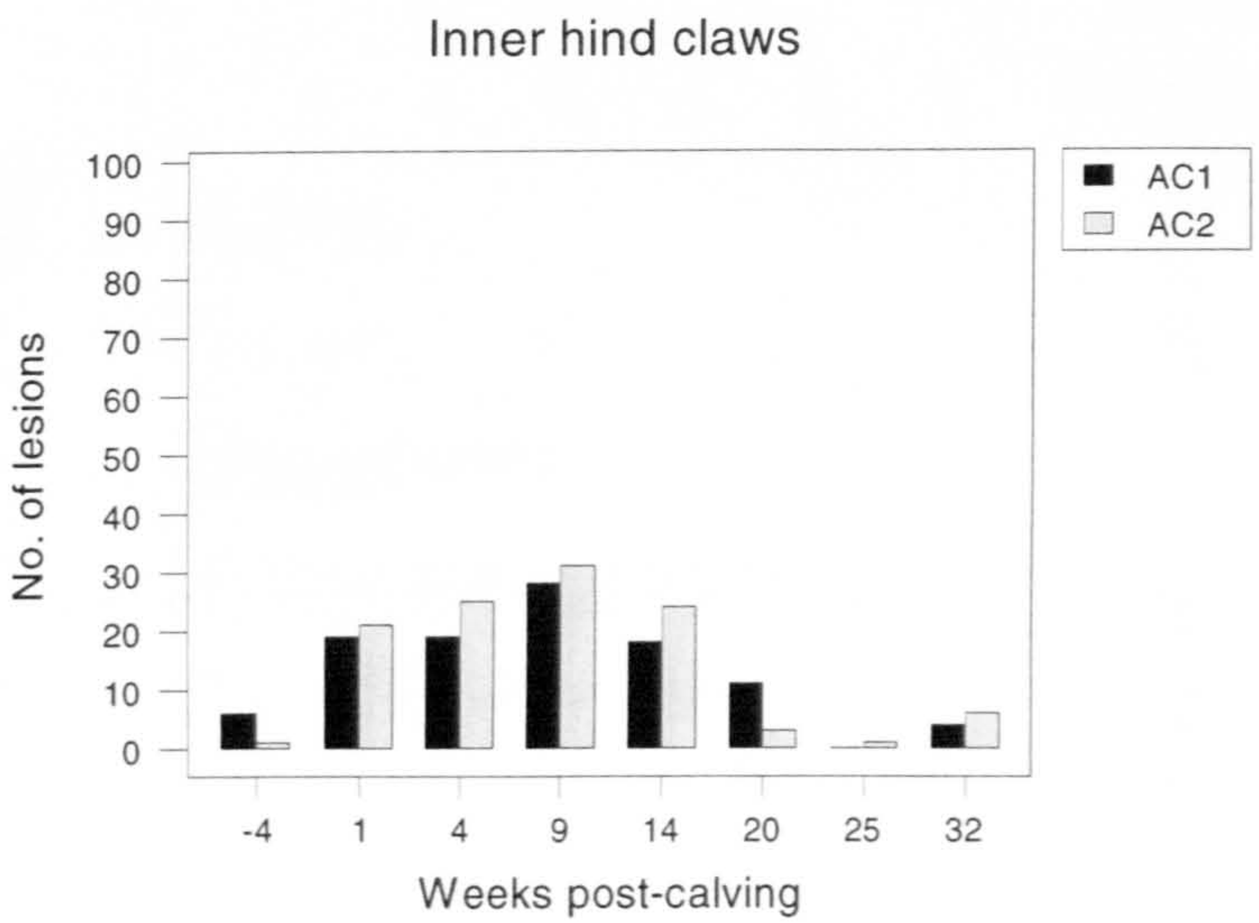
Inner hind claws
No. of lesions
100
90
80
70
60
50
40
30
20
10
0
-4
1
4
9
14
20
25
32
Weeks post-calving
AC1
AC2

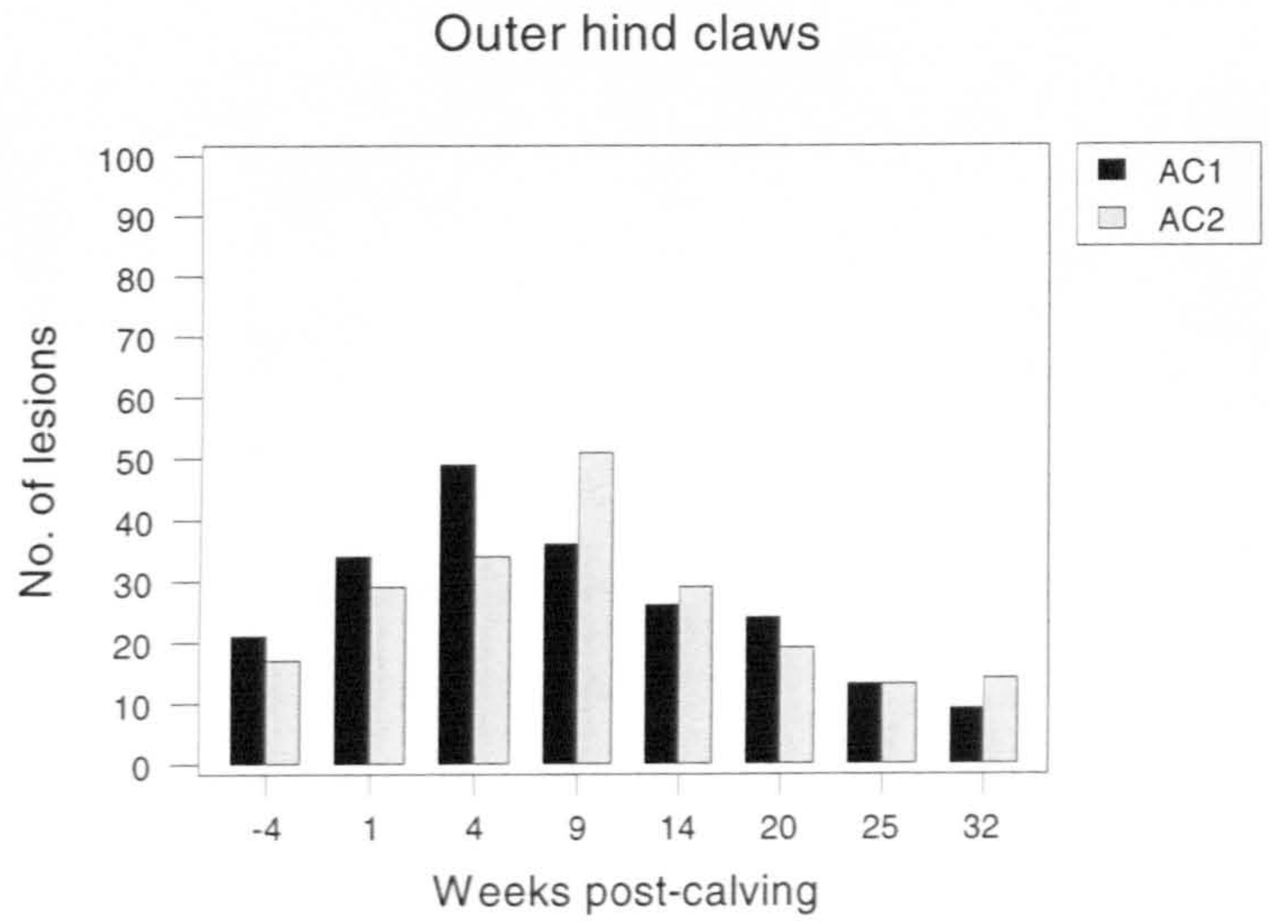
Outer hind claws
No. of lesions
100
90
80
70
60
50
40
30
20
10
0
-4
1
4
9
14
20
25
32
Weeks post-calving
AC1
AC2

Figure 4.11a
Distributions of lesions between zones of the sole: Group AC1

Zone 3 : Abaxial sole-bulb junction
Zone 4 : Sole-bulb junction
Zone 5 : Apex of sole
Zone 6 : Heel bulb

Inner front claws AC1

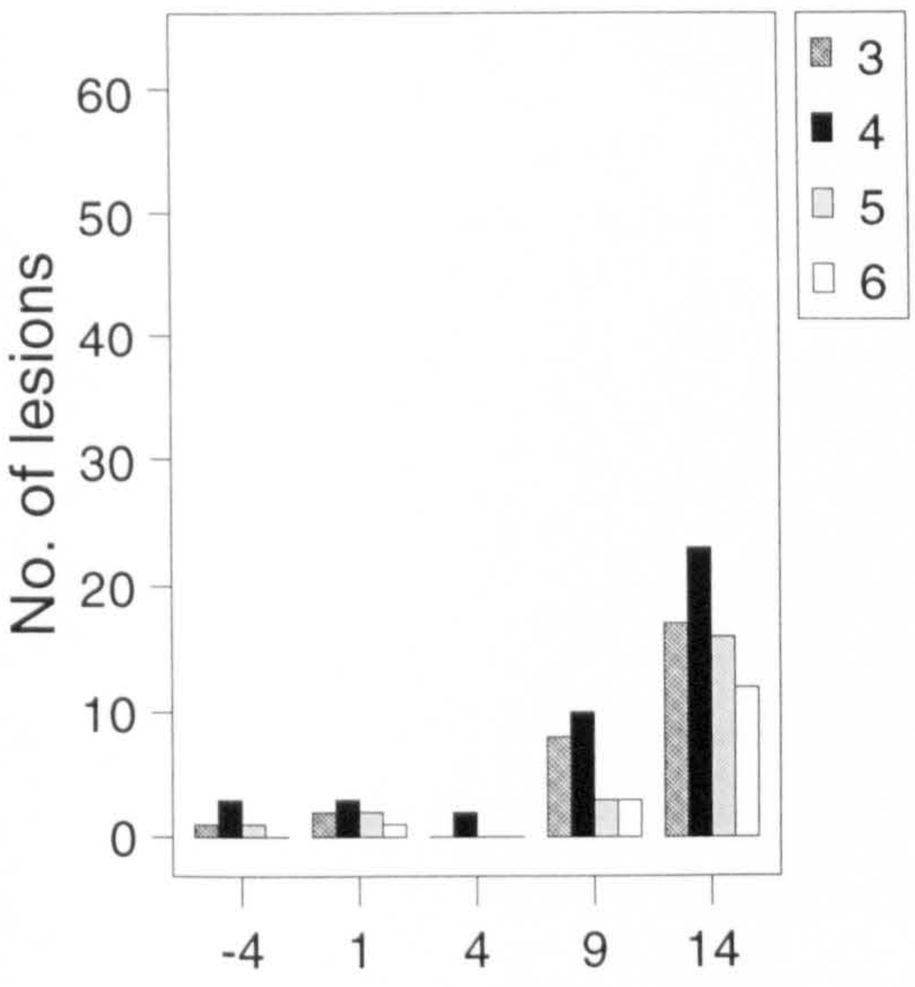

Outer front claws AC1

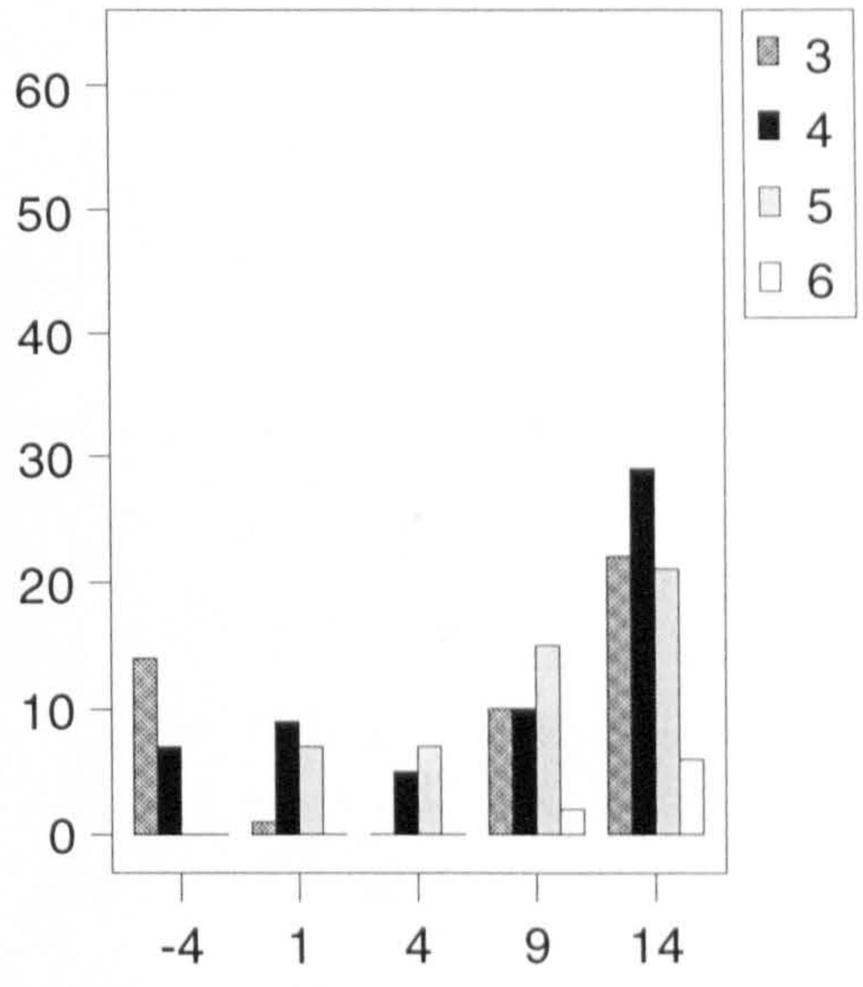

Inner hind claws AC1

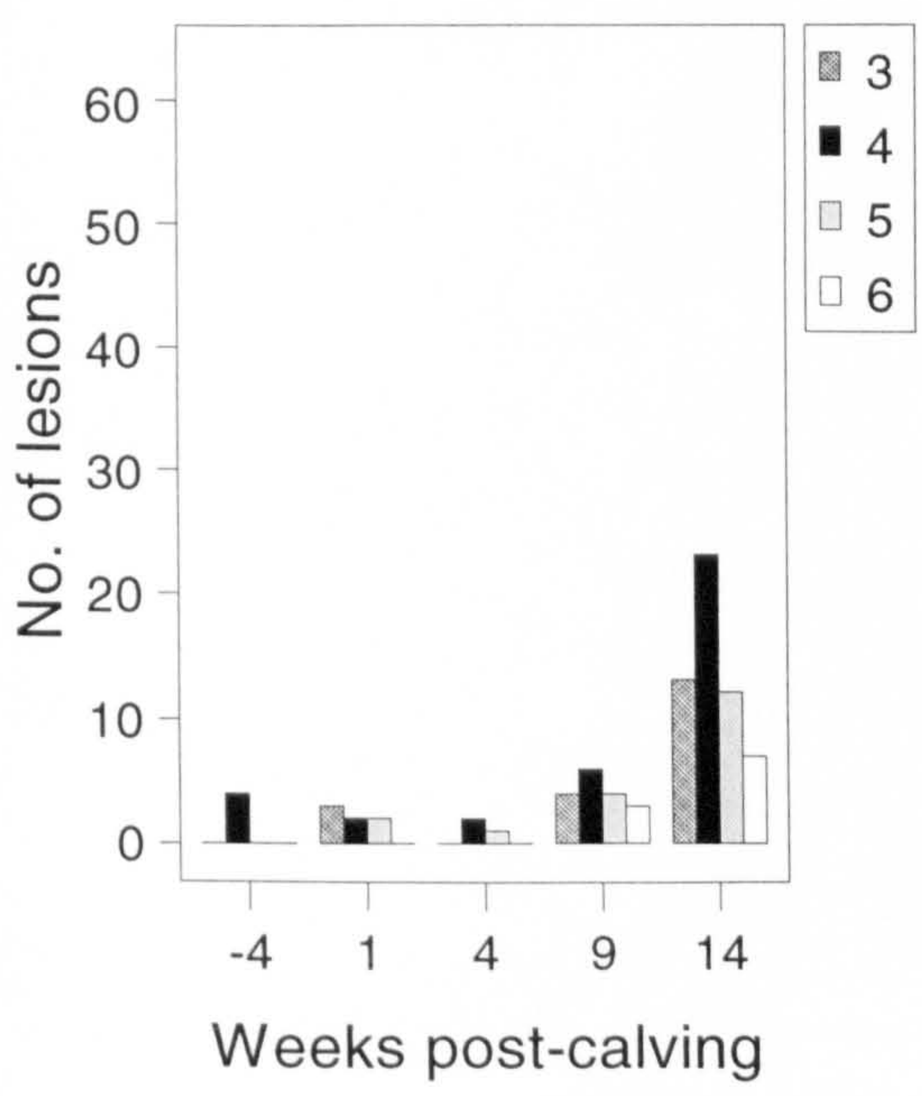

Outer hind claws AC1

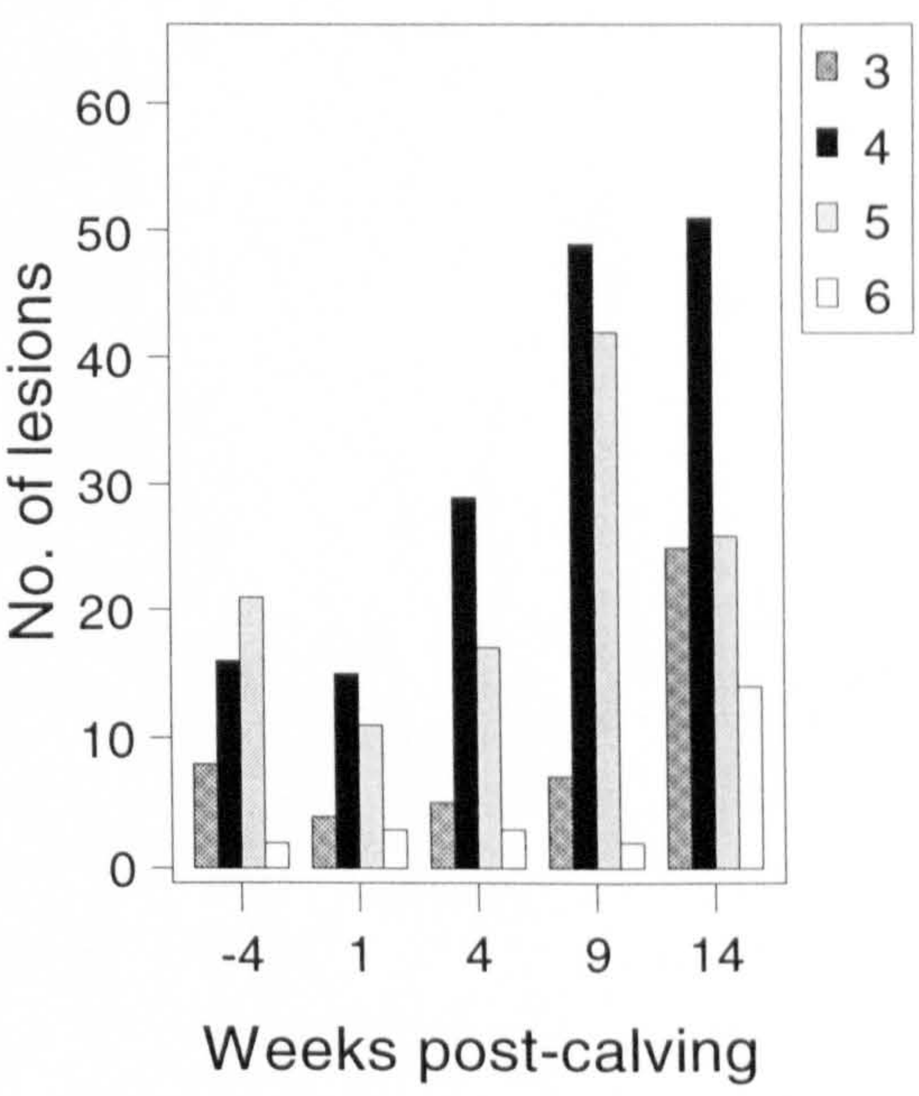

Figure 4.11b
Distributions of lesions between zones of the sole: Group AC2

Zone 3 : Abaxial sole-bulb junction
Zone 4 : Sole-bulb junction
Zone 5 : Apex of sole
Zone 6 : Heel bulb

Inner front claws AC2

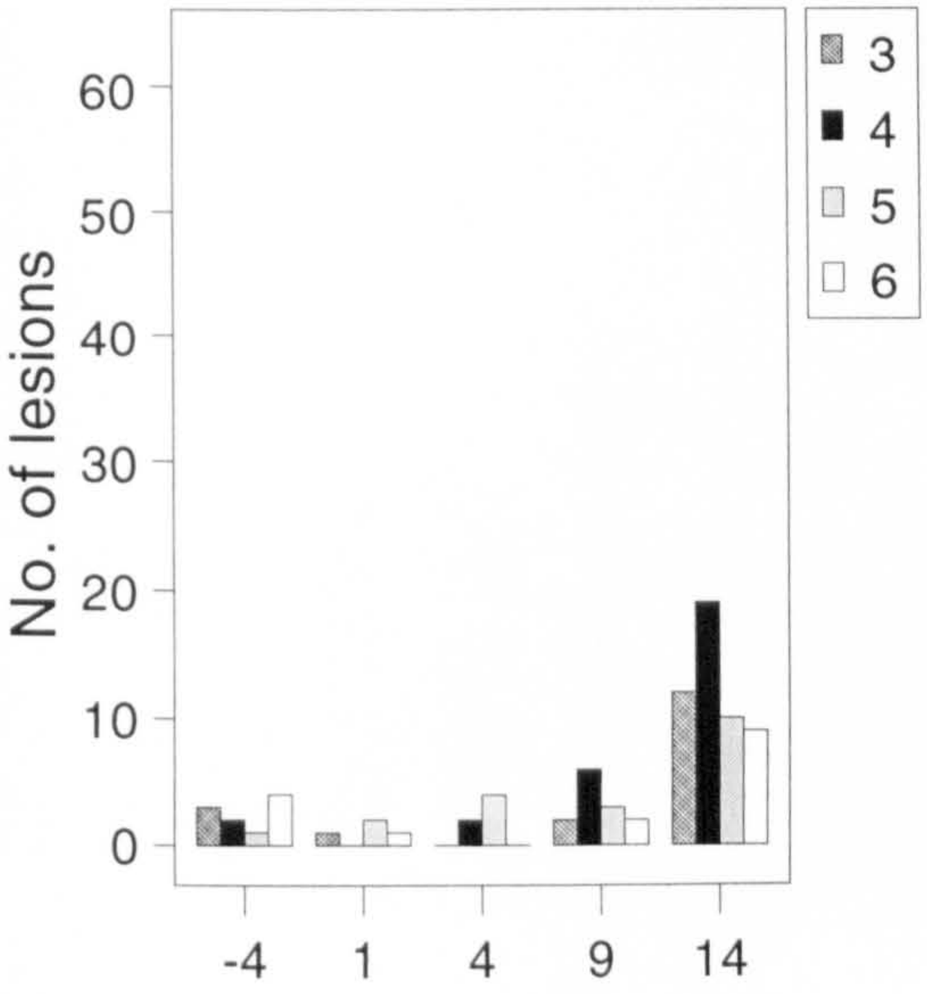

Outer front claws AC2

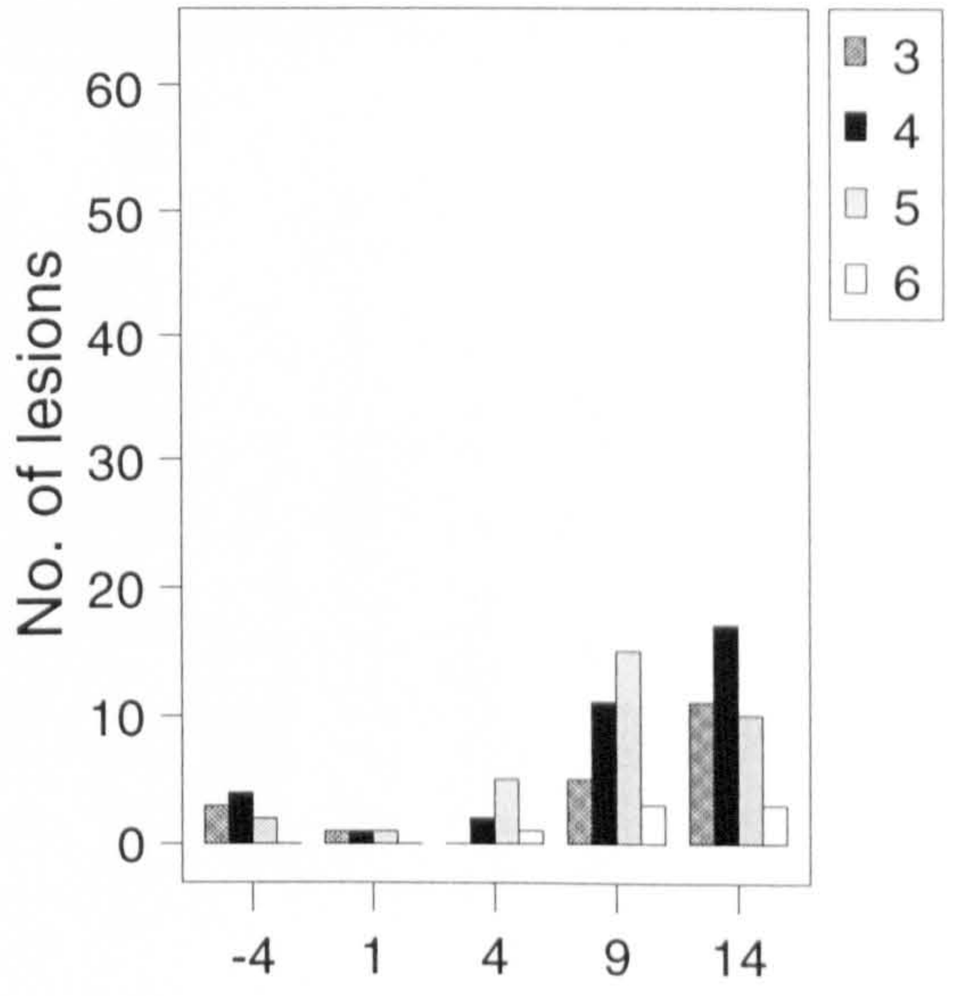

Inner hind claws AC2

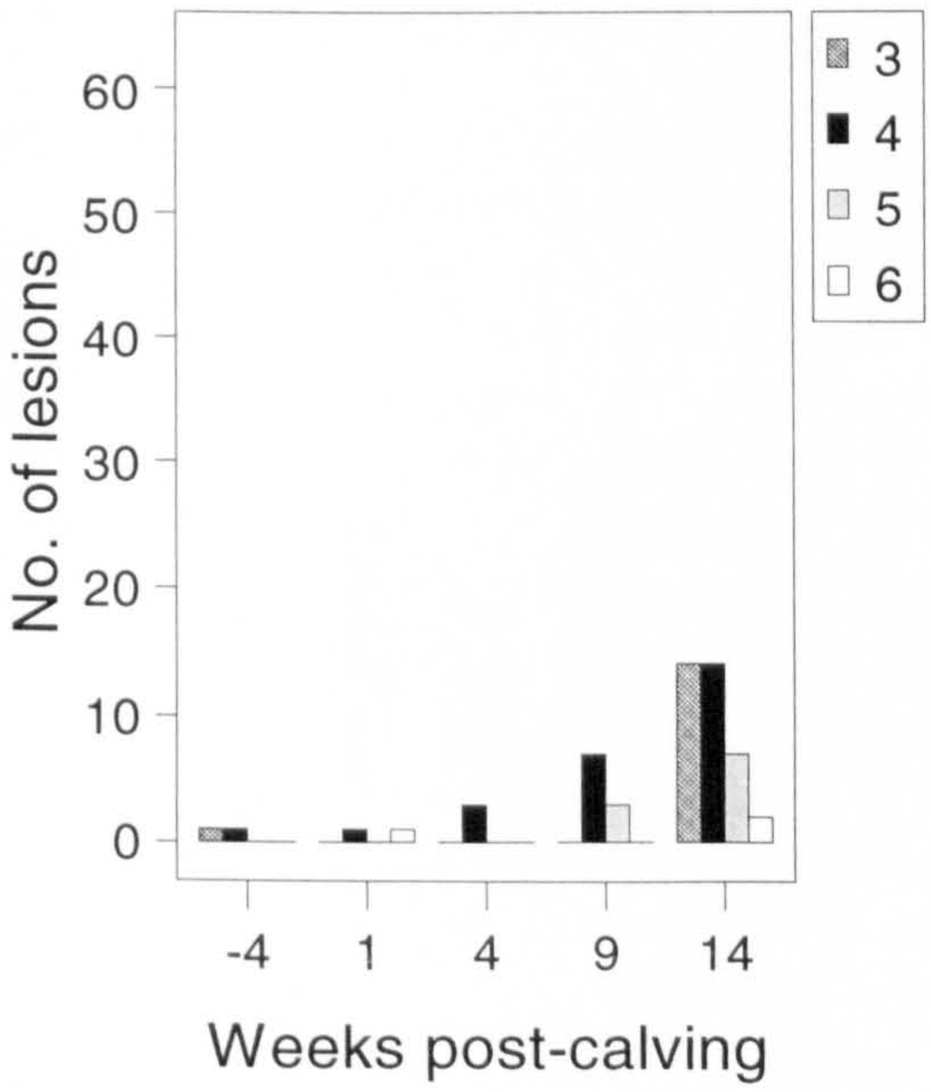

Outer hind claws AC2

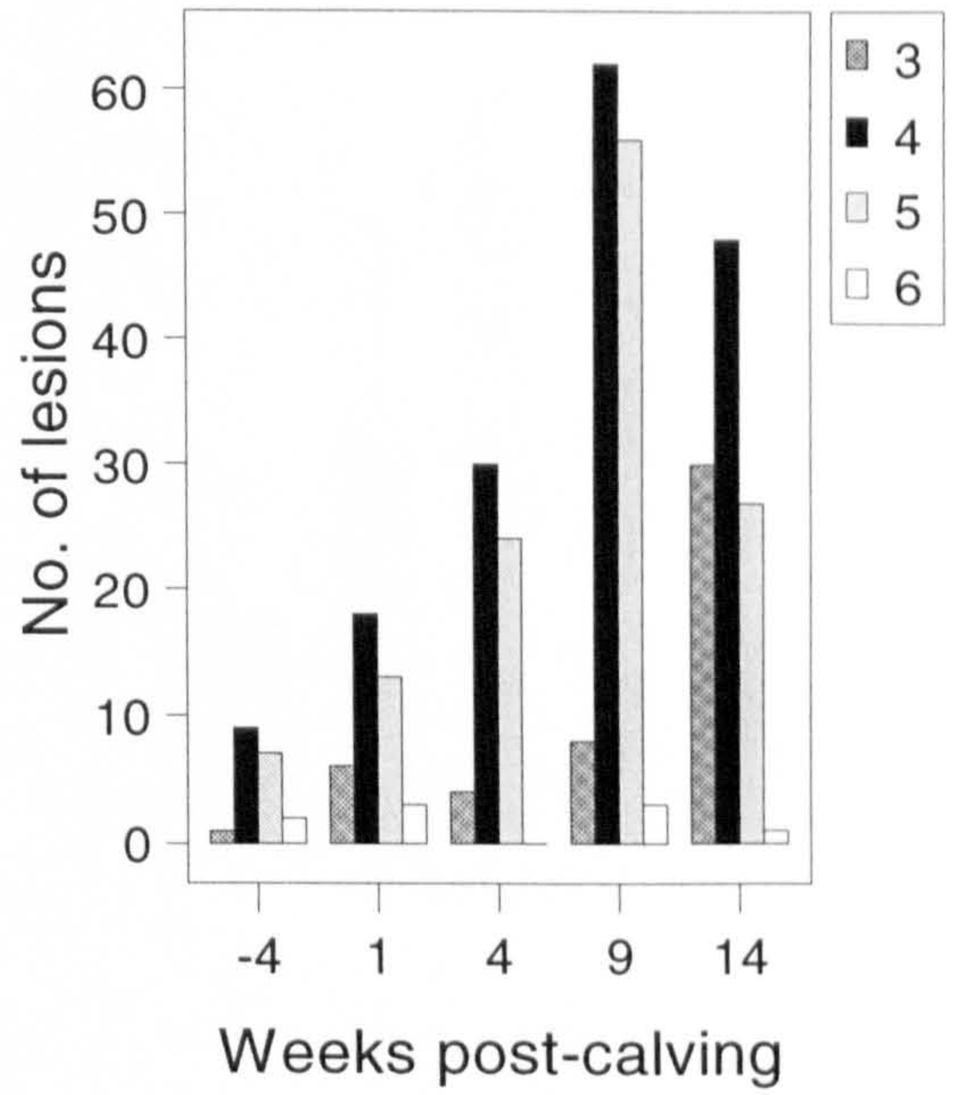

Figure 4.11c
Distributions of lesions between zones of the white line: Group AC1

Zone 1 : White line at toe
Zone 2 : Abaxial white line
Zone 3 : White line at sole-bulb junction
Zone 6 : White line caudal to the abaxial groove

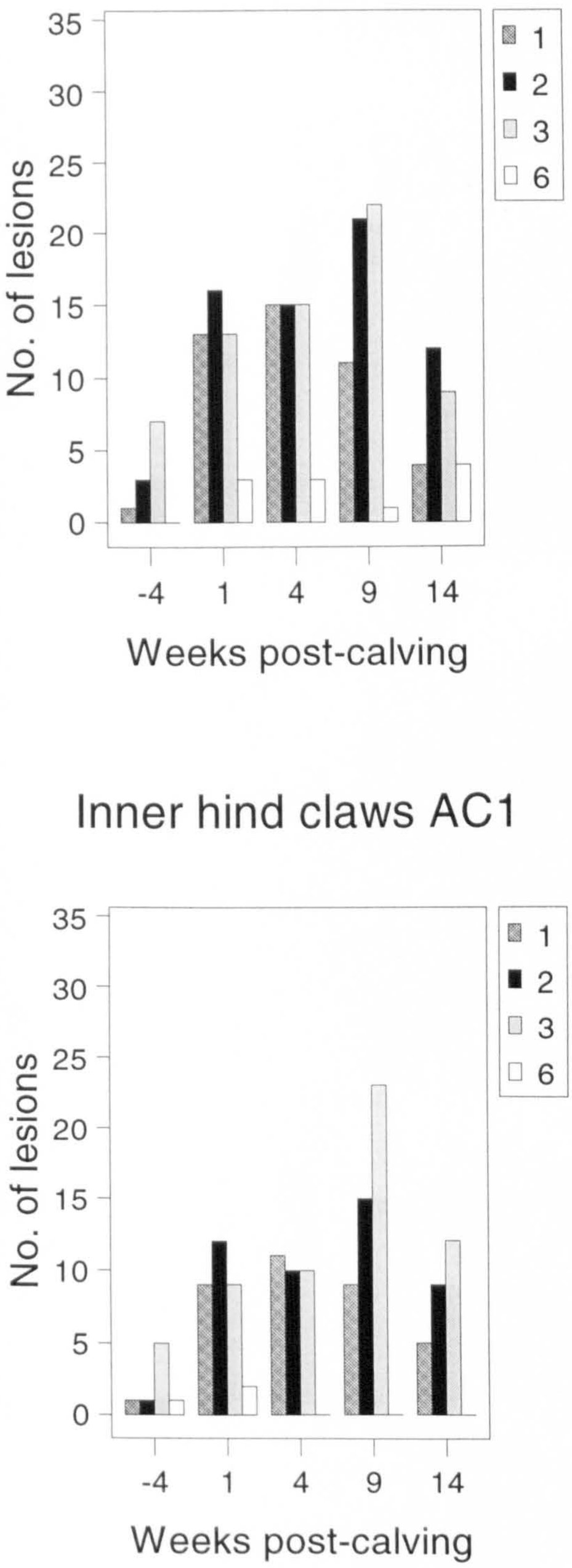
Inner front claws AC1
35
30
25
20
15
10
5
0
No. of lesions
-4
1
4
9
14
Weeks post-calving
1
2
3
6

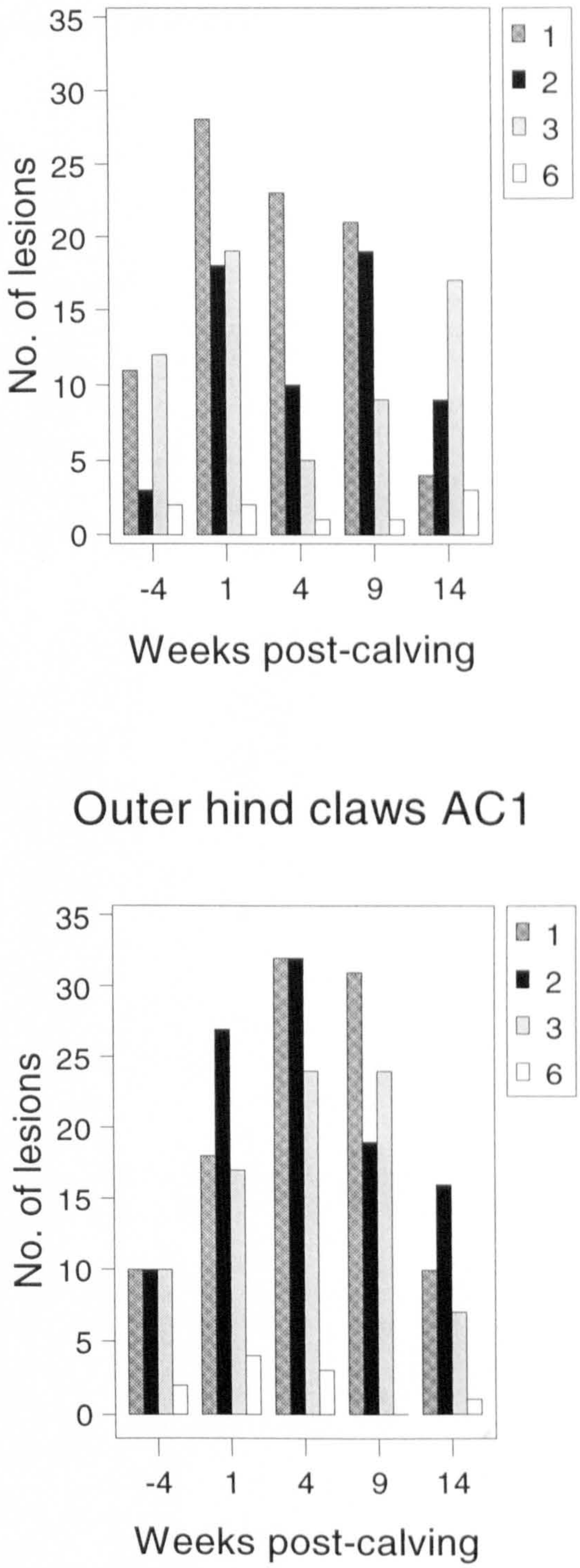
Outer front claws AC1
35
30
25
20
15
10
5
0
No. of lesions
-4
1
4
9
14
Weeks post-calving
1
2
3
6

Inner hind claws AC1
35
30
25
20
15
10
5
0
No. of lesions
-4
1
4
9
14
Weeks post-calving
1
2
3
6

Outer hind claws AC1
35
30
25
20
15
10
5
0
No. of lesions
-4
1
4
9
14
Weeks post-calving
1
2
3
6

Figure 4.11d
Distributions of lesions between zones of the white line: Group AC2

Zone 1 : White line at toe
Zone 2 : Abaxial white line
Zone 3 : White line at sole-bulb junction
Zone 6 : White line caudal to the abaxial groove

Inner front claws AC2

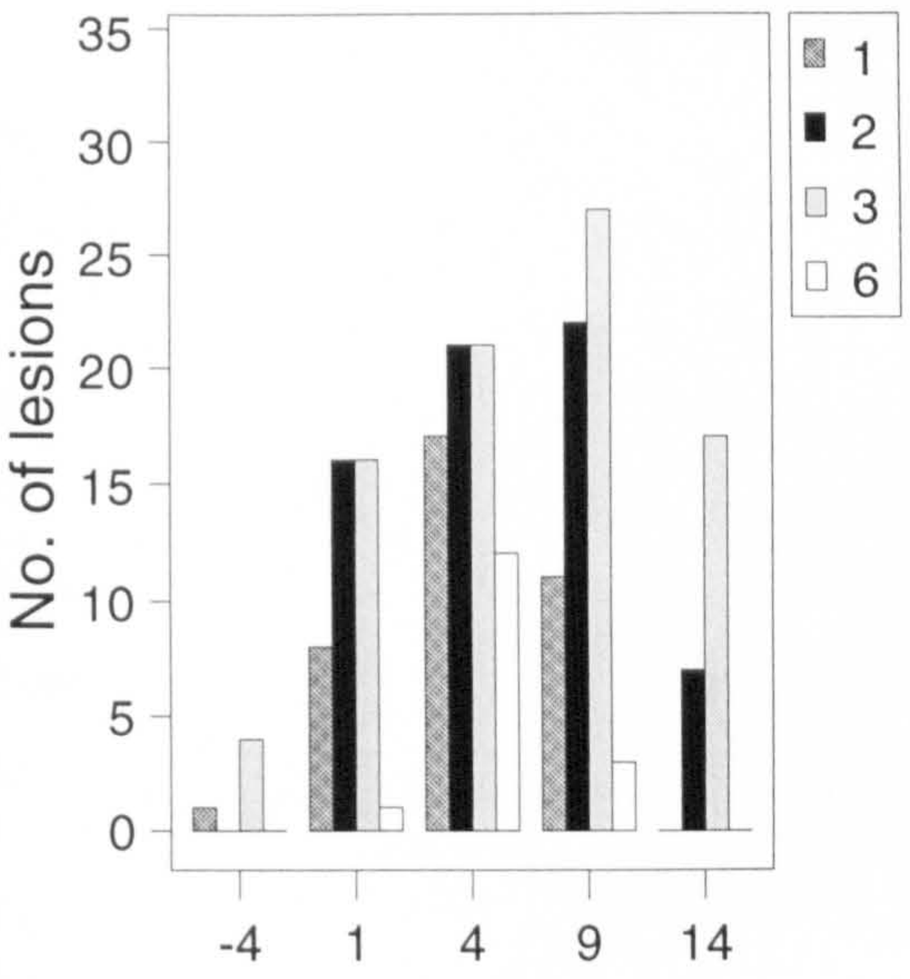

Outer front claws AC2

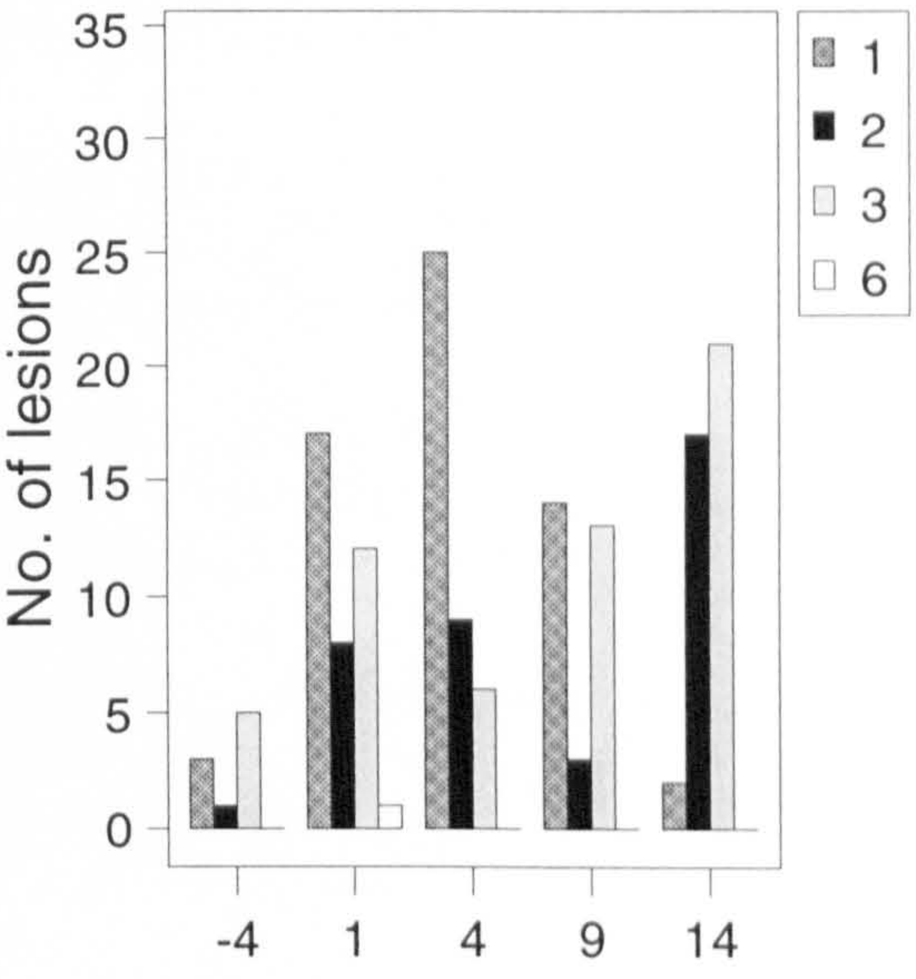

Inner hind claws AC2

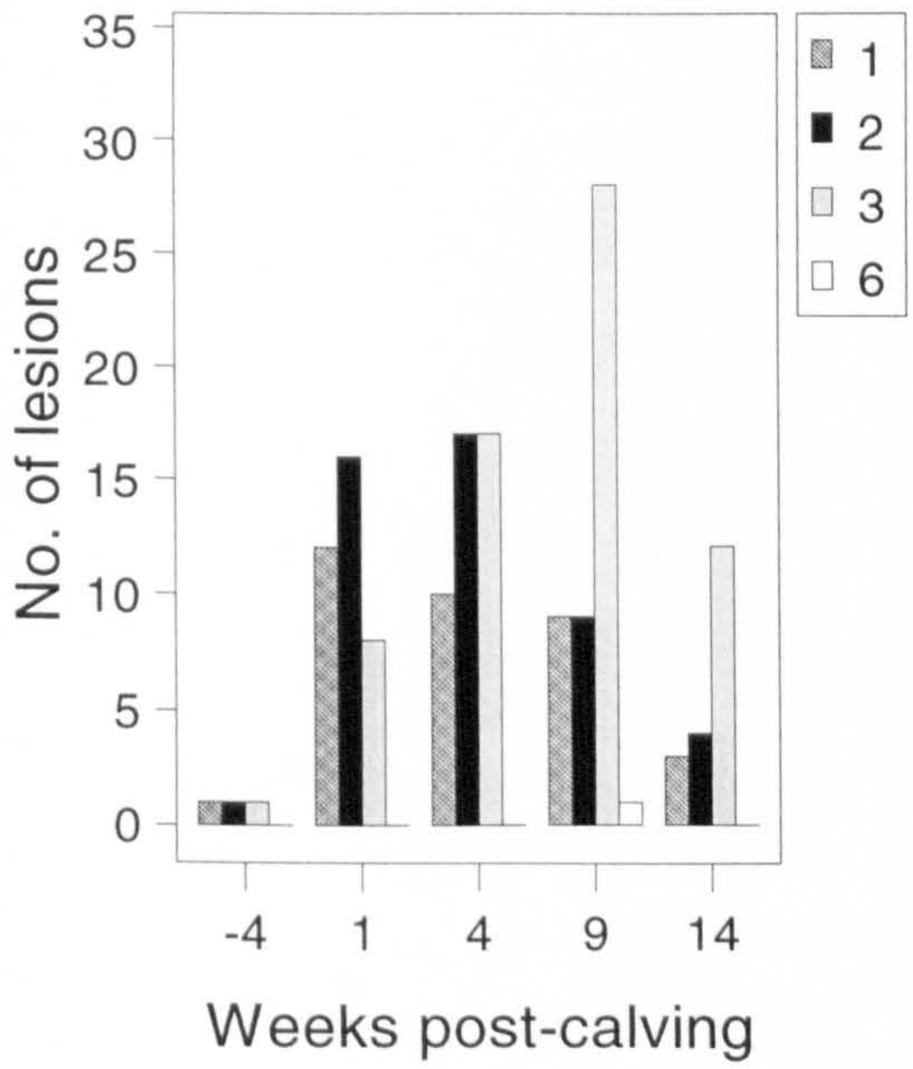

Outer hind claws AC2

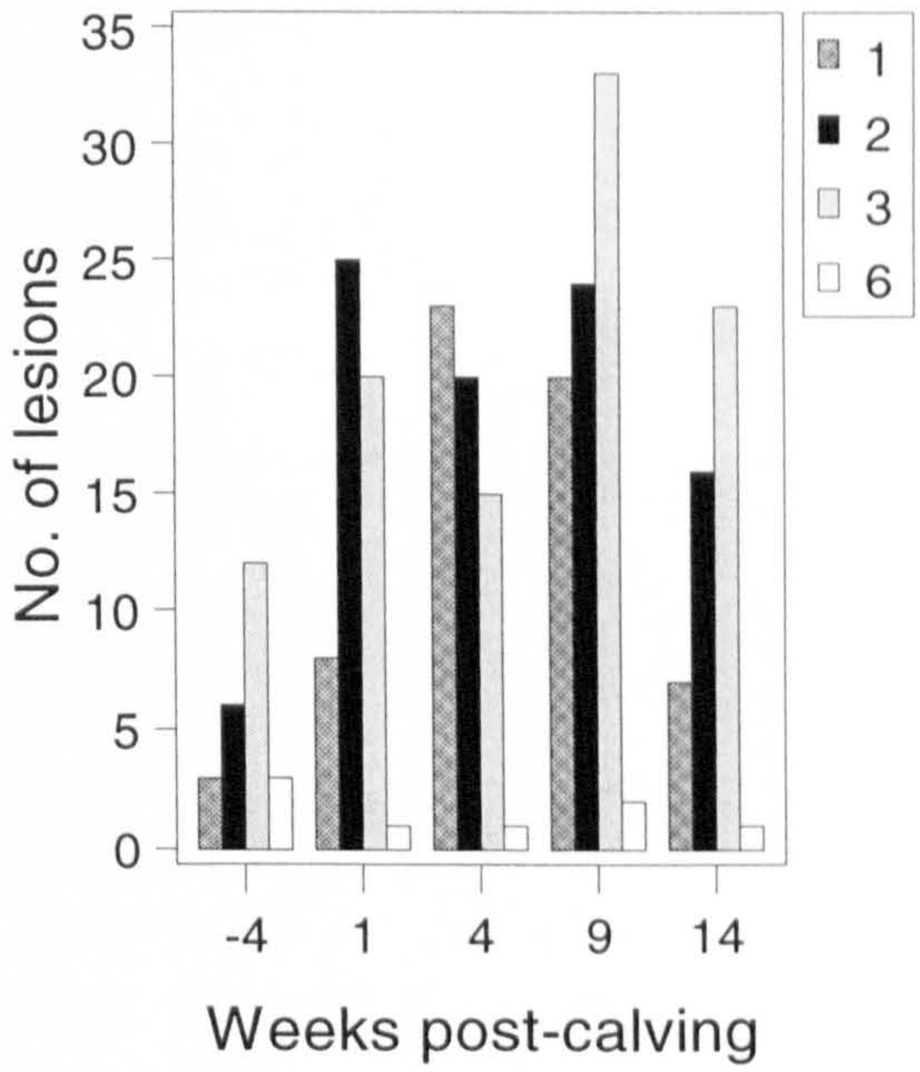

Figure 4.12
Median severity, size and combined lesion score for individual sole and white line lesions for Groups AC1 and AC2

aa1 : severity score for sole lesions, Group AC1
pa1 : size of sole lesions, Group AC1
ca1 : combined score for sole lesions, Group AC1

aa2 : severity score for sole lesions, Group AC2
pa2 : size of sole lesions, Group AC2
ca2 : combined score for sole lesions, Group AC2

al1 : severity score for white line lesions, Group AC1
pl1 : size of white line lesions, Group AC1
cl1 : combined score for white line lesions, Group AC1

al2 : severity score for white line lesions, Group AC2
pl2 : size of white line lesions, Group AC2
cl2 : combined score for white line lesions, Group AC2

(See Table 4.3 for full definitions of scores)

Sole Group AC1

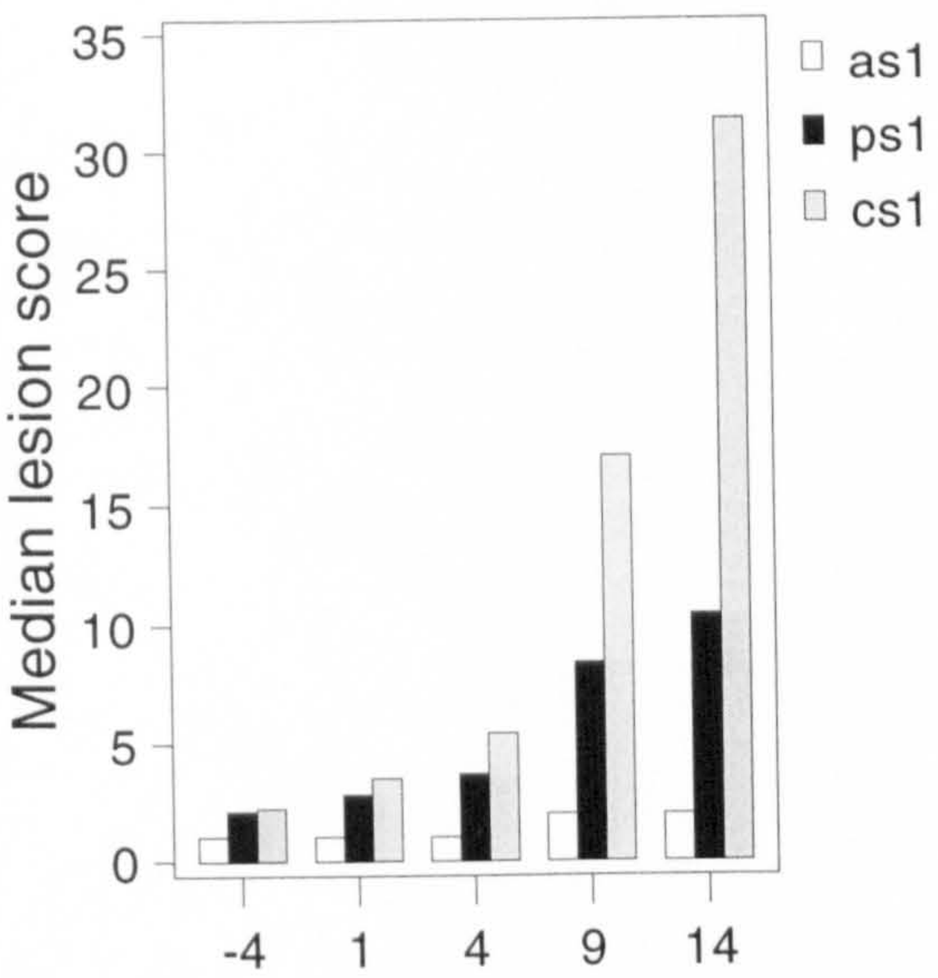

Sole Group AC2

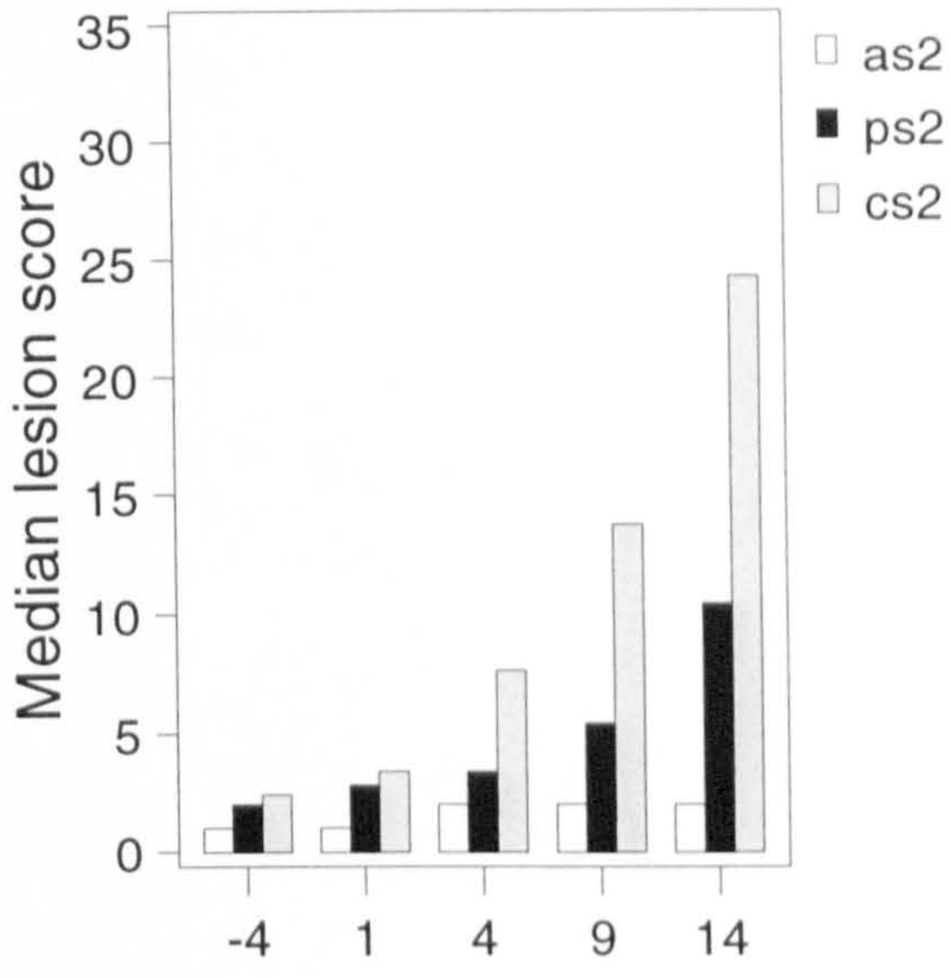

White line Group AC1

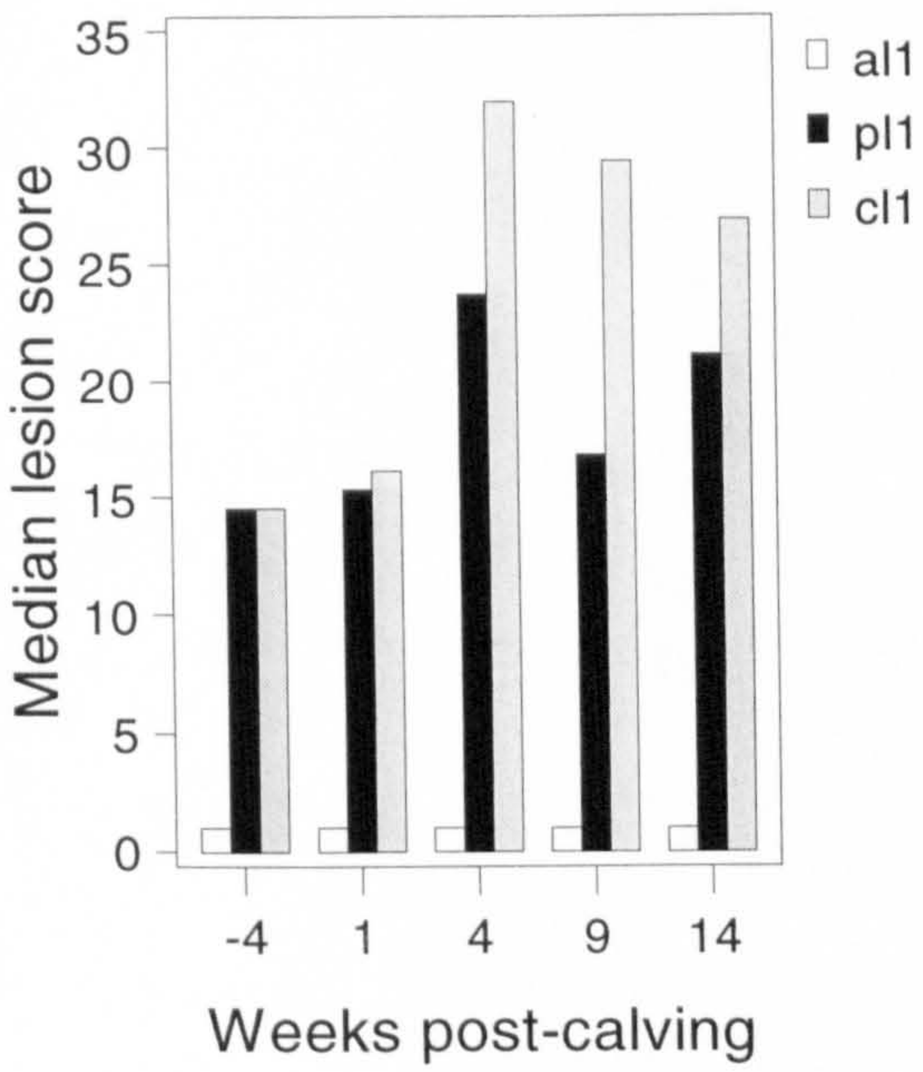

White line Group AC2

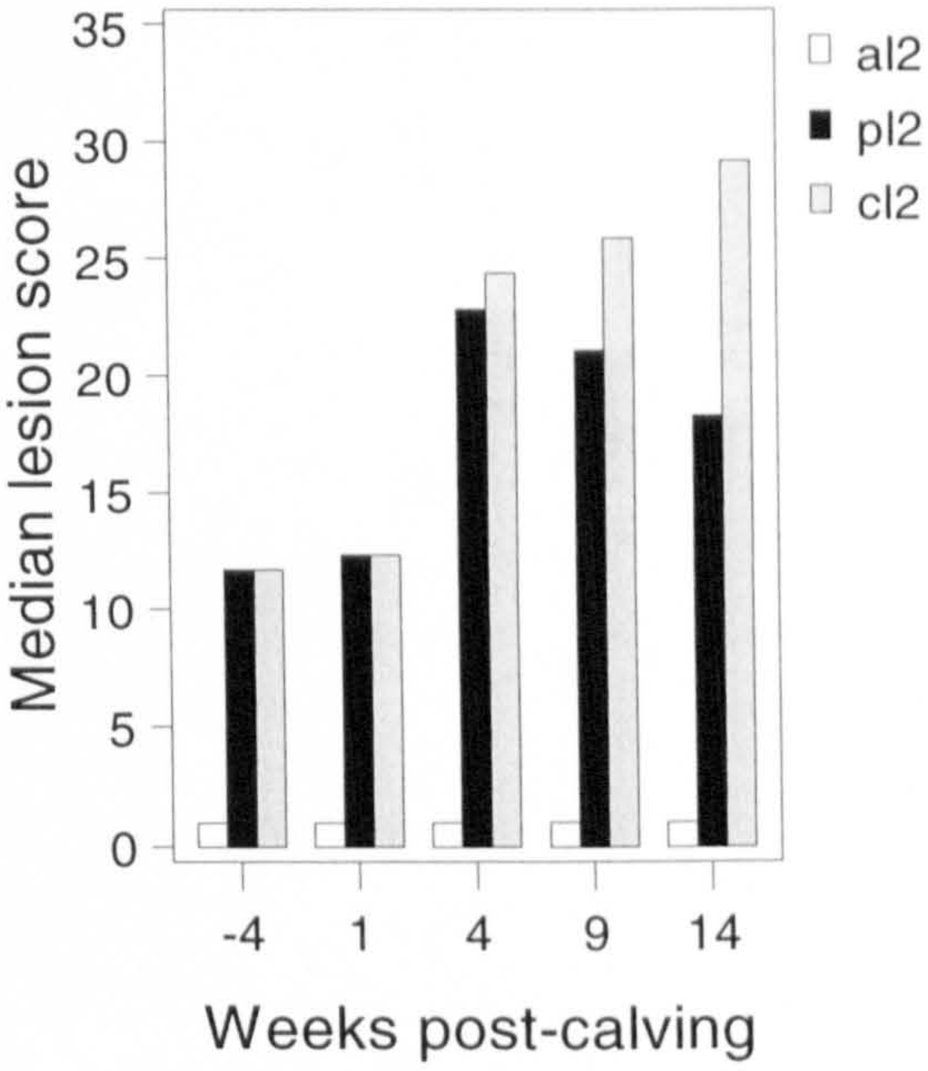

Figure 4.13a
The relationship between size and severity of individual lesions of the sole

(Pooled data for Groups AC1 and AC2)

-4 weeks post-calving

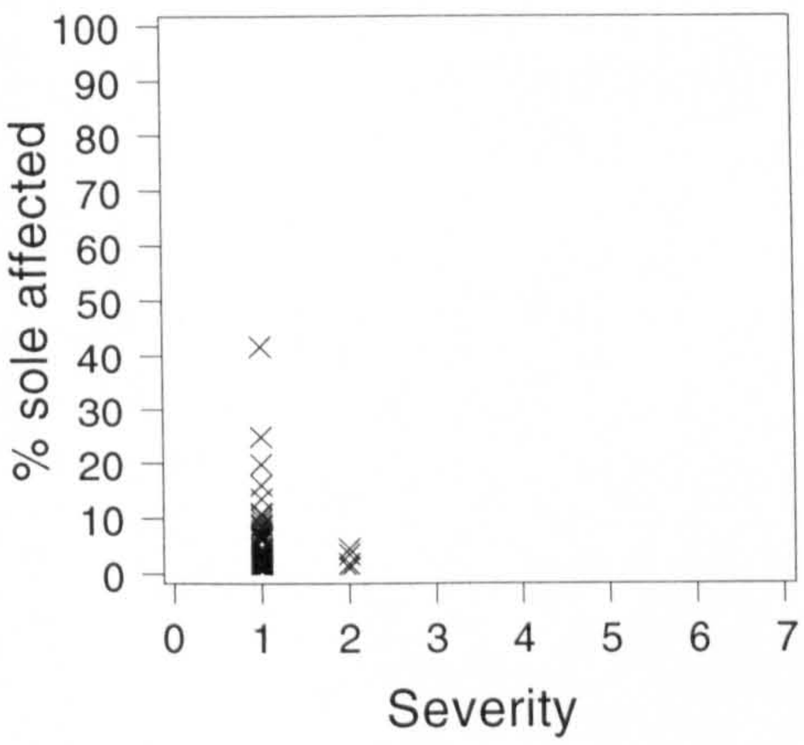

1 week post-calving

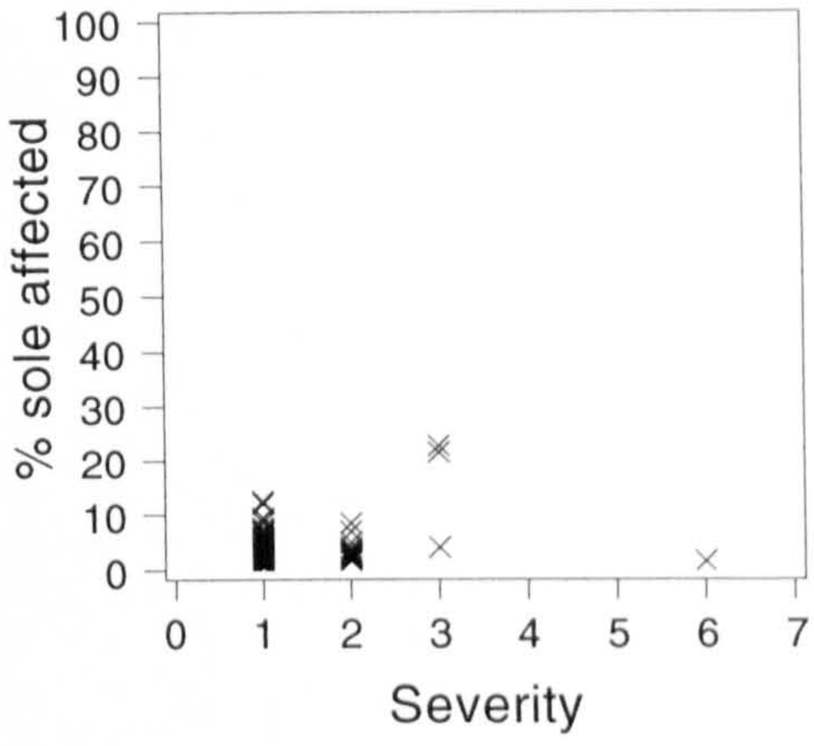

4 weeks post-calving

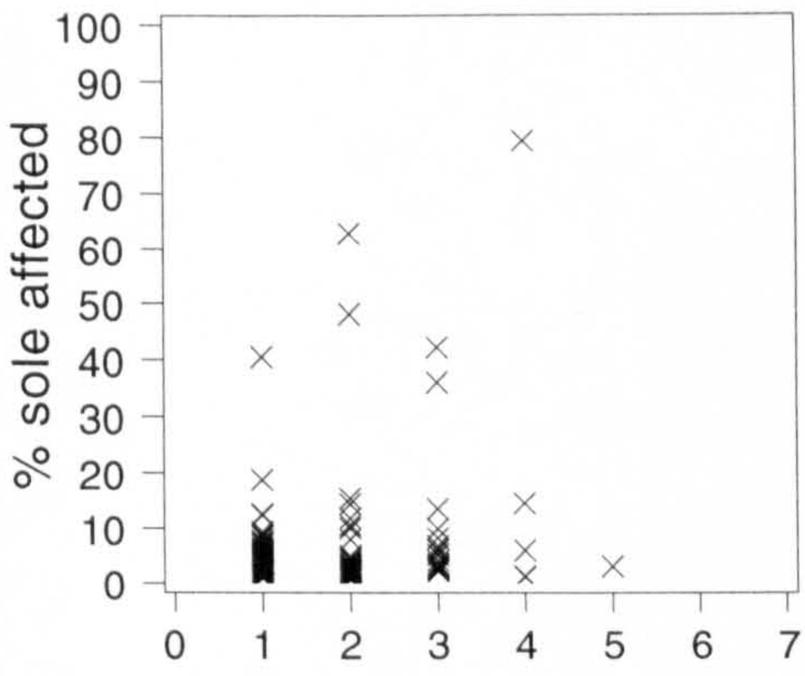

9 weeks post-calving

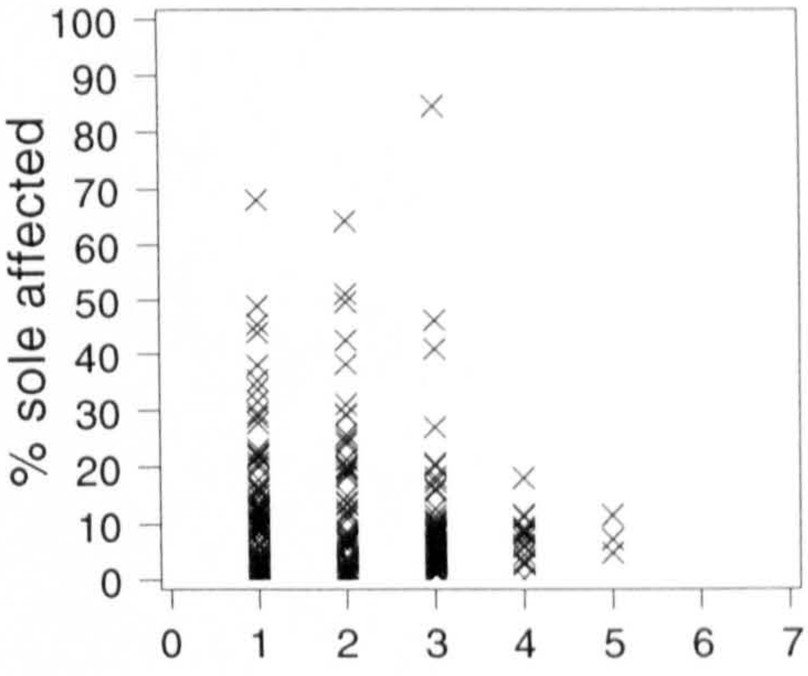

14 weeks post-calving

Figure 4.13b
The relationship between size and severity of individual lesions of the white line

(Pooled data for Groups AC1 and AC2)

-4 weeks post-calving

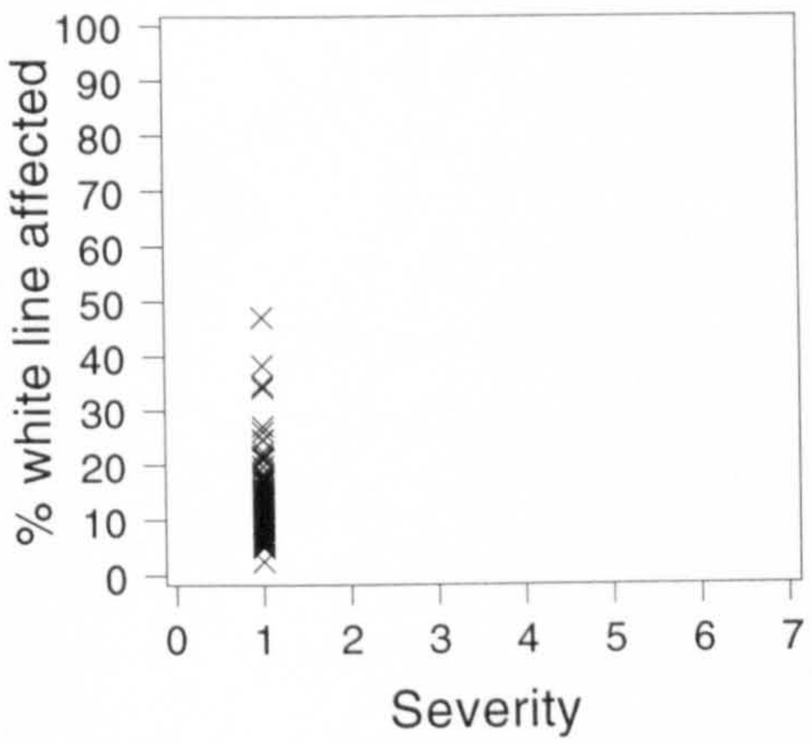

1 week post-calving

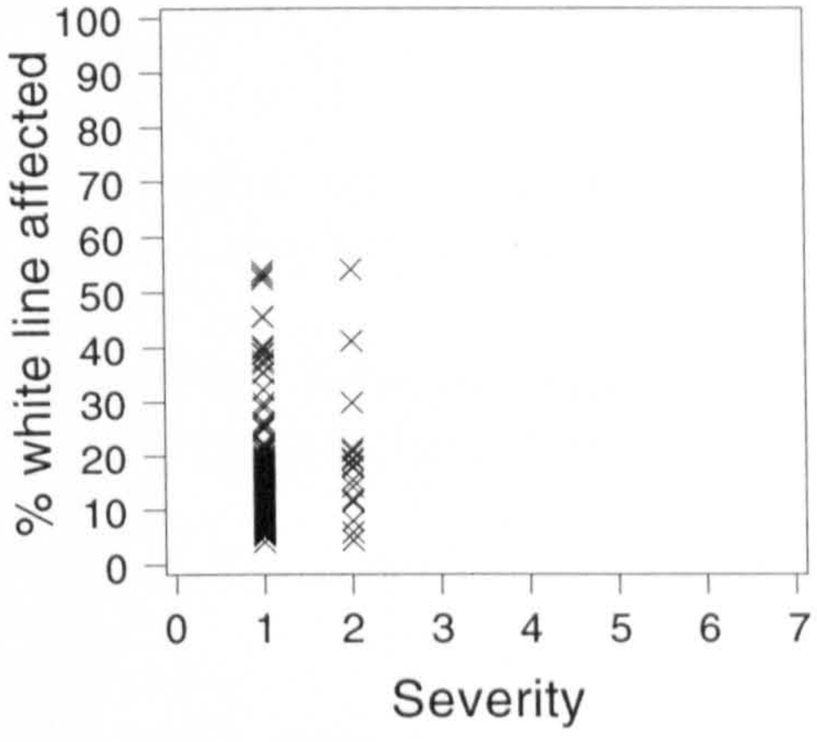

4 weeks post-calving

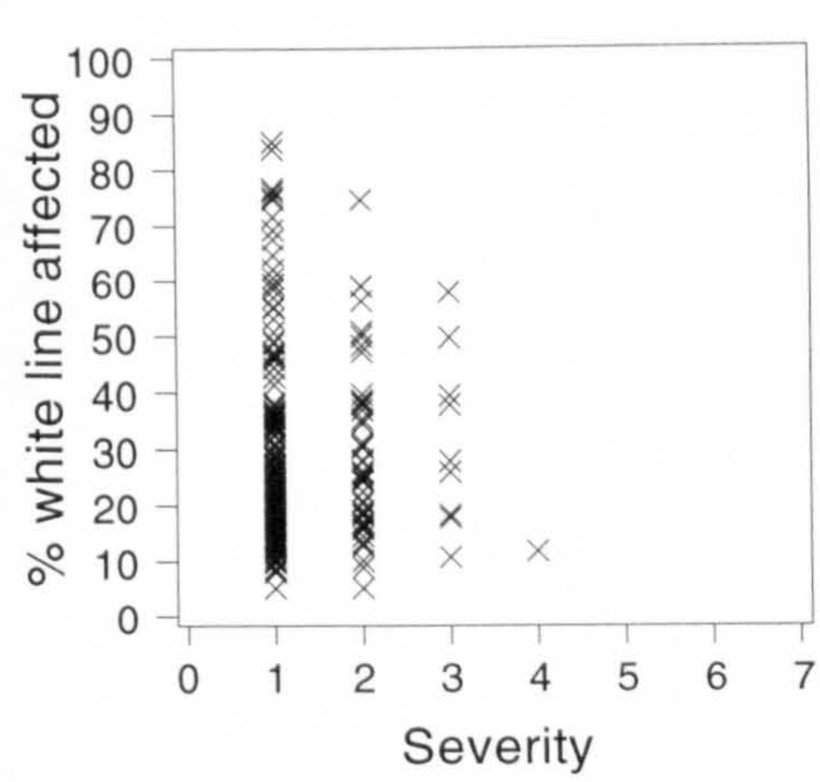

9 weeks post-calving

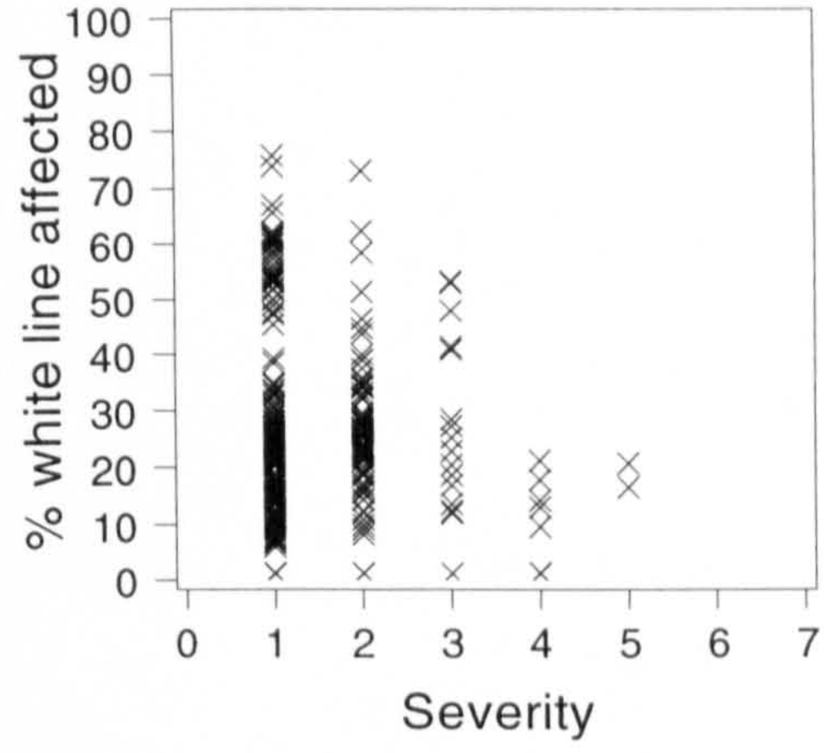

14 weeks post-calving

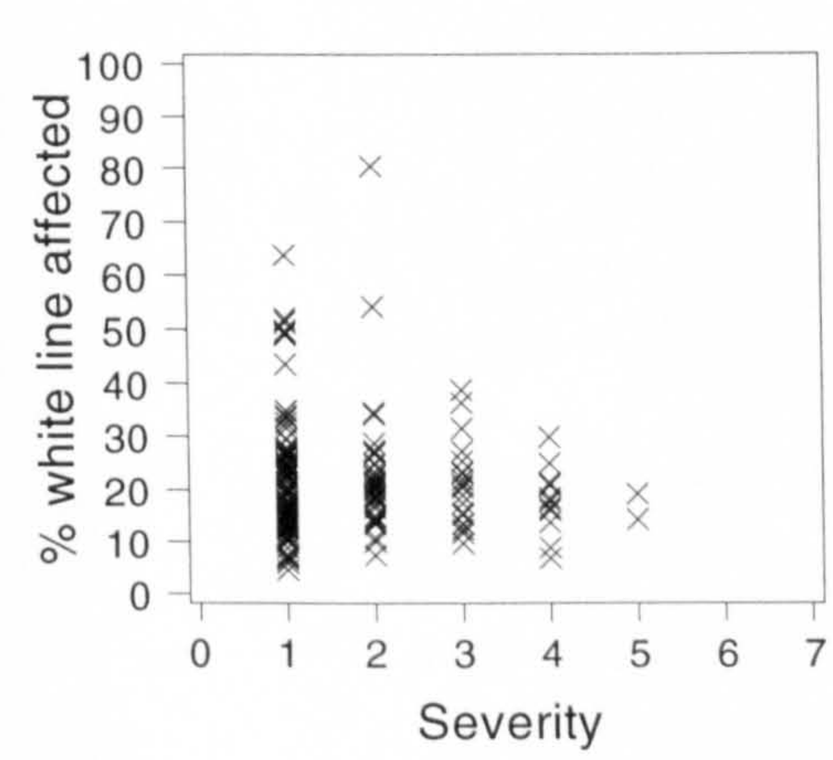

Figure 4.14

Median number of lesions and cumulative weighted severity score for lesions of the sole and white line of the outer hind claws

(Pooled data for Groups AC1 and AC2)

Ns claw : Number of sole lesions
Gs claw : Cumulative weighted severity score for sole lesions

Nl claw : Number of white line lesions
Gl claw : Cumulative weighted severity score for white line lesions

Sole lesions

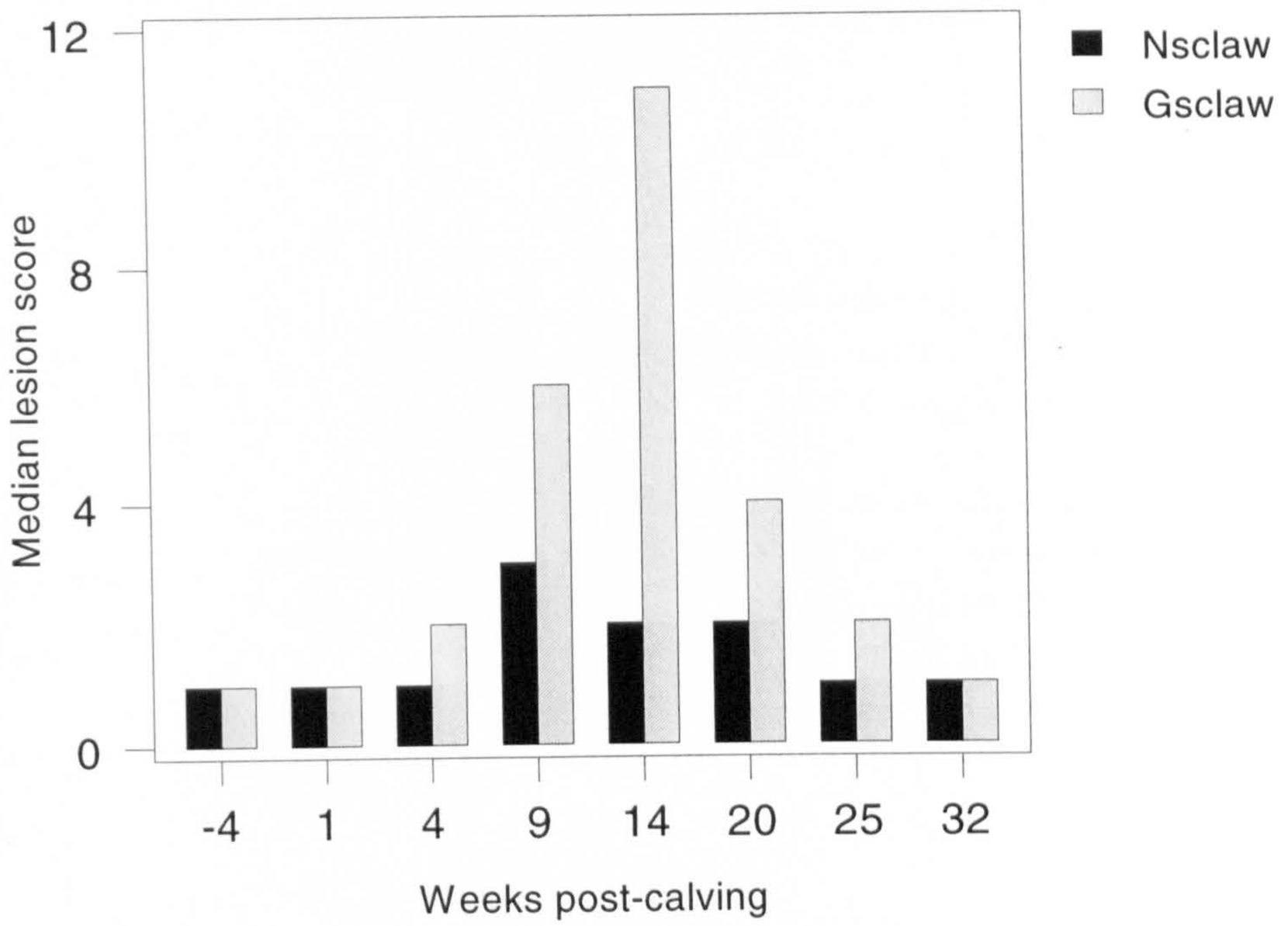

White line lesions

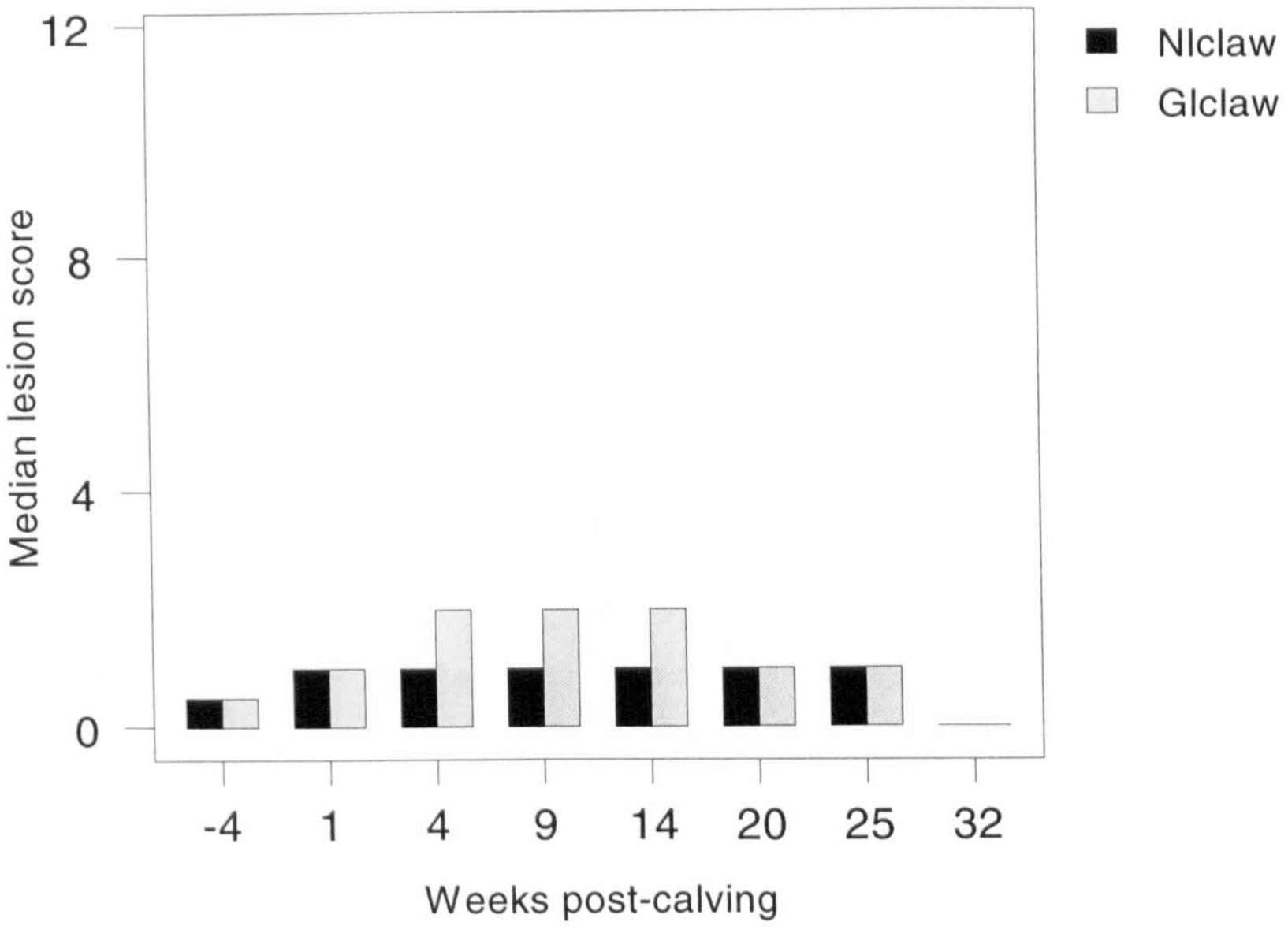

Figure 4.15
Median percentage of the sole and white line affected and the median cumulative combined score for sole and white line lesions for the outer hind claws

(Pooled data for Groups AC1 and AC2)

Ps claw : Percentage of the sole affected
Cs claw : Total combined lesion score for lesions of the sole
(weighted severity x size)

Pl claw : Percentage of the white line affected
Cl claw : Total combined lesion score for lesions of the white line
(weighted severity x size)

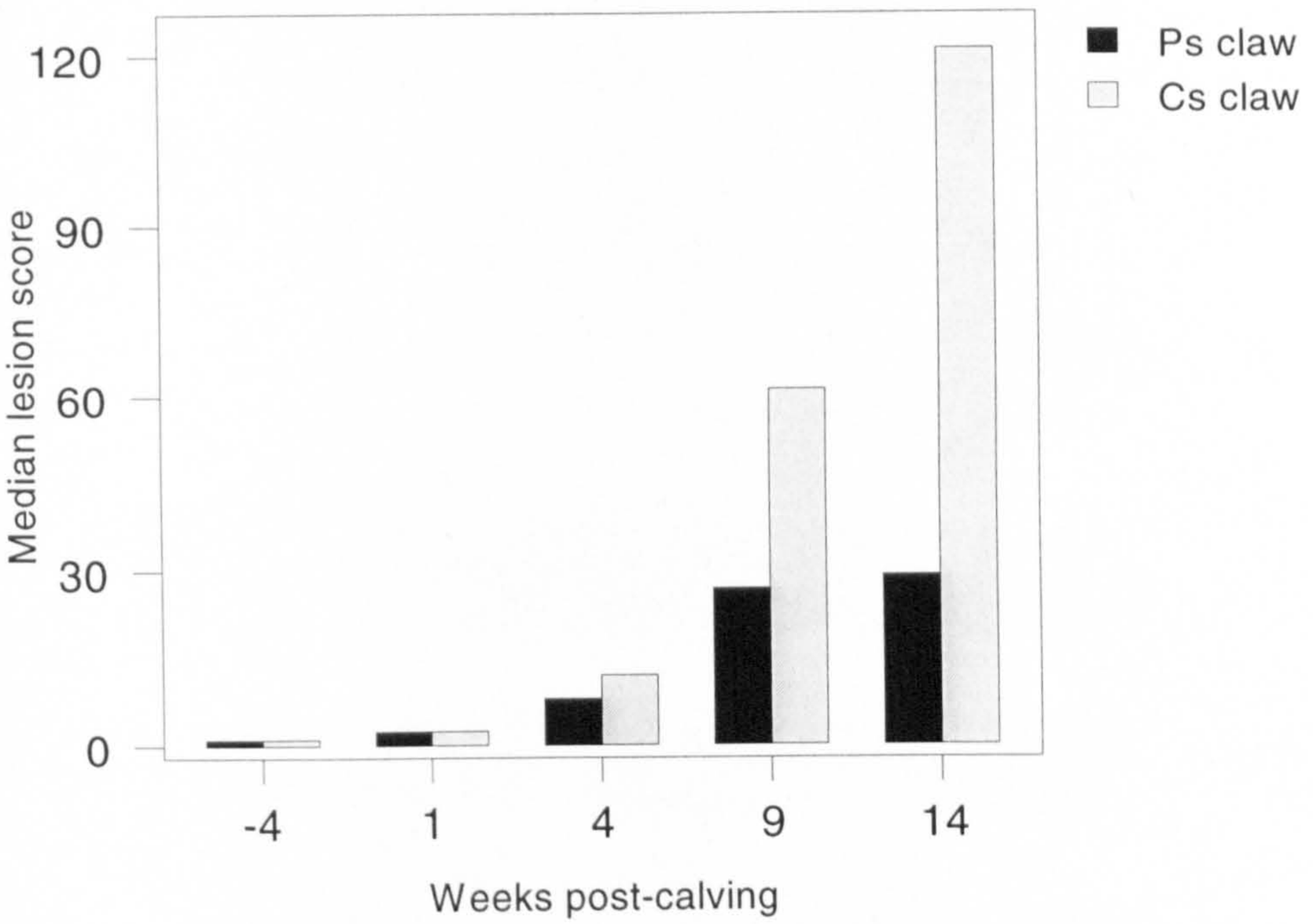
Sole lesions
Median lesion score
120
90
60
30
0
-4
1
4
9
14
Weeks post-calving
Ps claw
Cs claw

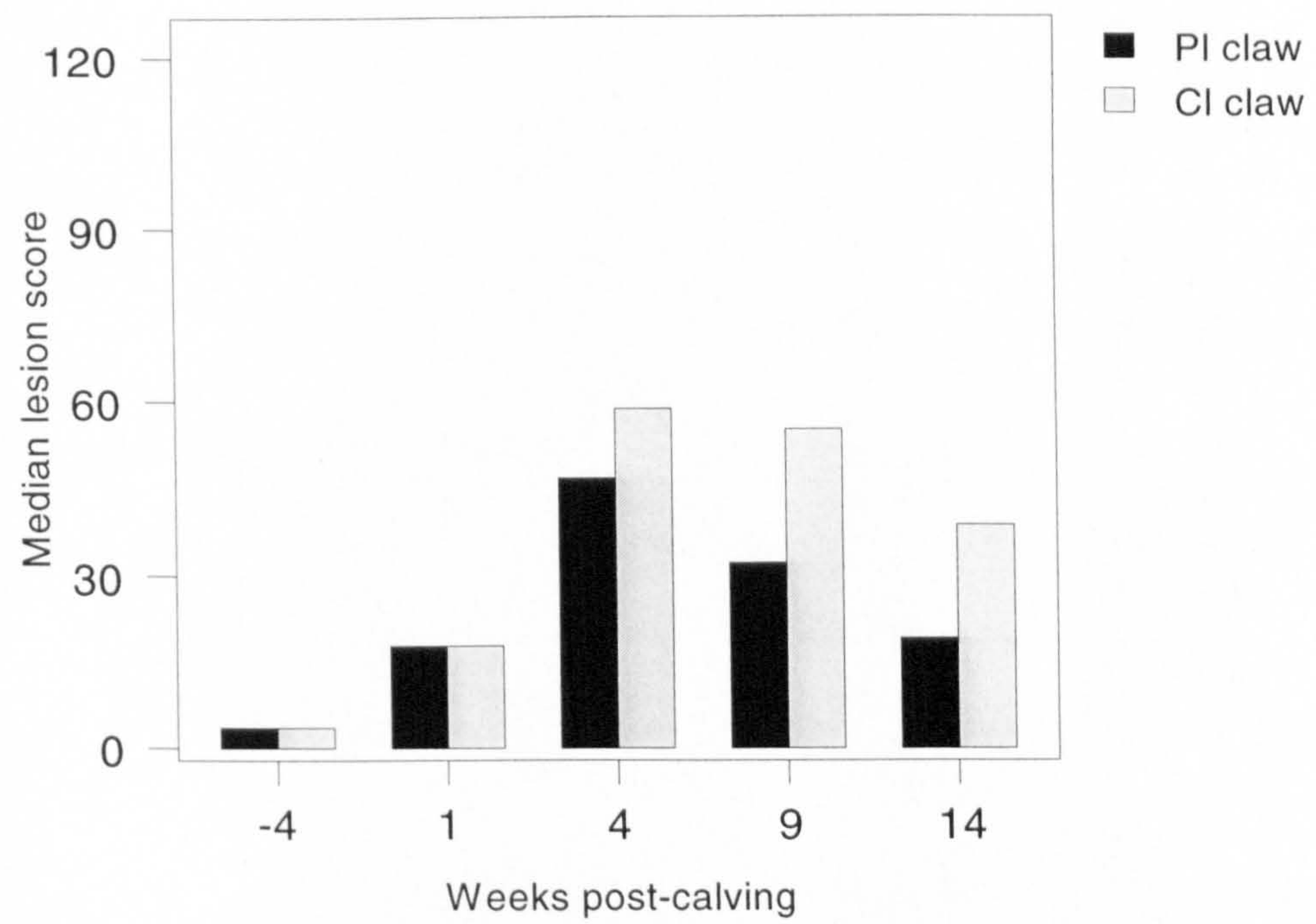
White line lesions
Median lesion score
120
90
60
30
0
-4
1
4
9
14
Weeks post-calving
Pl claw
Cl claw

Figure 4.16
Frequency of heel erosion of different severities throughout the lactation

(Pooled data for Groups AC1 and AC2)

HE 1: pitting of bulb horn
HE 2: oblique clefts in bulb horn
HE 3: substantial loss of bulb horn

H↑ - housing

T↑ - turnout

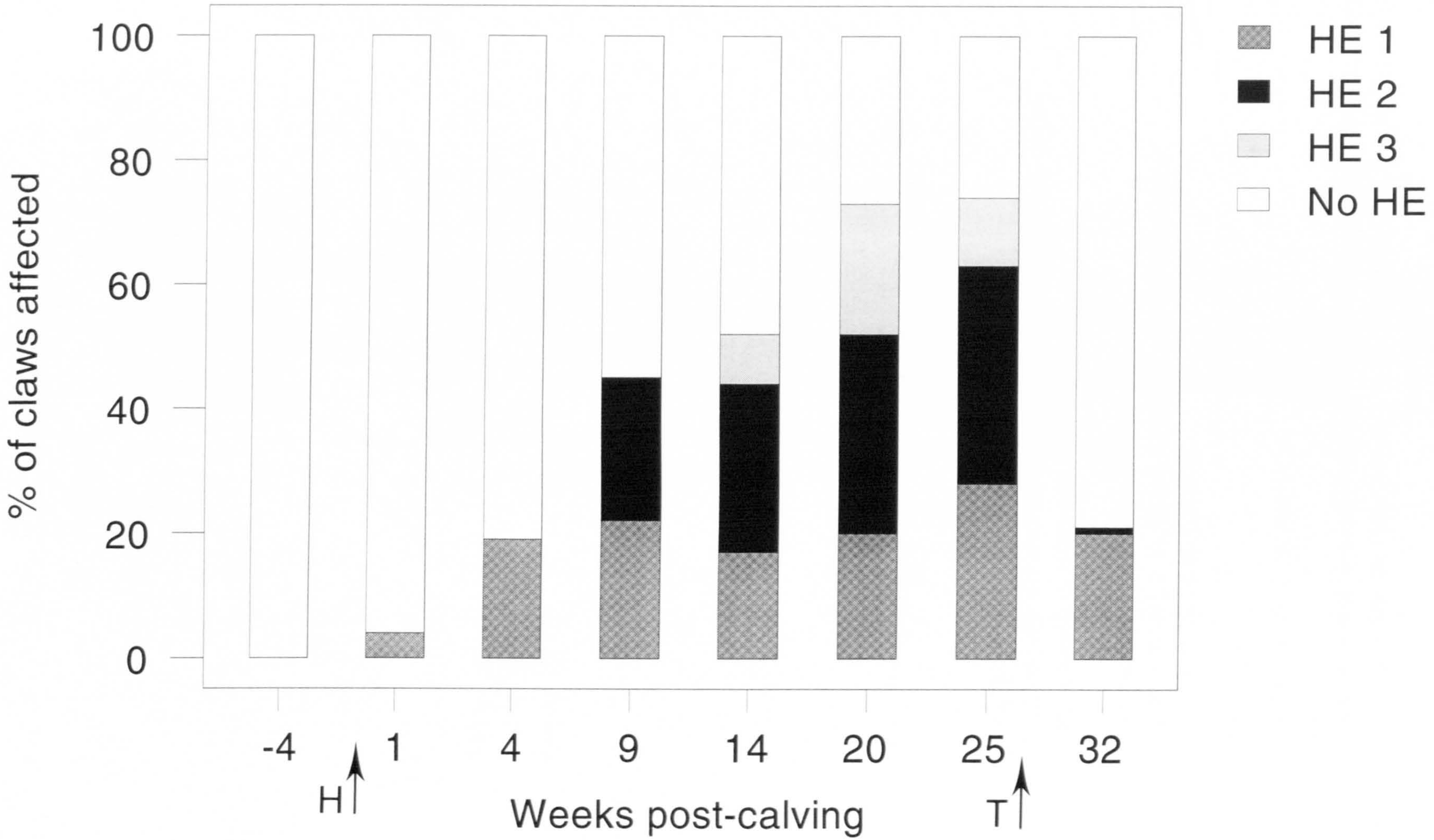
100
80
60
40
20
0
% of claws affected
HE 1
HE 2
HE 3
No HE
-4
1
4
9
14
20
25
32
H
T
Weeks post-calving

Figure 4.17
Median number of lesions and cumulative weighted severity per cow for sole and white line lesions and median total percentage of all eight claws affected

(Pooled data for Groups AC1 and AC2)

Ns cow : Total number of sole lesions
Gs cow : Total cumulative weighted severity score for sole lesions
Ps cow : Total percentage of the sole area affected

Nl cow : Total number of white line lesions
Gl cow : Total cumulative weighted severity score for white line lesions
Pl cow : Total percentage of the white line affected

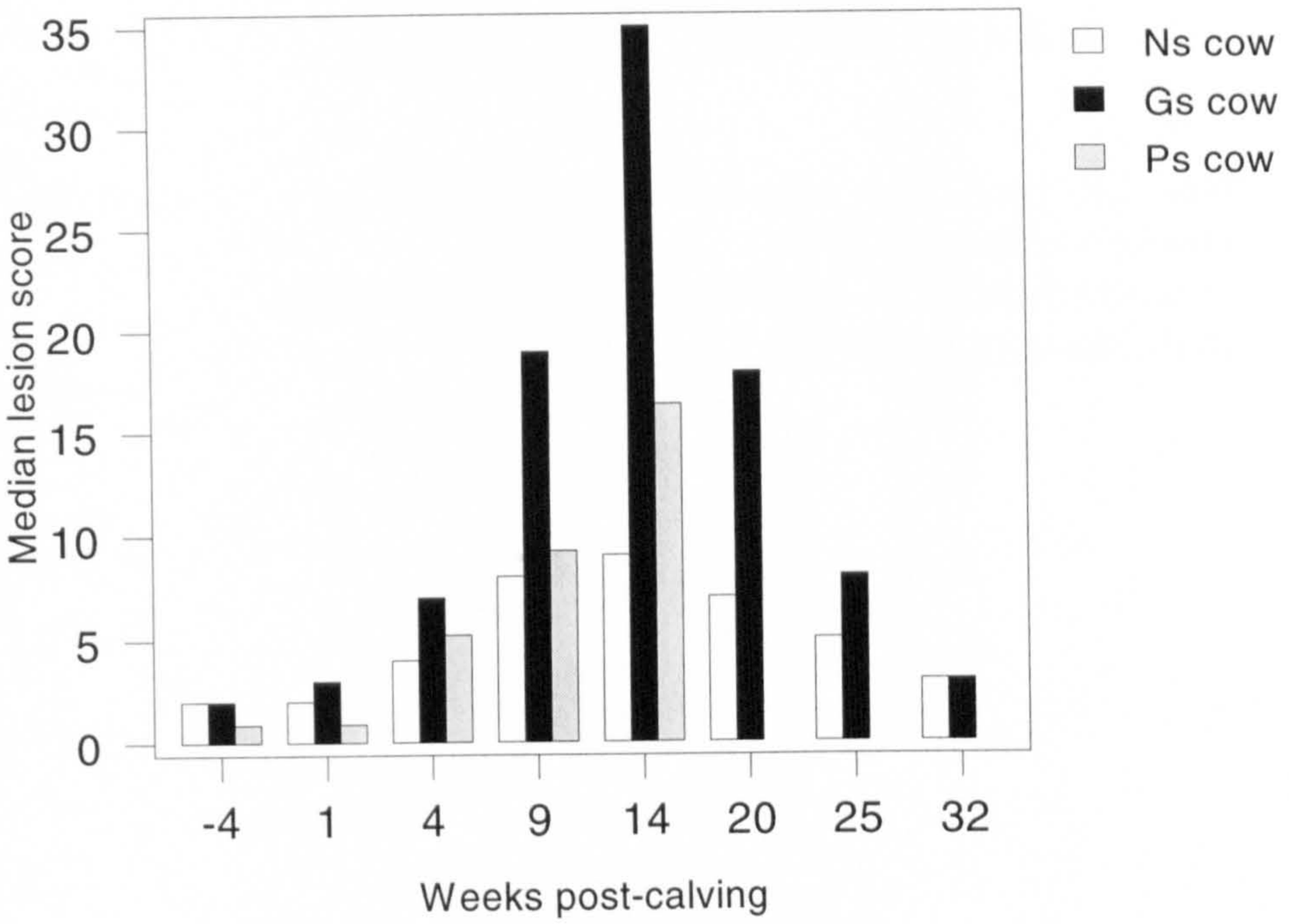
Sole lesions
Median lesion score
0
5
10
15
20
25
30
35
-4
1
4
9
14
20
25
32
Weeks post-calving
Ns cow
Gs cow
Ps cow

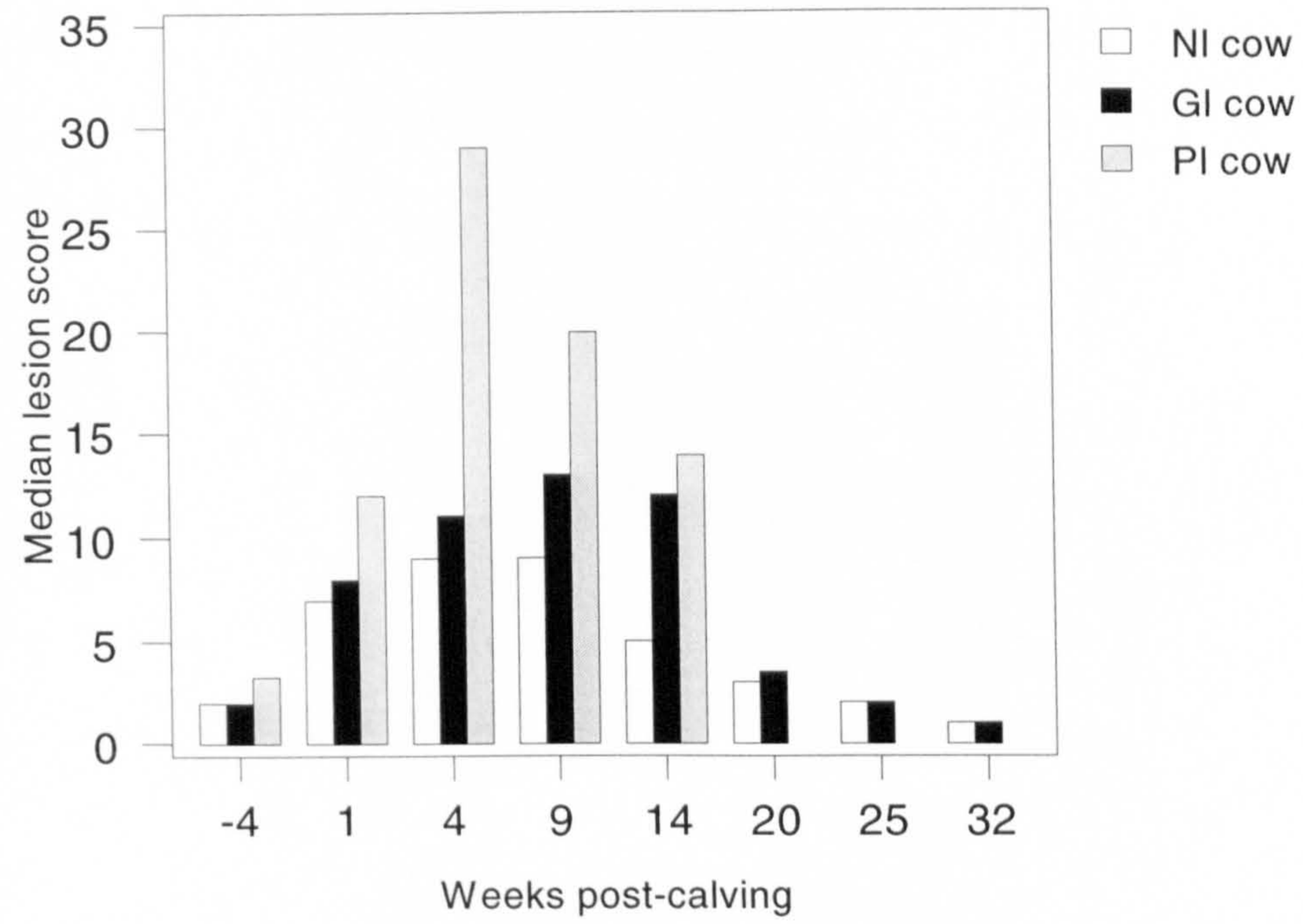
White line lesions
Median lesion score
0
5
10
15
20
25
30
35
-4
1
4
9
14
20
25
32
Weeks post-calving
Nl cow
Gl cow
Pl cow

Figure 4.18
Median total combined lesion score per cow for the sole and white line

(Pooled data for Groups AC1 and AC2)

Cs cow : Total combined lesion score for lesions of the sole
(weighted severity x size)
Cl cow : Total combined lesion score for lesions of the white line
(weighted severity x size)

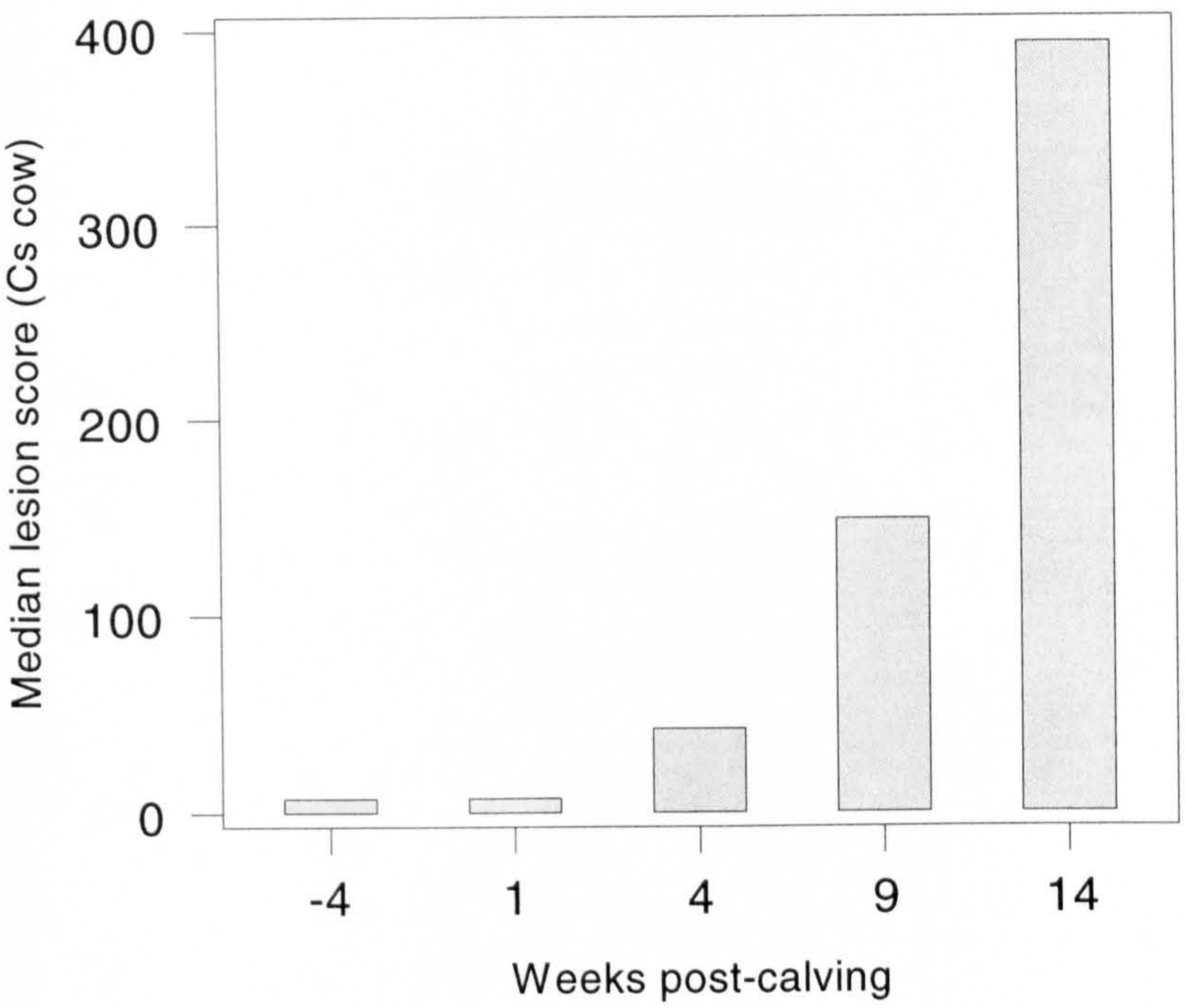
Sole lesions
Median lesion score (Cs cow)
400
300
200
100
0
-4
1
4
9
14
Weeks post-calving

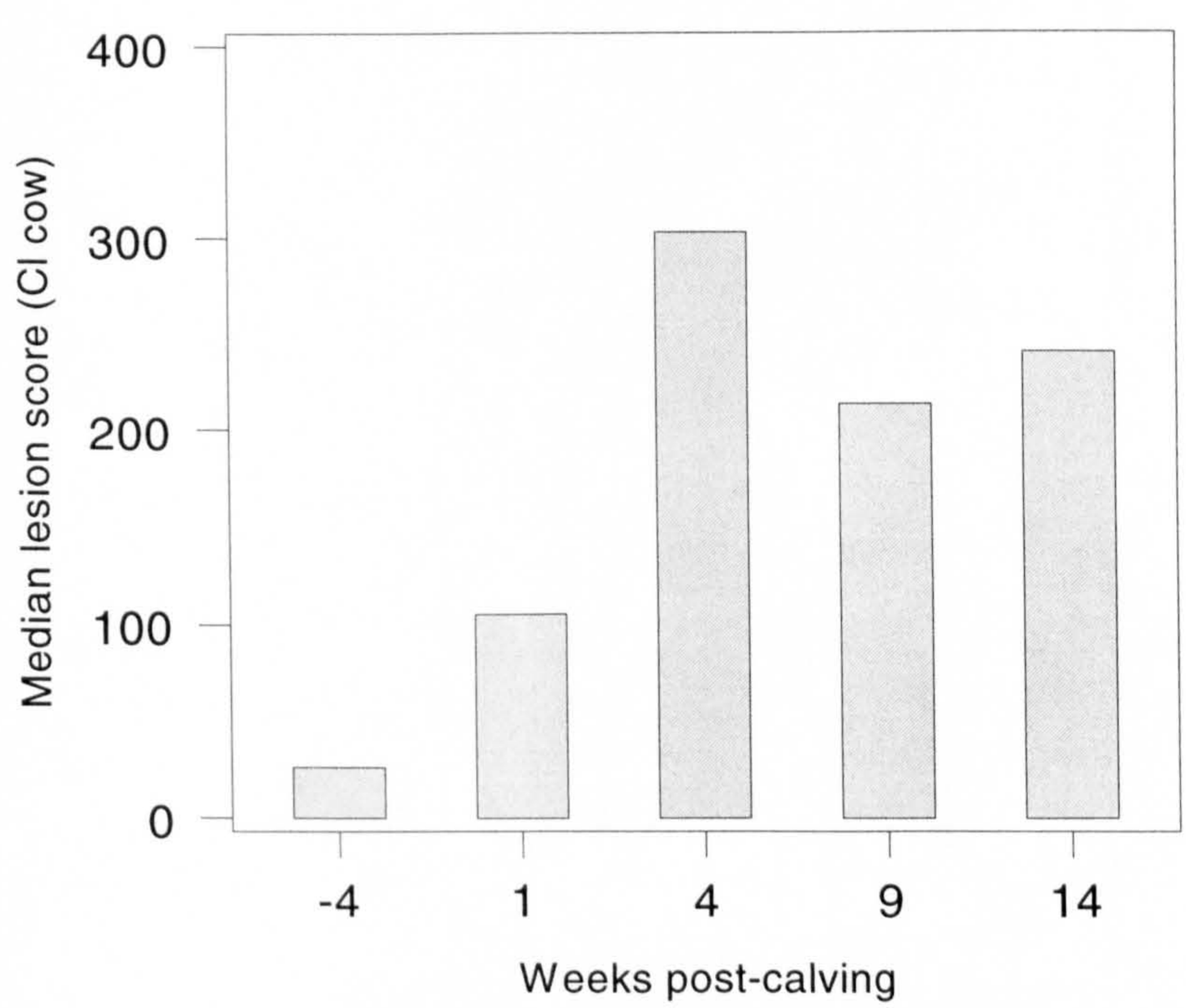
White line lesions
Median lesion score (Cl cow)
400
300
200
100
0
-4
1
4
9
14
Weeks post-calving

Figure 4.19
Variation in mean locomotion score over time in relation to calving and housing

(Pooled data for Groups AC1 and AC2)

(See Table 3.1 for definitions of locomotion score categories)

H ↑ - housing

T ↑ - turnout

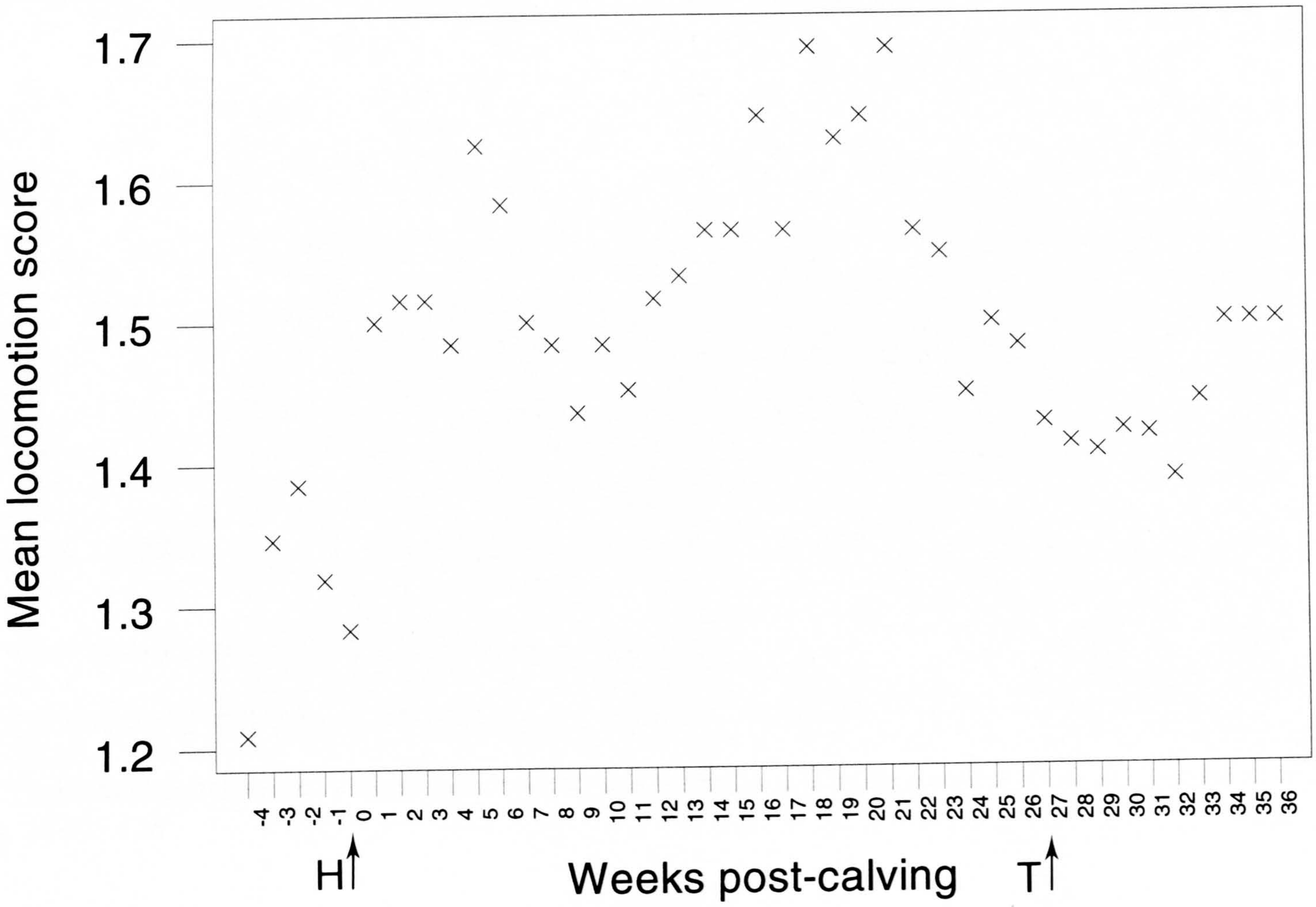
Mean locomotion score
1.7
1.6
1.5
1.4
1.3
1.2
-4 -3 -2 -1 0 1 2 3 4 5 6 7 8 9 10 11 12 13 14 15 16 17 18 19 20 21 22 23 24 25 26 27 28 29 30 31 32 33 34 35 36
H
Weeks post-calving
T

Figure 4.20
Frequency distribution of locomotion scores in relation to calving and housing

(Pooled data for Groups AC1 and AC2)

(See Table 3.1 for definitions of locomotion score categories)

H ↑ - housing

T ↑ - turnout

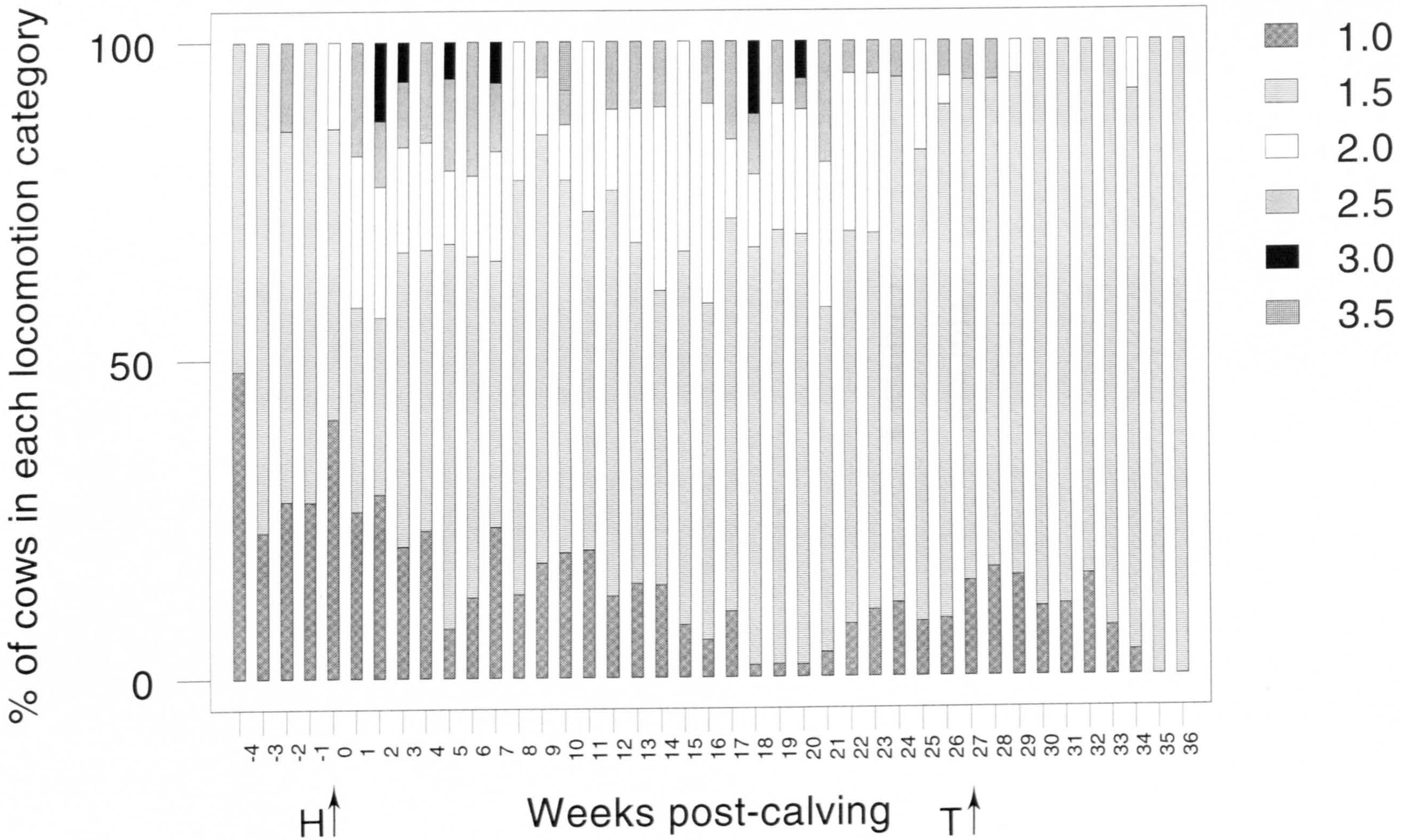
% of cows in each locomotion category
100
50
0
1.0
1.5
2.0
2.5
3.0
3.5
-4 -3 -2 -1 0 1 2 3 4 5 6 7 8 9 10 11 12 13 14 15 16 17 18 19 20 21 22 23 24 25 26 27 28 29 30 31 32 33 34 35 36
H
Weeks post-calving
T

FIGURES

CHAPTER 5

Figure 5.1
Diagram to show the site in the foot from which horn samples were taken and the procedure for sectioning these samples (not to scale)

1 Box shows site of sample sliver on abaxial white line of right hind outer claw

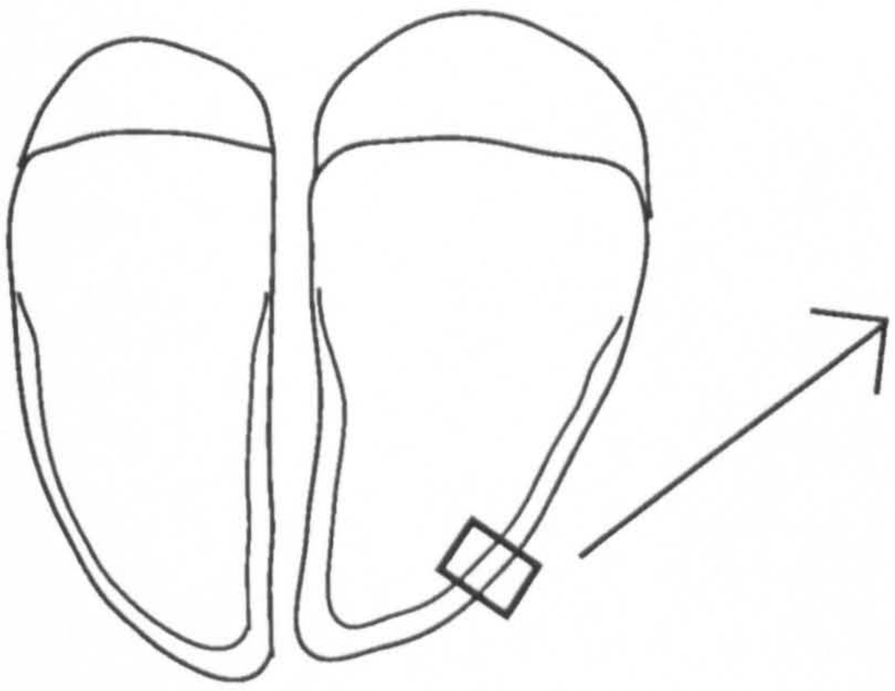

2 Horn sliver approx. 1 mm thick embedded in araldite

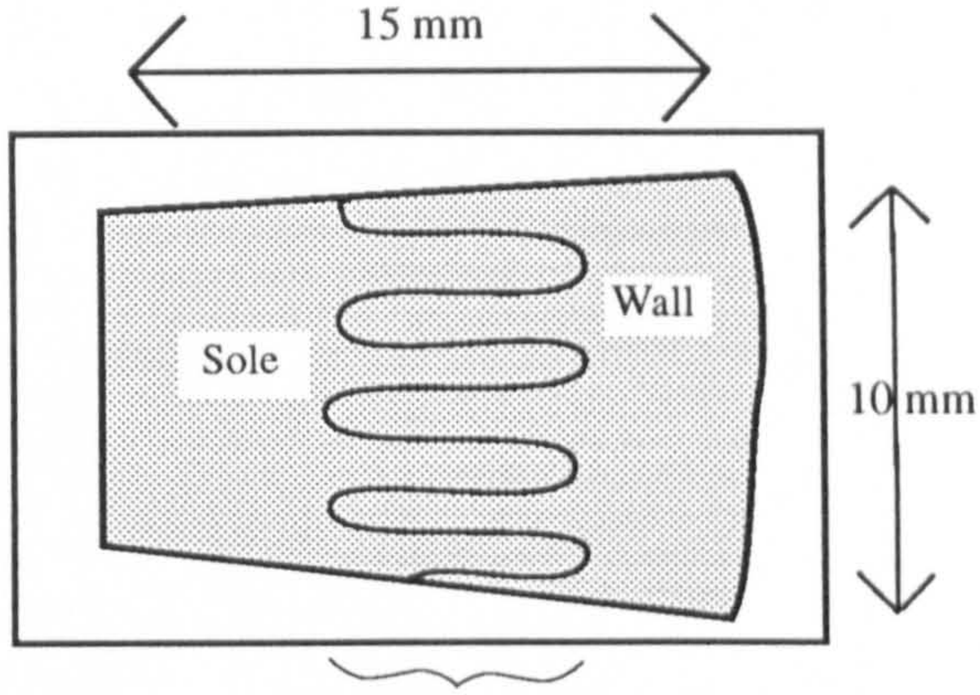

White line

3 Three blocks cut from white line region

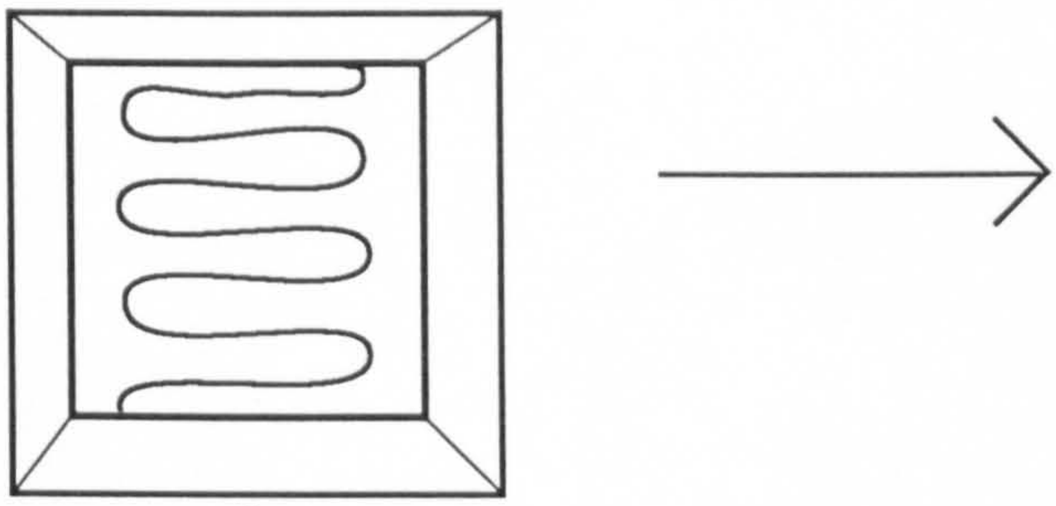

4 Sections for light microscope 1 micron thick

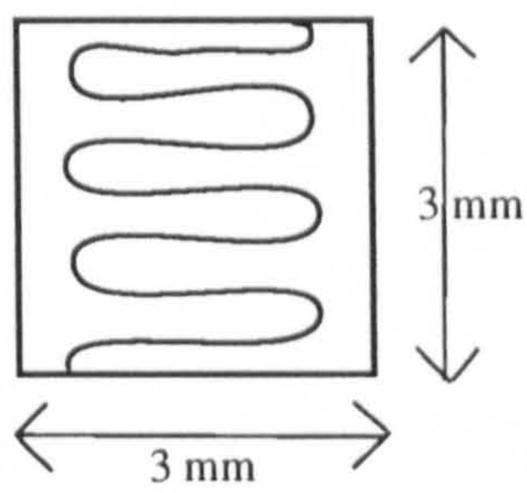

5 Block trimmed down to region of interest

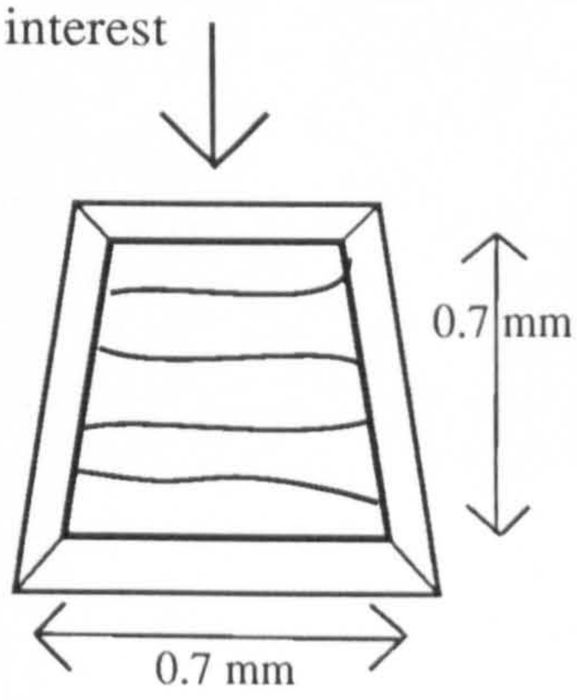

6 Sections for electron microscope 7 nm thick

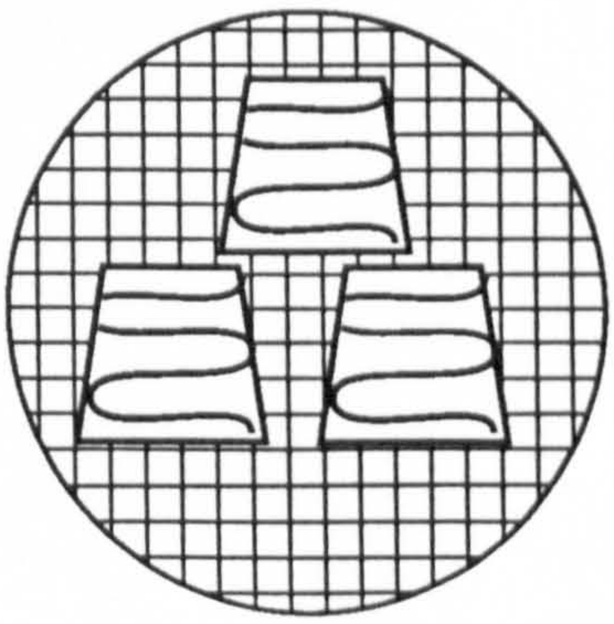

NB All sections are parallel to the distal surface of the foot

Figure 5.2
Micrograph of the laminar horn of the white line with grid overlaid for point-counting

Cell membranes (cm) of adjoining squames (s) are separated in places by electron lucent intercellular material (i).

x 25,000

Cow 84 Group L 4 weeks post-calving. Sample quadrat

The large grid (1 cm squares) was used for the pilot study.
In the main investigations, the large grid (1 cm squares) was used for estimating the volume fraction of cell membrane. The small grid (0.5 cm squares) was used for estimating the volume fraction of intercellular material. The volume fraction of intracellular material was obtained by subtraction.

\ : Points falling on membrane

o : Points falling on intercellular material

In this example, 16/285 points fell on membrane (5.6 %)
42/1073 points fell on intercellular material (4.4 %)

(A micrograph with a larger than average volume fraction of intercellular material was selected for clarity of illustration)

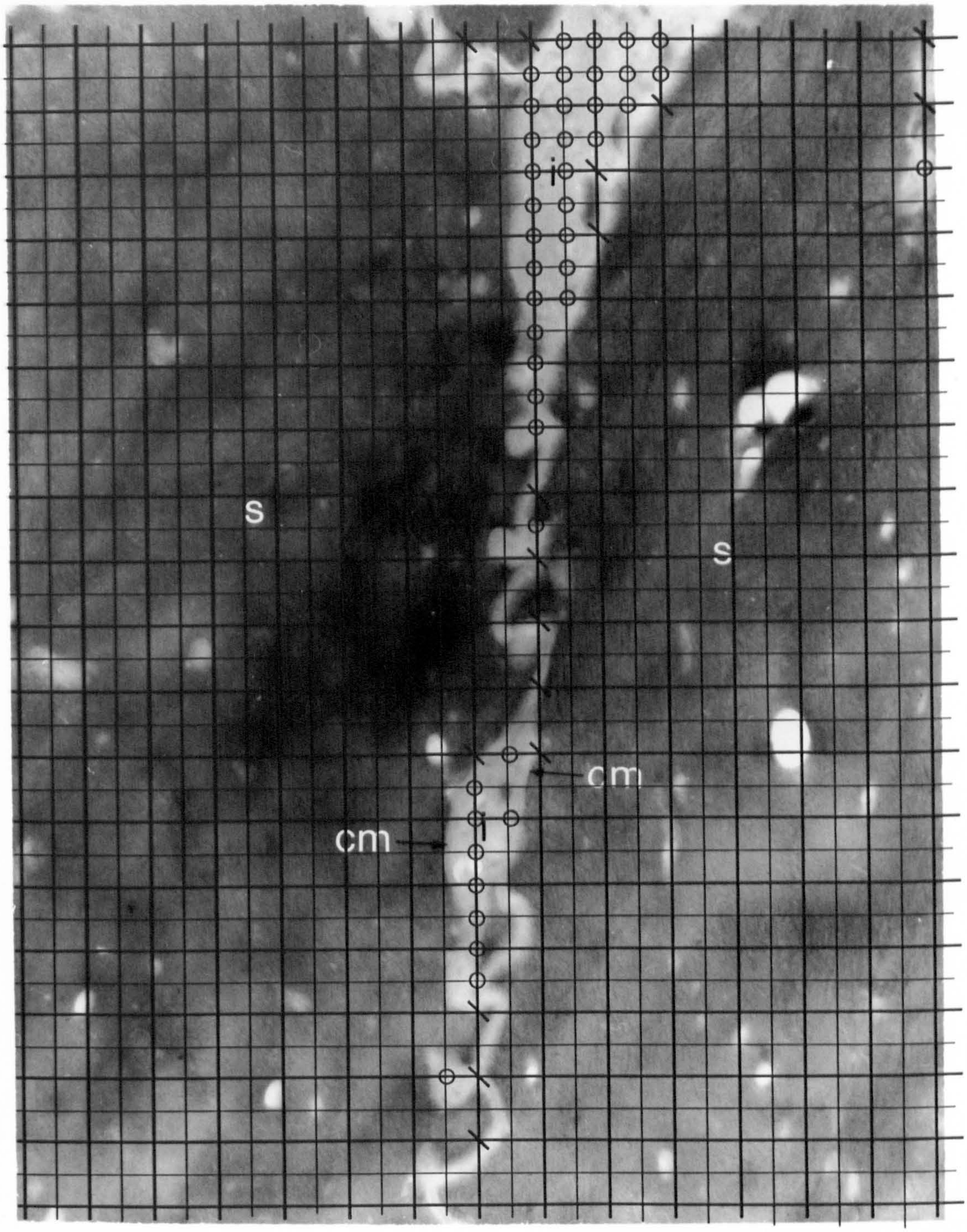
i
s
s
cm
cm

Figure 5.3
Micrograph of a sample of interdigitating horn with minimal intercellular material

Cell membranes (cm) of adjacent squames (s) are tightly apposed. Amounts of intercellular material (i) are minimal. Bundles of keratin fibres (kf ↑) are cut in transverse section.

x 25,000

Volume fraction of membrane = 13.7%.
Volume fraction of intercellular material = 0.74%

Cow 47 Group H Pre-calving. Sample quadrat.

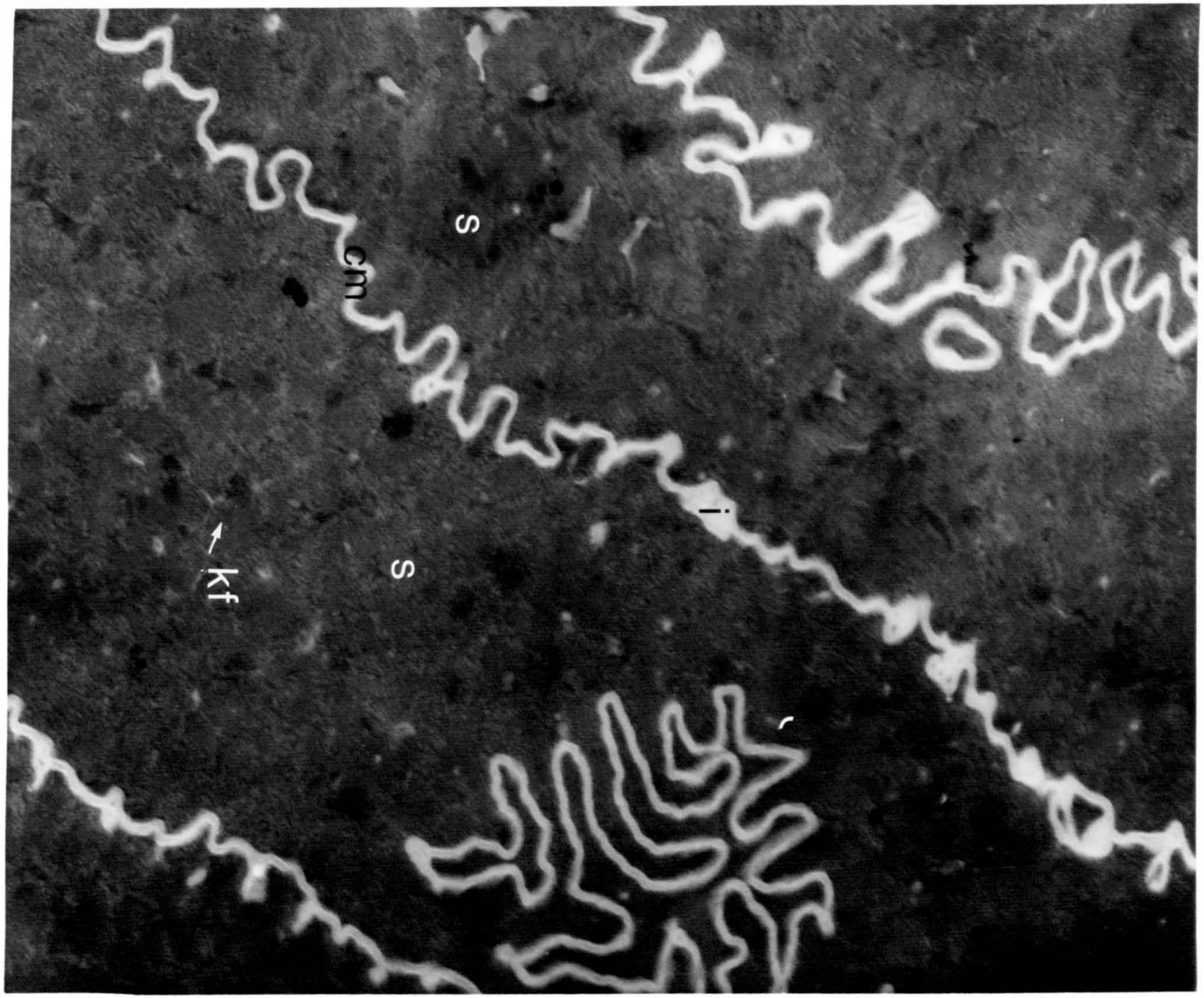
cm
s
kf
s
i
r

Figure 5.4
Micrograph of a sample of laminar horn with small amounts of reticulate intercellular material

Adjacent squames of laminar horn (s) are separated by small amounts of reticulate intercellular material (r) which are found in areas where the intercellular space is widened. Remnants of desmosomes (d) are visible where cell membranes (cm ↑) are closely apposed. There are shallow interdigitations (id) between adjoining squames. Bundles of keratin fibres (kf) are orientated parallel to the long axes of the squames.

x 28,750

Cow 30 Group H 9 weeks post-calving. Sample quadrat.

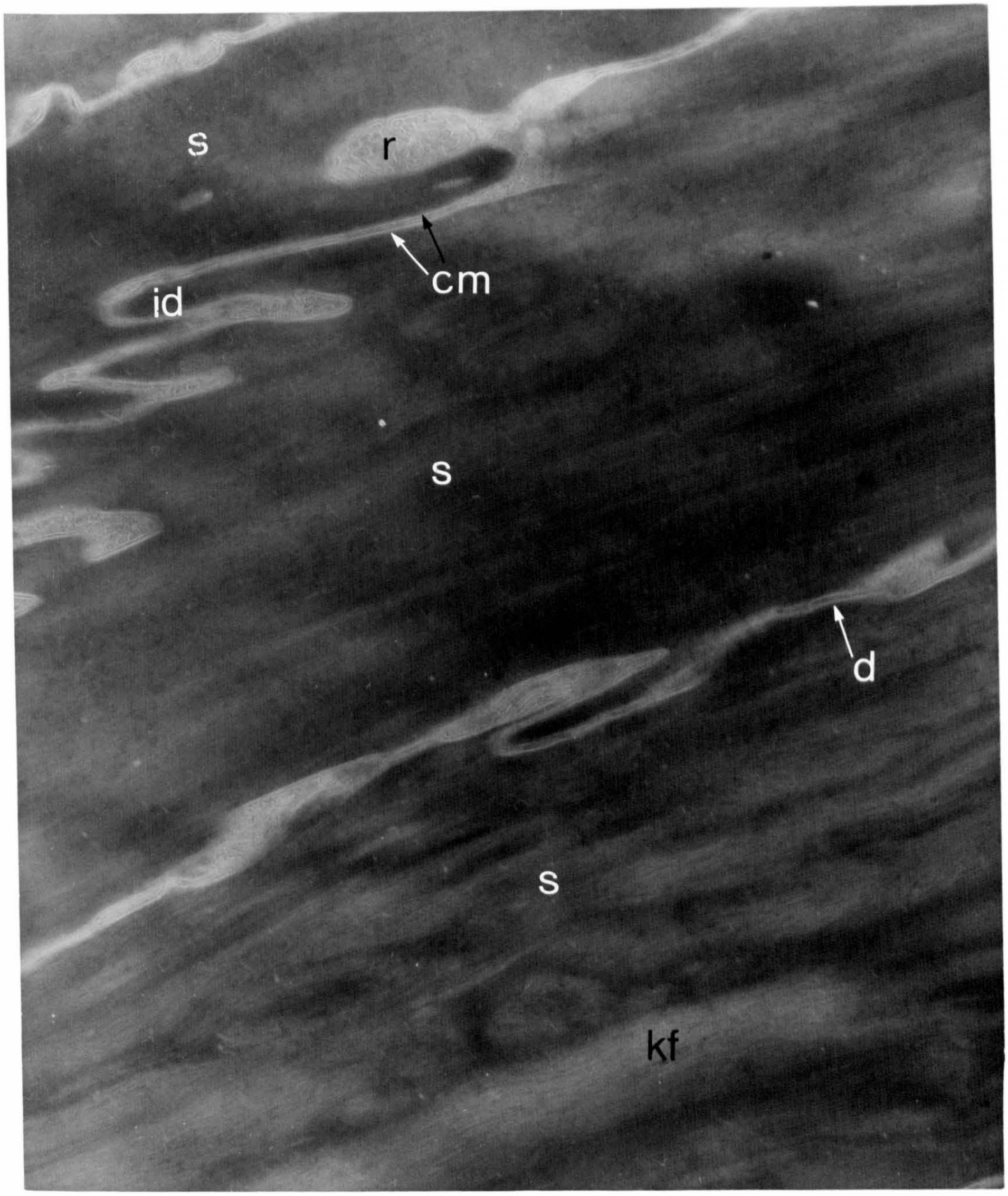
s
r
cm
id
s
d
S
kf

Figure 5.5
Micrograph of laminar horn showing reticulate and amorphous intercellular material

Adjacent squames (s) are separated by reticulate (r) and amorphous (a) intercellular material. The irregular electron density of cell contents and lack of organisation of keratin filaments indicate some disturbance of keratinization.

x 28,750

Cow 91 Group L 9 weeks post-calving. Sample quadrat.

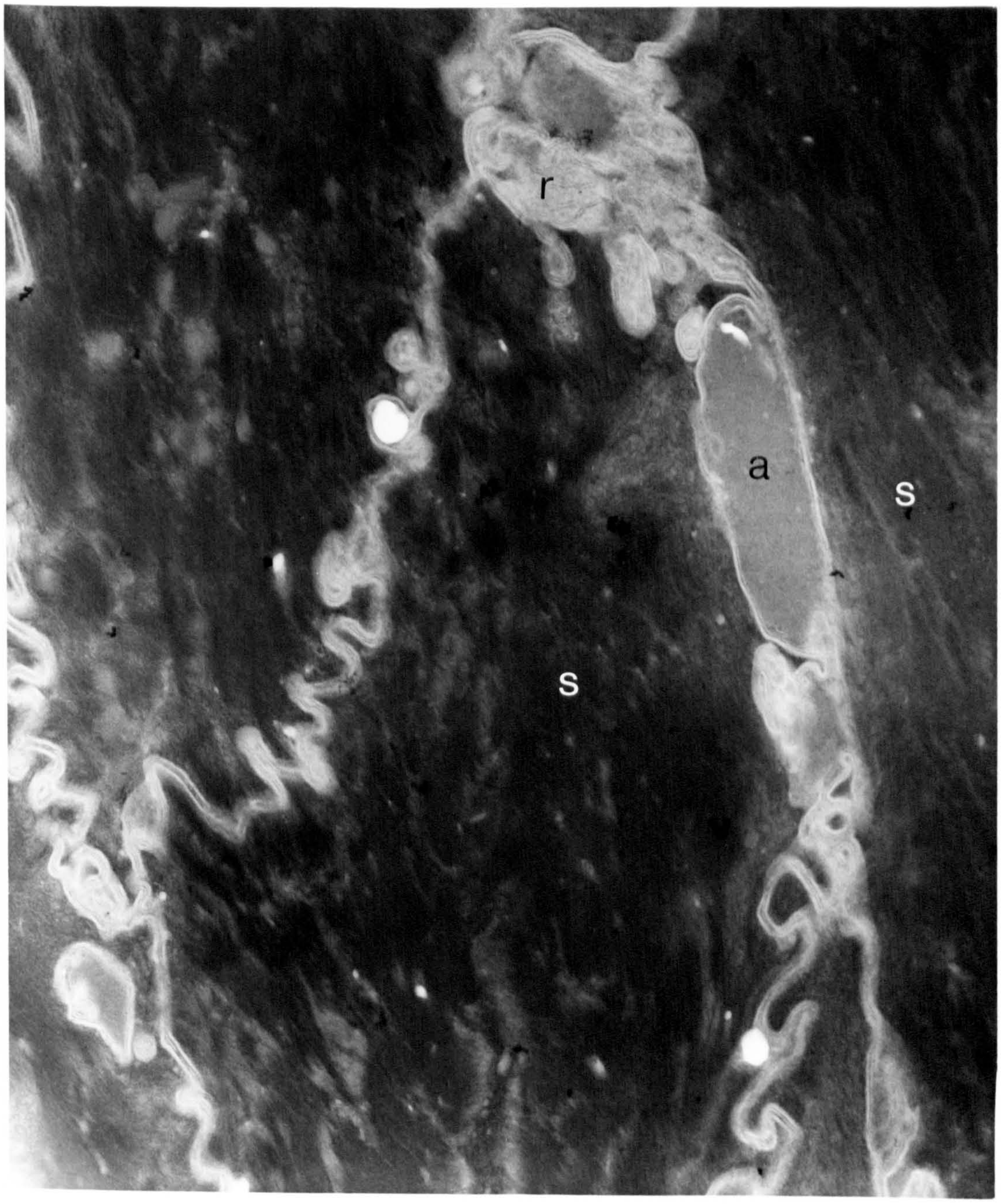
r
a
s
S

Figure 5.6
High power micrograph of electron lucent intercellular material

Parts of two adjacent squames (s) are visible in the top right hand corner of the micrograph. Between them the cell membranes are closely apposed. The majority of the micrograph, however, is occupied by electron-lucent intercellular material. A laminated pattern can be detected within the intercellular material at this high magnification.

x 115,500

Cow 47 Group H Pre-calving. Selected area.

Figure 5.7
High power micrograph of reticulate intercellular material

The intercellular space between adjacent cell membranes is widened and filled with intercellular material in which a reticulate pattern can be seen. A surviving desmosome (d) is visible.

x 88,750

Cow 84 Group L 28 weeks post-calving. Sample quadrat.

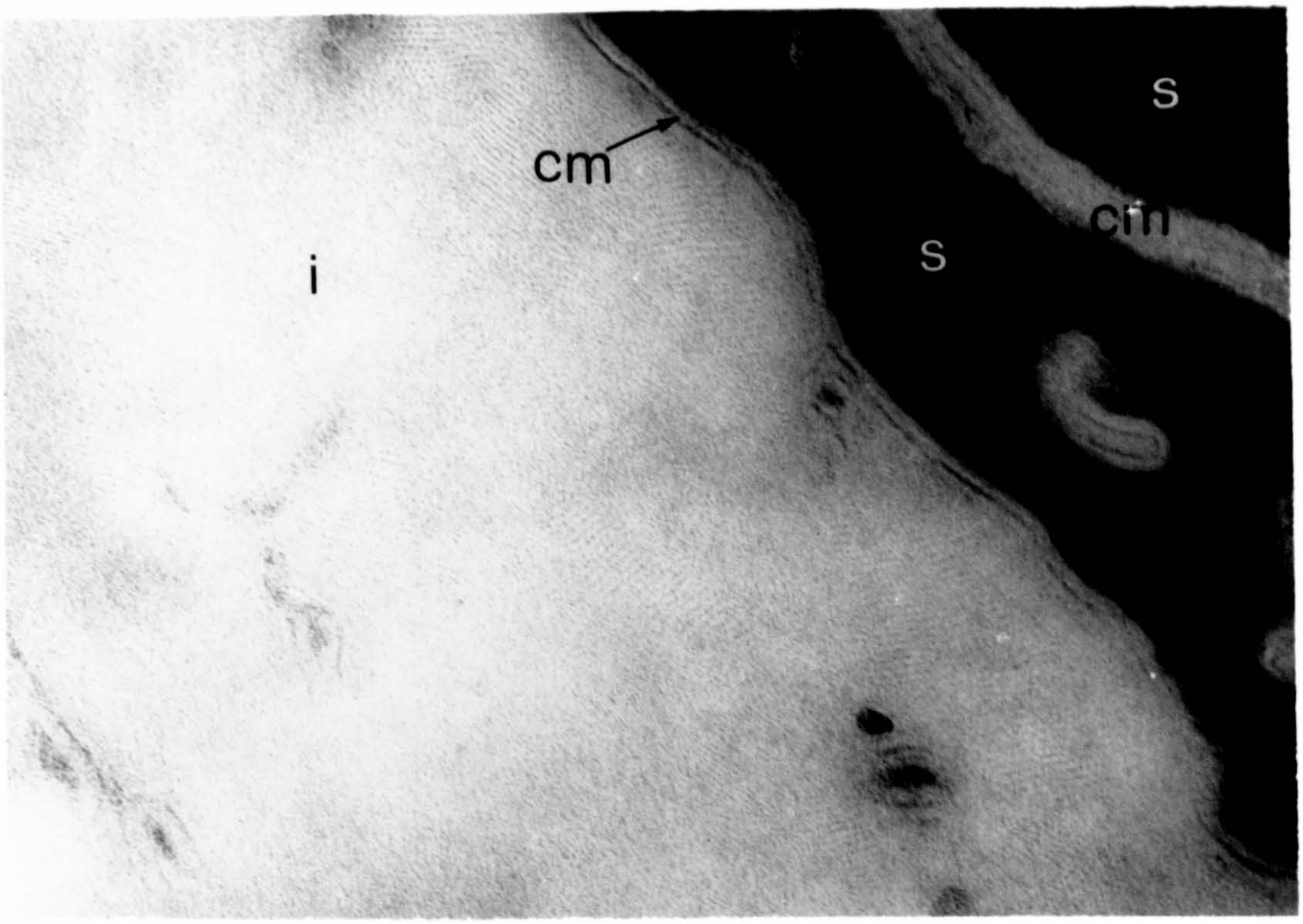
cm
S
cm
S
i

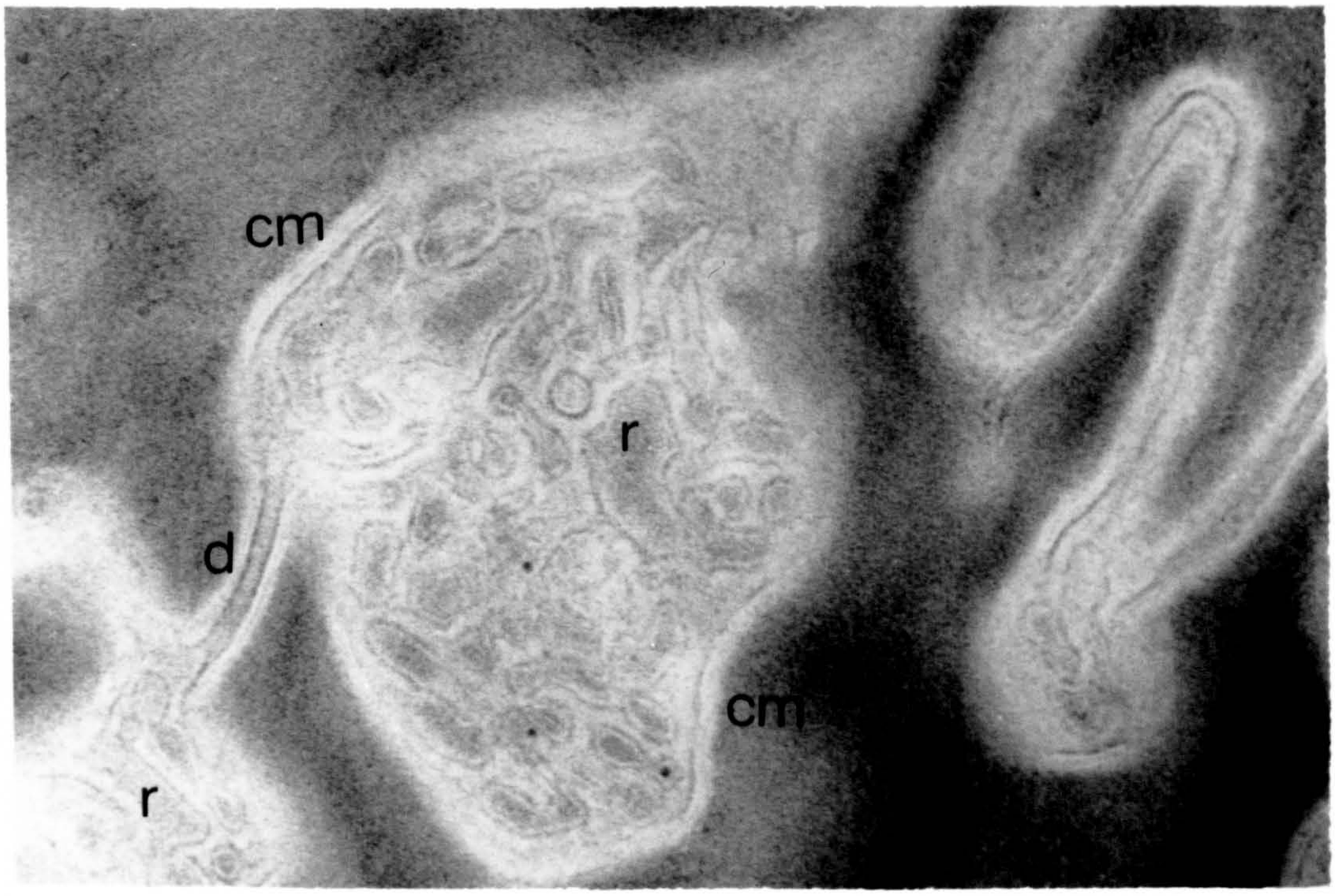
cm
r
d
r
cm

Figure 5.8
Micrograph of squames of laminar horn showing abnormal electron-dense intracellular structures

Discrete electron dense structures (ed) are visible within two squames. These are likely to be lipid remnants of organelles which have not become incorporated into the matrix.

x 28,750

Cow 53 Group H 9 weeks post-calving. Sample quadrat.

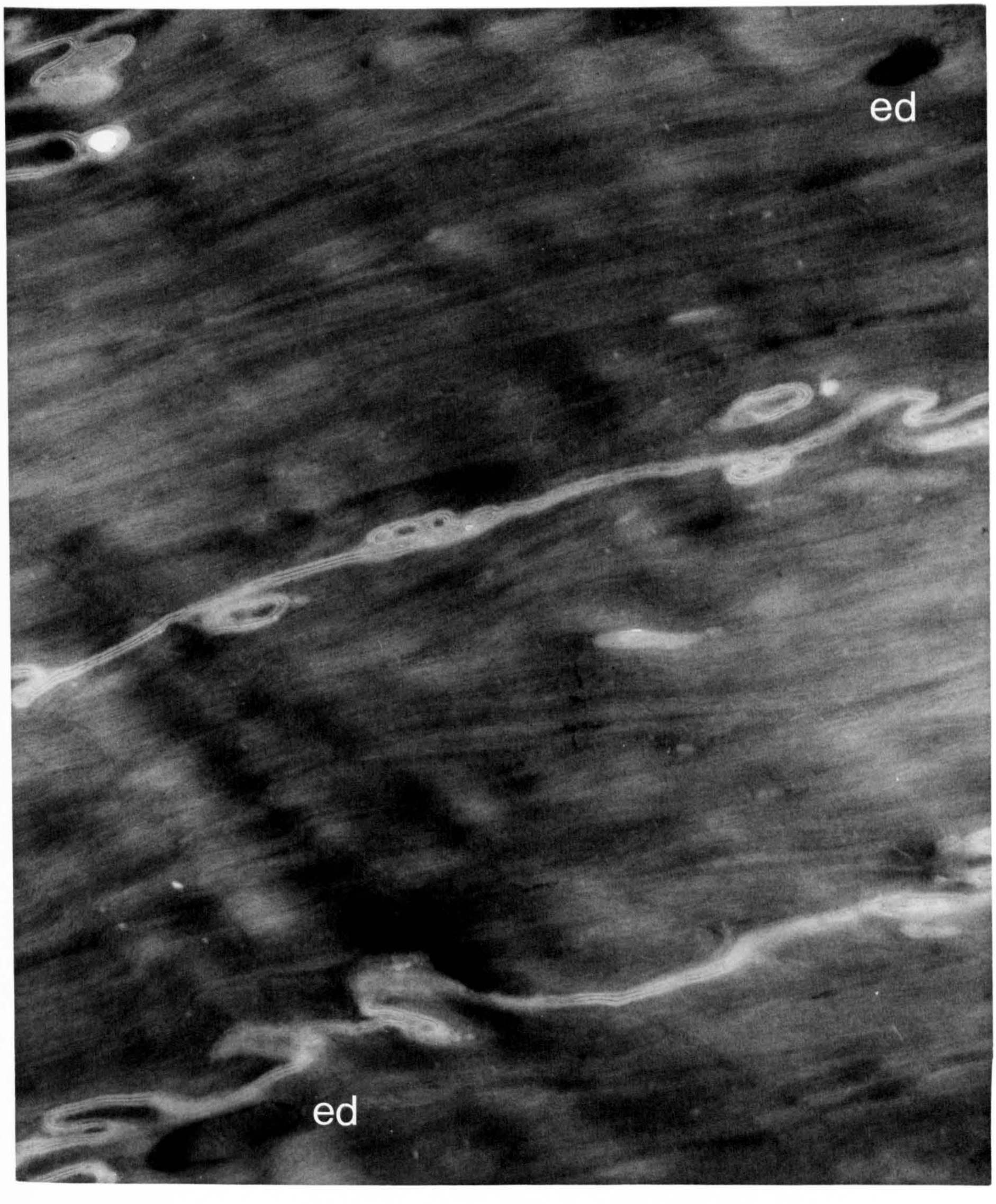
ed
ed

Figure 5.9
Micrograph of squames of laminar horn showing nuclear remnants

The remains of a nucleus (n) are visible in one squame. This is indicative of incomplete keratinization. The nucleus has become compressed and elongated. Like the keratin filaments (kf) it is orientated parallel to the long axis of the squame. Small amounts of intercellular material are present (i).

x 28,750

Cow 30 Group H 9 weeks post-calving. Sample quadrat.

Figure 5.10
Low power micrograph of an abnormal region of laminar horn

Intercellular material (i) is widespread. Squame contents show irregular electron density (ir) and in places the keratin filaments are very sparse (*).

x 10,350

Cow 84 Group L 20 weeks post-calving. Selected area

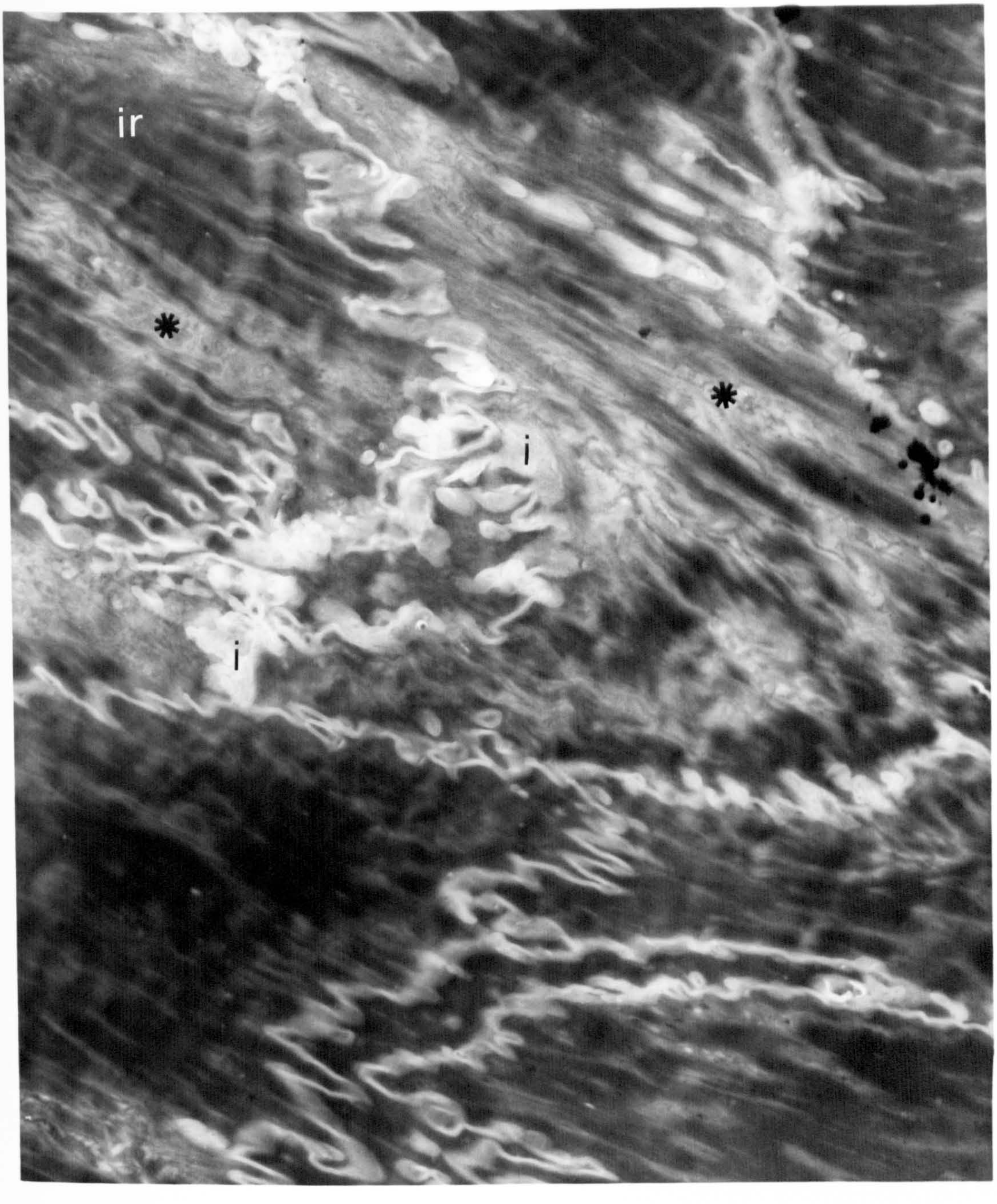
ir
*
*
i
i

Figure 5.11
Micrograph of squames of interdigitating horn with abnormal intracellular structure

Squame contents show irregular electron density (ir) and in places keratin fibres (kf) are sparse and poorly organised. A large nuclear remnant (n) is visible.

x 28,750

Cow 84 Group L 20 weeks post-calving Sample quadrat

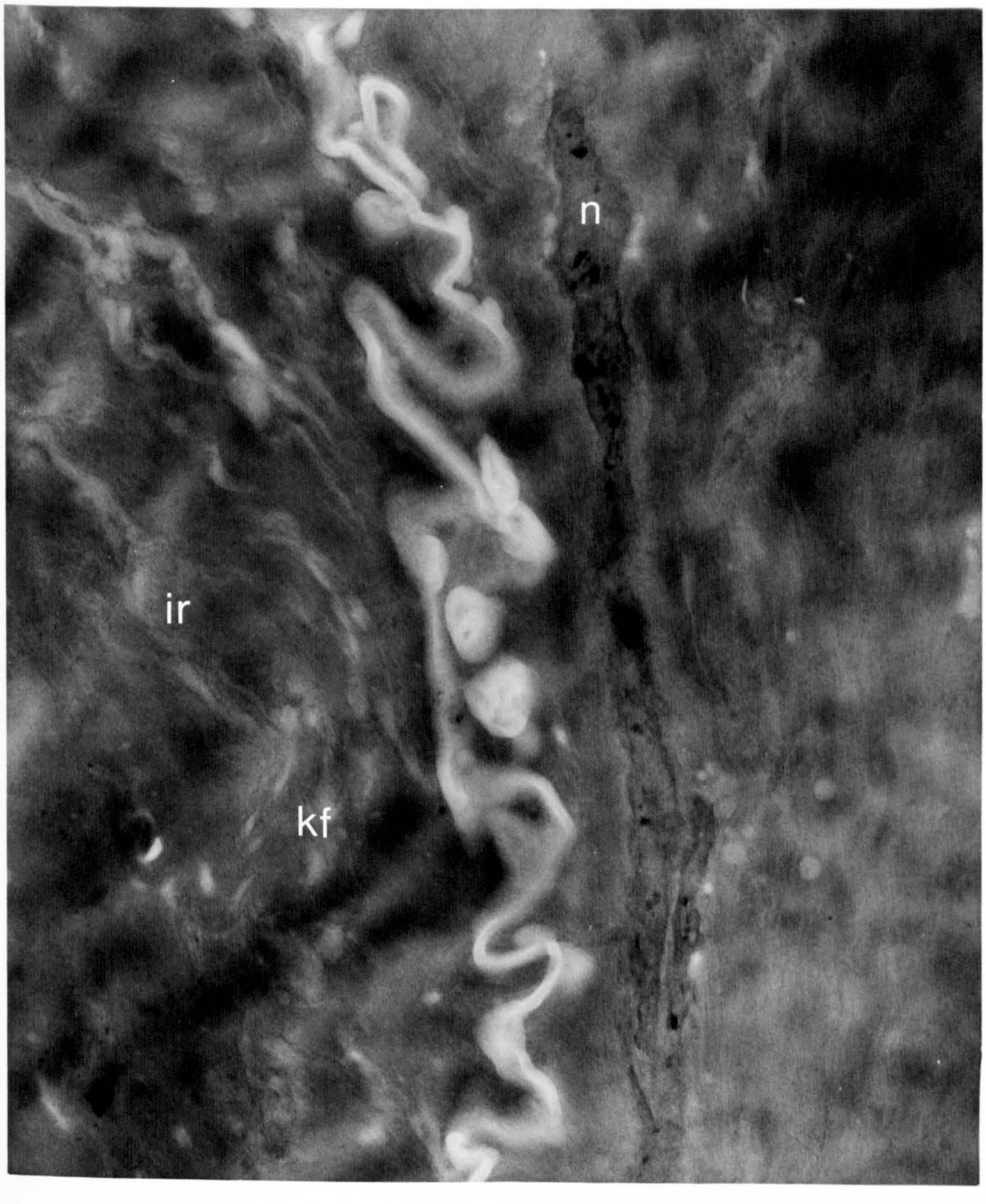
n
ir
kf

Figure 5.12
Micrograph of an extensive region of amorphous and reticulate intercellular material between squames of laminar horn

Large amounts of amorphous (a) and reticulate (r) intercellular material are present in the intercellular space. Intracellular material shows irregular electron density and remnants of organelles (↑) are visible within squames.

x 10,350

Cow 47 Group H 25 weeks post-calving. Sample quadrat.

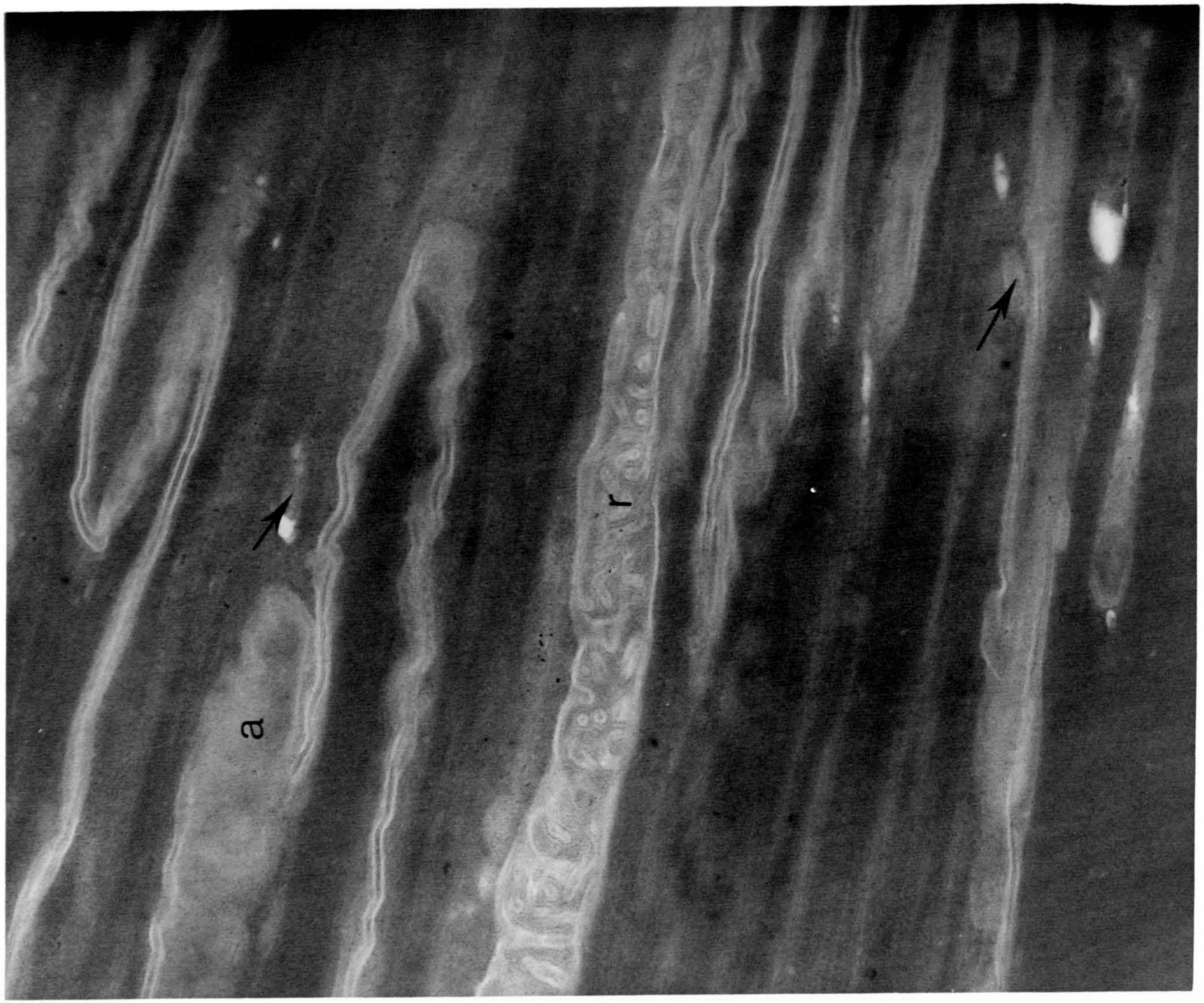
a

Figure 5.13
Micrograph showing a region of interdigitating horn with abnormal intercellular and intracellular structure

Cell membranes (↑) are widely separated by large areas of amorphous intercellular material (a). Remnants of desmosomes (d ↑) survive in places between regions of widened intercellular space. Keratin fibres (kf) within one squame are sparse and poorly organised. The adjacent squame contains granular electron dense deposits.

x 28,750

Cow 47 Group H 25 weeks post-calving. Selected area.


d
a
d
a
kf

Figure 5.14
Micrograph showing an extensive region of reticulate intercellular material between adjacent squames of laminar horn

Membranes of adjacent squames (cm) are separated by reticulate intercellular material (r).

x 28,750

Cow 84 Group L 25 weeks post-calving. Sample quadrat.

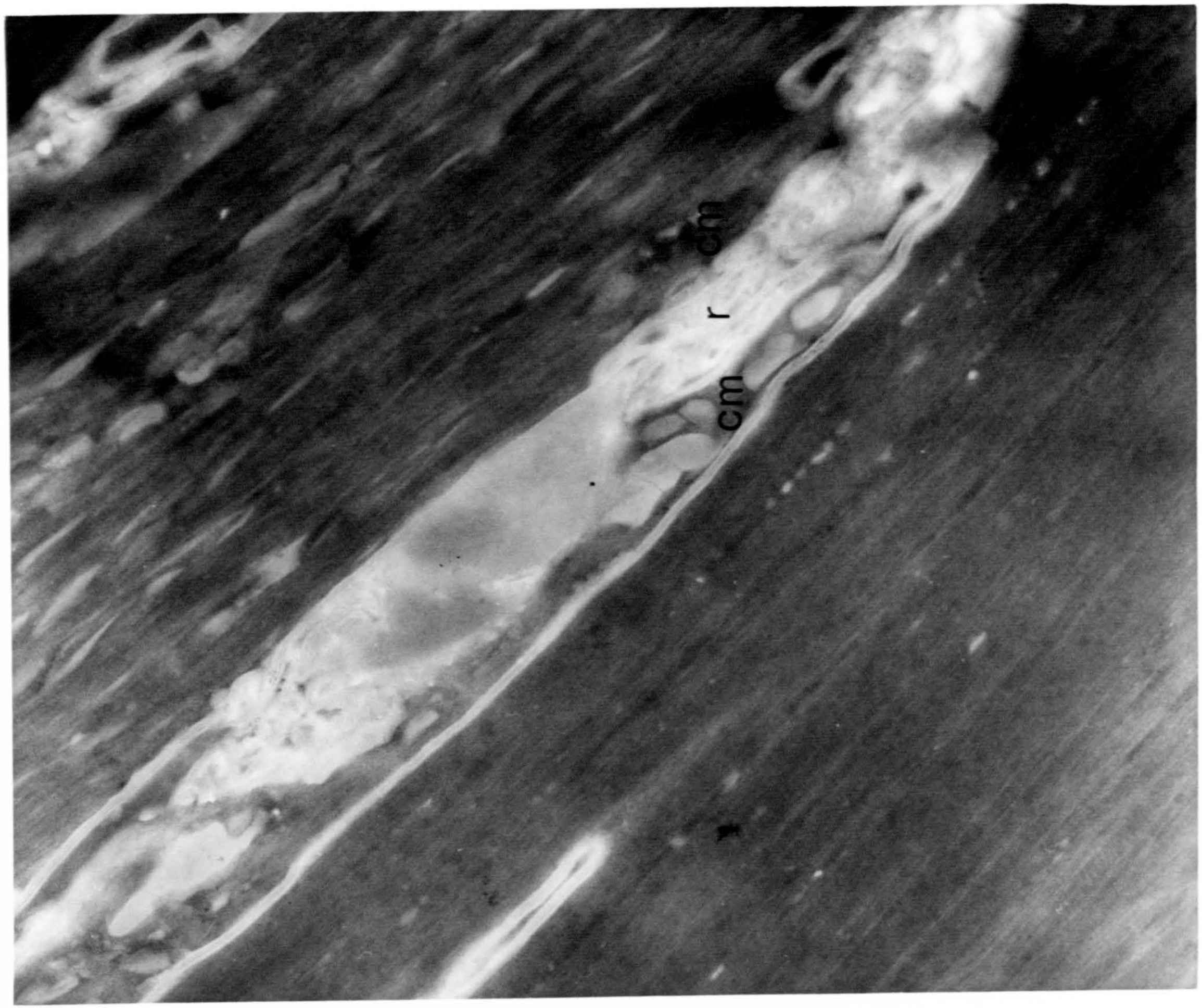
cm
r
cm

Figure 5.15
Low power micrograph of a region of abnormal structure at the edge of the laminar horn

Large amounts of amorphous intercellular material (a) fill the intercellular spaces, which have become widened in between surviving desmosomes (d ↑). Squames (s) are widely separated. The intracellular material has a "marbled" appearance (m) and the normal organisation of keratin filaments is lacking. Electron lucent intracellular structures (ly) are likely to be lysosomes.

x 10,350

Cow 47 Group H 25 weeks post-calving. Selected area.

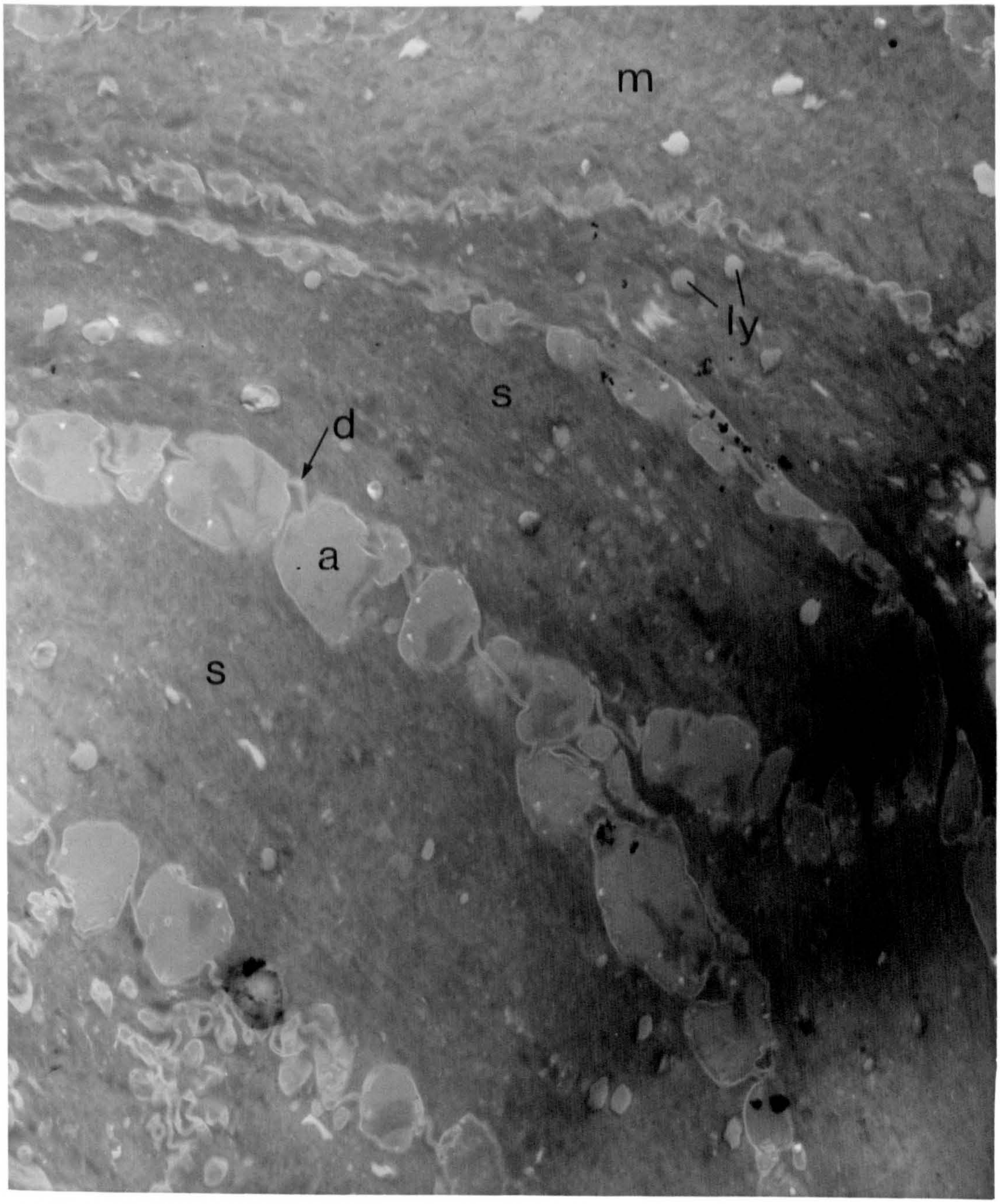
m
ly
s
d
a
s

Figure 5.16
Low power micrograph of a large area of disruption in the laminar horn

Some squames have a marbled appearance (m) while others are degenerate (ds). Keratin filaments (kf) are sparse and disorganised and there are distinct nuclear remnants (n). Extensive regions of amorphous intercellular material (i) separate the squames. Cell boundaries (b) are indistinct.

x 10,350

Cow 47 Group H 25 weeks post-calving. Selected area.

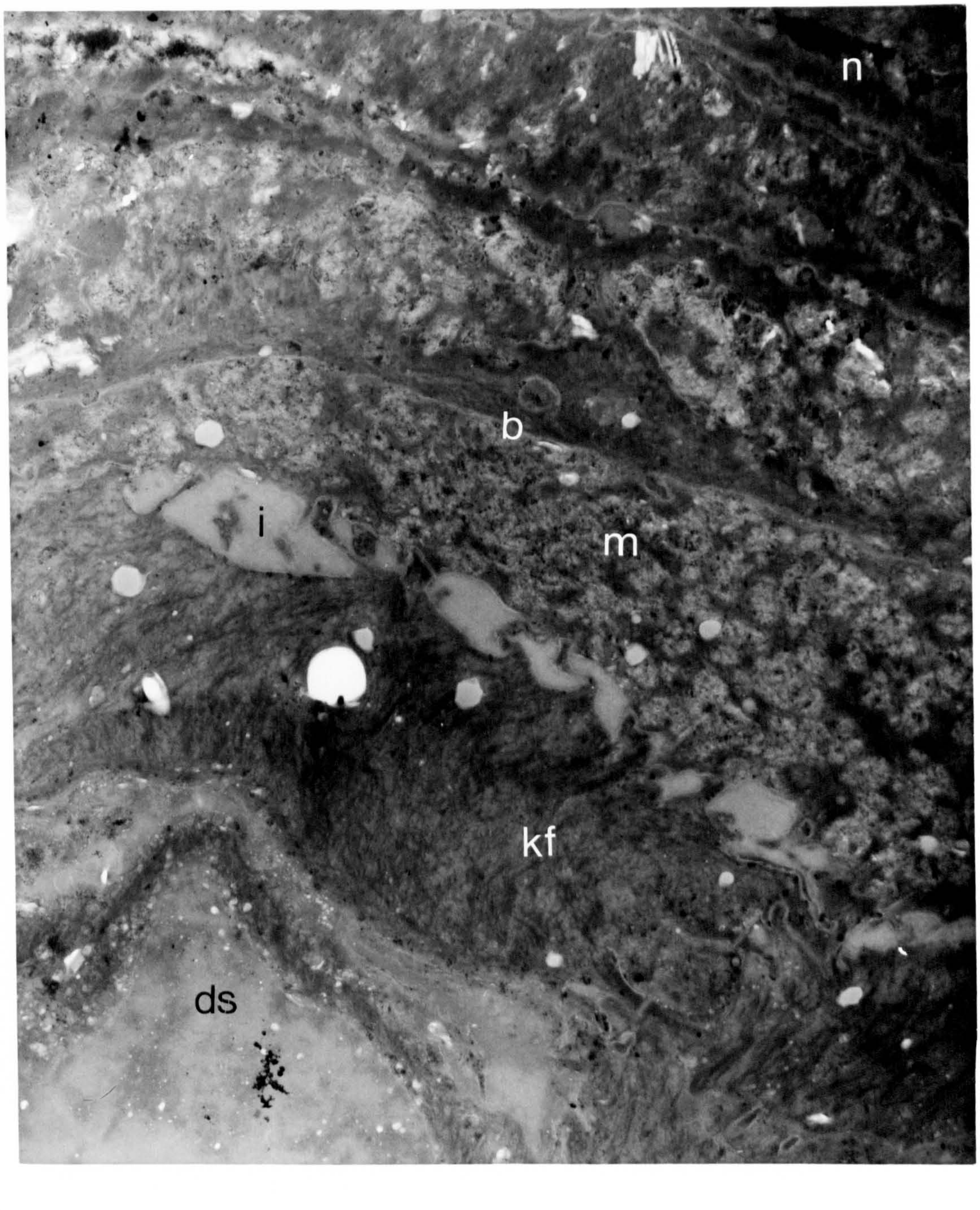
n
b
i
m
kf
ds

Figure 5.17
Micrograph of an abnormal region of interdigitating horn adjacent to the laminar horn shown in Figure 5.16

Cell boundaries (b) are contorted and discontinuous. Those squames which can be distinguished are degenerate (ds) or have a marbled appearance (m). Electron-dense lipid droplets (l) are visible and remnants of electron-dense nuclear material (n↑) are dispersed within squames. There are large areas of intercellular debris (i).

x 10,350

Cow 47 Group H 25 weeks post-calving. Selected area.


n
m
ds
b
n
l
i
i

Figure 5.18
Micrograph of a selected abnormal region in laminar horn

The electron-density of squames is very variable. One squame has a marbled appearance (m) while in another there is a large nuclear remnant (n). Squame boundaries are very contorted and there are considerable amounts of intercellular material.

x 10,350

Cow 84 Group L 25 weeks post-calving. Selected area.


i
c
i
m

Figure 5.19
High power micrograph of an intracellular region with marbled appearance

The marbled appearance of squames was due to electron lucent areas (*) with sparse keratin fibres (kf). Physical weakness in these areas often resulted in the formation of holes in the sections during preparation or viewing.

x 12,500

Cow 84 Group L 20 weeks post-calving. Selected area.

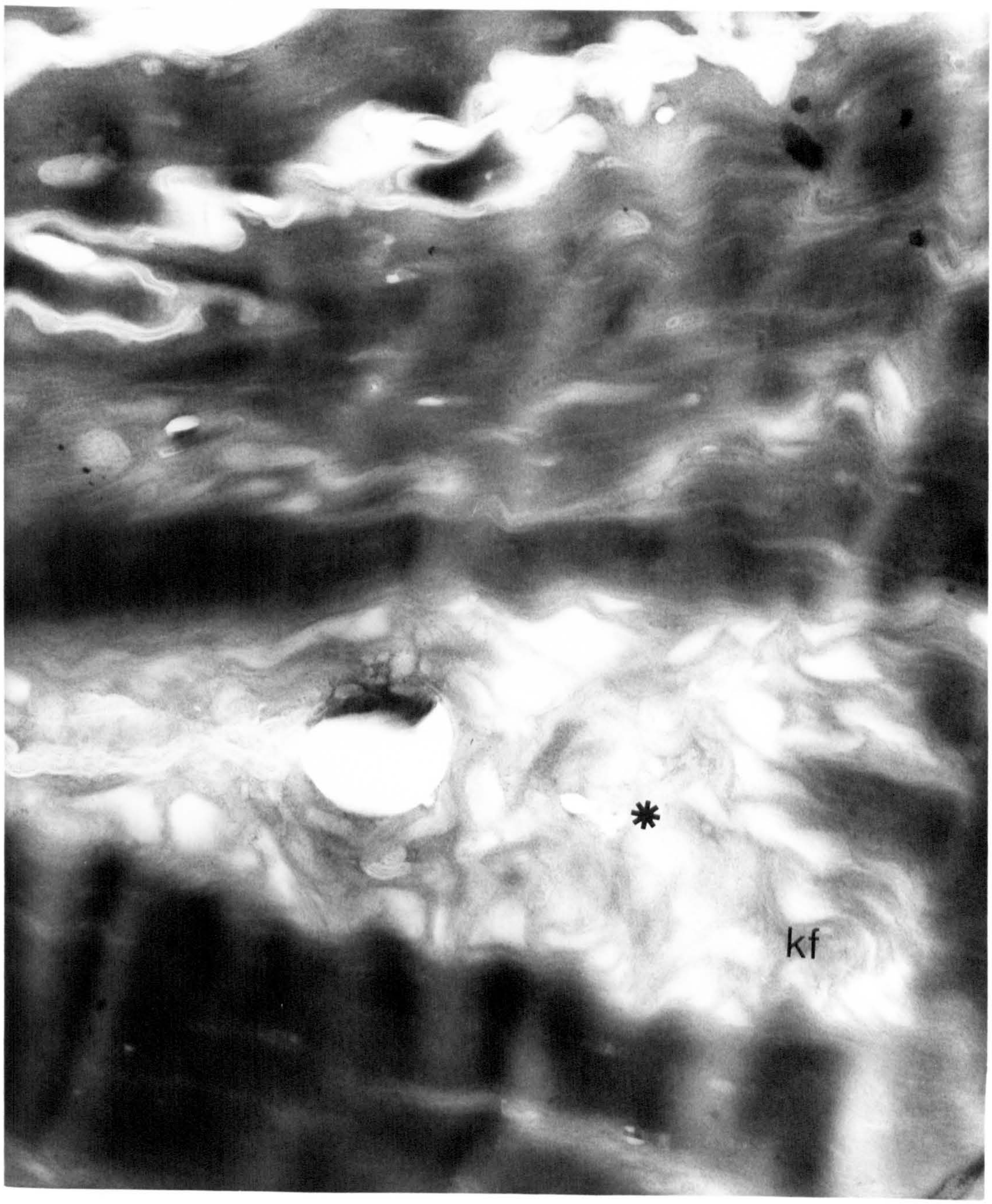
*
kf

Figure 5.20
Variation in lesion score and horn ultrastructure score over time for two cows, one with high and one with low gross lesion score

In this comparison the animals were ranked on the total combined lesion score for the right hind outer claw (*Ct claw8* = *Cs claw8* + *Cl claw8* - see Table 4.3) at nine weeks post-calving.
Cow 47 had a high gross lesion score at nine weeks post-calving
(i.e. large and severe lesions of the sole and white line). Cow 84 had a low score at this time.

A. Lesion scores for the outer hind claws plotted against time

Ct = combined score for sole and white line
Cl = combined score for white line only

B. Volume fraction (%) of intercellular material (ICM) in the laminar horn (LH) of the white line plotted against time

C. Volume fraction (%) of intercellular material (ICM) in the interdigitating horn (IDH) of the white line plotted against time

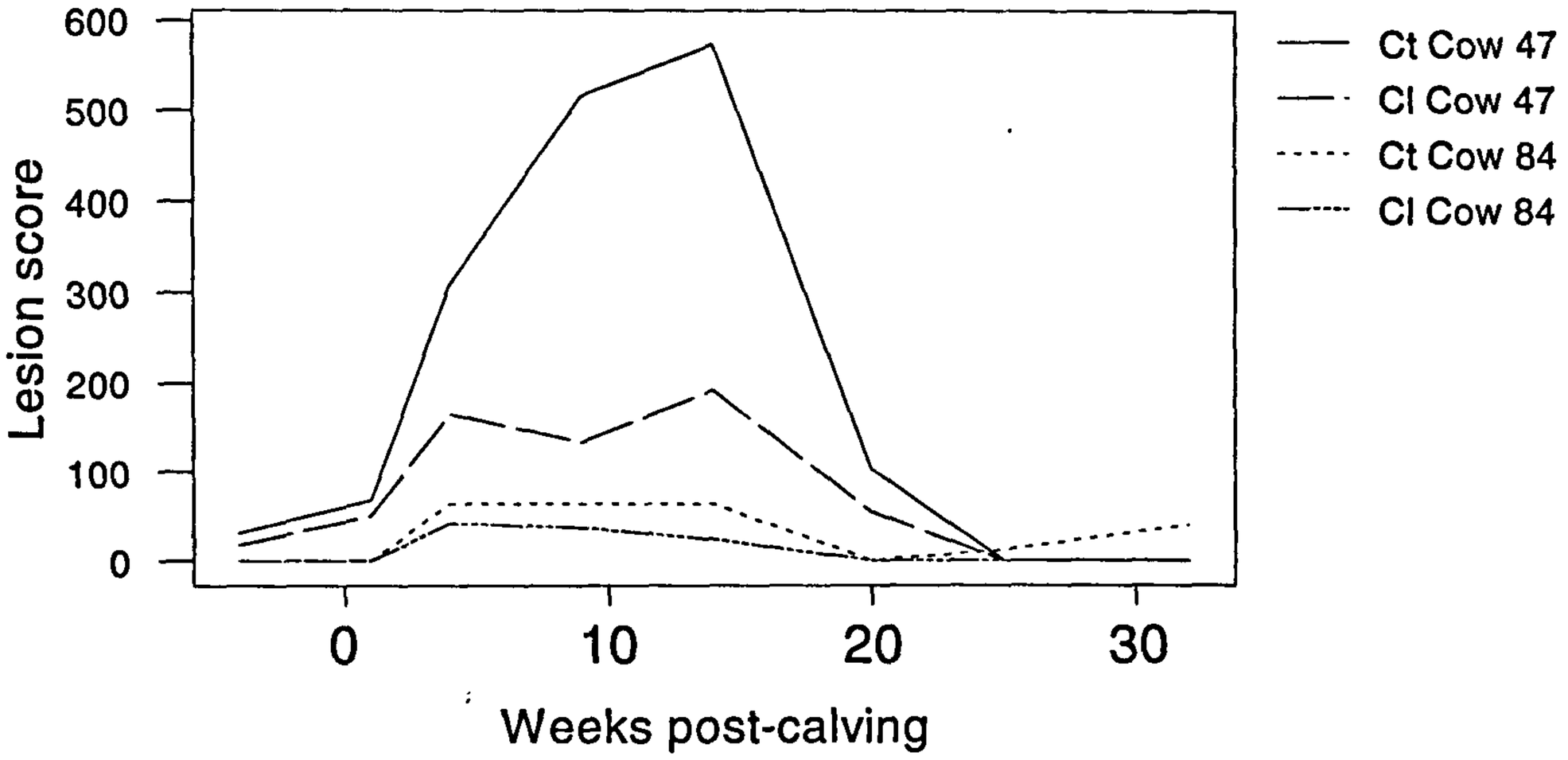
Lesion score
600
500
400
300
200
100
0
0
10
20
30
Weeks post-calving
Ct Cow 47
Cl Cow 47
Ct Cow 84
Cl Cow 84

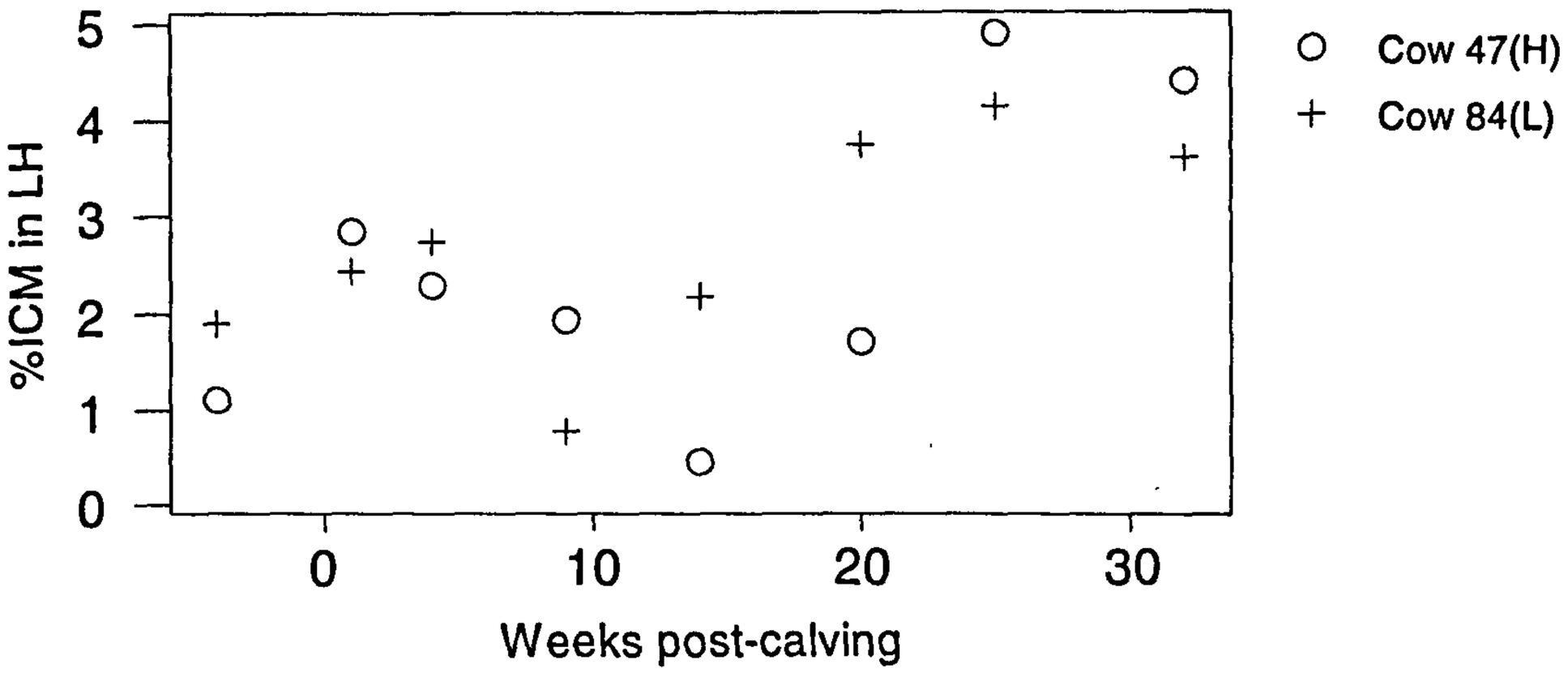
%ICM in LH
5
4
3
2
1
0
0
10
20
30
Weeks post-calving
Cow 47(H)
Cow 84(L)

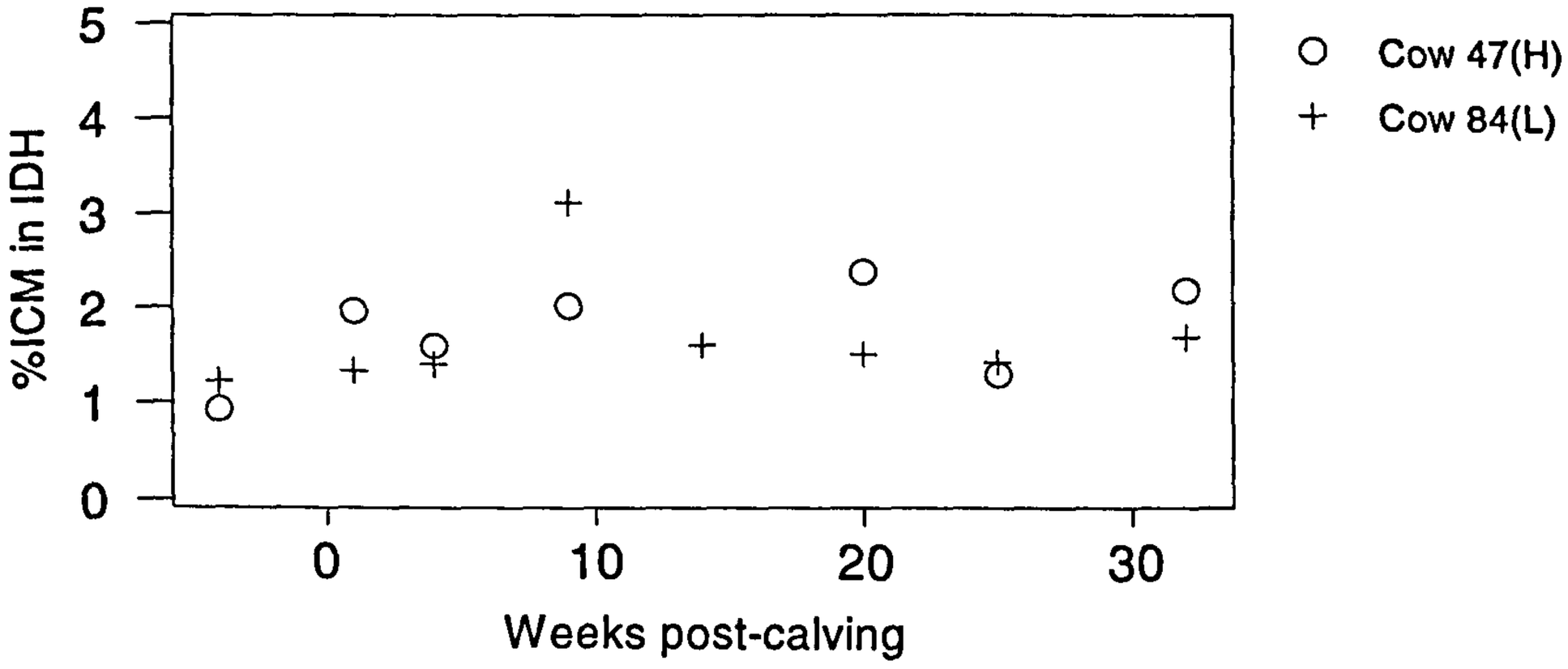
%ICM in IDH
5
4
3
2
1
0
0
10
20
30
Weeks post-calving
Cow 47(H)
Cow 84(L)

FIGURES

CHAPTER 6

Figure 6.1
Schematic diagram of the dermis and epidermis to illustrate the production of horn in the distal laminar region

The horn is shown on the left, separated from the underlying epidermal layer (maturation zone) and dermis (on the right).

LHL	Laminar horn leaflets
L1, L2	Dermal laminae
CH	Cap horn
MZ	Maturation zone
W	Wall horn


Direction of "migration" of laminar horn and cap horn


Direction of generation of laminar horn

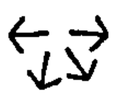
Direction of generation of cap horn


Direction of generation of interdigitating horn
(Interdigitating horn itself is not shown in this diagram)

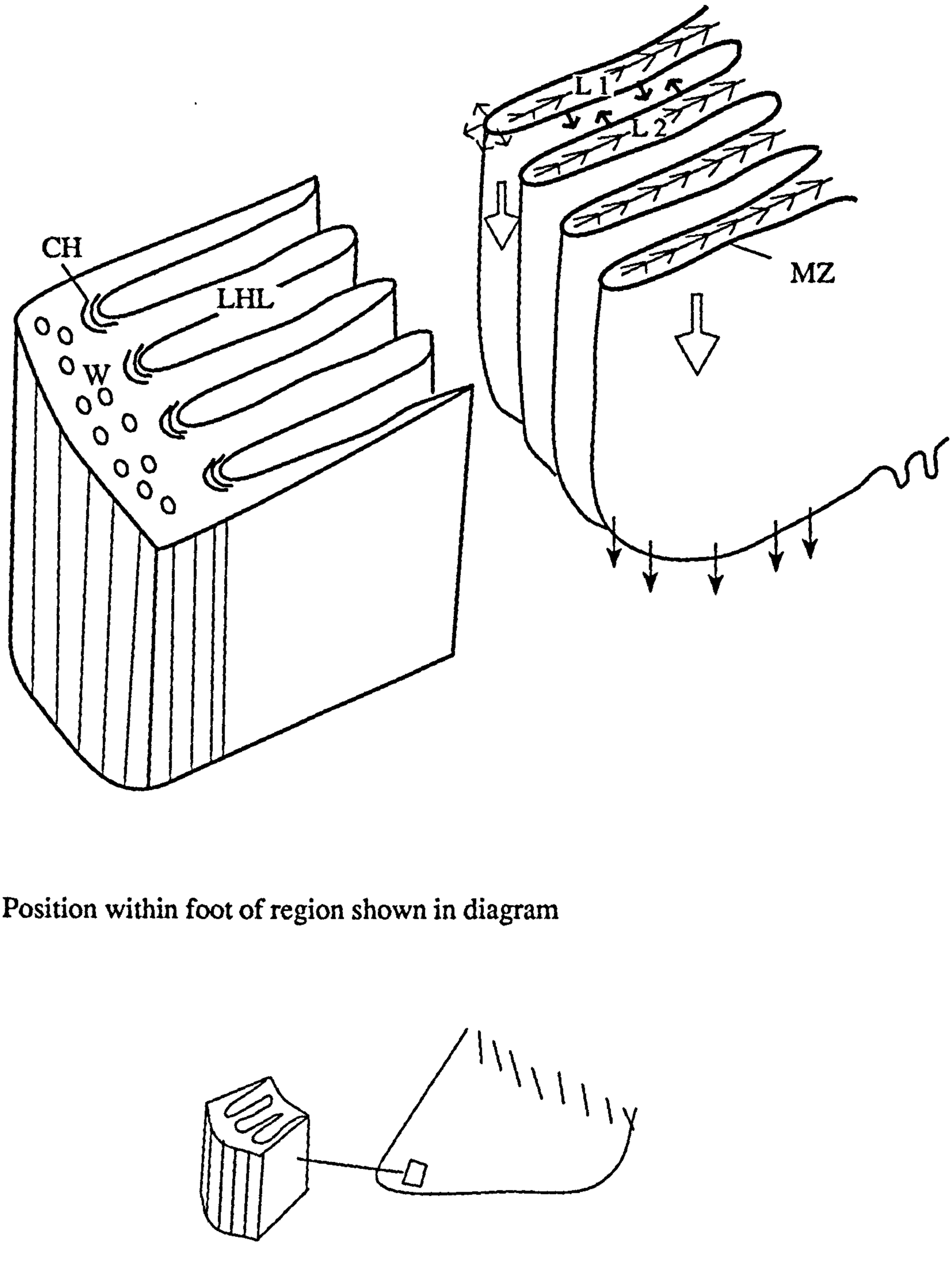

Position within foot of region shown in diagram

Figure 6.2
Schematic diagram showing longitudinal and transverse sections through the distal laminar region and white line

Section 1 : Longitudinal section through a dermal lamina.

Section 2 : Transverse section showing dermal laminae (DL) interdigitating with laminar horn leaflets (LH).

Section 3 : Longitudinal section through a dermal lamina at the level where the crest begins to curve away from the outer wall and the width of the lamina is reduced.

Section 4 : Transverse section through dermal laminae over which interdigitating horn is being produced. The peripheral space between laminar horn leaflets (LH) is filled by interdigitating horn (IDH).

Section 5 : Longitudinal section including the distal limit of a dermal lamina (DL). The space distal to the dermal lamina is occupied by interdigitating horn (IDH), which forms part of the white line. There is debate over whether the distal surface of a lamina is normally divided into "terminal papillae" (dotted outline).

Section 6 : Transverse section through the fully formed white line, consisting of laminar horn leaflets (LH) and interdigitating horn or "terminal horn" (IDH). There is debate over whether the terminal horn normally contains tubules (dotted outlines).

Section 7 : Longitudinal section through a laminar horn leaflet of the white line.

Positions of sections 1 to 7

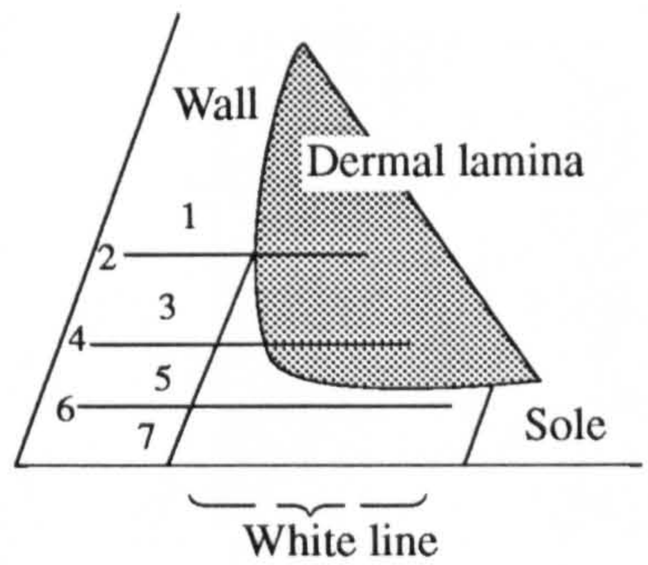

Dermis

Epidermis

Horn tubules

Cap horn

Terminal papillae

Terminal tubule

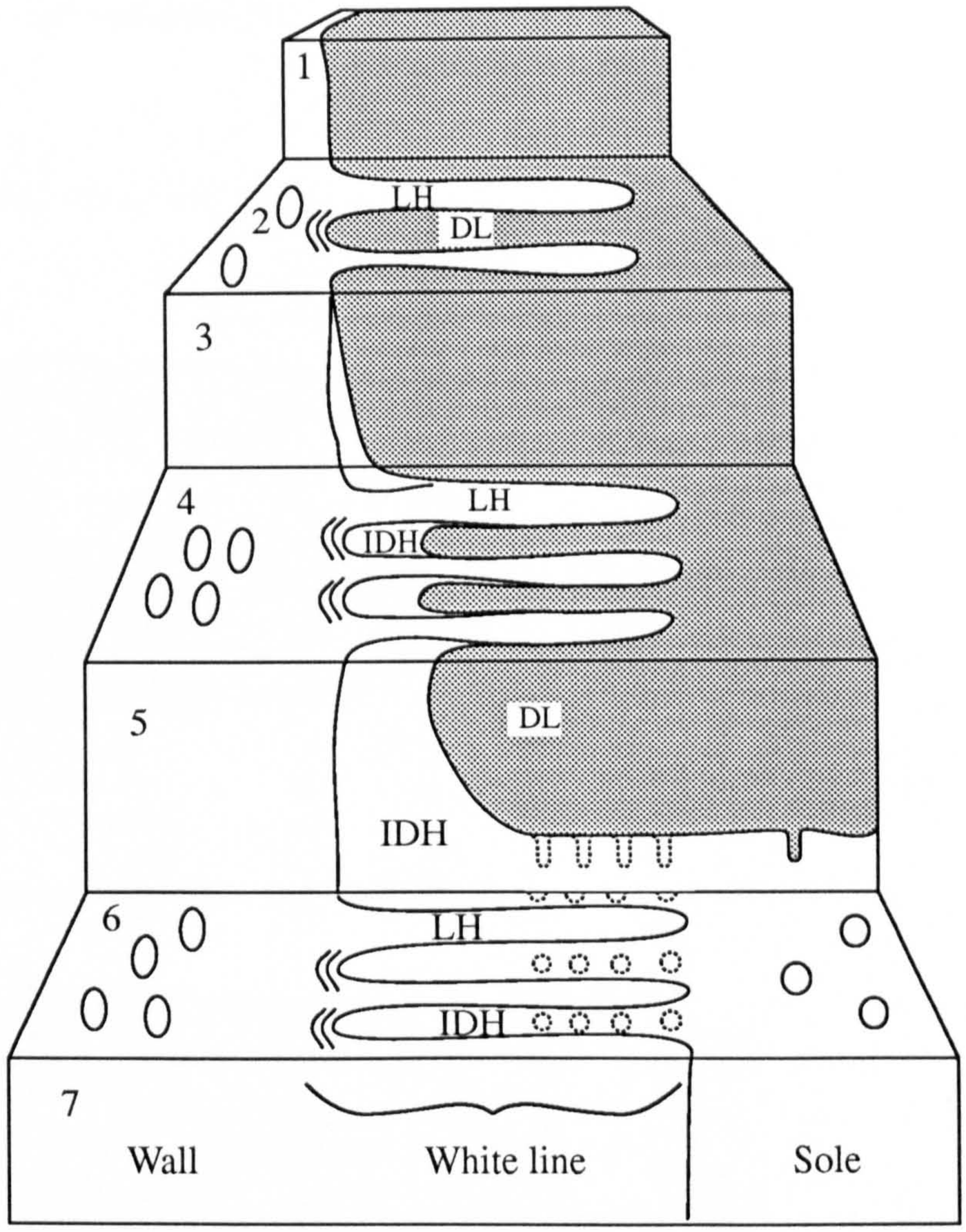

Figure 6.3
Diagrams illustrating changes in the dimensions of the white line and its components

i). Normal white line in transverse section

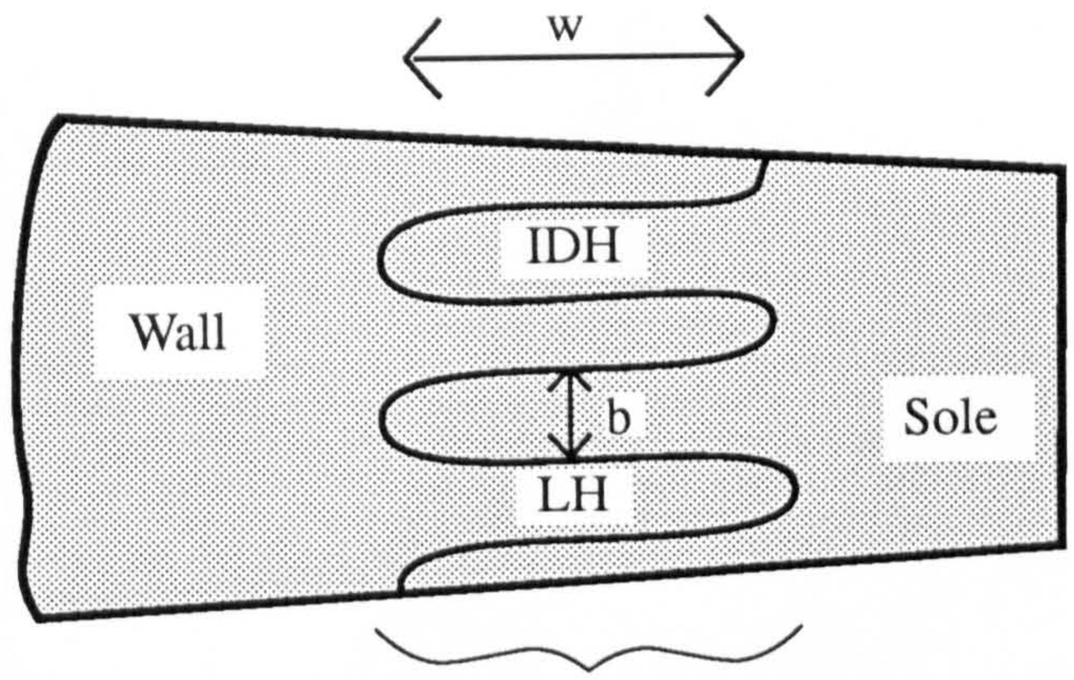

LH : laminar horn　　IDH : interdigitating horn

w : width of white line　　b : breadth of a sheet of interdigitating horn

ii). Widening of the white line (w +)

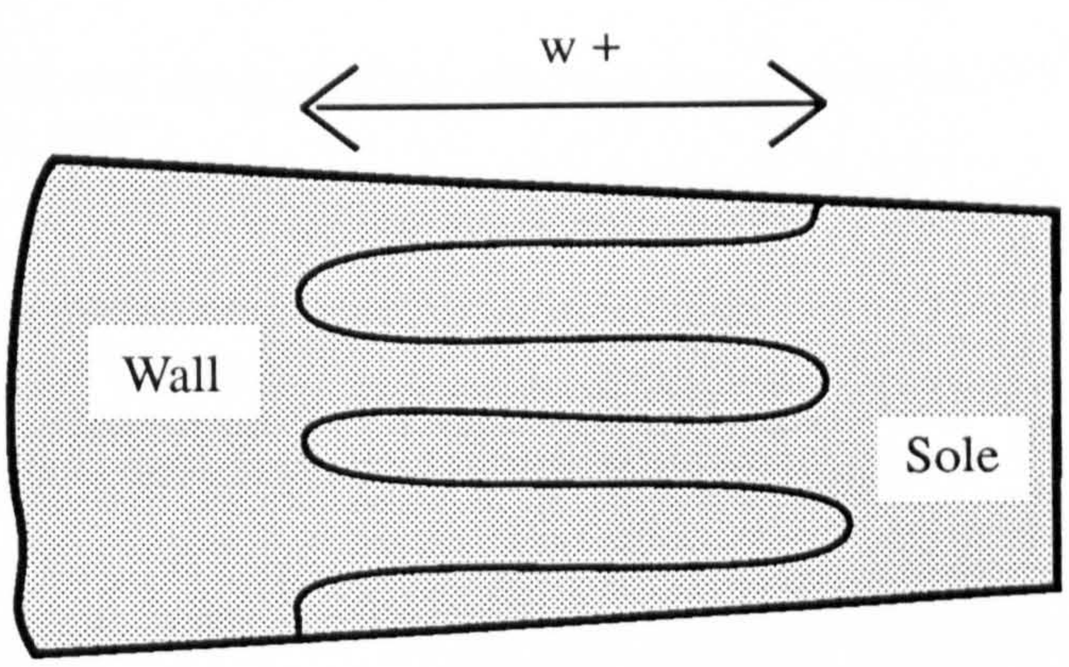

iii). Broadened interdigitating horn (b +)

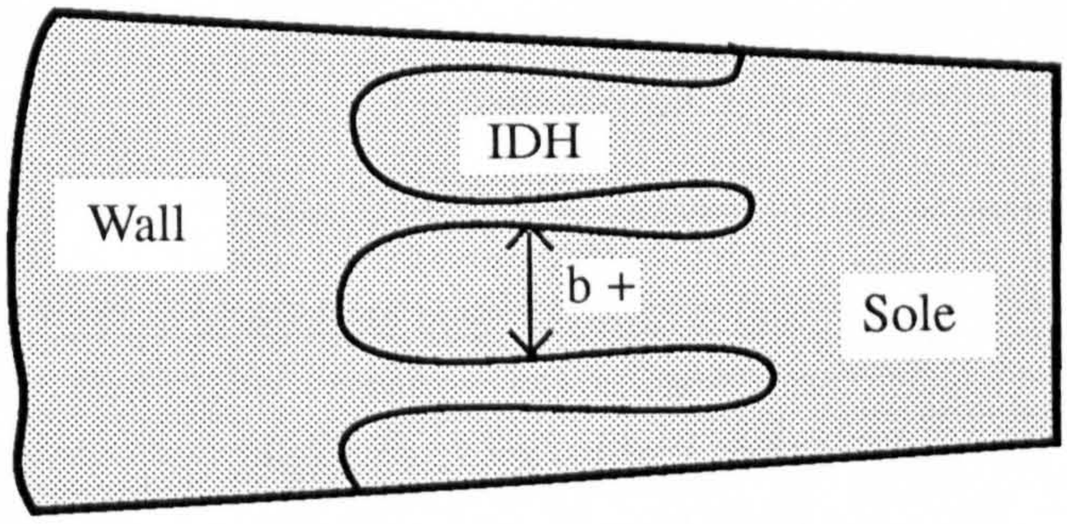

Figure 6.4
Diagrams to illustrate the effects on the coria resulting from rotation of the distal phalanx

A. Normal position of distal phalanx

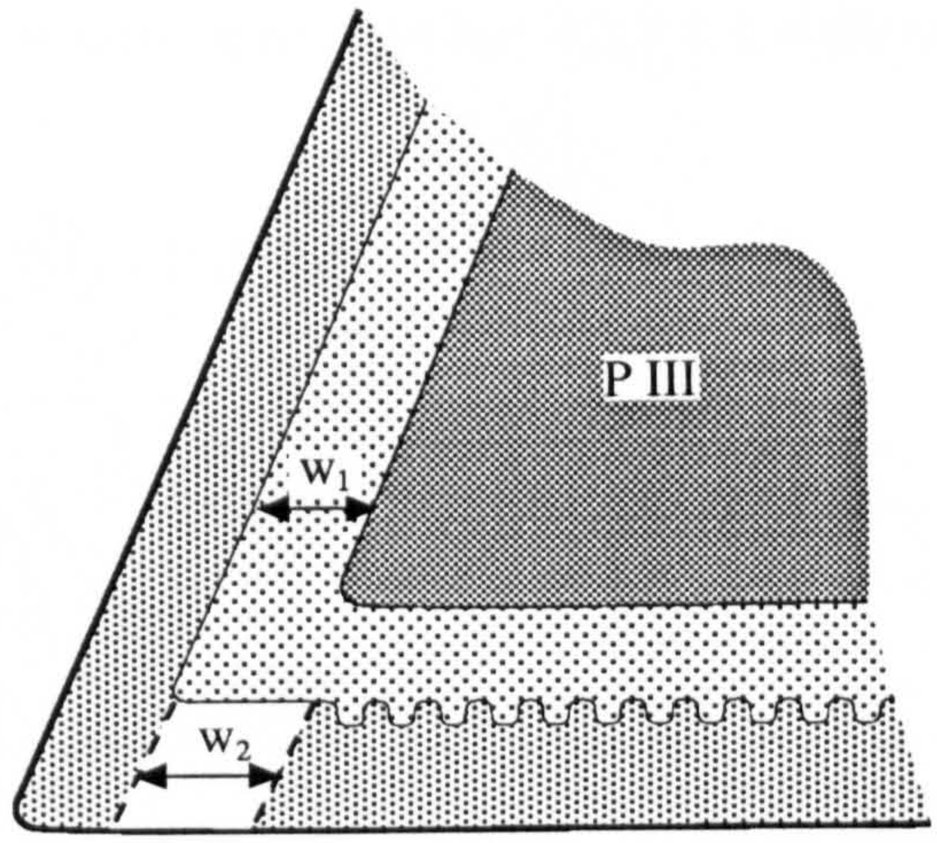

w_1 Normal width of distal laminar corium

w_2 Normal width of white line

B. Rotation of distal phalanx when dermal-epidermal attachment in the laminar region is lost

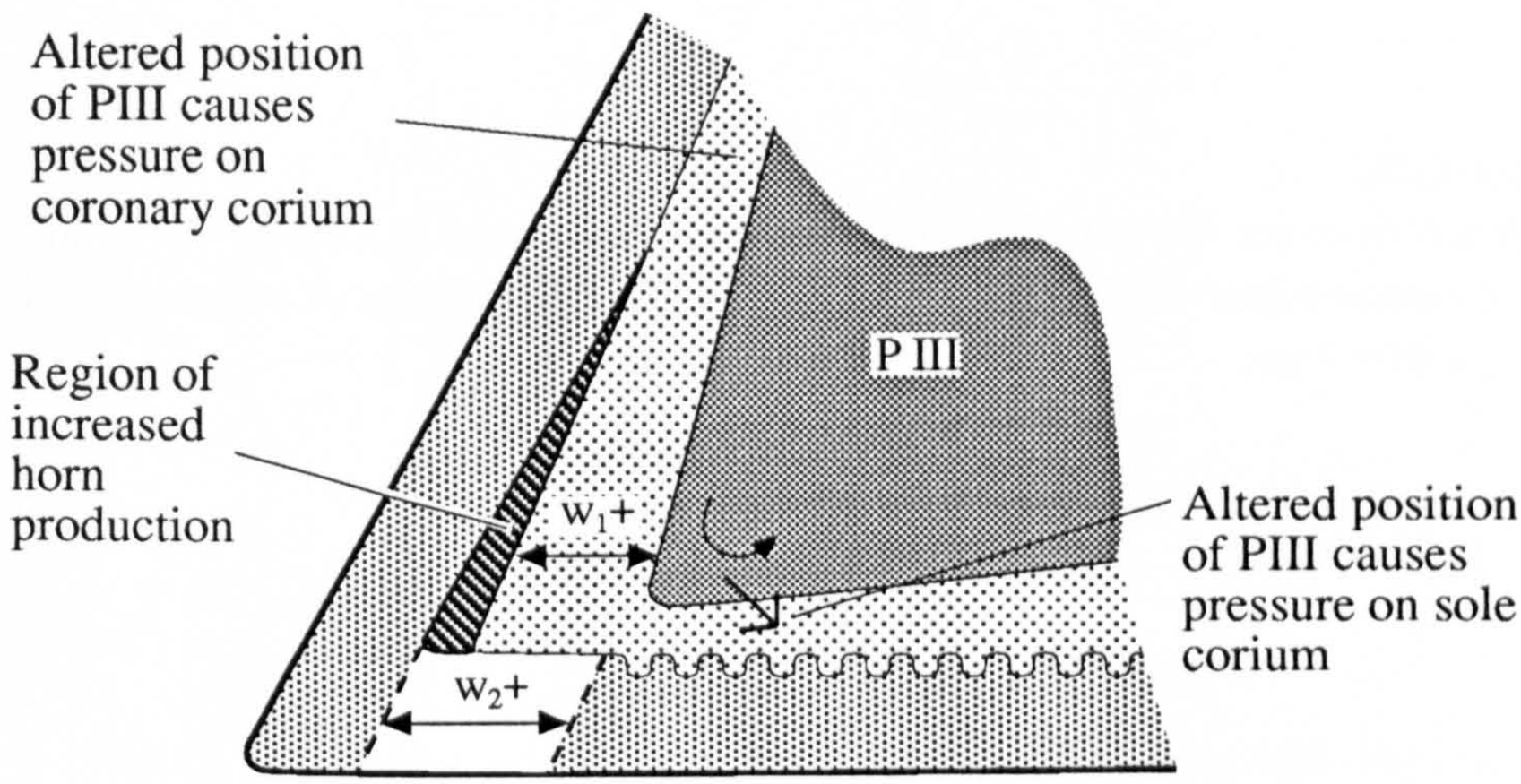

Direction of rotation of PIII

w_1+ Increased width of distal laminar corium

w_2+ Increased width of white line

Figure 6.5a
Diagram to show the positions of sample blocks of tissue taken from the dorsal and lateral walls of the claw for light and scanning electron microscopy

Figure 6.5b
Diagram to show the positions of samples taken from the distal surface of the claw to determine within-foot variation in the proportion of interdigitating horn in the white line

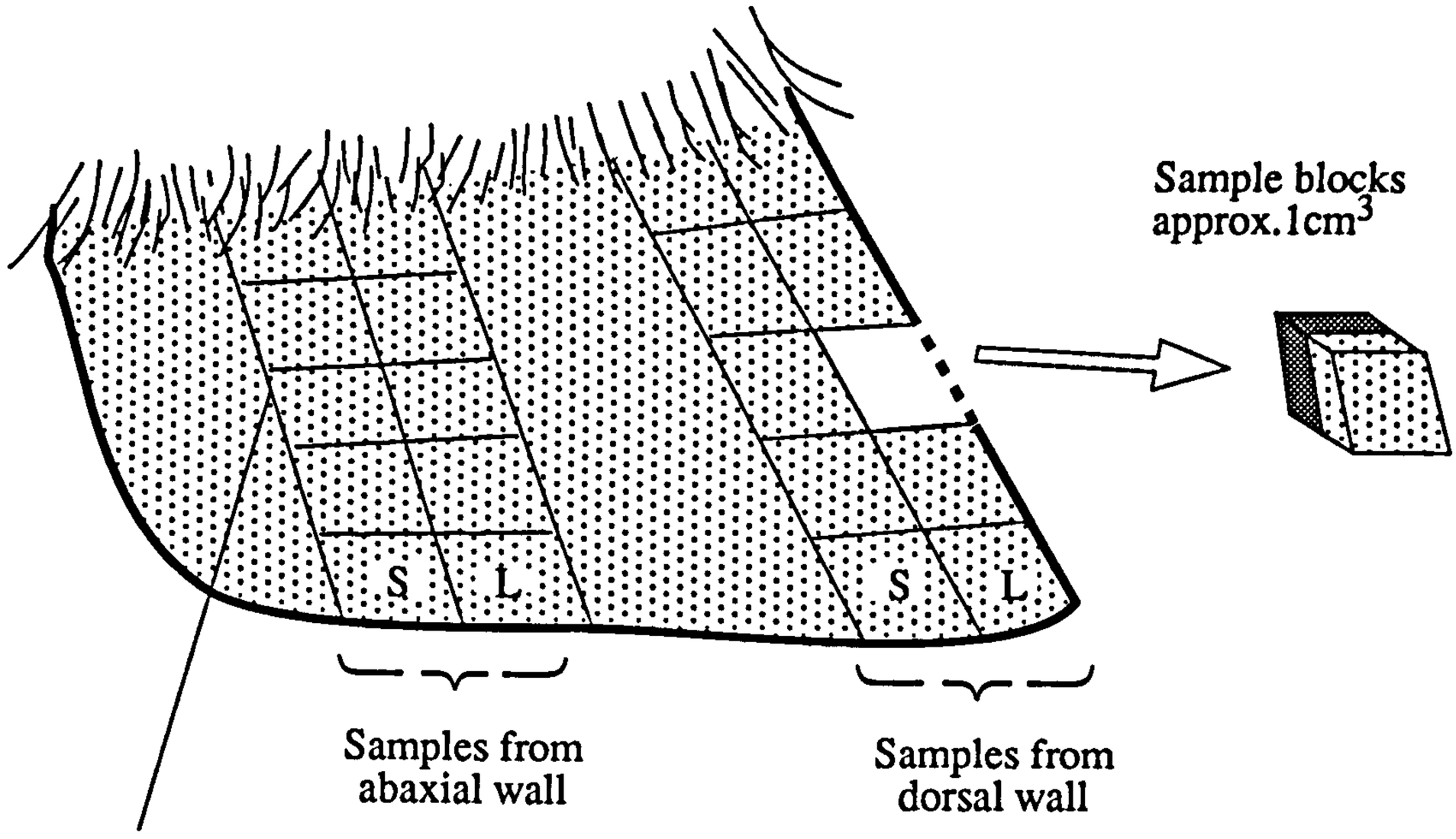

Sample blocks
approx. 1cm^3

Samples from
abaxial wall

Samples from
dorsal wall

Abaxial groove

S : samples for scanning electron microscopy
L : samples for light microscopy

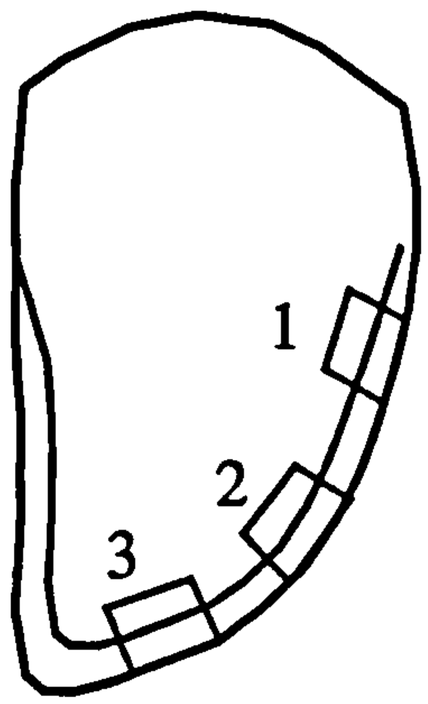

Sample sites

1. Sole-bulb junction
2. Abaxial white line
3. Adjacent to point of toe

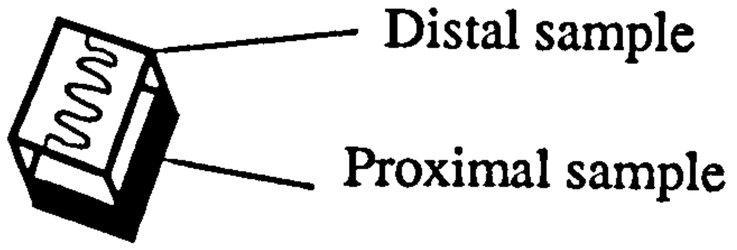

Sample blocks
approx.
1cm x 1cm x
0.6 cm thick

Figure 6.6
Position within the white line of sample quadrats used for measurement of the volume fraction of interdigitating horn

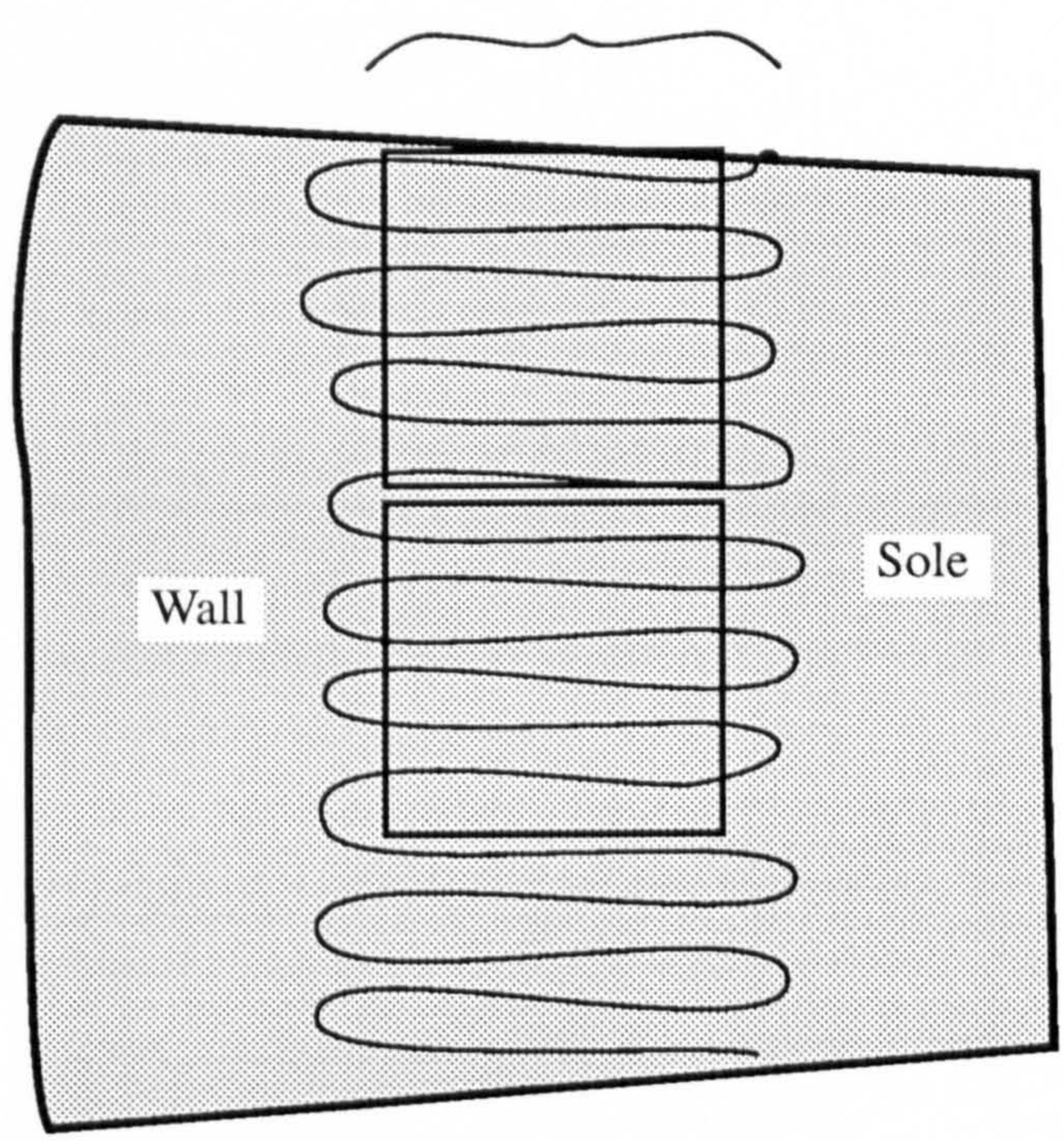

Position of sample quadrat delineated by 1mm square eyepiece graticule

Figure 6.7
A sliver of horn from the distal surface of the claw on the abaxial border viewed in the dissection microscope

The cut surface (proximal surface) has been photographed. The white line (wl) is the region of horn separating wall (w) and sole (s). Discrete regions of haemorrhage (h ↑) can be seen in the sole. The blood is mostly confined to individual tubule cores.

x 7

Figure 6.8
A higher power view of a sliver of horn from the white line in the dissection microscope

Within the white line two components can be distinguished. The lighter interdigitating horn (idh ↑) is continuous with the sole (s). It interdigitates with the darker laminar horn leaflets (lh ↑). The laminar horn leaflets and interdigitating horn are slightly distorted from their normal position perpendicular to the outer wall. Three regions of haemorrhage (h) are visible. Each is confined to a few adjacent sheets of laminar and interdigitating horn.

x 22

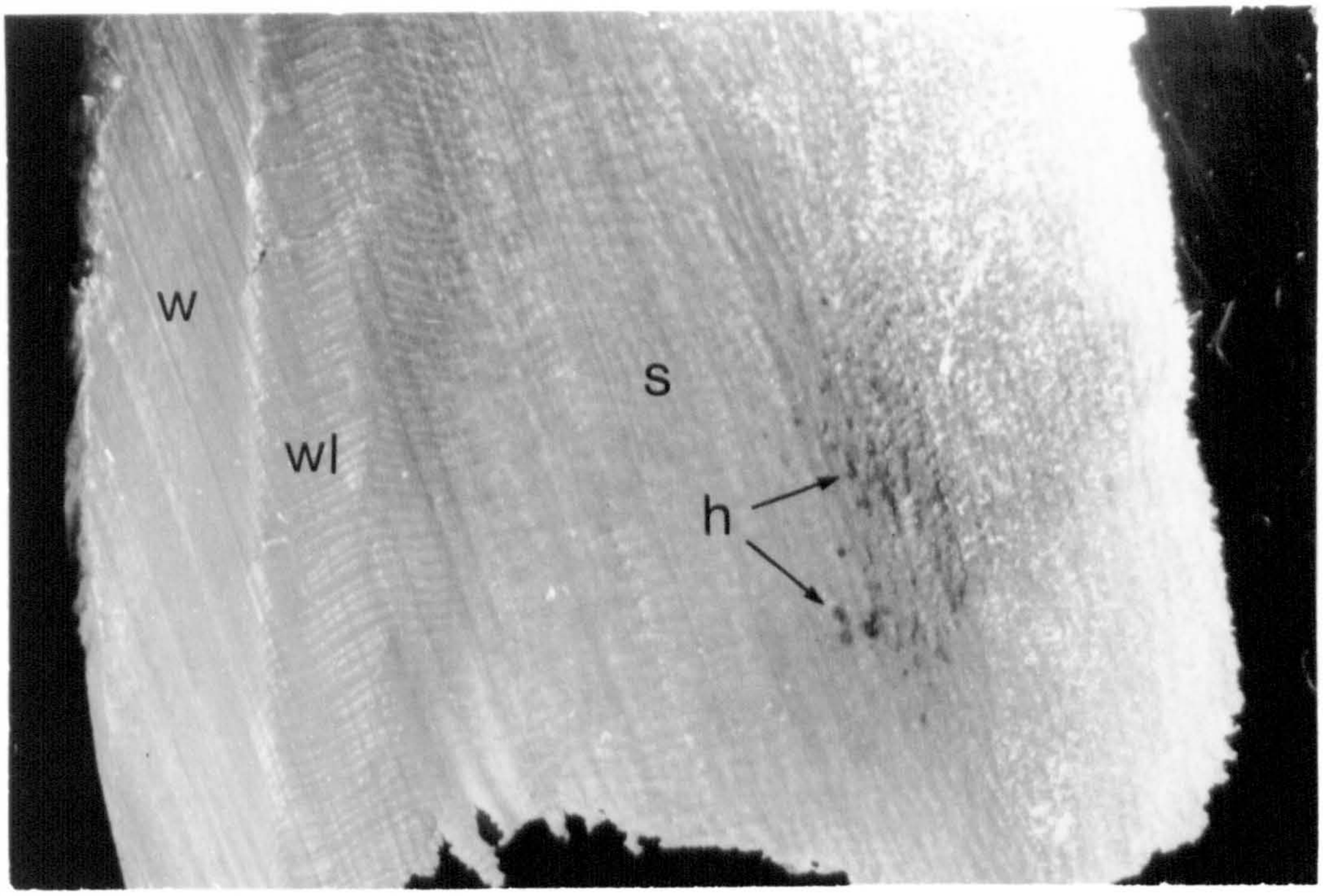
w
wl
s
h

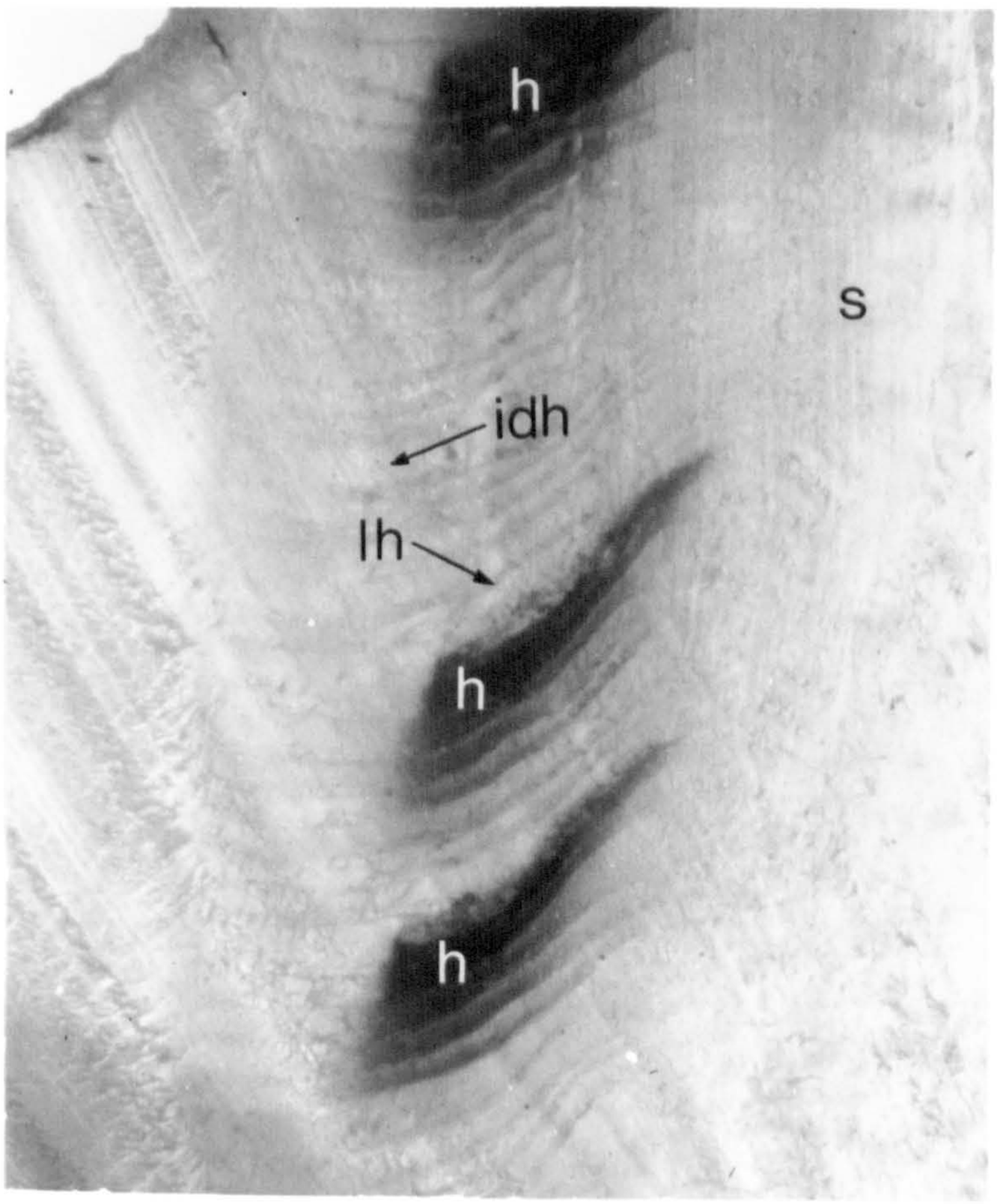
h
s
idh
lh
h
h

Figure 6.9
A sliver of horn from the distal surface of the abaxial border of the claw viewed in the dissection microscope

The cut surface (proximal surface) had been photographed. Small regions of haemorrhage in the sole (s) are confined to tubule cores (h1 ↑). Larger regions affect the intertubular horn as well (h2). In this sample the white line (wl) is free from haemorrhage. Some blood is visible in tubules of the wall (w).

x 22

Figure 6.10
The uncut (distal) surface of a sliver of horn from the distal surface of the abaxial border of the claw, photographed in the dissection microscope

The striated nature of the white line (wl) is distinguishable. There is considerable separation between the laminar horn and the interdigitating horn of the white line (↑). One crack (*) has extended from the white line into the sole (s). Cracks in the wall (w) and breakdown (↑↑) at the junction between wall and white line are also visible.

x 11

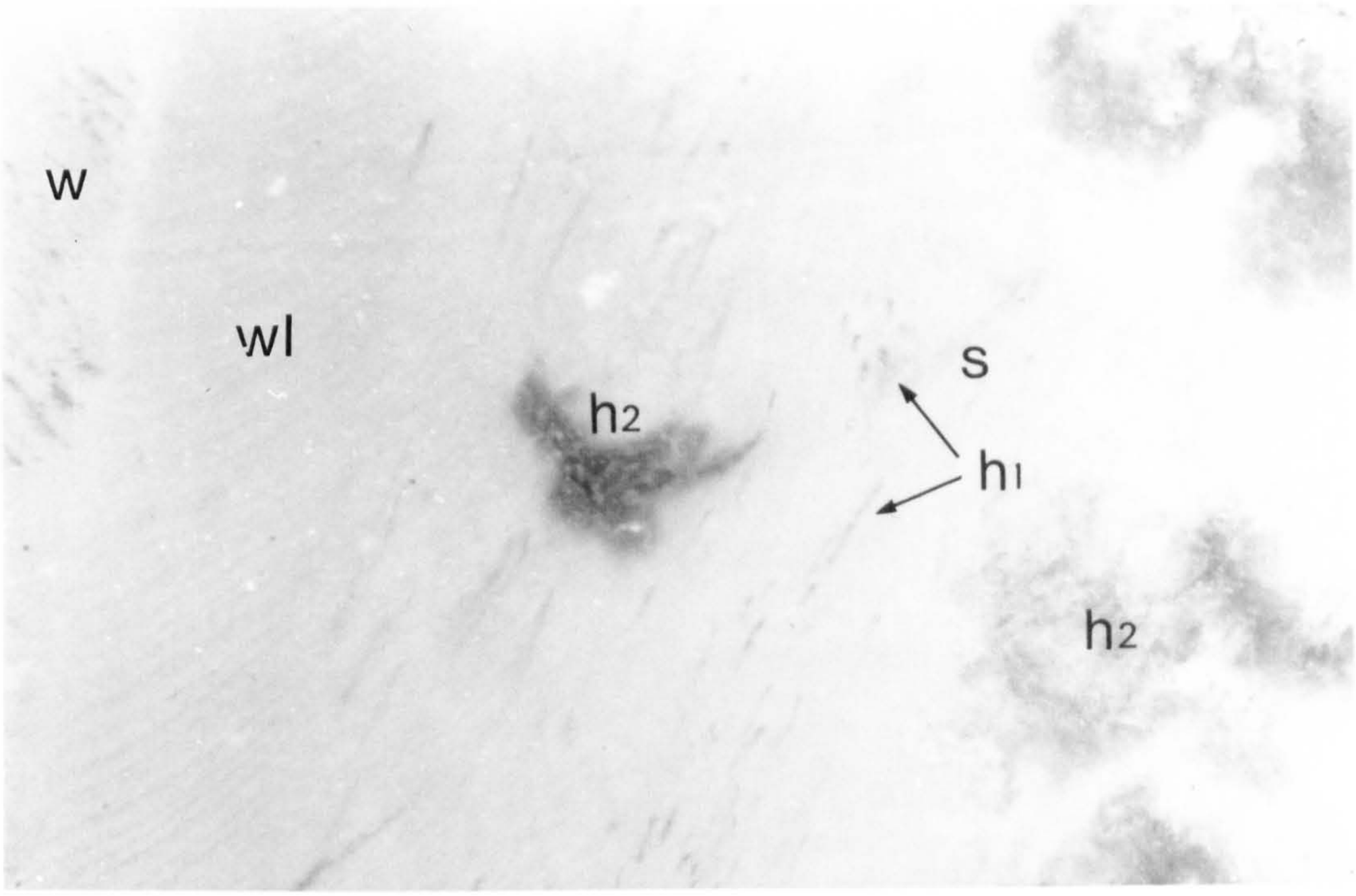
w
wl
h2
s
h1
h2

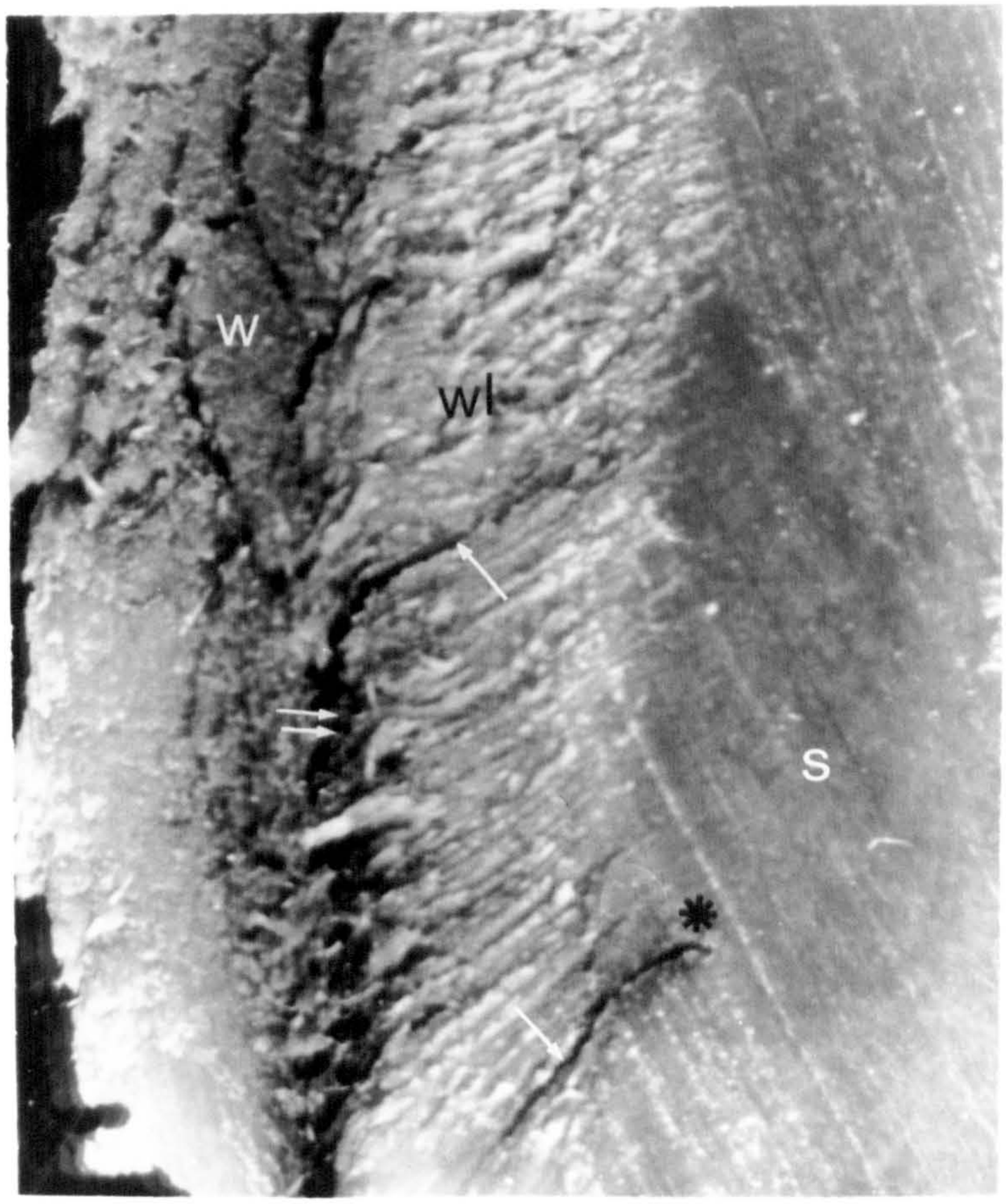
w
wl
s

Figure 6.11
Light micrograph of a transverse section of horn from the edge of the white line adjoining the wall

The laminar horn (lh) is more intensely stained than the interdigitating horn (idh). A layer of connecting cells (cc ↑) is distinguishable by particularly dark staining, at the junction between laminar and interdigitating horn.

x 144

Stain : Toluidine Blue

Figure 6.12
Light micrograph of a transverse section of horn of the wall, sole and white line

The interdigitating horn (idh) was stained red while the laminar horn (lh) was more yellow. Medullae of tubules (t ↑) in the wall (w) and the sole (s) stained dense red. Arches of squames forming the cap horn (↑) are visible over the tips of sheets of interdigitating horn.

x 45

Stain : Martius Scarlet-Blue

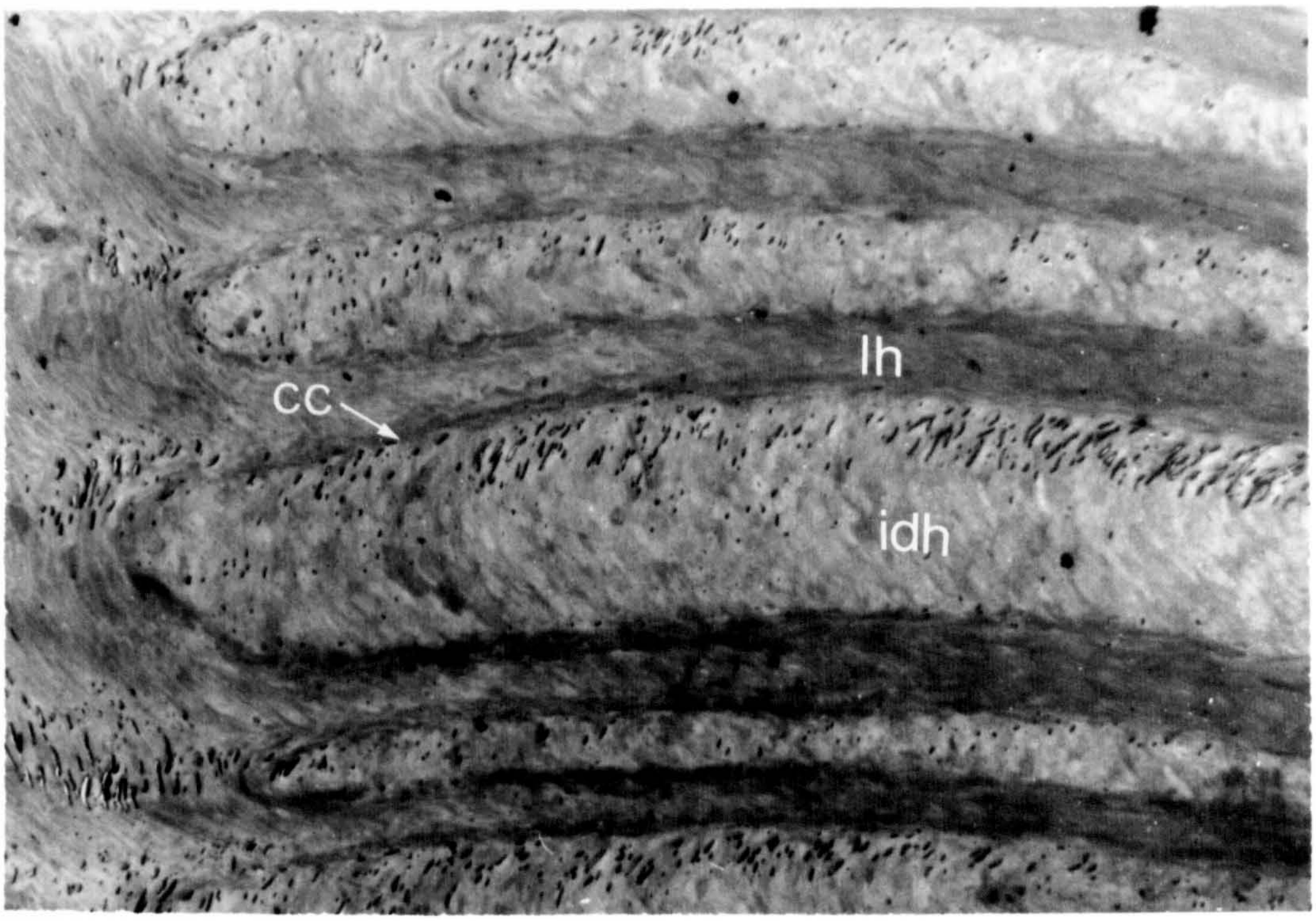
lh
cc
idh

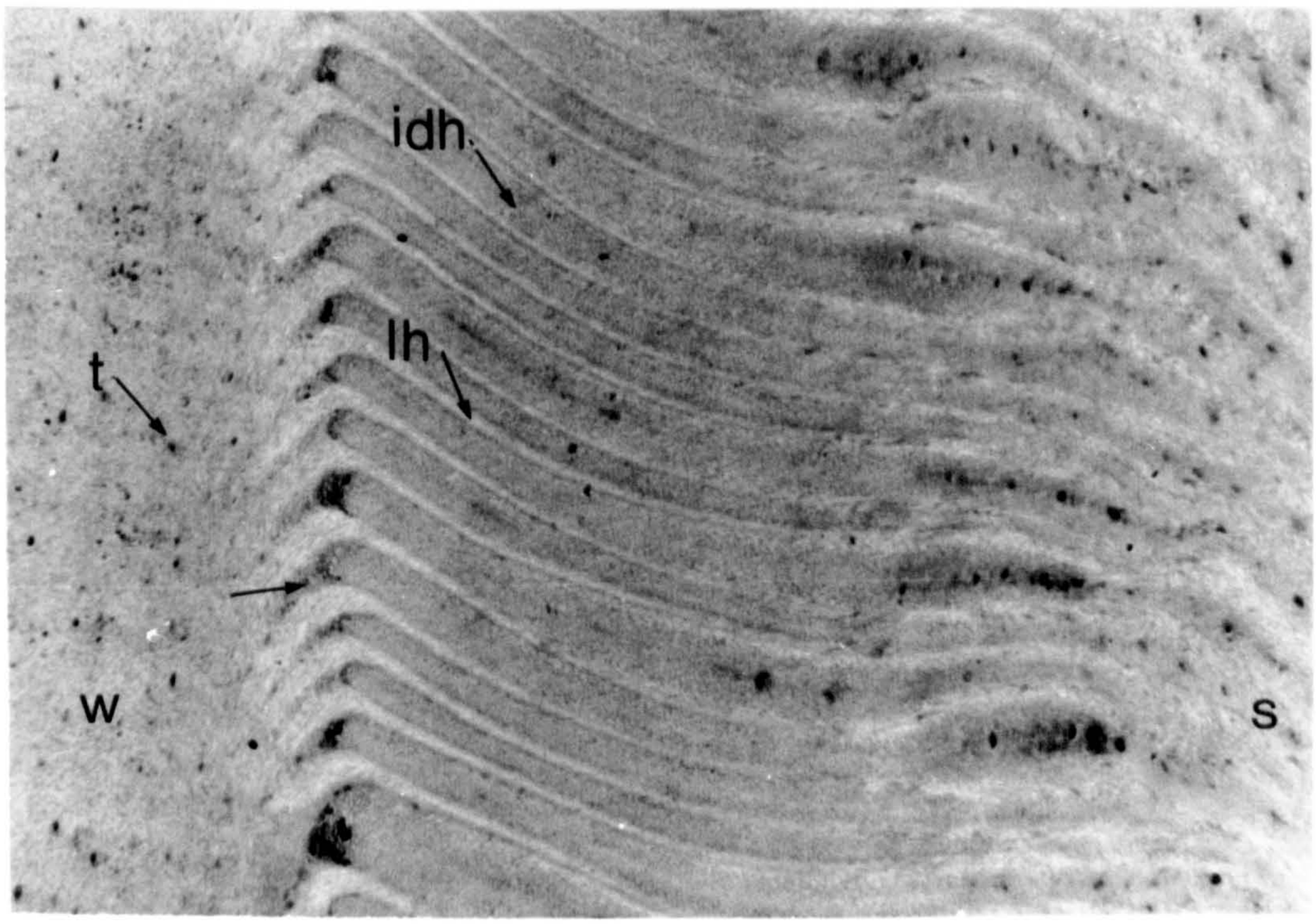
idh
lh
t
W
S

Figure 6.13
Light micrograph of the white line in transverse section showing broadening of the interdigitating horn and abnormal staining

Broadened regions (br) and round densely stained regions (↑) are visible within sheets of interdigitating horn (idh). In places the continuity of the laminar horn (lh) is interrupted (*).

x 72

Stain : Toluidine Blue.

Figure 6.14
Light micrograph showing abnormality of the dermal - epidermal junction proximal to the white line (transverse section)

This section is taken proximal to the complete formation of the white line, at the level of Section 4 in Figure 6.2.
Expanded dermal laminae (ed) are adjacent to broadened sheets of interdigitating horn (br). The dermal tissue is very sparse and has suffered much damage during preparation and sectioning. This does not normally occur and suggests that pathological changes had affected the structure of the dermis.

x 94

Stain : Phloxine-Tartrazine

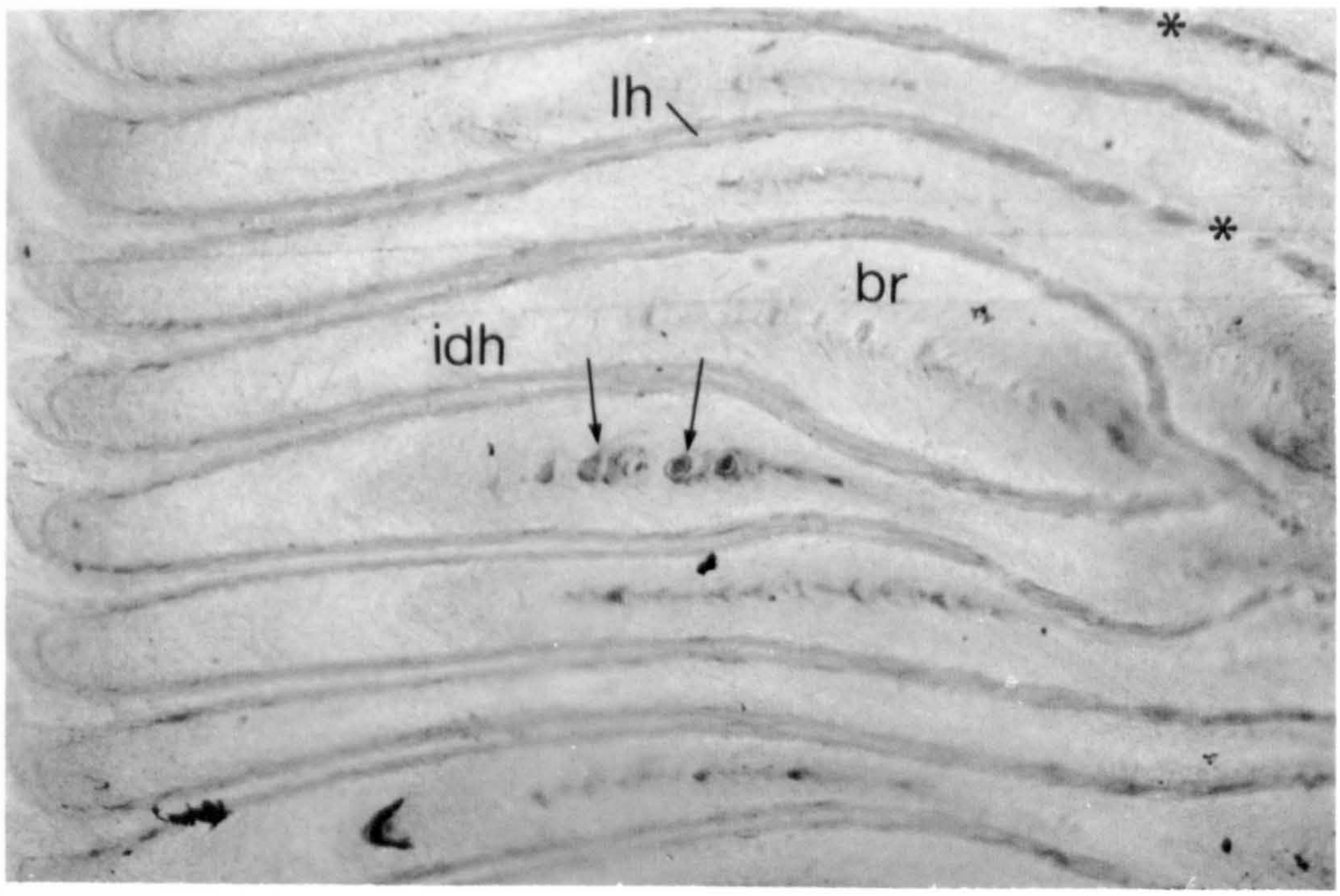
lh
*
*
br
idh

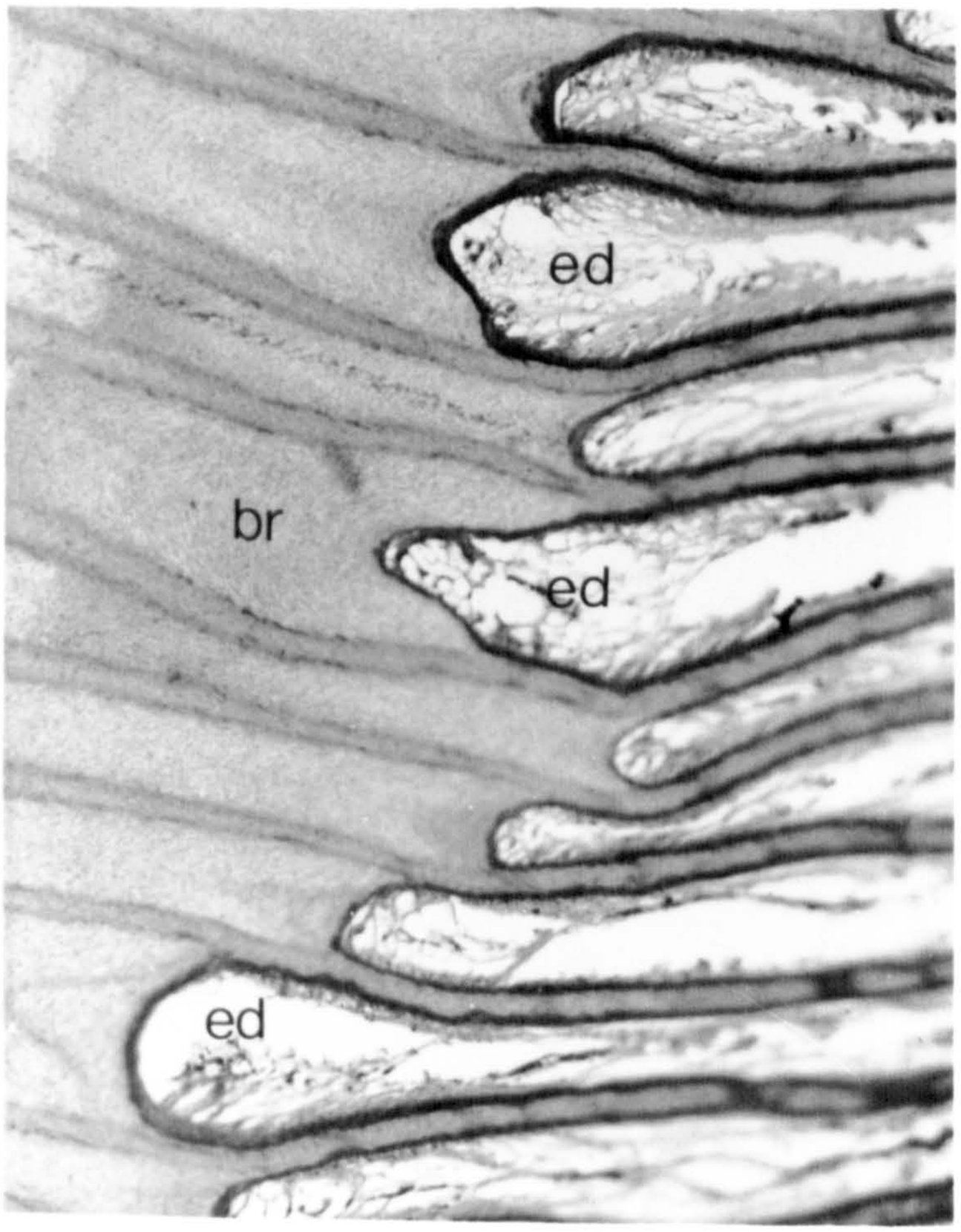
ed
br
ed
ed

Figure 6.15
Scanning electron micrograph of the dermal-epidermal junction proximal to the white line (at the level of Section 4 in Figure 6.2)

Formation of interdigitating horn has begun at this level. The space between laminar horn leaflets (lh) is occupied in the inner layers by dermal laminae (dl) but peripherally by interdigitating horn (idh). The central dermal lamina (*) is expanded and shows some breakdown of normal internal structure compared to adjacent dermal laminae. It gives rise to a broadened sheet of interdigitating horn.

x 110

Figure 6.16
Light micrograph showing abnormality of the dermal-epidermal junction proximal to the white line (at the level of Section 4 in Figure 6.2)

This micrograph illustrates breakdown in the normal dermal and epidermal structure. The dermal laminae (dl), the overlying epidermis and the adjacent laminar horn leaflets (lh) are very distorted in shape. There is an accumulation of collagen bundles and a decrease in cells in the dermal laminae (dl). Blood capillaries (ca) are conspicuous but were reduced in number. The basement membrane (bm ↑) is thickened. The basal cells (bc) are elongated and the basal cell layer has retreated towards the bone (to the right of the picture). There is proliferation of the maturation zone (mz) over the tips of the dermal laminae (dl). Cells within the maturation zone are irregular in size and arrangement. At the tips of the epidermal laminae, spaces within the maturation zone are filled with exudate (ex).

x 216

Stain : Martius Scarlet-Blue

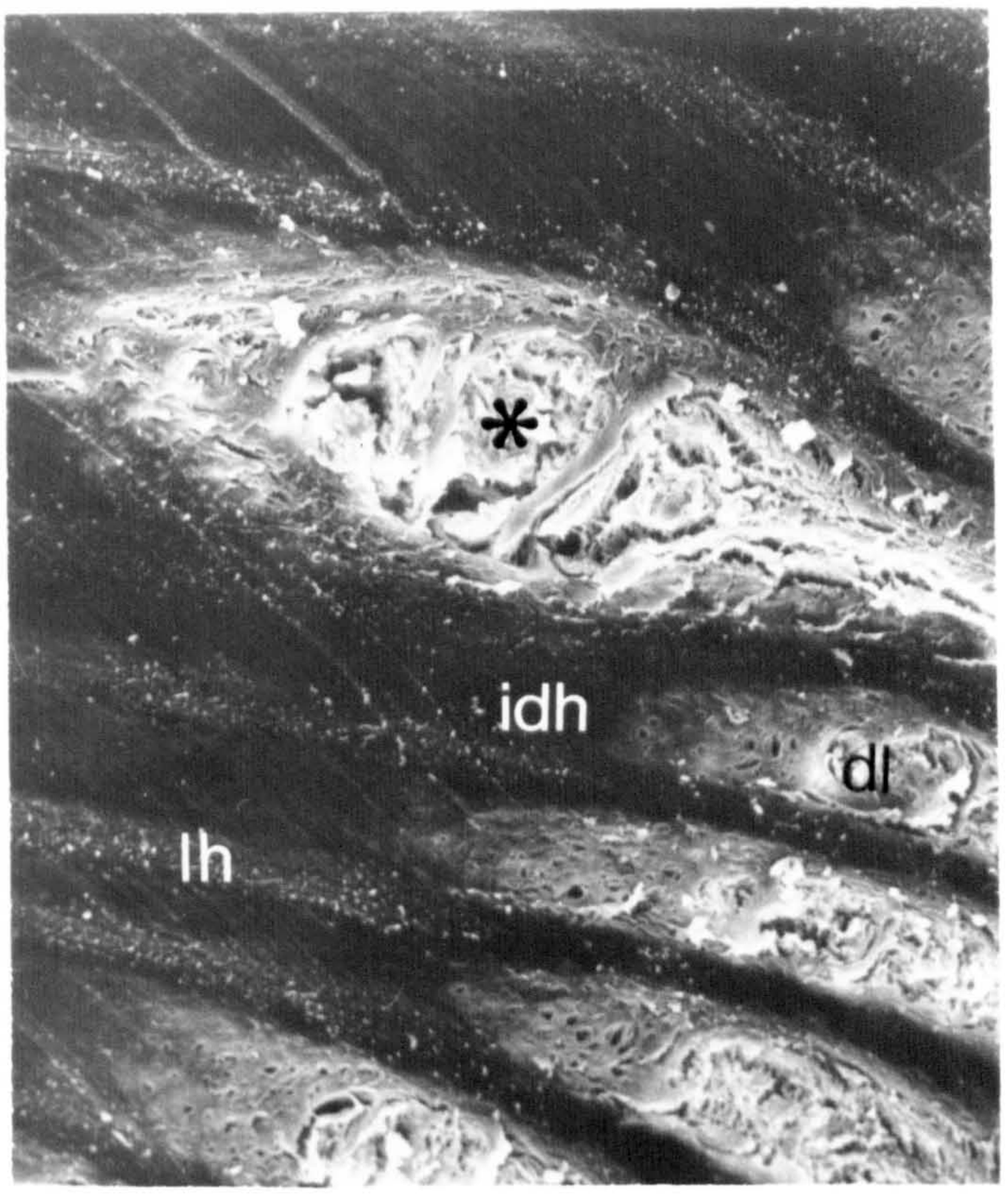
*
idh
dl
lh

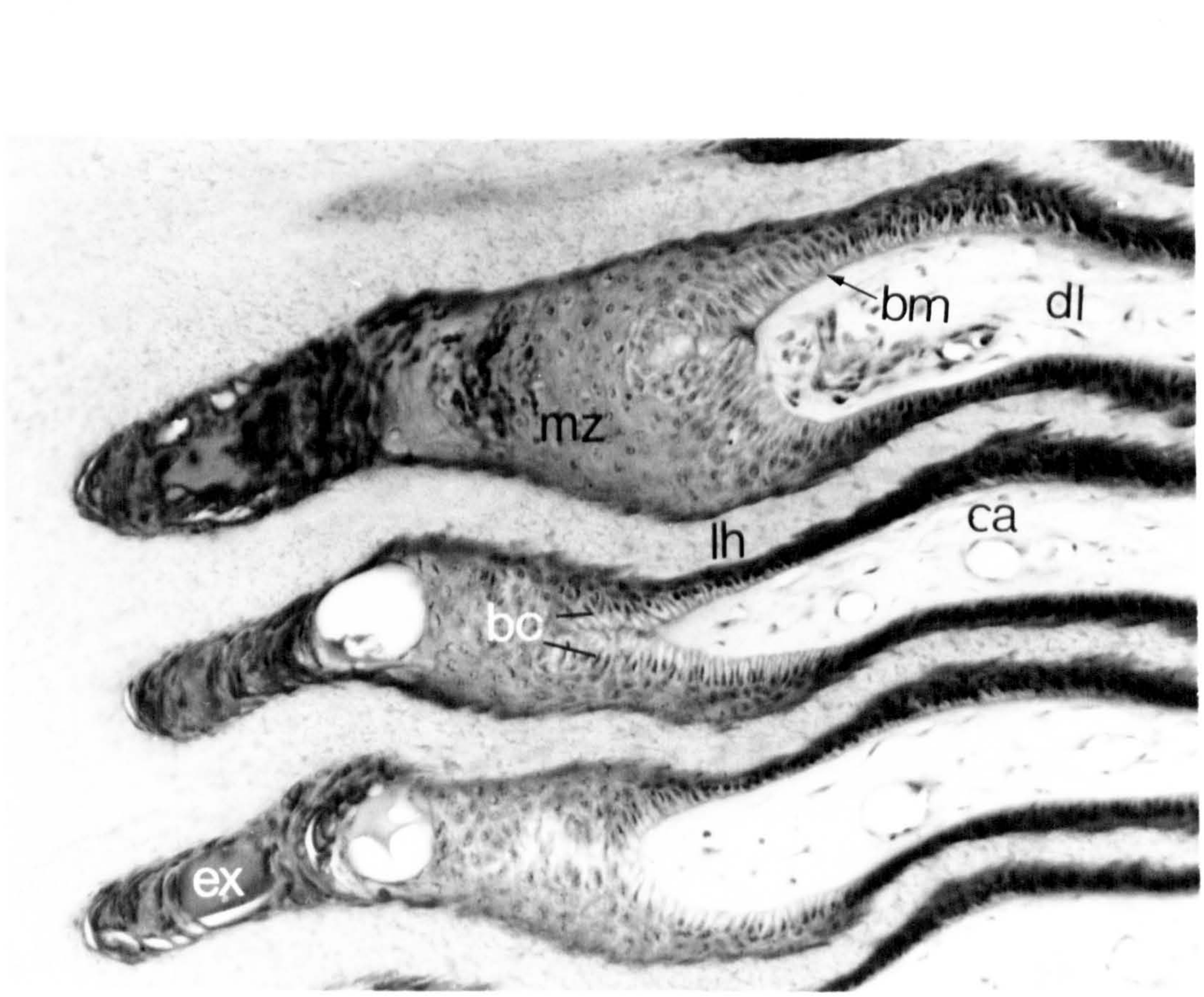
bm
dl
mz
ca
lh
bo
ex

Figure 6.17
Light micrograph of a section of the white line showing abnormal structure and staining

Sheets of interdigitating horn (idh) and laminar horn leaflets (lh) are distorted in shape. Within a broadened sheet of interdigitating horn round, densely stained regions (↑) are visible. In these regions cellular structure is hard to distinguish.

x 144

Stain : Toluidine Blue

Figure 6.18
Light micrograph of a broadened sheet of interdigitating horn with abnormal staining properties

Within the majority of the broadened sheet of interdigitating horn (idh), only the squame boundaries are densely stained. In arrowhead shaped regions (a) all material is densely stained. This may be intercellular exudate from the dermis, or the product of squame degeneration. Arch-shaped arrangements of squames are found on either side of these regions (↑).

x 115

Stain : Toluidine Blue

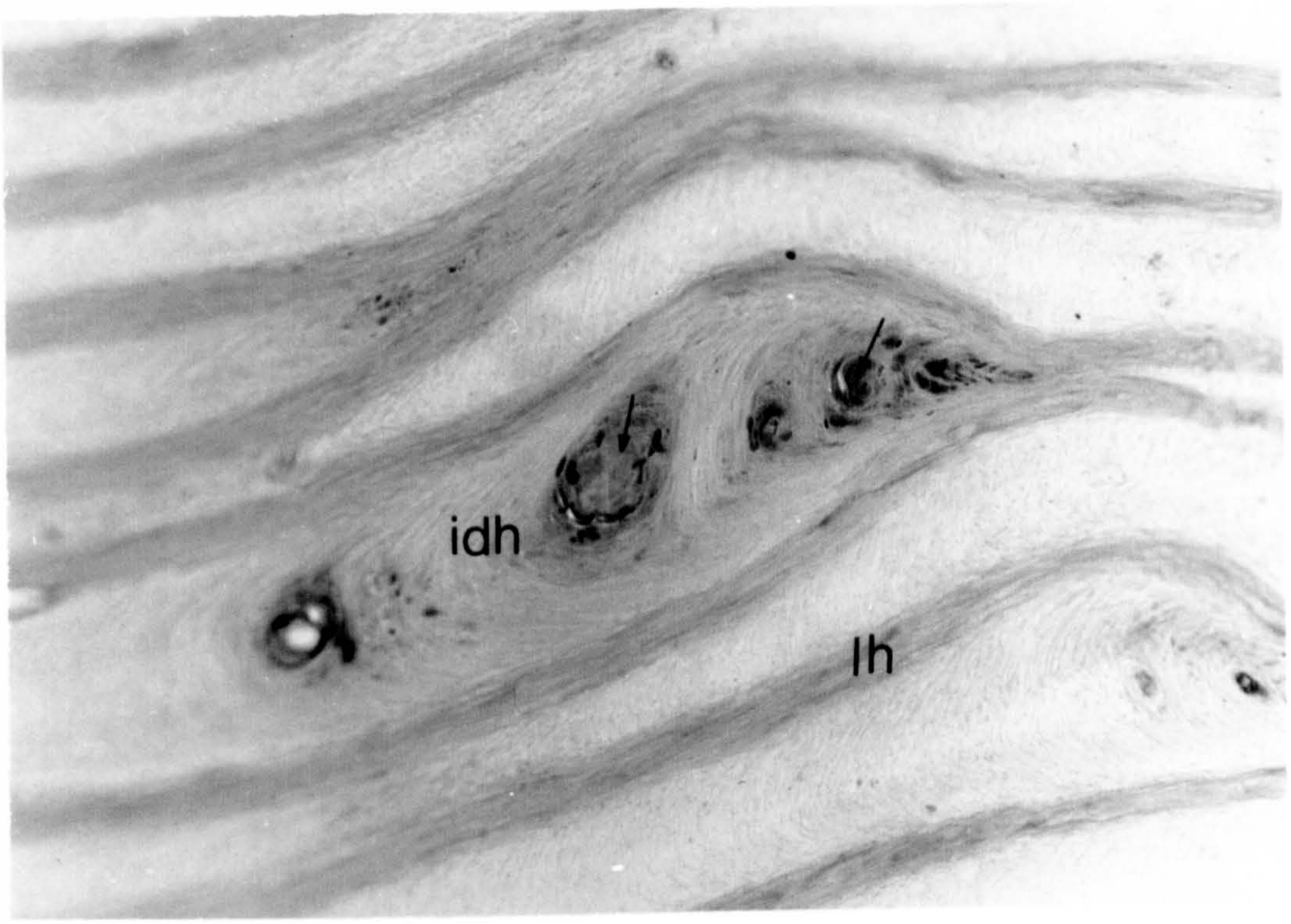
idh
lh

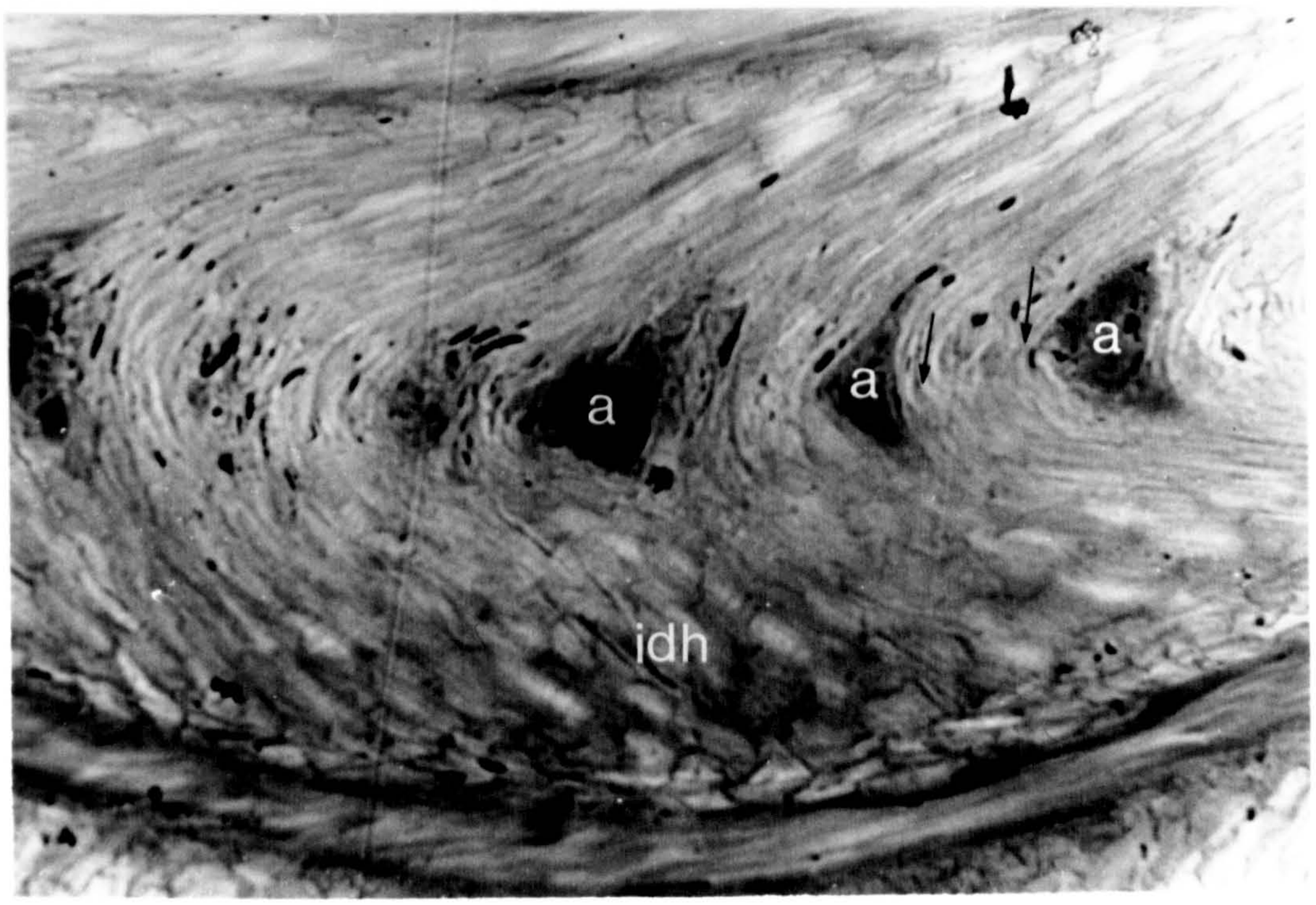
a
a
a
idh

Figure 6.19
Light micrograph of broadened regions of interdigitating horn with extensive dense staining

All sheets of interdigitating horn (idh) are distorted in shape and two are considerably broadened. Within these broadened sheets of interdigitating horn, extensive dark stained areas are visible (*). The intense staining arises from staining of intracellular and intercellular material in addition to the squame boundaries.

x 90

Stain : Toluidine Blue

Figure 6.20
High power light micrograph of densely stained regions at the tips of broadened sheets of interdigitating horn

The profiles of sheets of interdigitating horn (idh) are distorted. Near the tips of the interdigitating horn, close to the junction with the wall, amorphous, densely stained regions are visible (↑). Cellular structure cannot be distinguished in these regions and they are thought to result from the disintegration of squames and the presence of exudate from the dermis.

x 160

Stain : Toluidine Blue

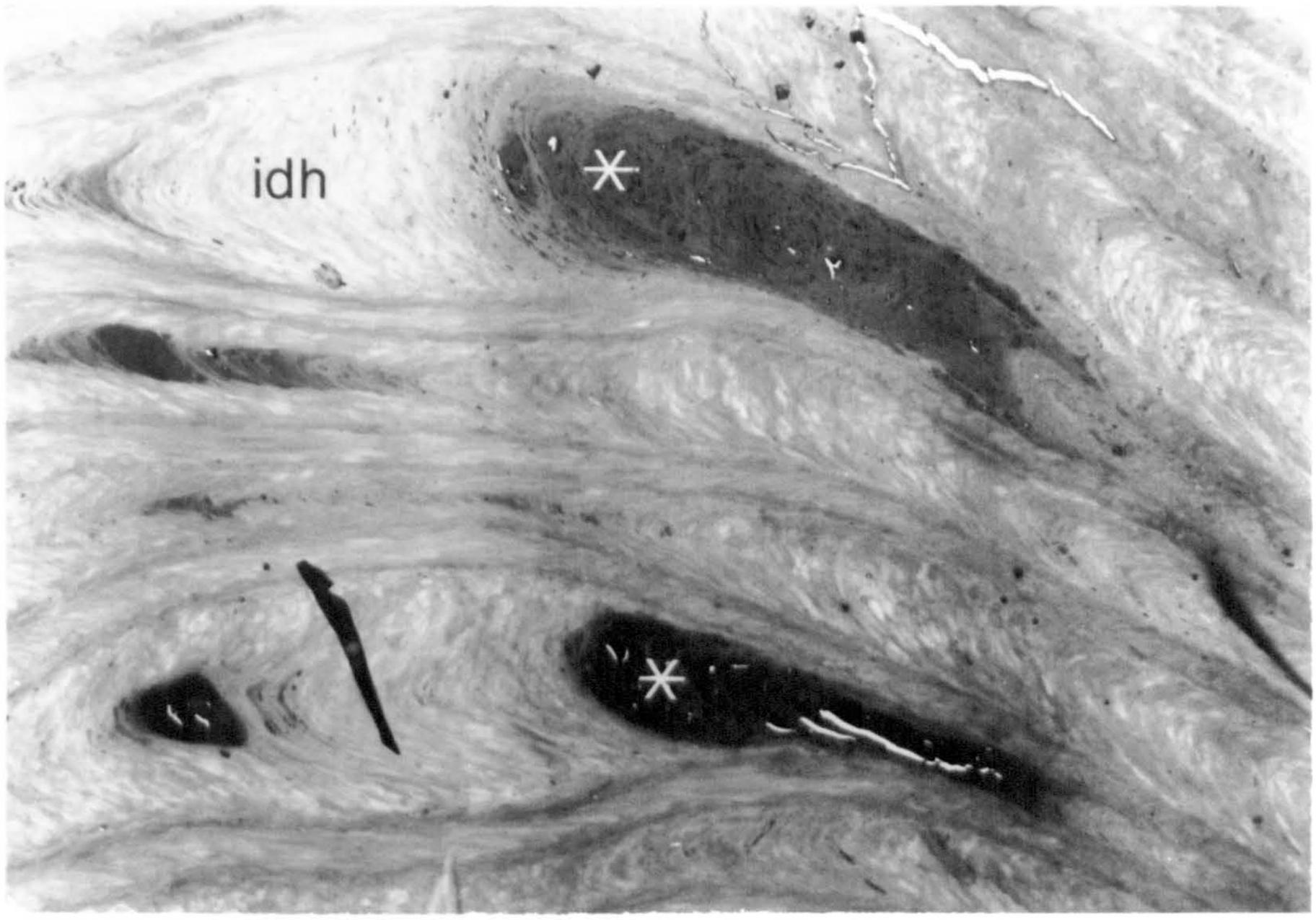
idh

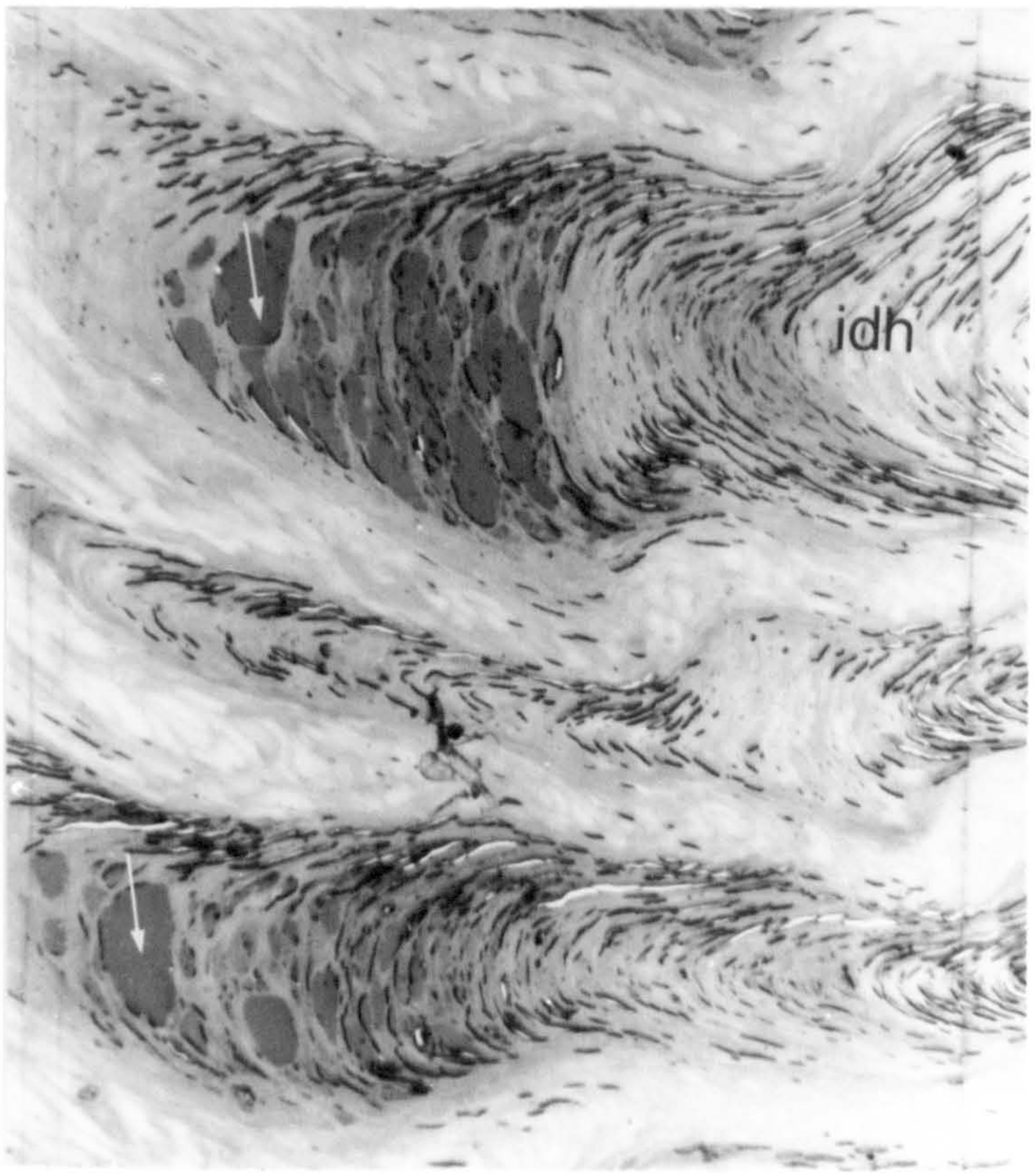
idh

Figure 6.21
Scanning electron micrograph of horn from the white line

Laminar horn (lh) and interdigitating horn (idh) can be clearly distinguished in the scanning electron microscope. Within broadened and distorted regions of interdigitating horn, cracks have developed (↑). These are filled with debris and loose squames. Some of the cracks follow an arrowhead shape, pointing towards the wall. The shape and position of these cracks corresponds to the boundary of arrowhead-shaped regions of abnormal staining detected in the light microscope and illustrated in Figure 6.18.

x 110

Figure 6.22
High power light micrograph of a section of the white line stained with Perl's Prussian Blue

The cell boundaries are stained by the background stain (Neutral Red). The granular black stain indicates the presence of haemosiderin. This blood breakdown product is found concentrated in an almost circular region (*) corresponding to an area which stained densely with Martius Scarlet Blue in an adjacent section. Haemosiderin is also found in discrete granules in the intercellular spaces (i↑) and concentrated in two linear defects in the horn (↑).

x 360

Stain : Perl's Prussian Blue

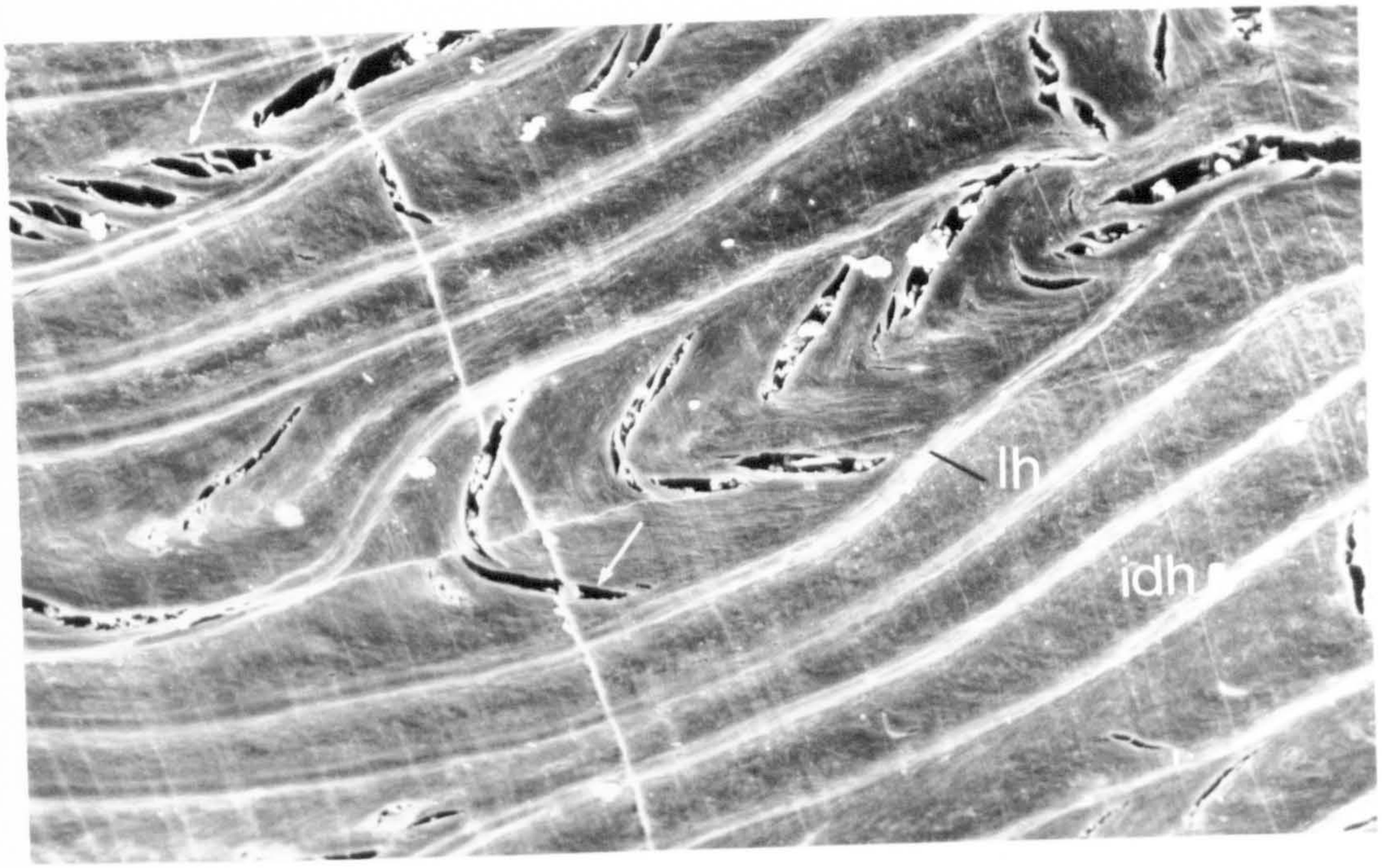
lh
idh

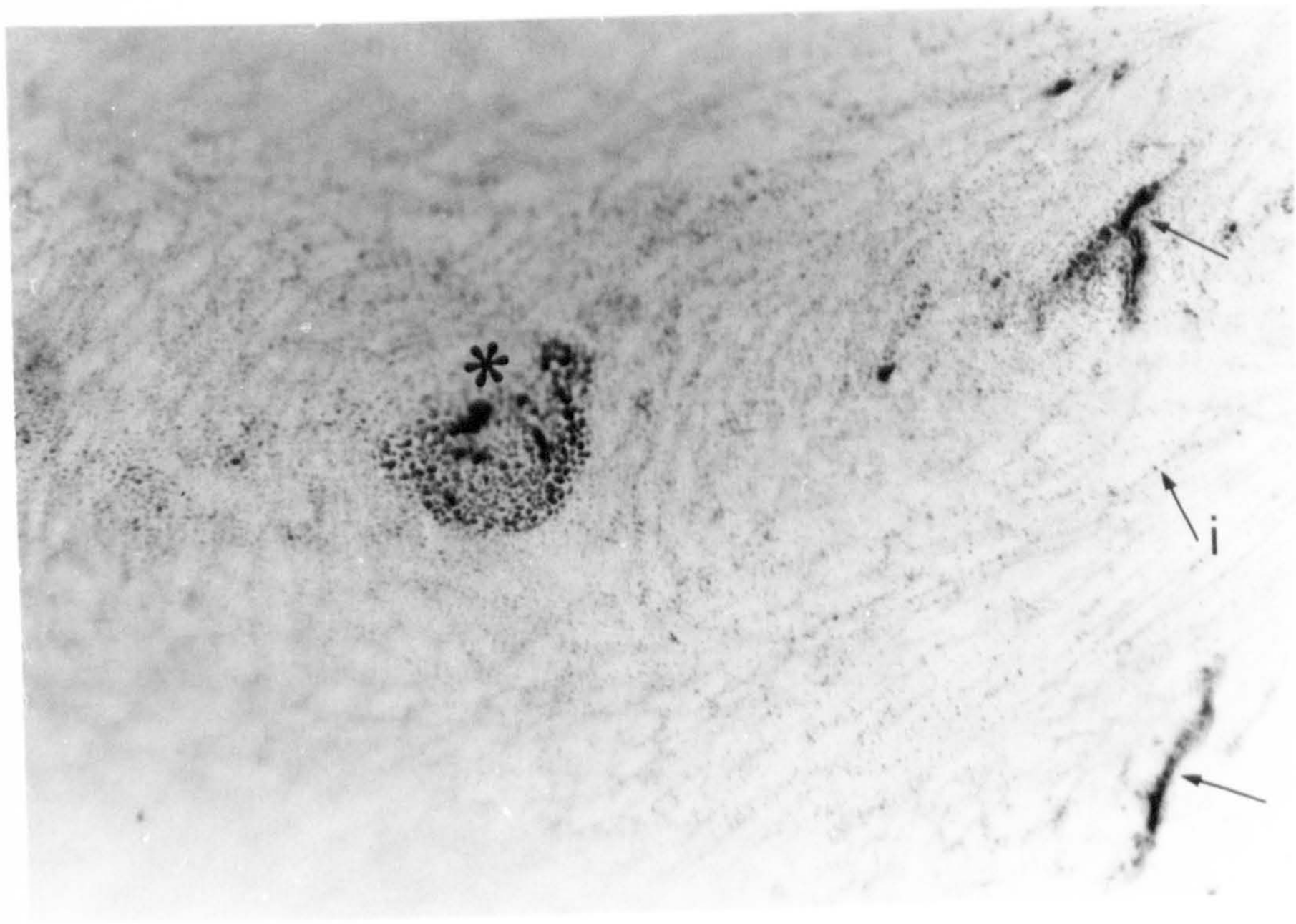
*
i

Figure 6.23
Light micrograph of a region of broadened interdigitating horn in a section stained with Perl's Prussian Blue

The broadened interdigitating horn (idh) is stained much more strongly with the counterstain Neutral Red than is the laminar horn (lh). Within the broadened interdigitating horn there are specific deposits of haemosiderin indicated by the granular black staining (↑).

x 144

Stain : Perl's Prussian Blue

Figure 6.24
Light micrograph of a section from the sole horn stained with Perl's Prussian Blue

Haemosiderin is concentrated granular deposits in the tubule medulla (m).

x 360

Stain : Perl's Prussian Blue

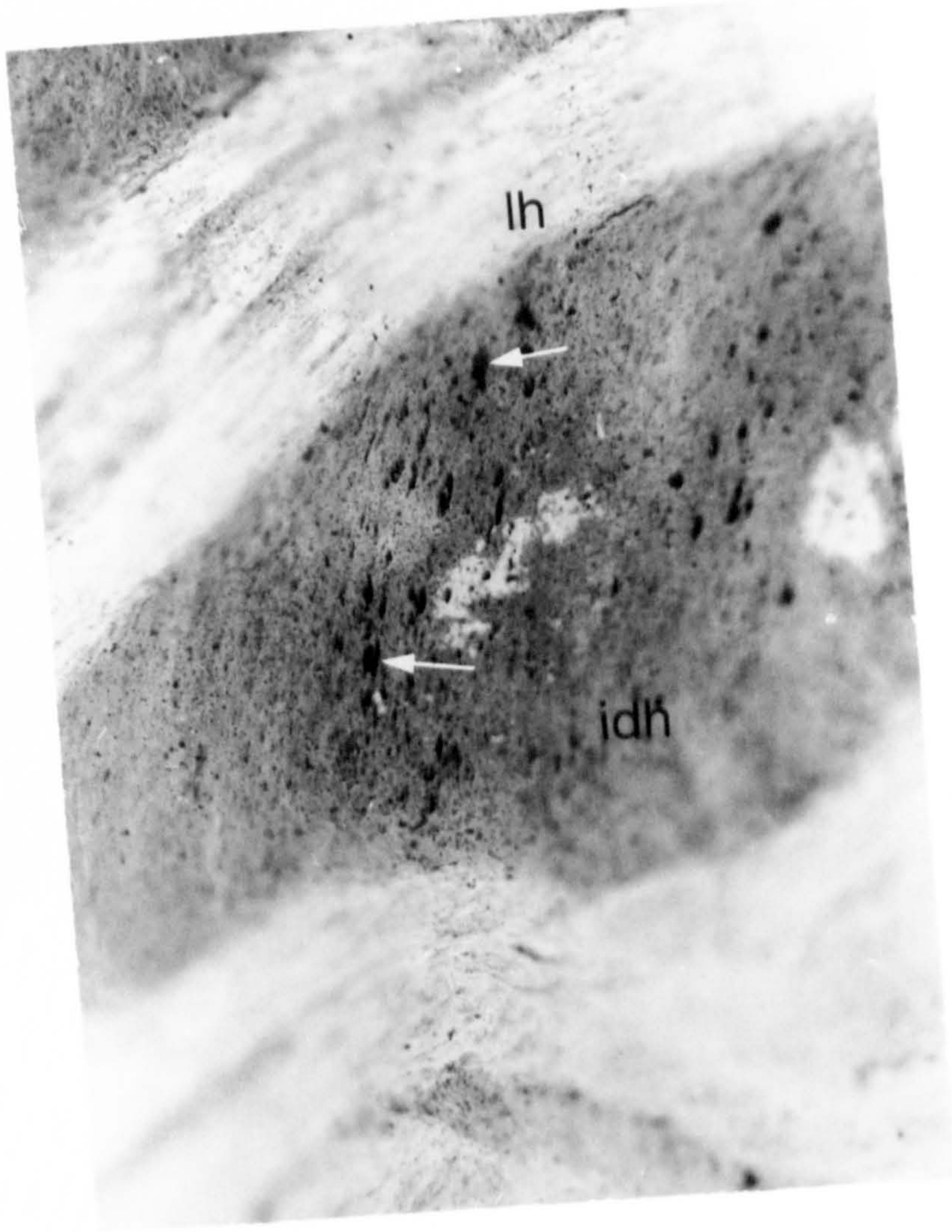
lh
idh

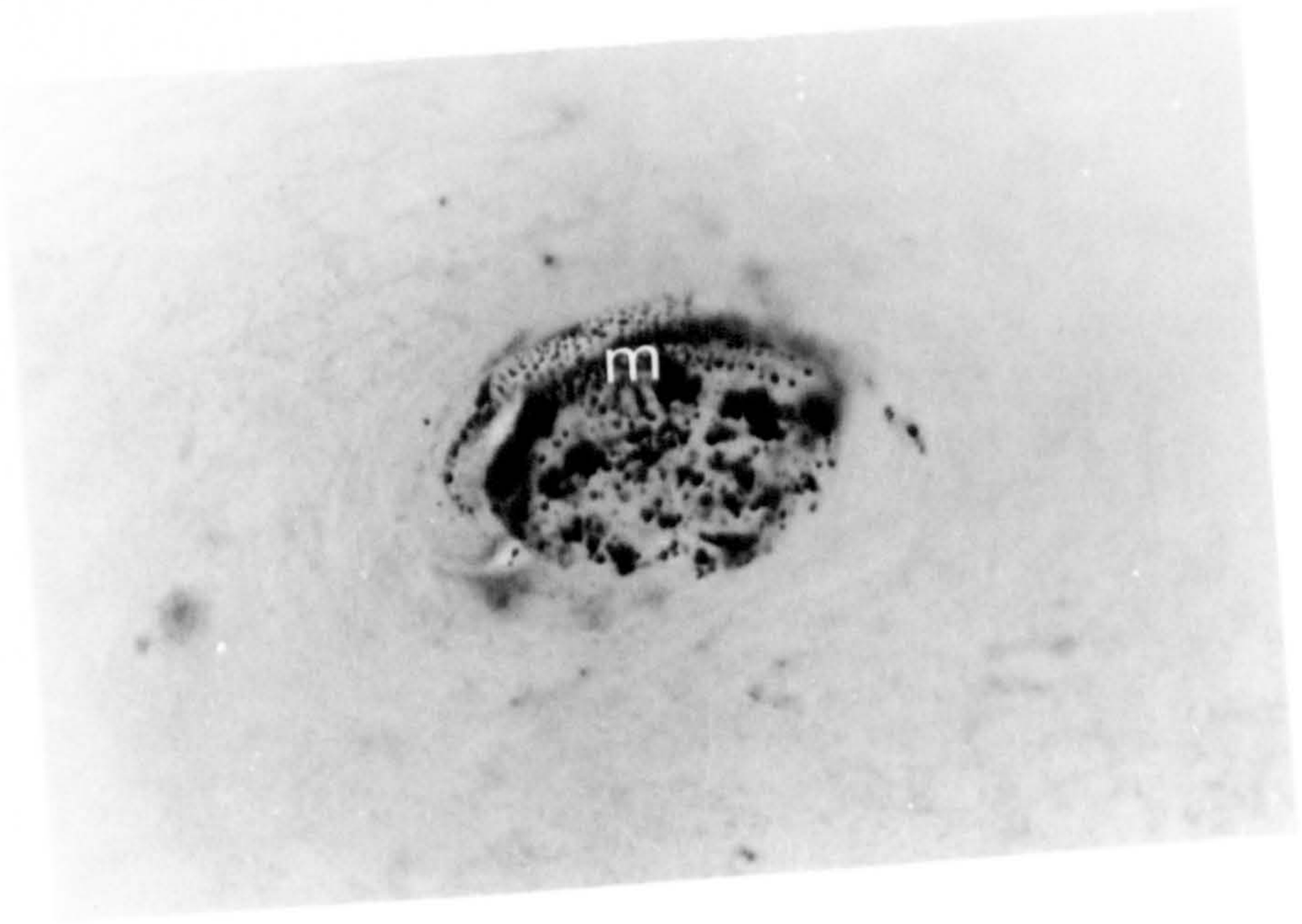
m

Figure 6.25
Light micrograph of a section from a sole exhibiting gross haemorrhage, stained with Perl's Prussian Blue

Haemosiderin forms a network (n ↑) spread over a large area. Interspersed within the network are discrete granules of haemosiderin (↑).

x 360

Stain : Perl's Prussian Blue

Figure 6.26
Low power light micrograph of a section including wall, sole and white line, stained with Perl's Prussian Blue

Haemosiderin is present in tubules of the wall (t ↑), and in cracks (↑) which extend from the white line (wl) into the wall (w) and the sole (s).

x 36

Stain : Perl's Prussian Blue

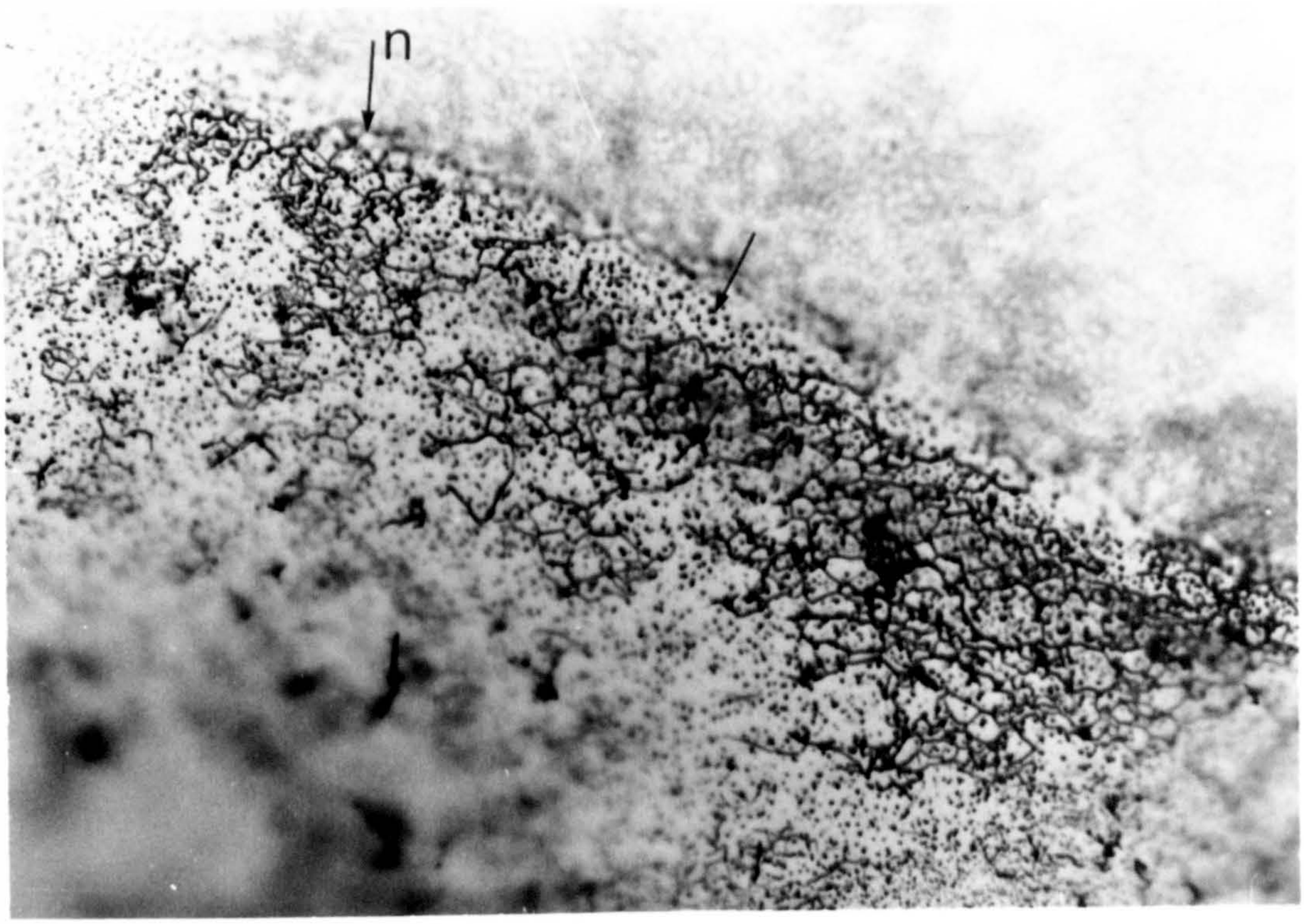
n

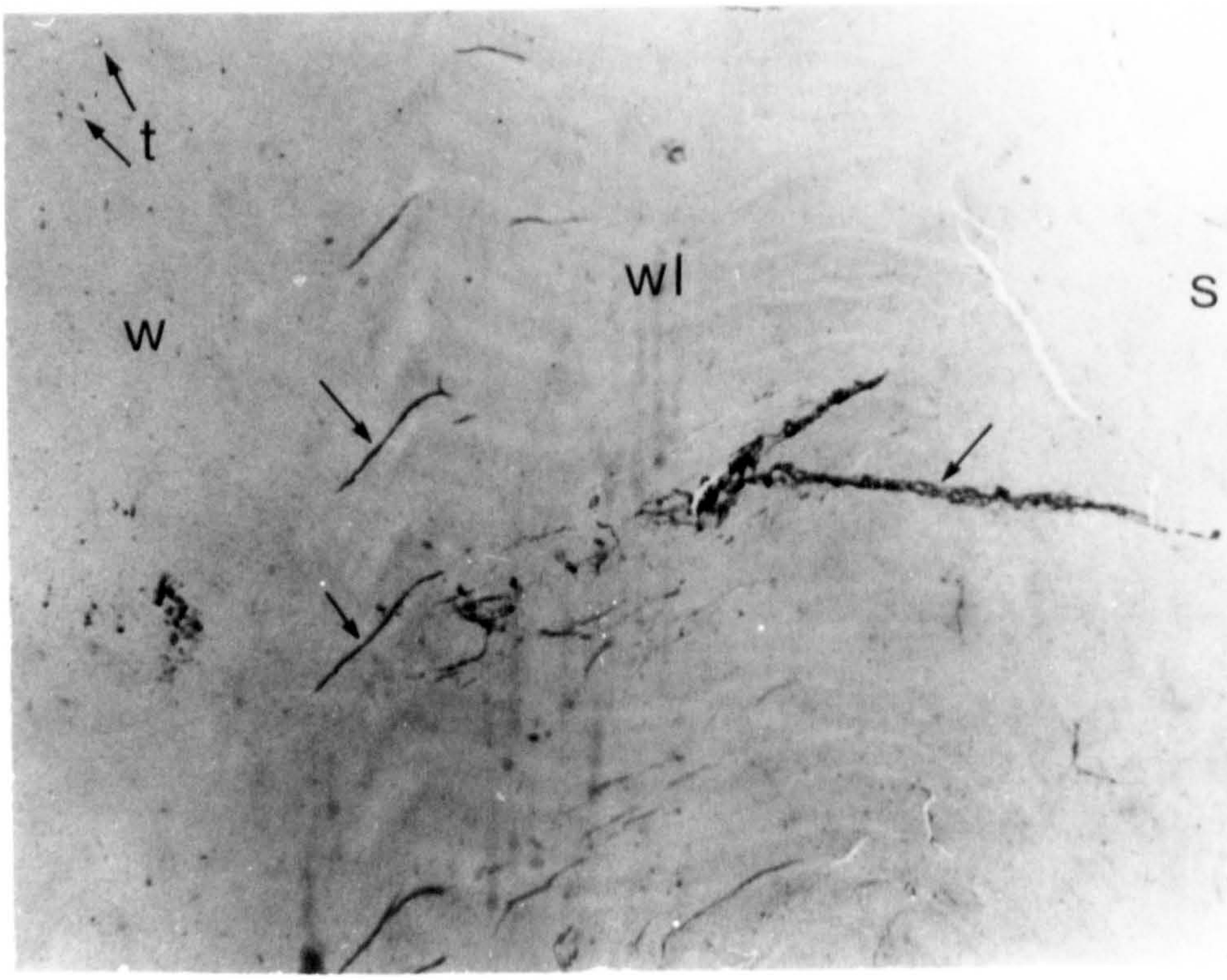
t
w
wl
s

Figure 6.27
The percentage of interdigitating horn in the white line (%IDH) plotted against weeks post-calving, for two cows

Cow 47 had severe and extensive gross lesions of the sole and white line at nine weeks post-calving.
Cow 84 had only mild gross lesions at this time.

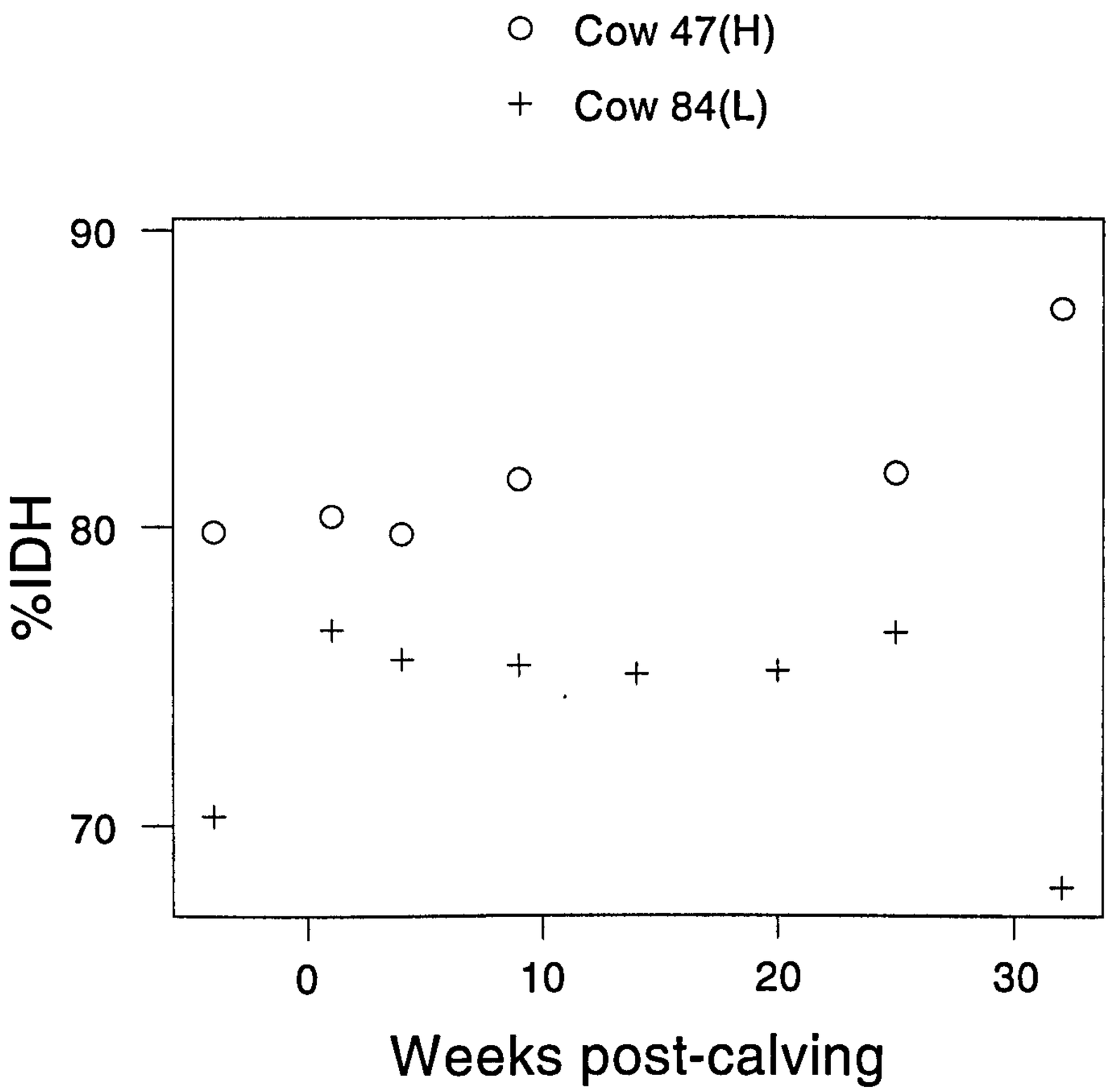
Cow 47(H)
Cow 84(L)
90
80
70
%IDH
0
10
20
30
Weeks post-calving

Figure 6.28
The mean percentage of interdigitating horn in the white line (%IDH) plotted against weeks post-calving, for two groups of five cows

Group HS had high severity gross lesions of the sole at 14 weeks post-calving.
Group LS had low severity gross lesions at this time.

Figure 6.29
The percentage of broadened sheets of interdigitating horn in the white line, plotted against weeks post-calving, for two groups of cows, one with high and one with low severity gross lesions of the sole

Data for the individual cows are plotted

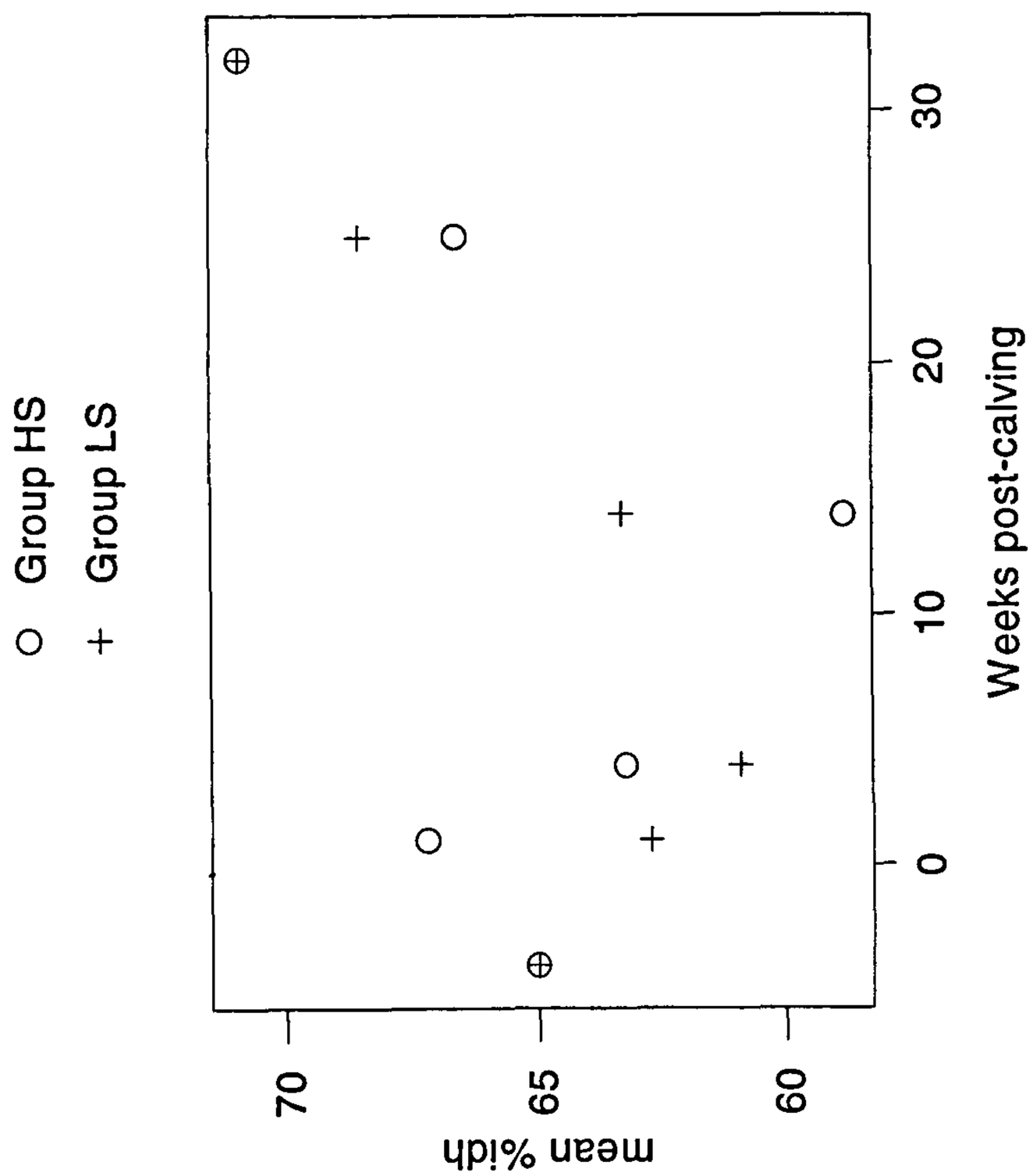
Group HS
Group LS
mean %idh
70
65
60
0
10
20
30
Weeks post-calving

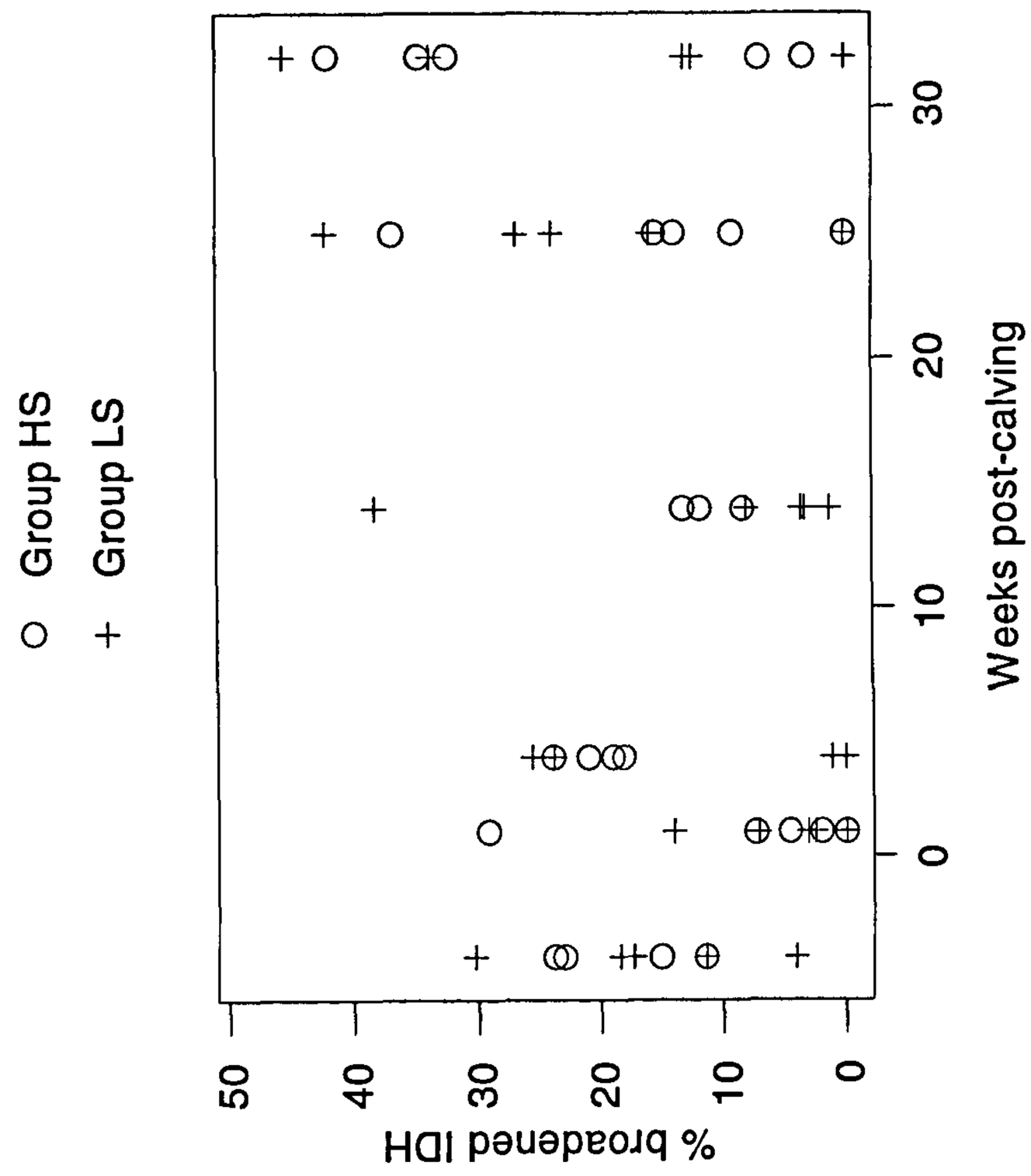
Group HS
Group LS
% broadened IDH
50
40
30
20
10
0
10
20
30
Weeks post-calving

Figure 6.30
Graphs to illustrate the percentage of sheets of interdigitating horn (IDH) exhibiting abnormalities of staining in two groups of five cows at different times during the lactation

Group HS had high severity gross lesions of the sole at 14 weeks post-calving.
Group LS had low severity lesions at this time.

Data for the individual cows are plotted

Figure 6.30a
Percentage of sheets of IDH containing discrete, round densely stained areas (% round stain) plotted against weeks post-calving

Figure 6.30b
Percentage of sheets of IDH containing extensive densely stained areas (% extensive stain) plotted against weeks post-calving

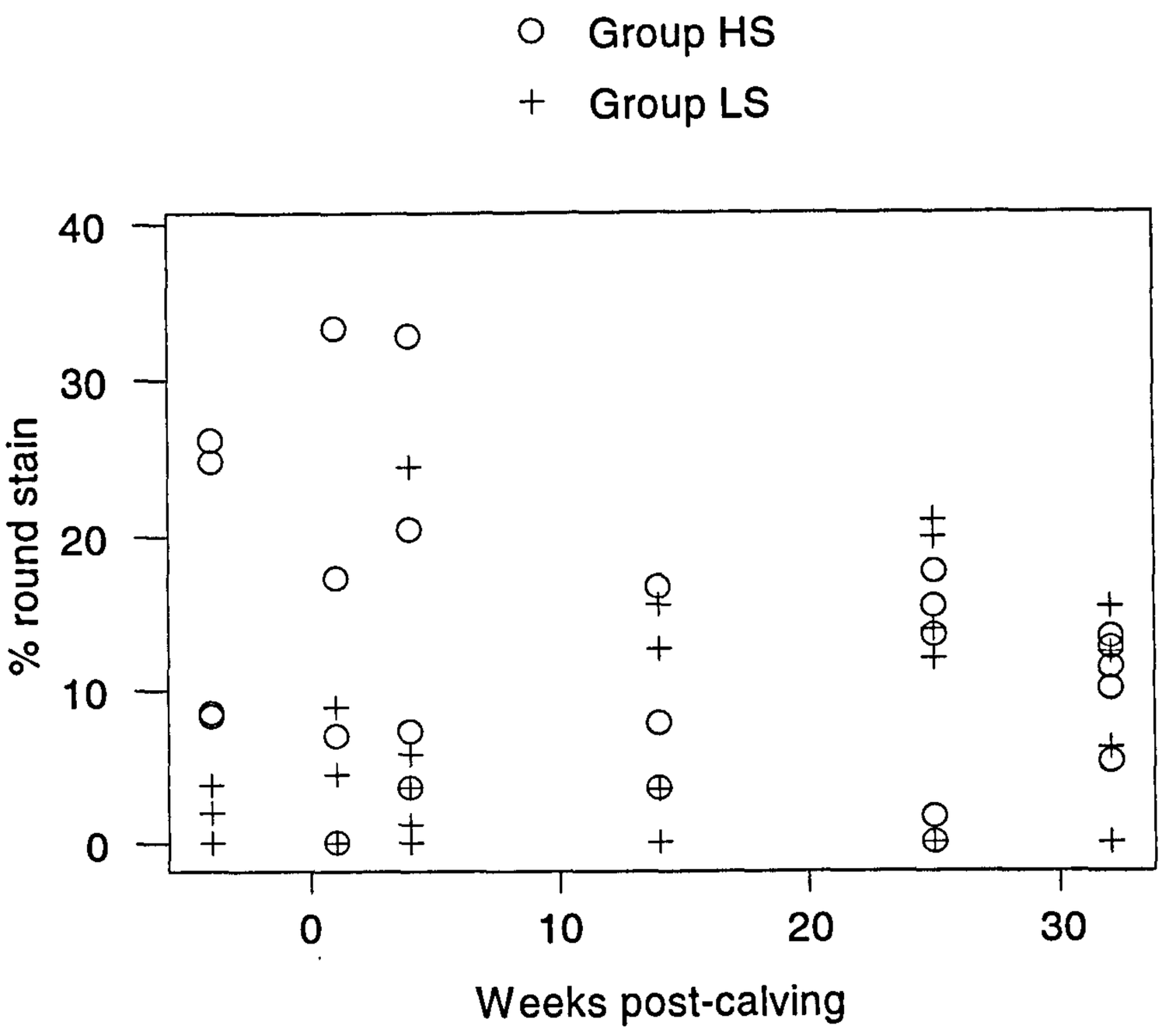
Group HS
Group LS
% round stain
40
30
20
10
0
0
10
20
30
Weeks post-calving

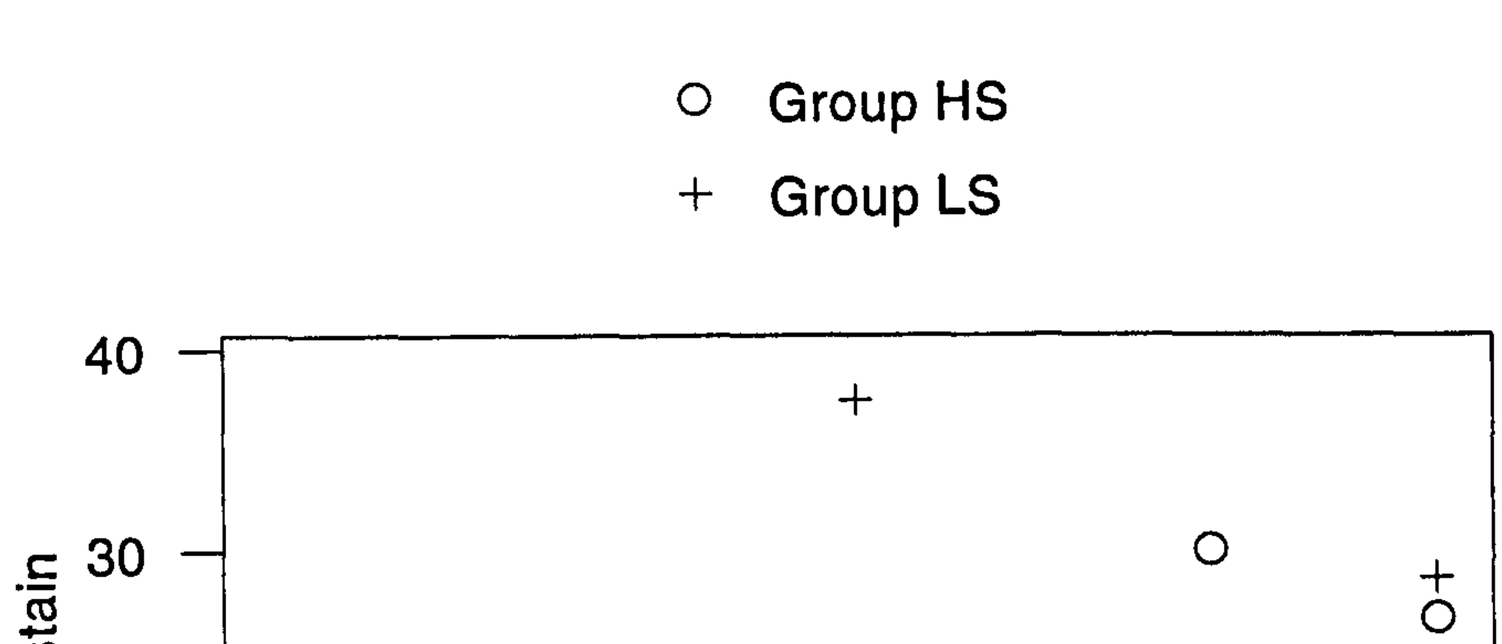
Group HS
Group LS
% extensive stain
40
30
20
10
0
0
10
20
30
Weeks post-calving

FIGURES

CHAPTER 7

Figure 7.1
Diagrams to illustrate selective sampling of broadened regions of interdigitating horn for transmission electron microscopy (not to scale)

1 Embedded horn slivers viewed in dissection microscope to select those with broadened regions of IDH

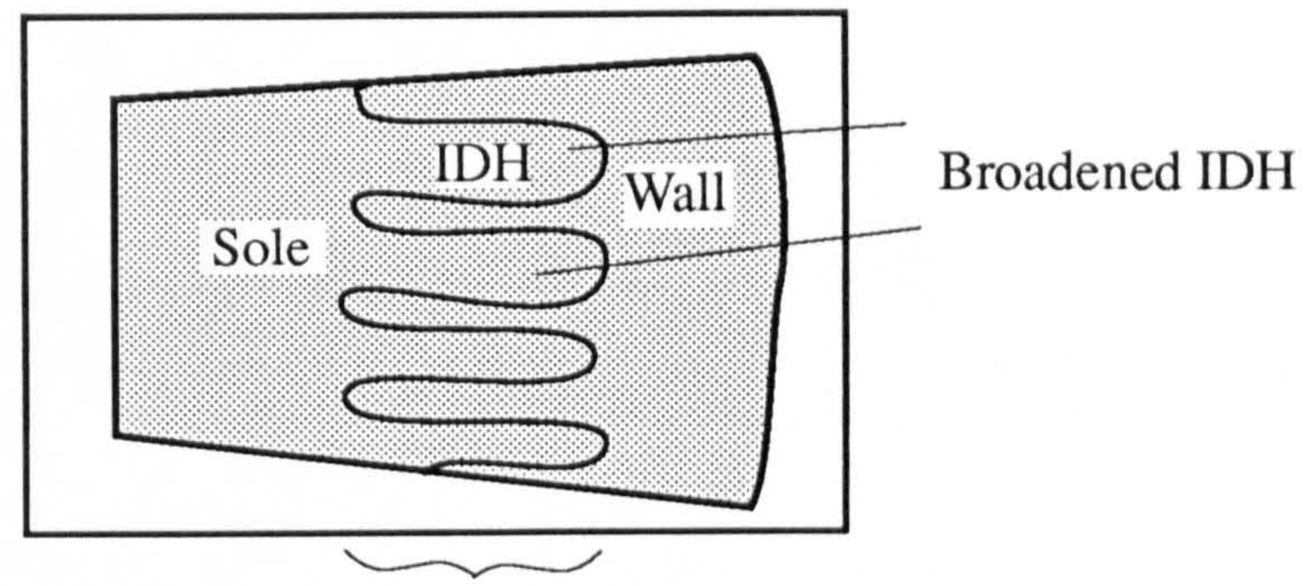

2 One block cut from white line to include broadened IDH

3 Survey sections stained with Toluidine Blue and viewed in light microscope

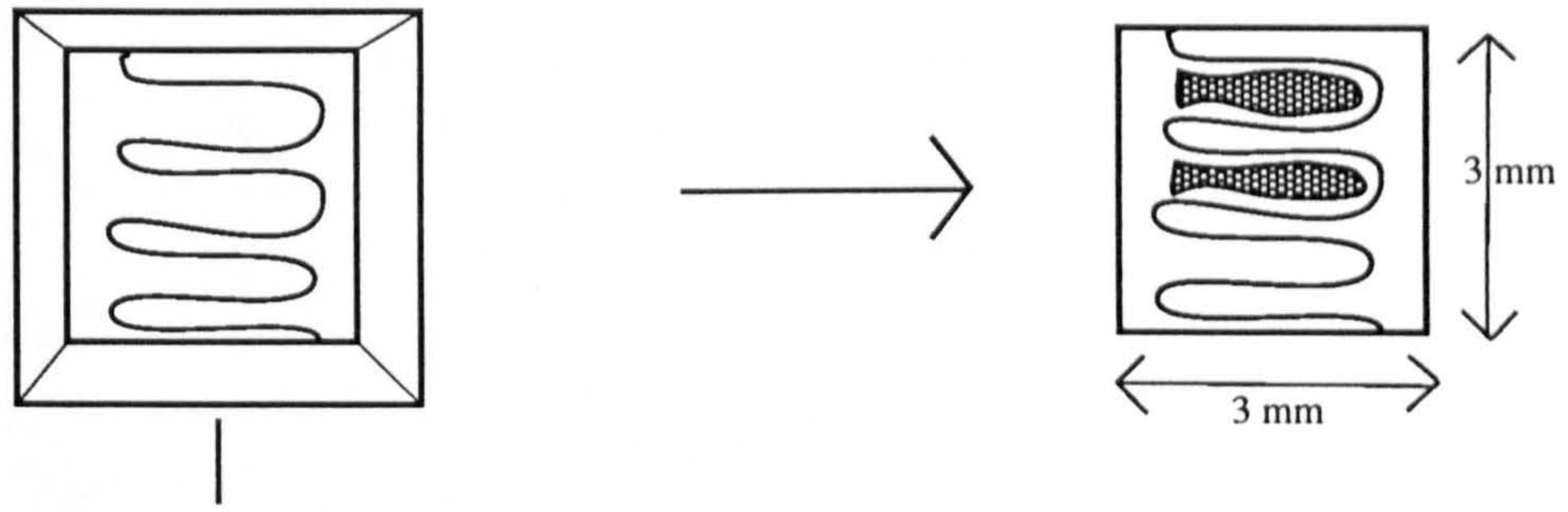

4 Block trimmed down to region of broadened densely stained IDH

5 7 nm sections for electron microscope

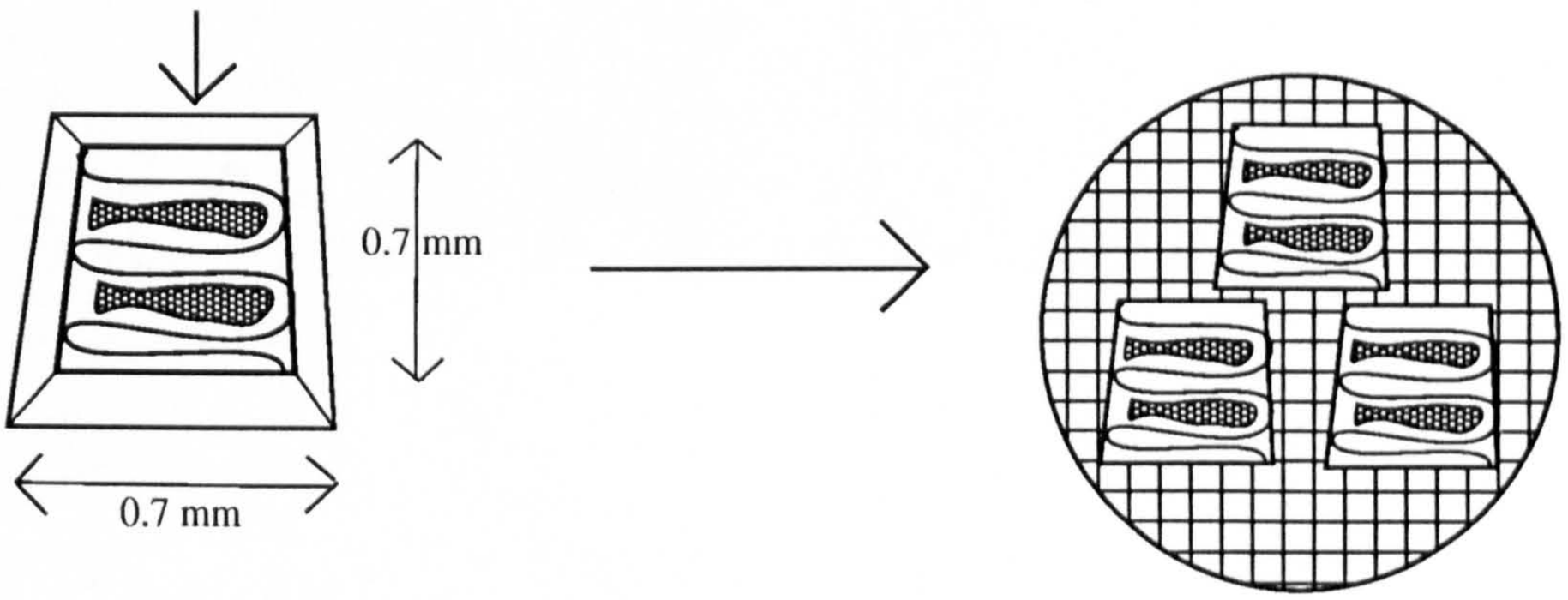

NB All sections are parallel to the distal surface of the foot

Figure 7.2
Low power transmission electron micrograph of the tip of a broadened sheet of interdigitating horn and the adjacent laminar horn

Squames of interdigitating horn (idh) and laminar horn (lh) are irregularly shaped. The intracellular material shows much variation in electron density, giving a "marbled" appearance (m). Well preserved remains of nuclei (n) are visible, indicating that keratinization has not proceeded normally. Squame boundaries are distorted (↑) and intercellular material (i) is present in enlarged intercellular spaces in the laminar horn.

x 6,200

Cow 47 25 weeks post-calving

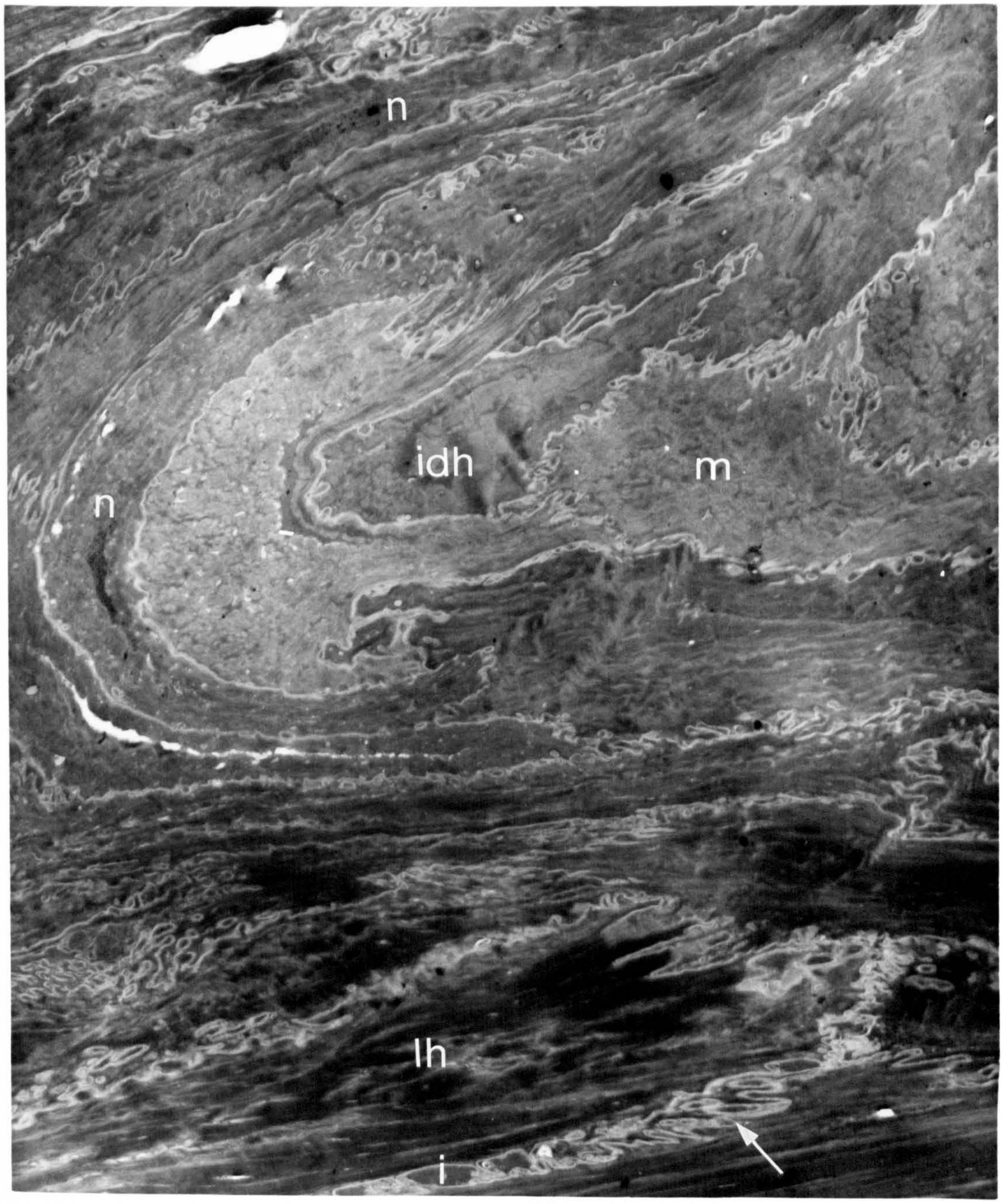
n
idh
m
n
lh
i

Figure 7.3
Higher power transmission electron micrograph of the junction between broadened interdigitating horn and the adjacent laminar horn

In this region the "marbled" appearance of squames of interdigitating horn (idh) and laminar horn (lh) is due to irregular arrangement of keratin fibres (kf ↑) and failure of the normal close association between keratin fibres and interfilamentous matrix (ma). Cell boundaries (cb ↑) are very distorted and in places are separated by intercellular material (i). In some regions a reticulate pattern can be distinguished in the intercellular material (ri).

x 9,700

Cow 84 9 weeks post-calving

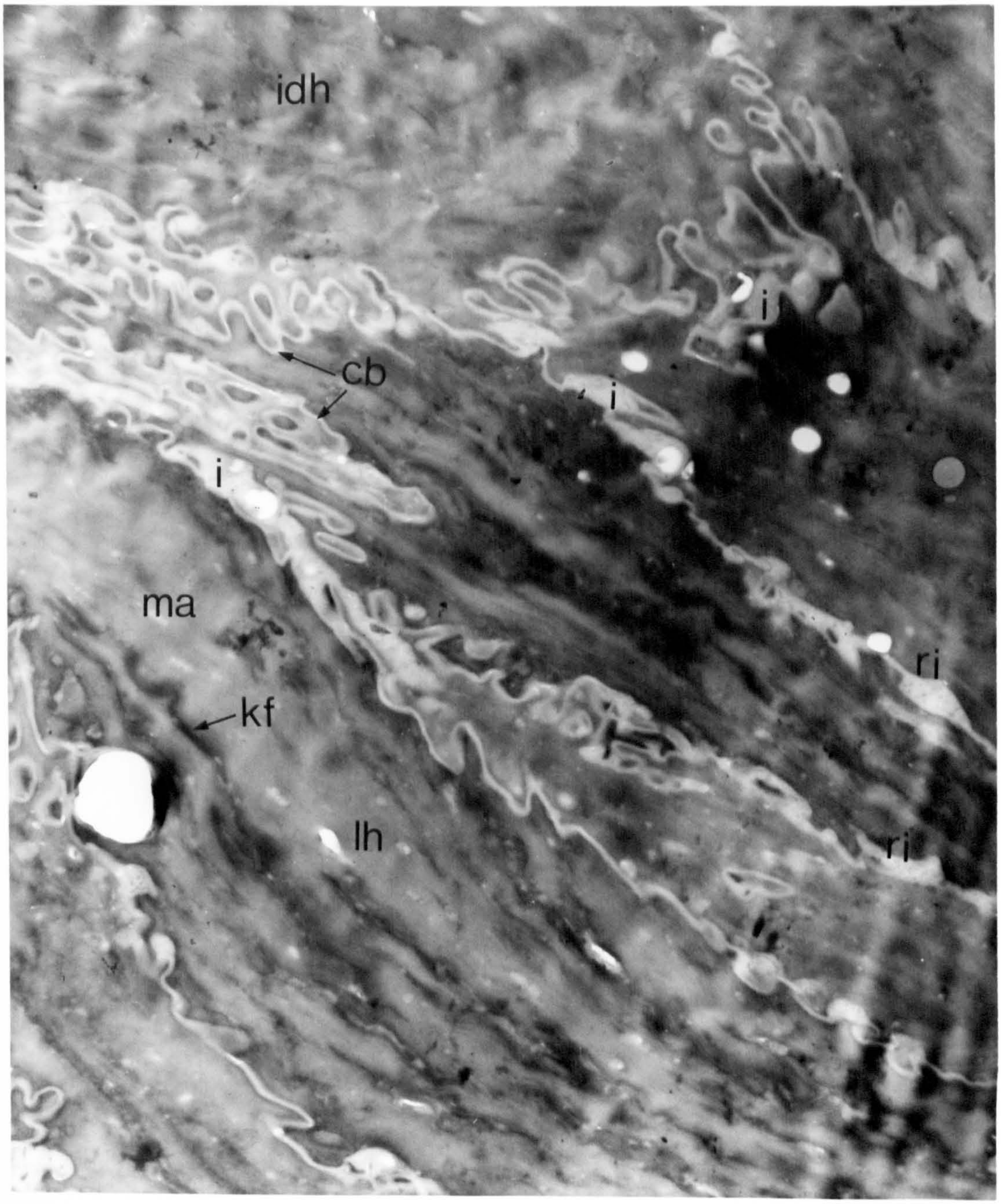
idh
cb
i
i
i
ma
kf
ri
lh
ri

Figure 7.4
Transmission electron micrograph of broadened interdigitating horn and adjacent laminar horn

In this micrograph the mottled appearance of squames of the interdigitating horn (idh) arises from the presence of electron-lucent areas within the squames (↑). These have a similar appearance to the intercellular material (i) which is found in enlarged intercellular spaces in the laminar horn (lh).

x 5,775

Cow 60 14 weeks post-calving

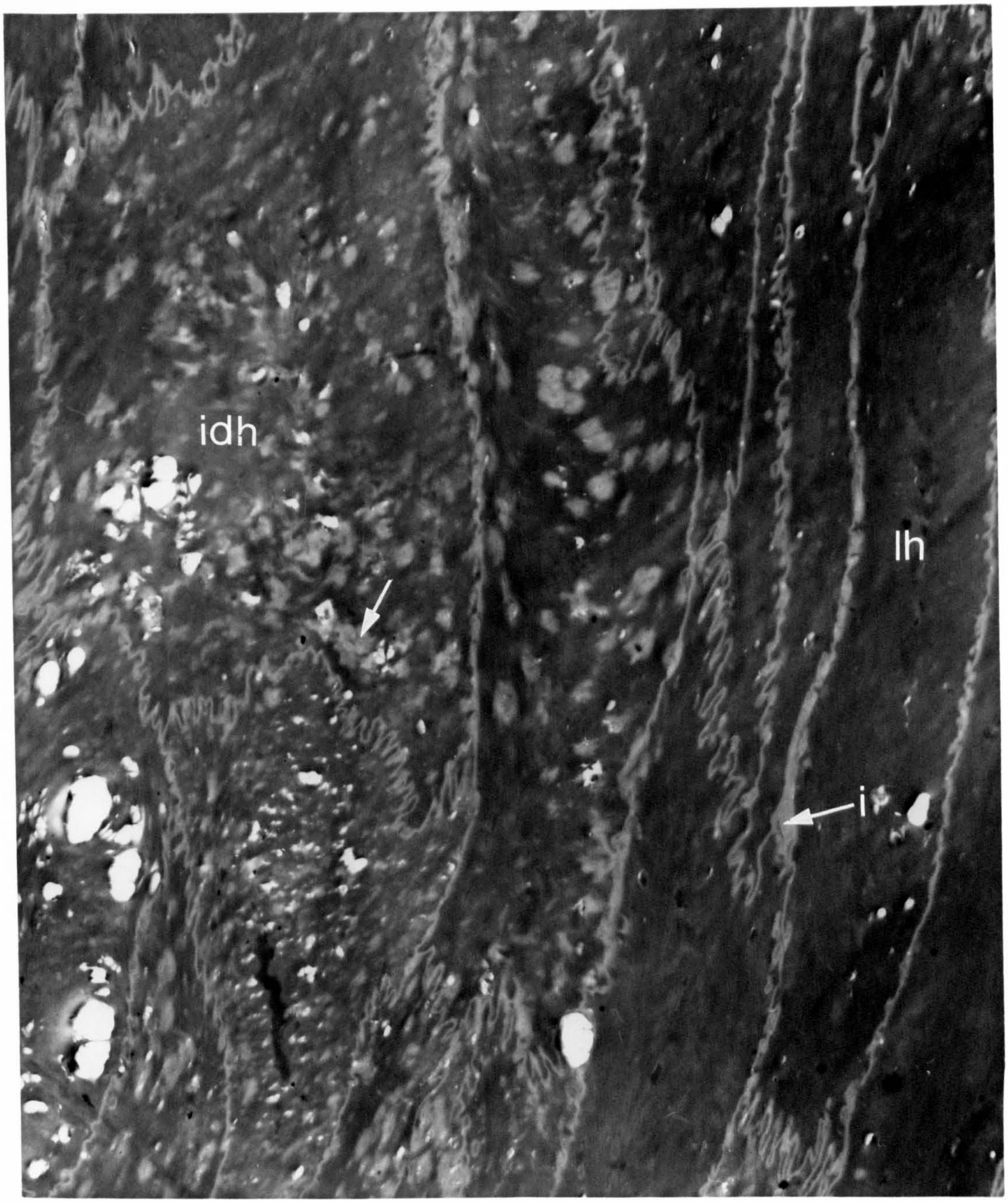
idh
lh
i

Figure 7.5
Transmission electron micrograph of broadened interdigitating horn and adjacent laminar horn

In the interdigitating horn (idh) the lack of matrix makes individual keratin fibres (kf ↑) clearly visible. There is an electron-dense deposit on the intracellular aspect of the squame boundaries (↑). In the laminar horn (lh) matrix is present but filament-matrix association is poor. Several pale oval bodies are visible which may be the remains of mitochondria (*).

x 7,100

Cow 47 14 weeks post-calving

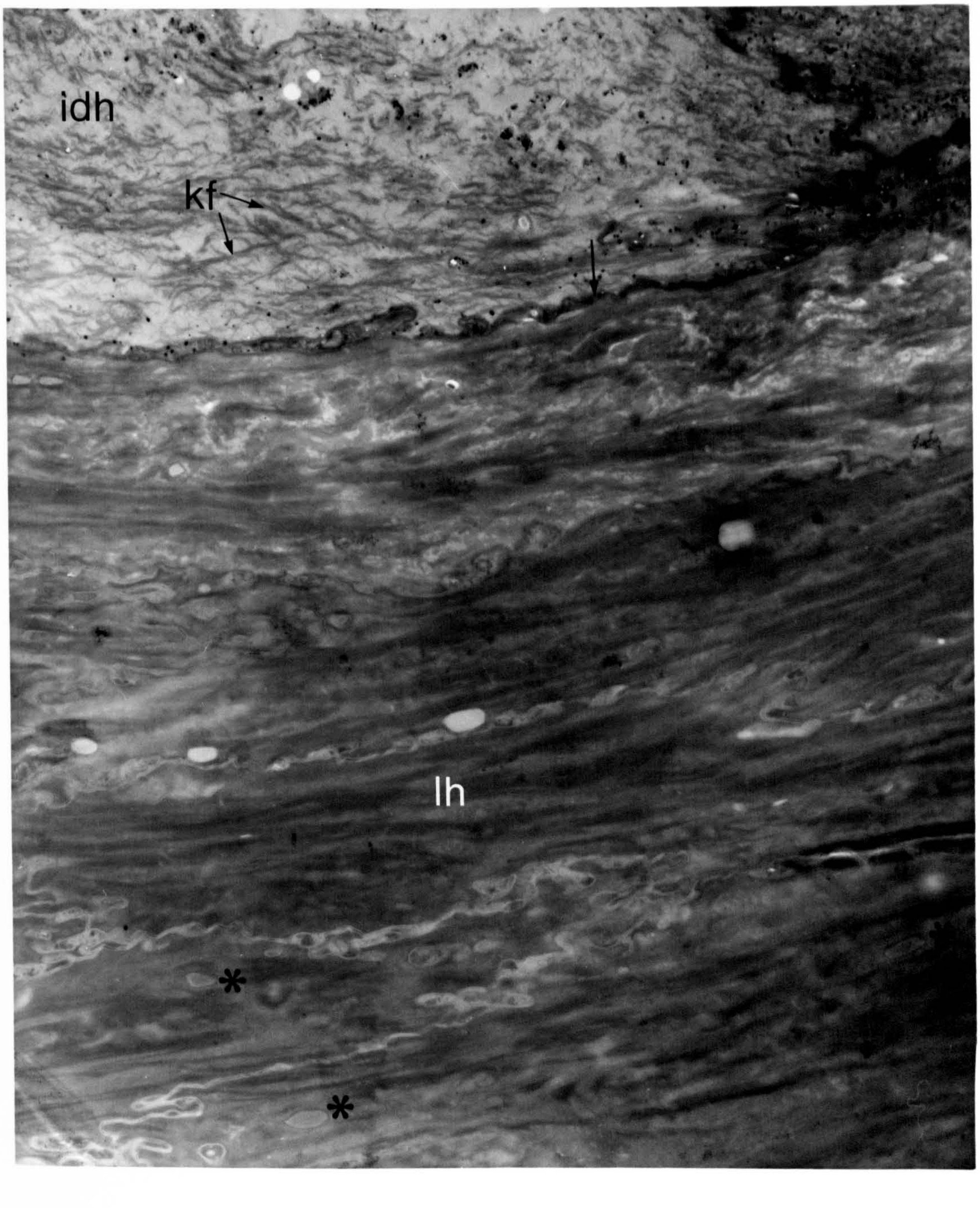
idh
kf
lh
*
*

Figure 7.6
High power transmission electron micrograph of the remains of a nucleus in a squame within a broadened sheet of interdigitating horn

The nucleus (n) is well-preserved. It contains granular electron-dense material.
The nucleus shows signs of separating from the surrounding material.

x 35,000

Cow 47 4 weeks post-calving

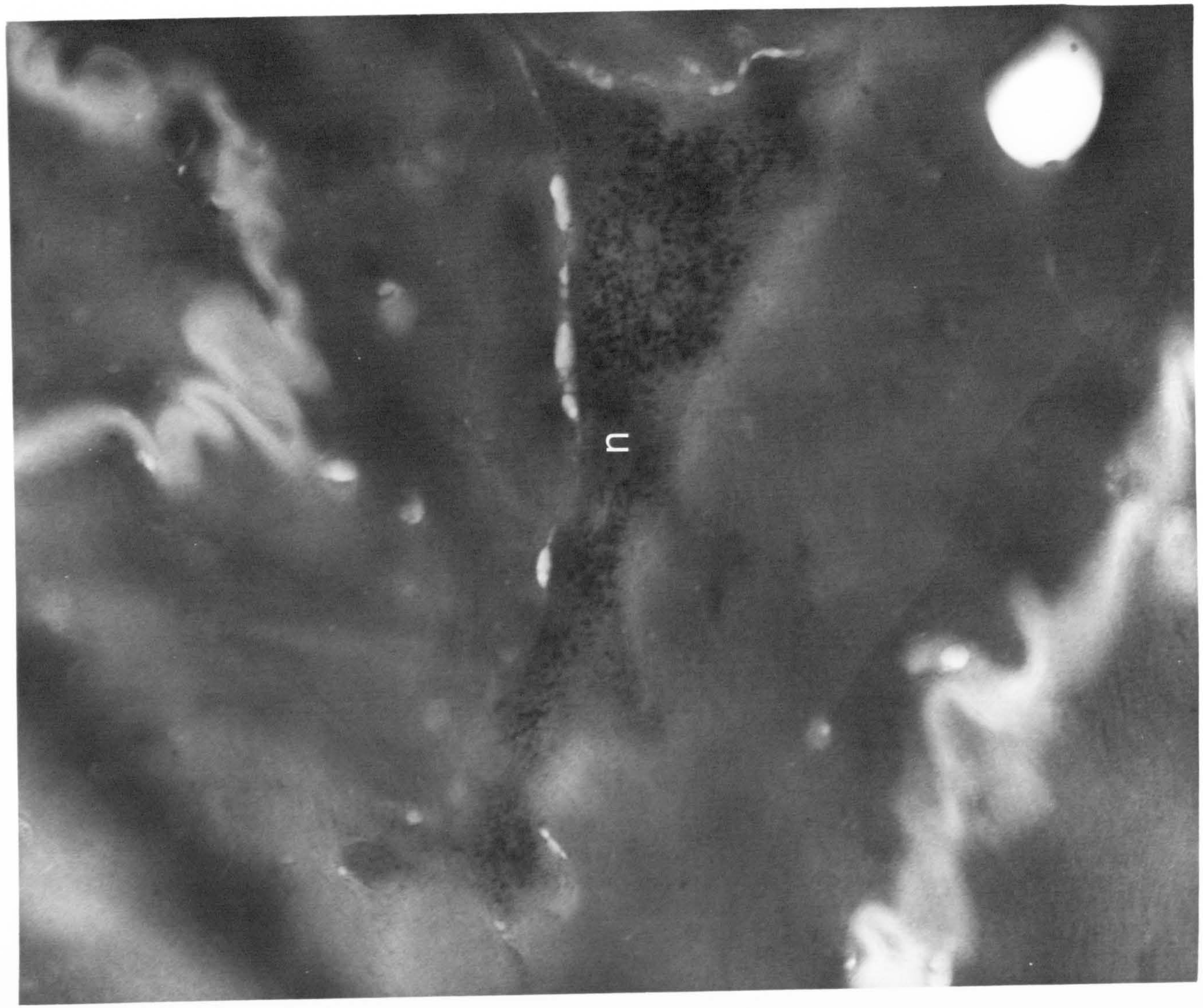

Figure 7.7
Transmission electron micrograph of squames of interdigitating horn from an area with high affinity for histological stains

The tissue is very fragile and holes (h) inevitably develop during preparation or viewing. The contents of squames is highly variable in electron density. Remnants of organelles (o) can be seen. The remains of the nucleus (n) are visible as granular electron-dense material.

x 13,300

Cow 47 14 weeks post-calving

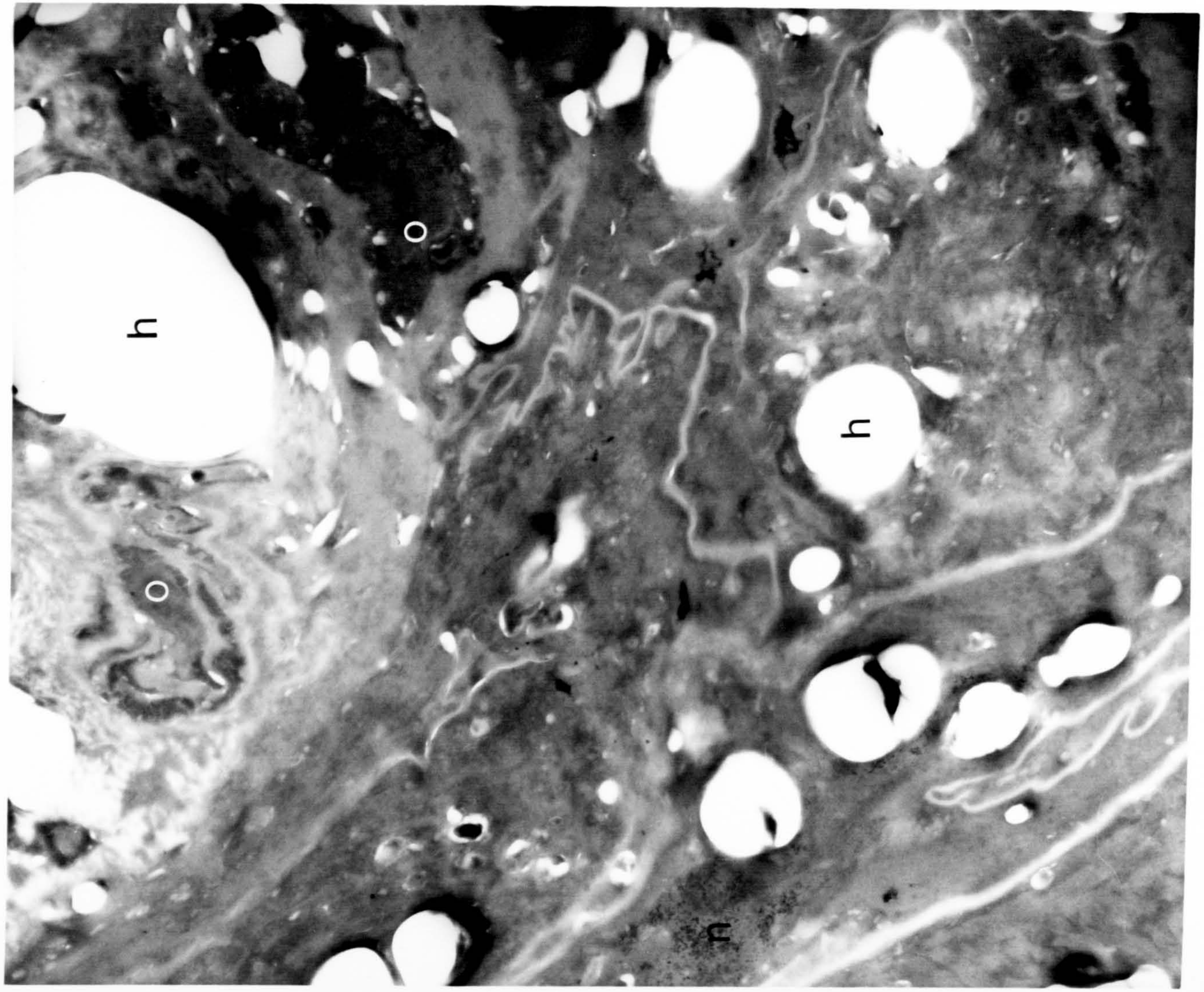
h
O
h
O
F

Figure 7.8
High power transmission electron micrograph of squames of interdigitating horn from an area with high affinity for histological stains

Discrete oval bodies can be detected within squames, which often show signs of separation from the surrounding tissue (*). These are thought to be the remains of mitochondria. Electron-dense material (ed) scattered throughout the squame gives an appearance similar to that found in less complete forms of keratinization.

x 30,360

Cow 47 14 weeks post-calving

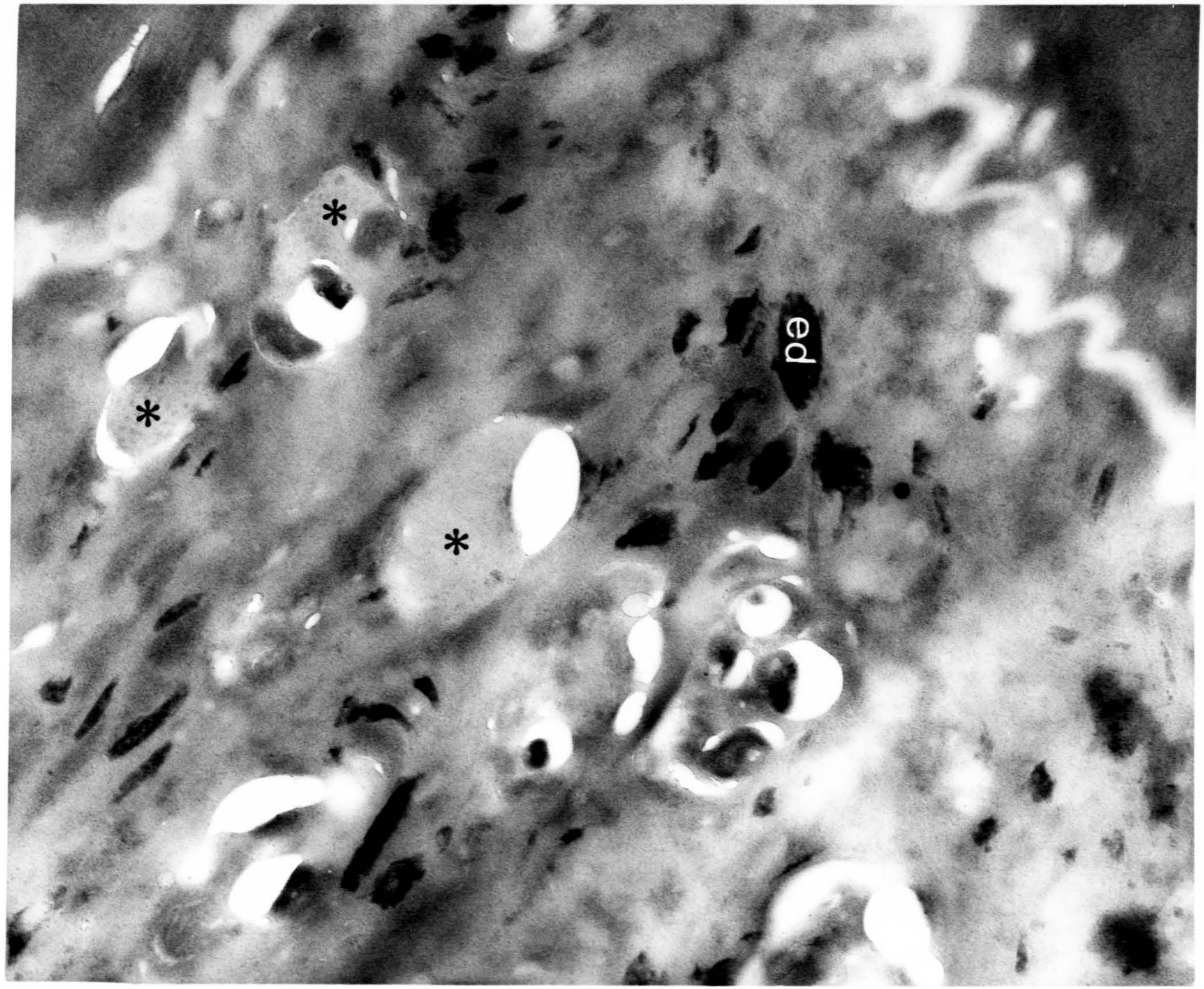
*
*
*
ed

Figure 7.9
Transmission electron micrograph of squames of interdigitating horn from an area with high affinity for histological stains

The central squame (s) contains a large amount of electron-dense material (ed). The appearance of this squame is similar to that seen in less complete forms of keratinization. The space between this squame and one of its neighbours is widened in places and contains amorphous intercellular material (i). The neighbouring squames contain smaller amounts of granular electron-dense material and have a mottled appearance. It is thought that the abnormal keratinization process has reached a different stage in these squames.

x 8,500

Cow 47 14 weeks post-calving

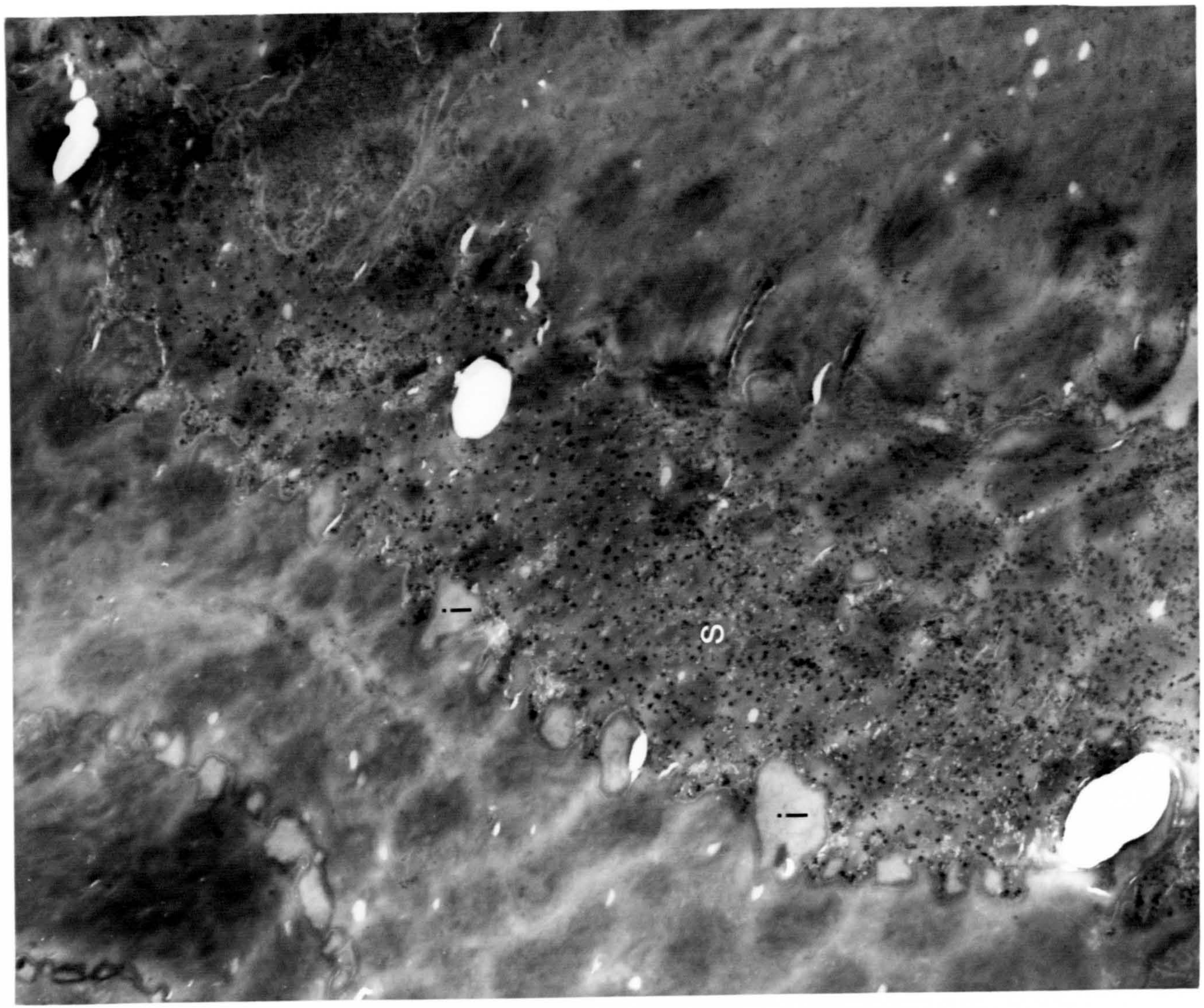
S

Figure 7.10
High power transmission electron micrograph of the boundary of a squame of interdigitating horn containing electron-dense deposit

The electron dense deposit is concentrated at the boundary of the squame (↑). It appears to be limited by the squame boundary as none is present in the adjacent squame. The neighbouring squame nevertheless has an irregular intracellular structure.

x 33,000

Cow 47 14 weeks post-calving

Figure 7.11
High power transmission electron micrograph of electron dense particles present in a squame displaying abnormal keratinization

At high power the electron dense particles (*) show no limiting membranes. The internal structure is not uniform, but gives the particles a mottled appearance. Within the particles, electron dense granules can be distinguished which have a crystalline appearance (↑).

x 161,700

Cow 47 14 weeks post-calving

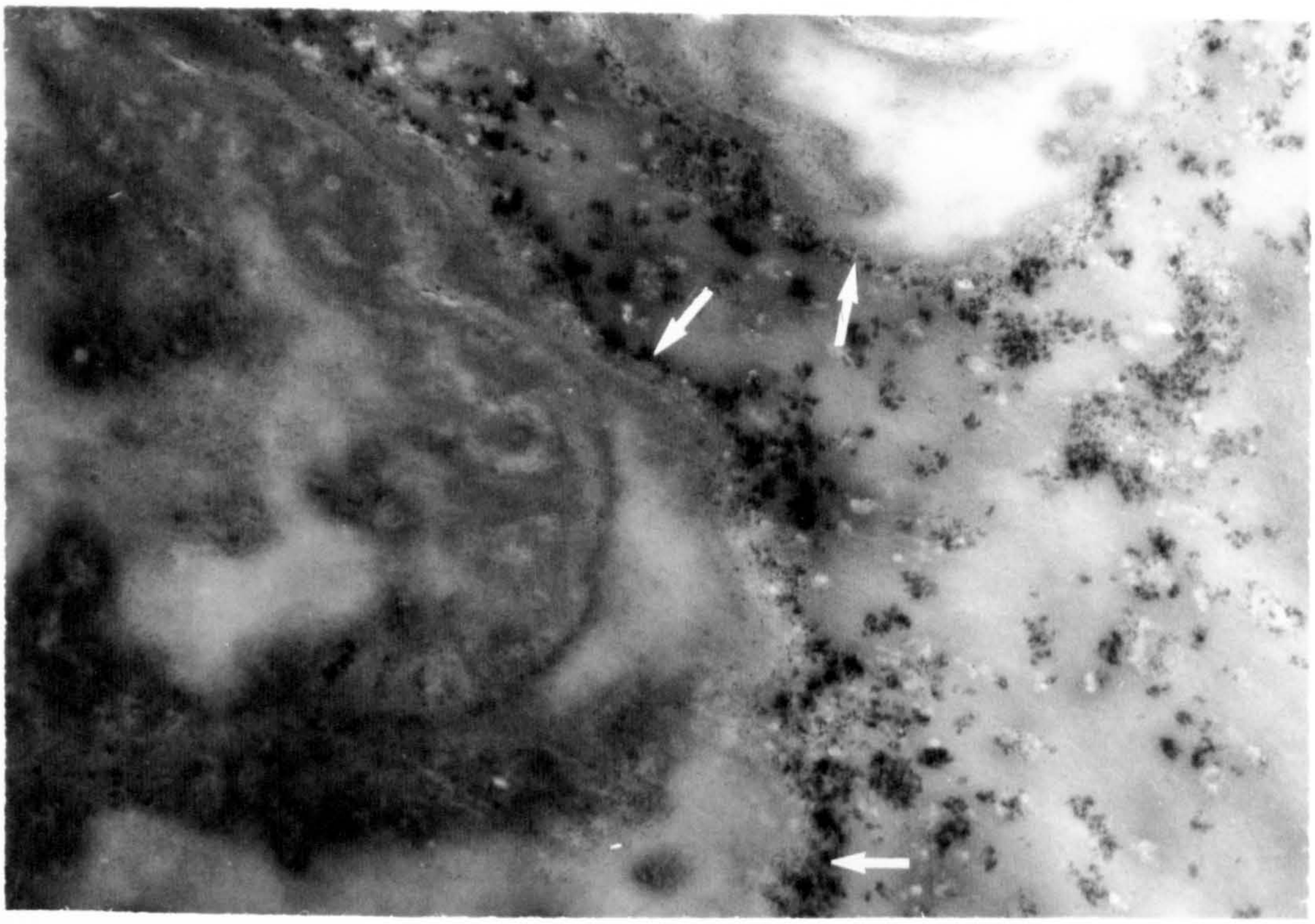

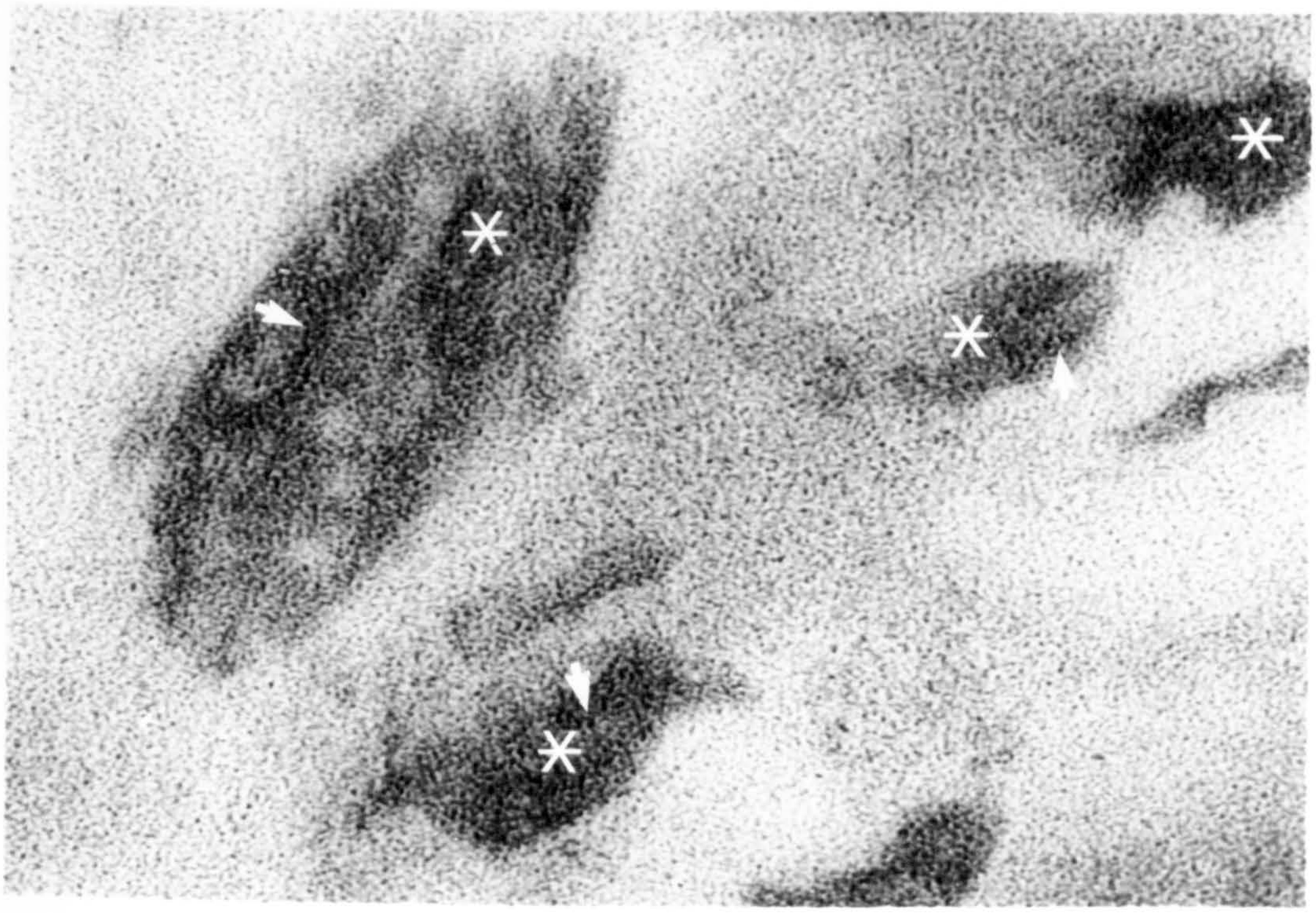

Figure 7.12
Transmission electron micrograph of squames of interdigitating horn from an area with high affinity for histological stains

The normal intracellular structure is disturbed and there is lack of association between keratin fibres and matrix. Electron-dense material has been deposited on the intracellular aspect of squame boundaries (↑).

x 31,250

Cow 47 14 weeks post-calving

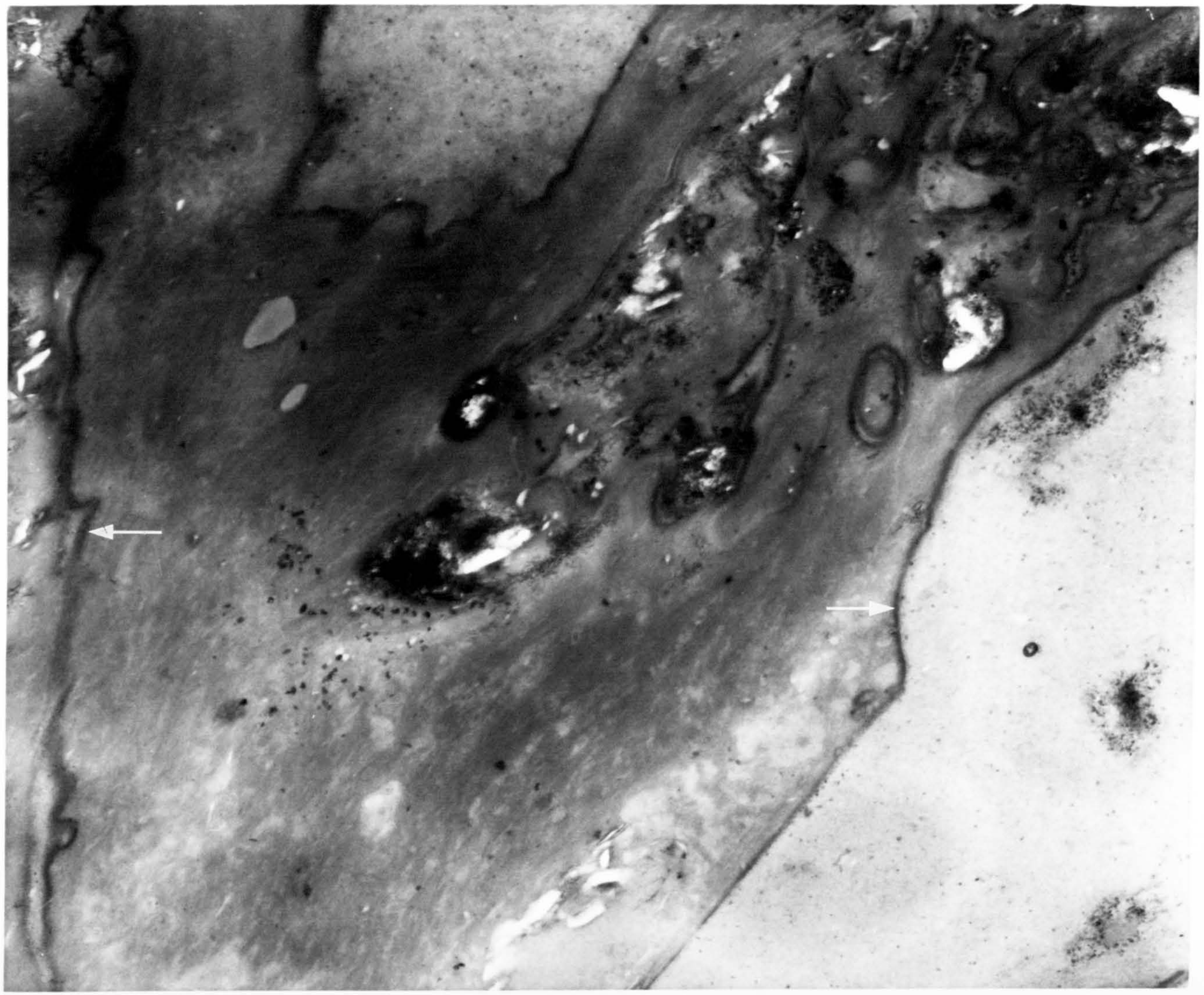

Figure 7.13
Transmission electron micrograph of interdigitating horn including a round region corresponding to an area with high affinity for histological stain

Within the interdigitating horn (idh) five squames form an oval shape which corresponds to an oval region of dense staining on the survey section. These squames are of highly variable electron density. In two of them, keratin fibres (kf) are concentrated at the periphery while the remainder of the squame is filled with unstructured intracellular debris (u). This material is very susceptible to damage during preparation and viewing.

The surrounding squames of interdigitating horn show less extreme abnormalities of keratinization, containing granular electron-dense deposits (ed) and nuclear remnants (n). Surrounding squames form an arch (a) over the aspect of the oval region closest to the wall. Electron dense deposits are also visible in the adjacent laminar horn (lh).

x 7,300

Cow 47 14 weeks post-calving

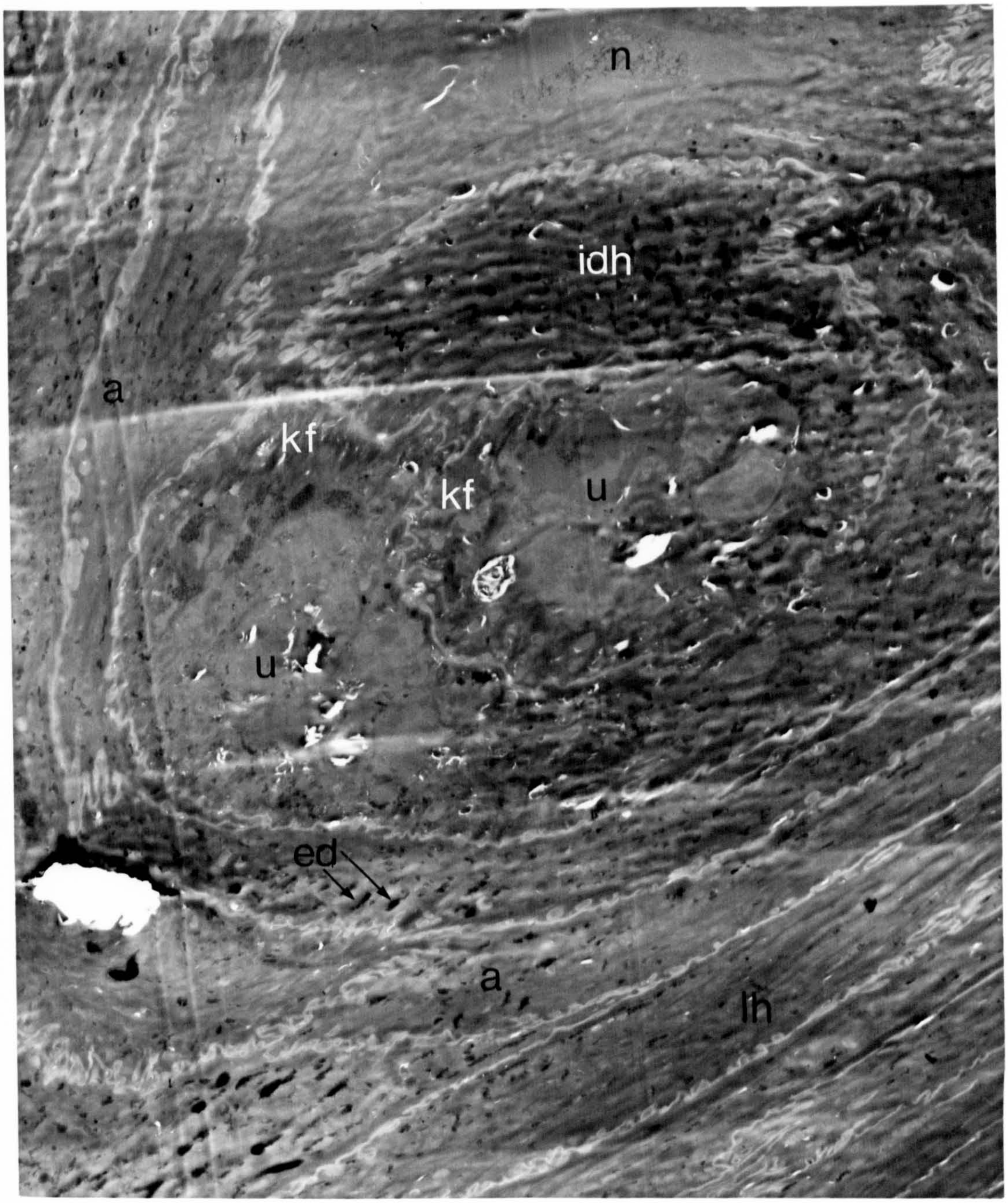
n
idh
a
kf
kf
u
u
ed
a
lh

Figure 7.14
Higher power transmission electron micrograph of squames of interdigitating horn within a round region corresponding to an area with high affinity for histological stain

Four squames (1 - 4) make up a circular region corresponding to a circular area with high affinity for Toluidine Blue in the survey section. The tissue of the central squame (1) has been severely damaged during preparation and viewing. The majority of holes (h) have developed as a result of damage to discrete oval structures (*) or separation of these from the surrounding tissue. Similar oval structures are present in squames 2 and 4. Small amounts of intercellular material (i) are present in widened intercellular spaces. Very few keratin fibres can be distinguished in any of the squames.

x 9,200

Cow 84 9 weeks post-calving

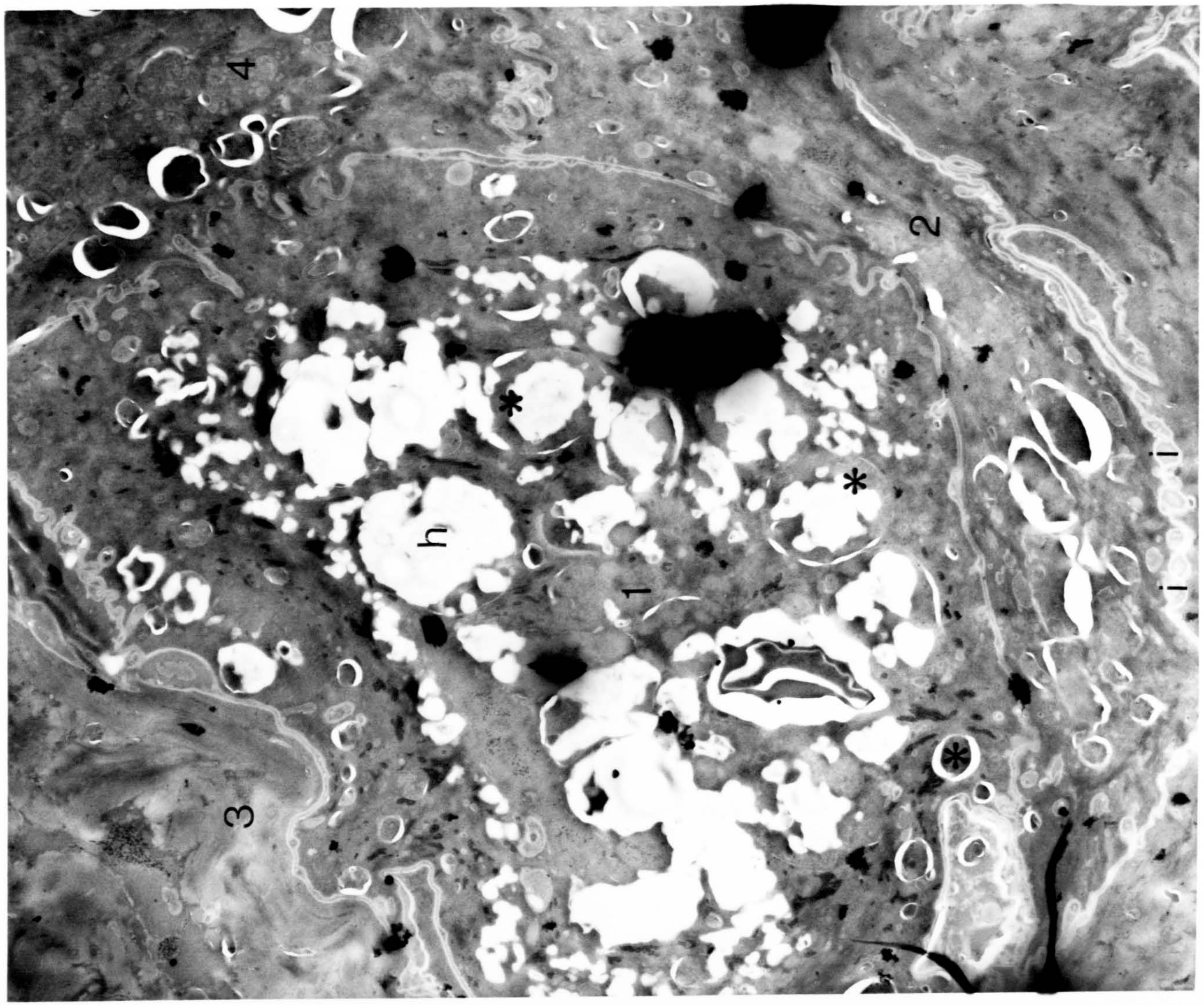
4
2
1
3
h
i
*
*
*

Figure 7.15
Low power transmission electron micrograph of a broadened sheet of interdigitating horn with high affinity for histological stains

The position of this micrograph corresponds to a small region at the junction between the laminar horn and the tip of the interdigitating horn, in a section similar to that illustrated in Figure 6.20. Large amounts of grey amorphous intercellular material (i) are present between the squames of interdigitating horn (idh). It is thought that these develop from smaller, separate areas of intercellular material, with the destruction of surviving desmosomes (d ↑). The adjacent squames of laminar horn (lh) have a marbled appearance.

x 2,500

Cow 60 9 weeks post-calving

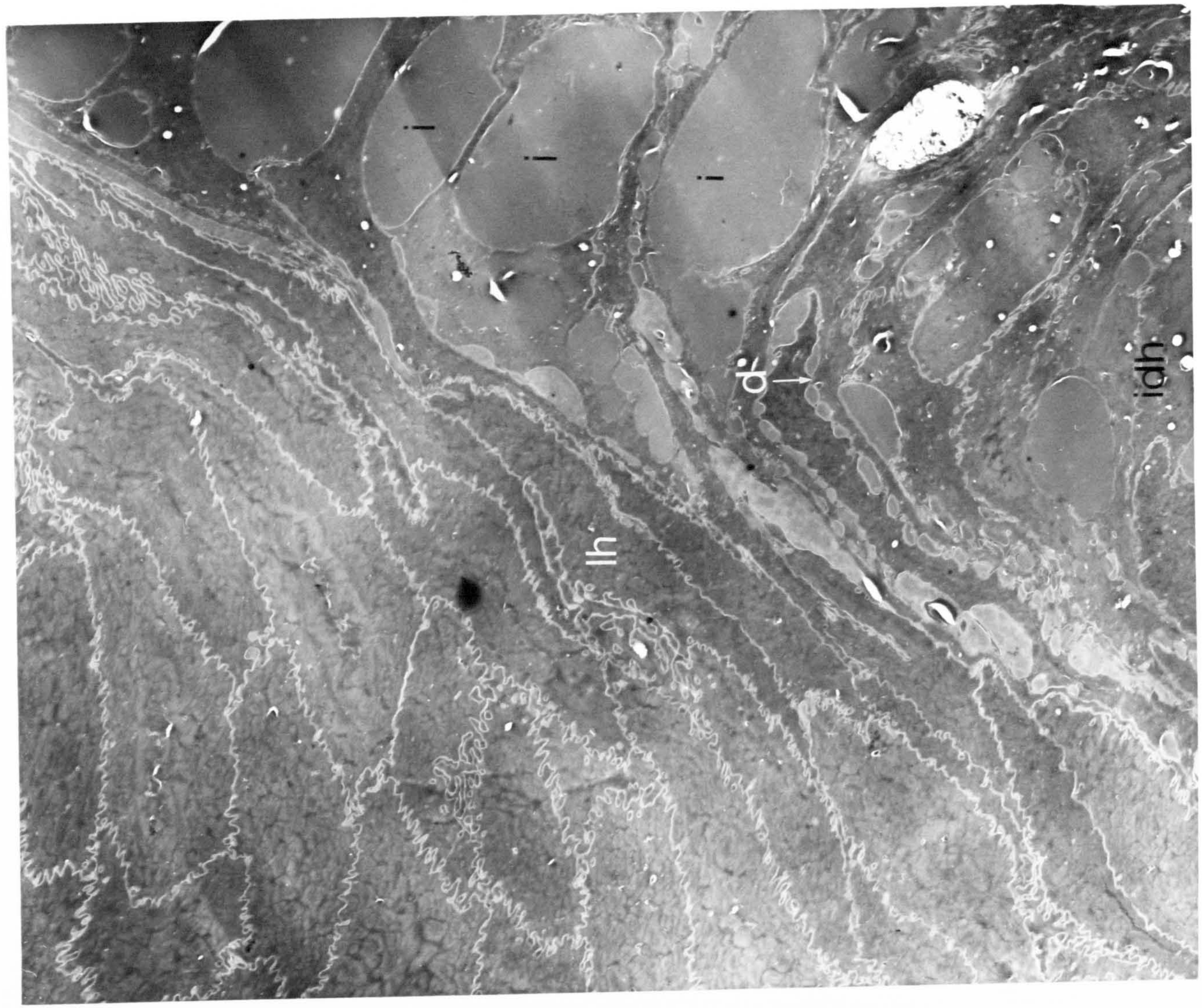
ih
ihi
ihi

Figure 7.16
Transmission electron micrograph of an abnormal region at the tip of a broadened sheet of interdigitating horn

Highly abnormal squames (s) are separated by large amounts of grey amorphous intercellular material (i). Within squames interfilamentous matrix is sparse and keratin filaments (kf) are unevenly distributed. Remnants of a nucleus (n) and organelles (*) have survived. One squame is almost completely degenerate (ds). Electron-dense deposits (↑) are present on the intra-cellular aspects of squame membranes.

x 10,350

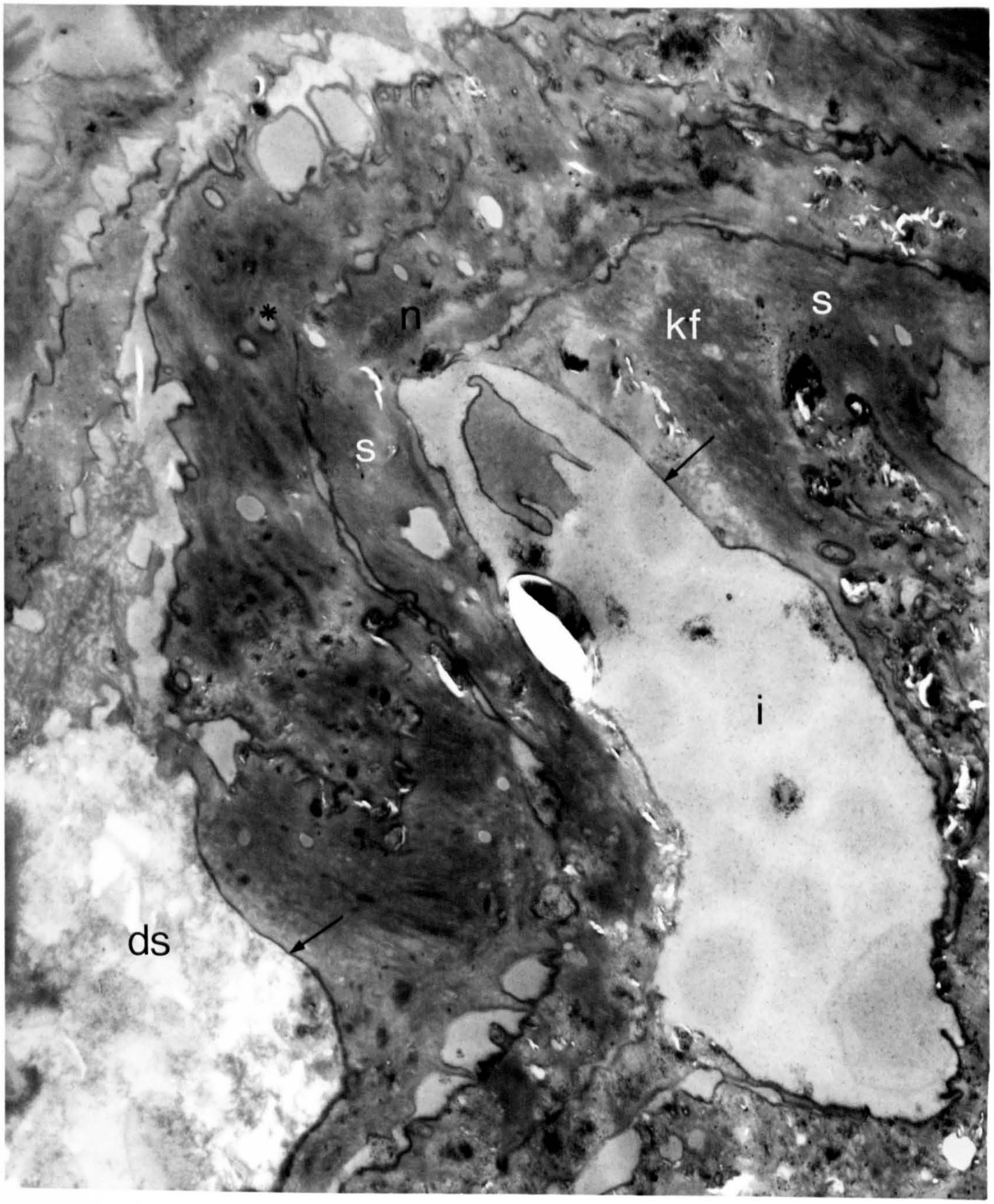
*
n
s
kf
s
i
ds

Figure 7.17
High power transmission electron micrograph of an abnormal region at the tip of a broadened sheet of interdigitating horn

Lack of association between keratin filaments (kf) and interfilamentous matrix (ma) results in a highly abnormal intracellular structure. Adjacent squames remain attached by some surviving desmosomes (d↑) but in between these points the intercellular space is greatly widened and filled with amorphous intercellular material (i). An electron dense deposit is present on the intracellular aspect of the squame membranes (↑).

x 12,000

Cow 47 14 weeks post-calving

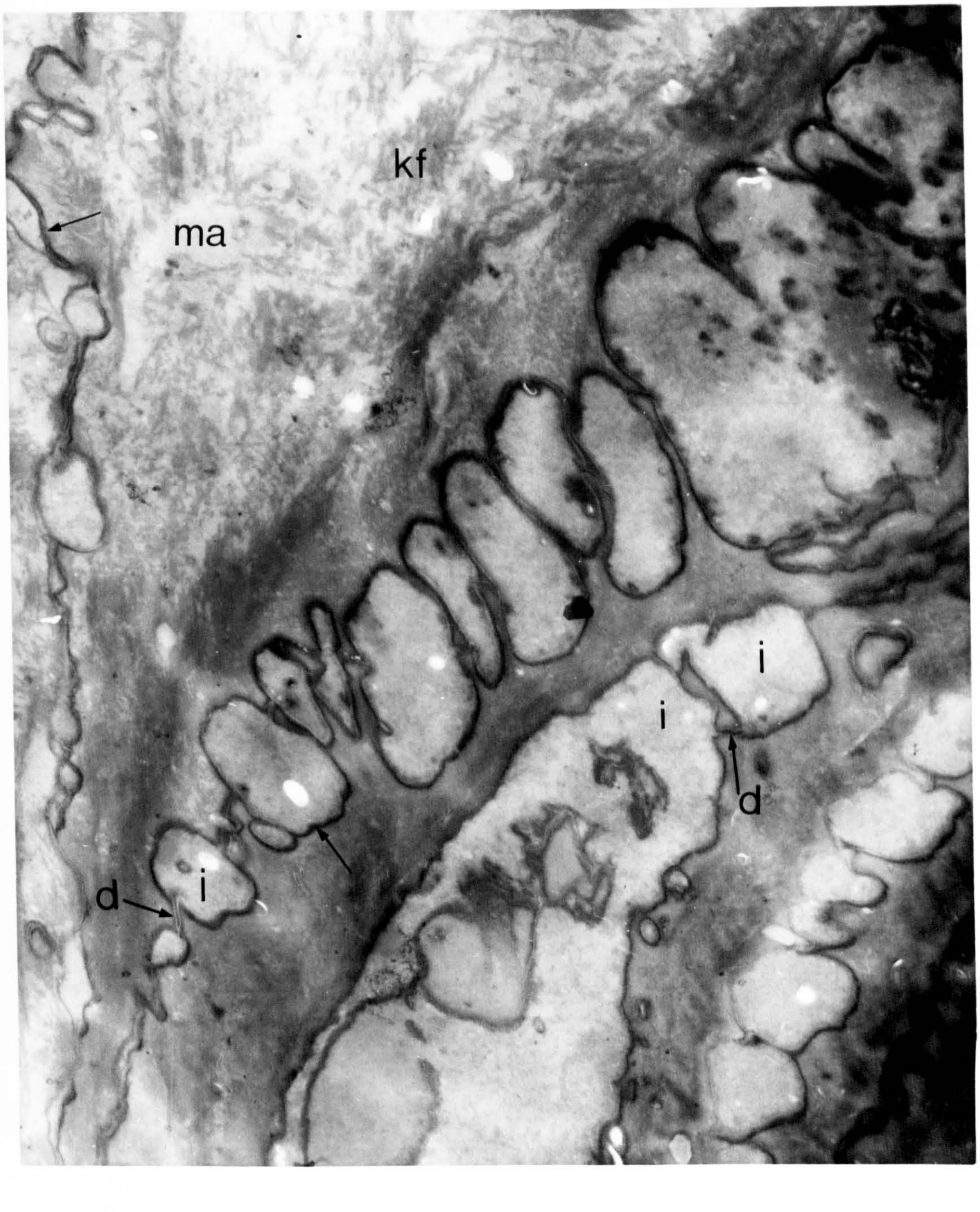
kf
ma
i
i
d
d
i

Figure 7.18
Low power transmission electron micrograph of a cleft in the horn of the white line containing bacteria

A cleft (c) between the laminar horn (lh) and the interdigitating horn (idh) contains a large population of bacteria (b). The bacteria are invading further into the laminar horn and the interdigitating horn through the intercellular spaces (↑). Islands of horn (*) have been surrounded by bacteria.

x 8,300

Cow 47 14 weeks post-calving


Ih
c
b
*
*
*
b
idh

Figure 7.19
High power transmission electron micrograph of bacteria found in the horn of the white line

A number of different types of bacteria (b) are present within the squame, digesting the intracellular material. One bacterium (b*) is in the process of division while another is degenerate.

x 36,900

Cow 44 9 weeks post-calving

Figure 7.20
Transmission electron micrograph of plant material found in a cleft of horn in the white line

The majority of the cleft is filled by plant tissue (p). Small areas of degenerate horn (dh) are visible and these have been invaded by bacteria (b↑).

x 2,000

Cow 48 9 weeks post-calving

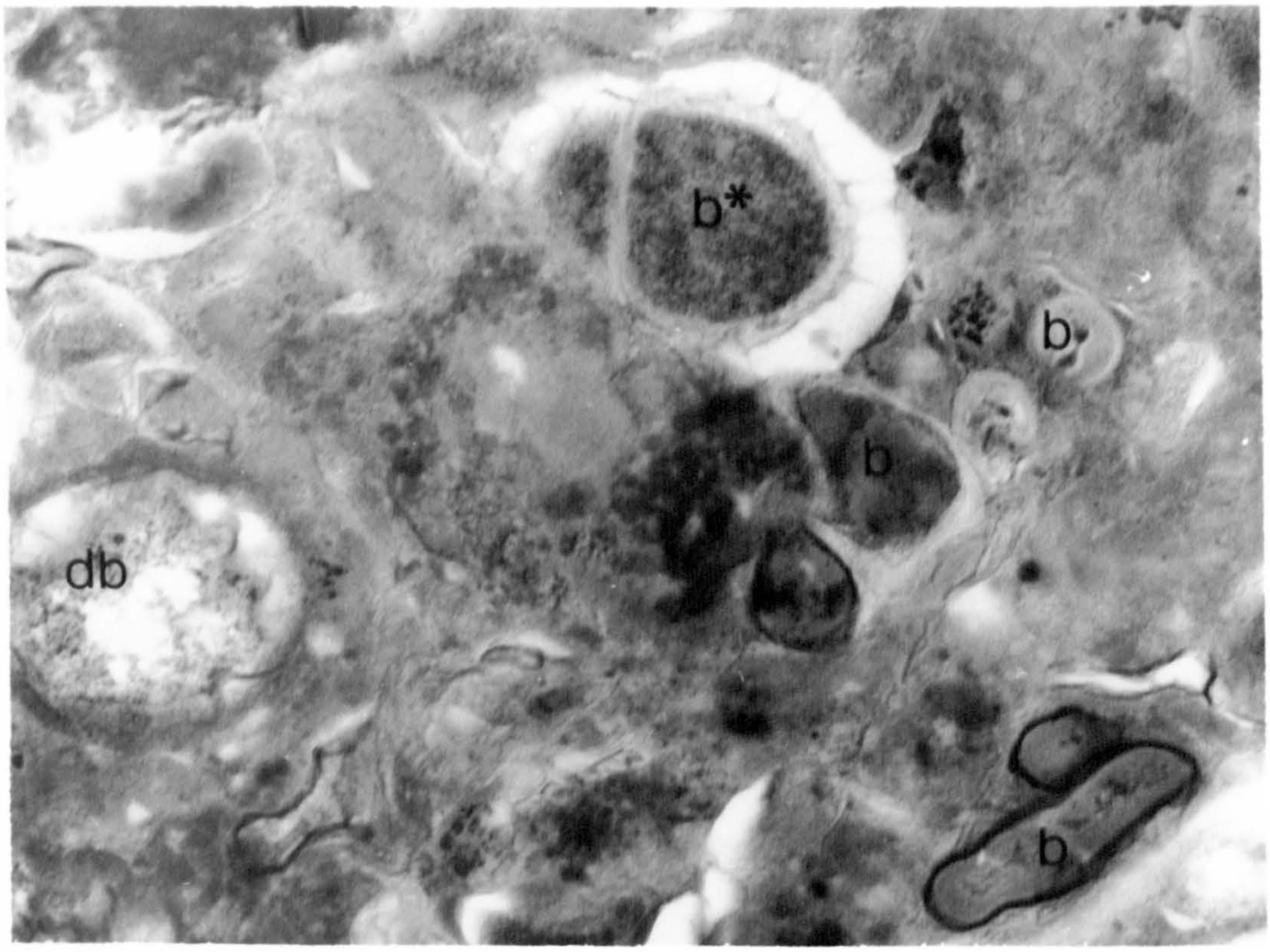
b*
b
db
b

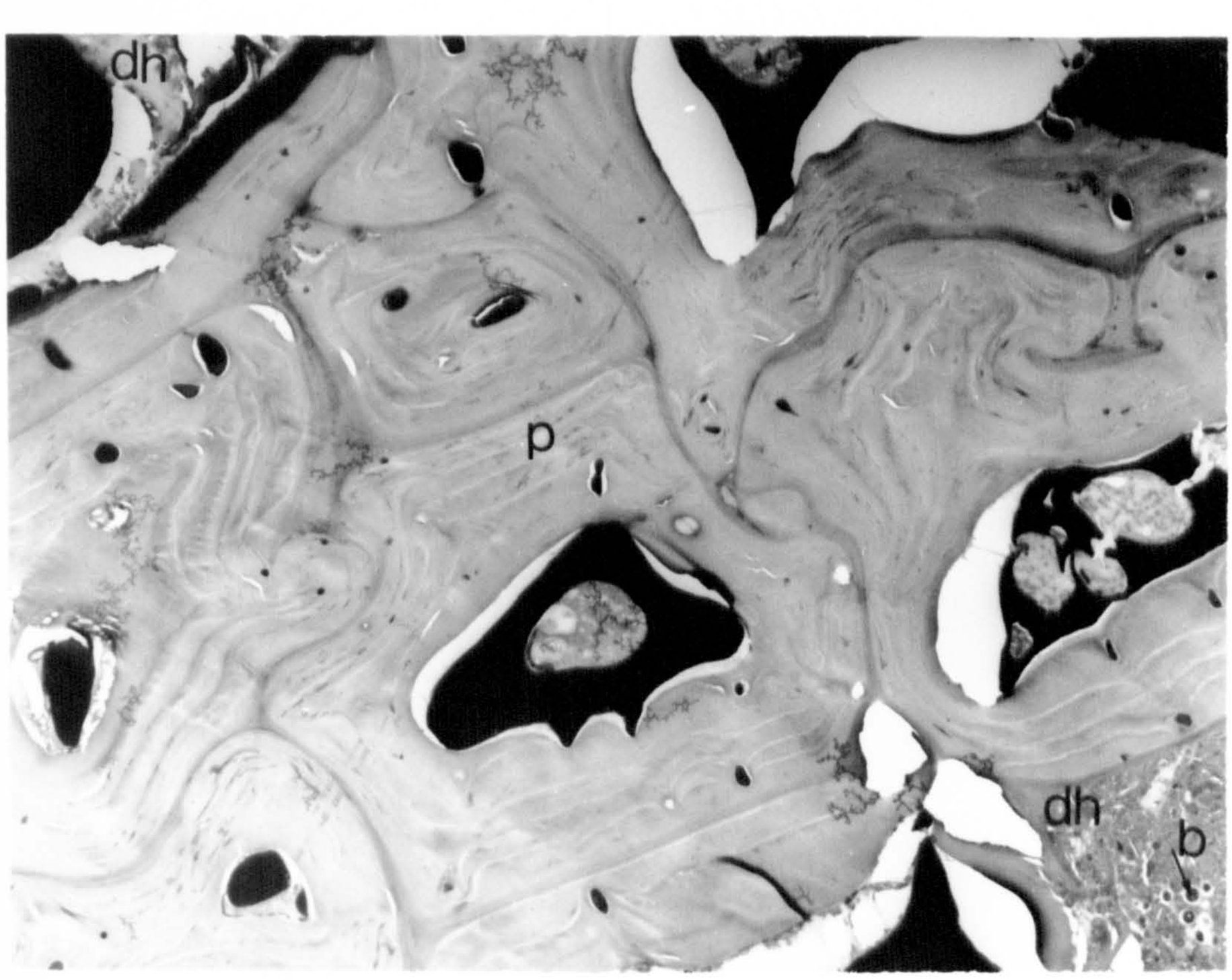
dh
p
dh
b

Figure 7.21
Transmission electron micrograph of the interdigitating horn in a sample with signs of haemorrhage in the white line at the gross level

Squames (s) are incompletely keratinized. Filament - matrix association is poor and damage has occurred during sectioning. Electron-dense deposits (ed) are present in the central squame. There is a large amount of grey amorphous intercellular material (i) which is thought to originate from blood that has escaped from the dermis.

x 17,500

Cow 30 32 weeks post-calving

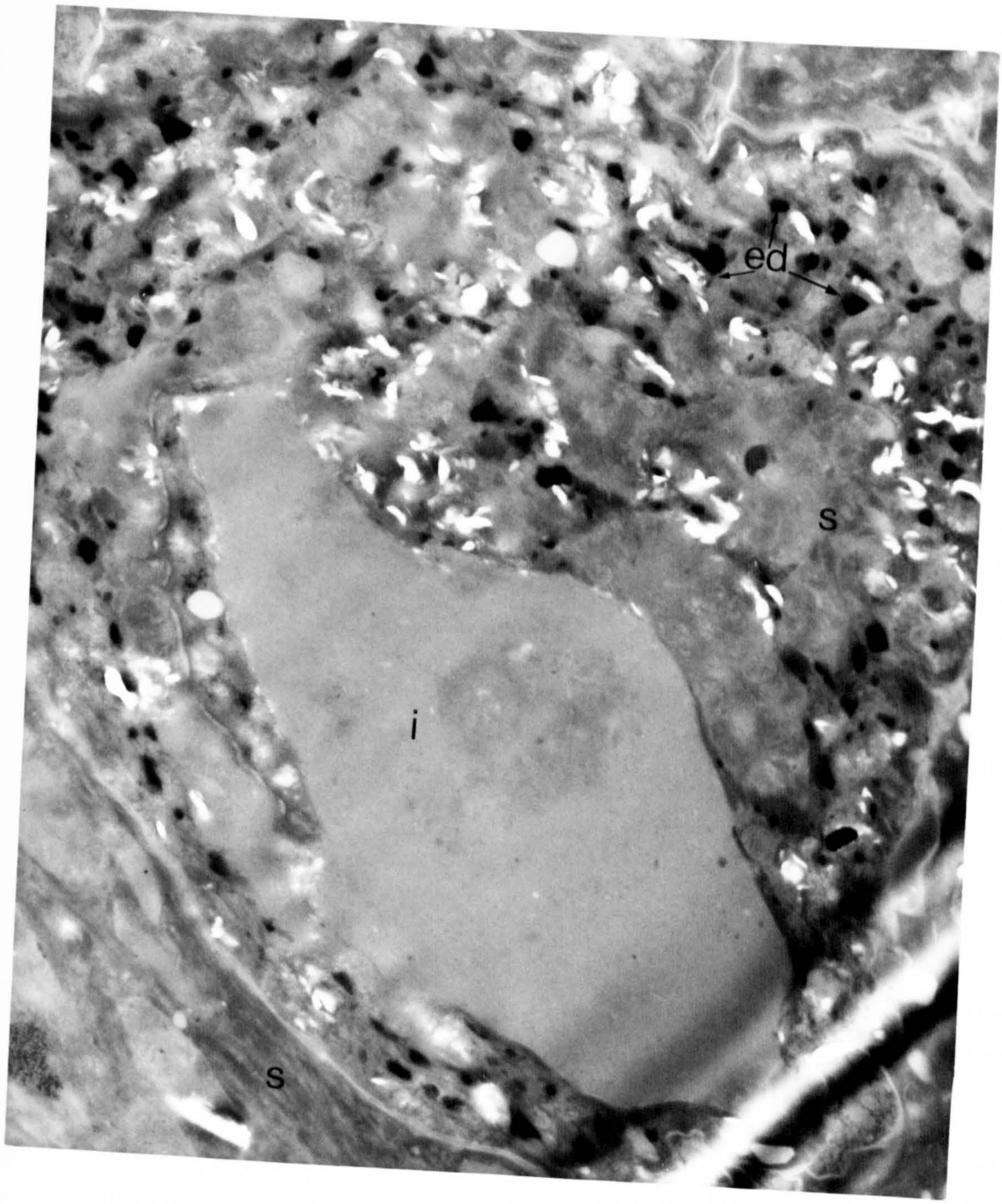
ed
s
i
s

Figure 7.22
Low power transmission electron micrograph of fungus and bacteria found in a cleft in the white line in a sample exhibiting gross haemorrhage

A large cleft (cl) separates laminar horn (lh) and interdigitating horn (idh). Fungal hyphae (f) and bacteria (b) are present in the cleft.

x 3,870

Cow 63 14 weeks post-calving

Figure 7.23
Transmission electron micrograph of fungus and bacteria found in a cleft in the white line

In this case the fungus (f) has penetrated between squames of laminar horn (lh). The immediately adjacent horn is degenerate (dh) but the adjoining squames have a fairly normal appearance. Bacteria (b) are also present in the cleft.

x 8,360

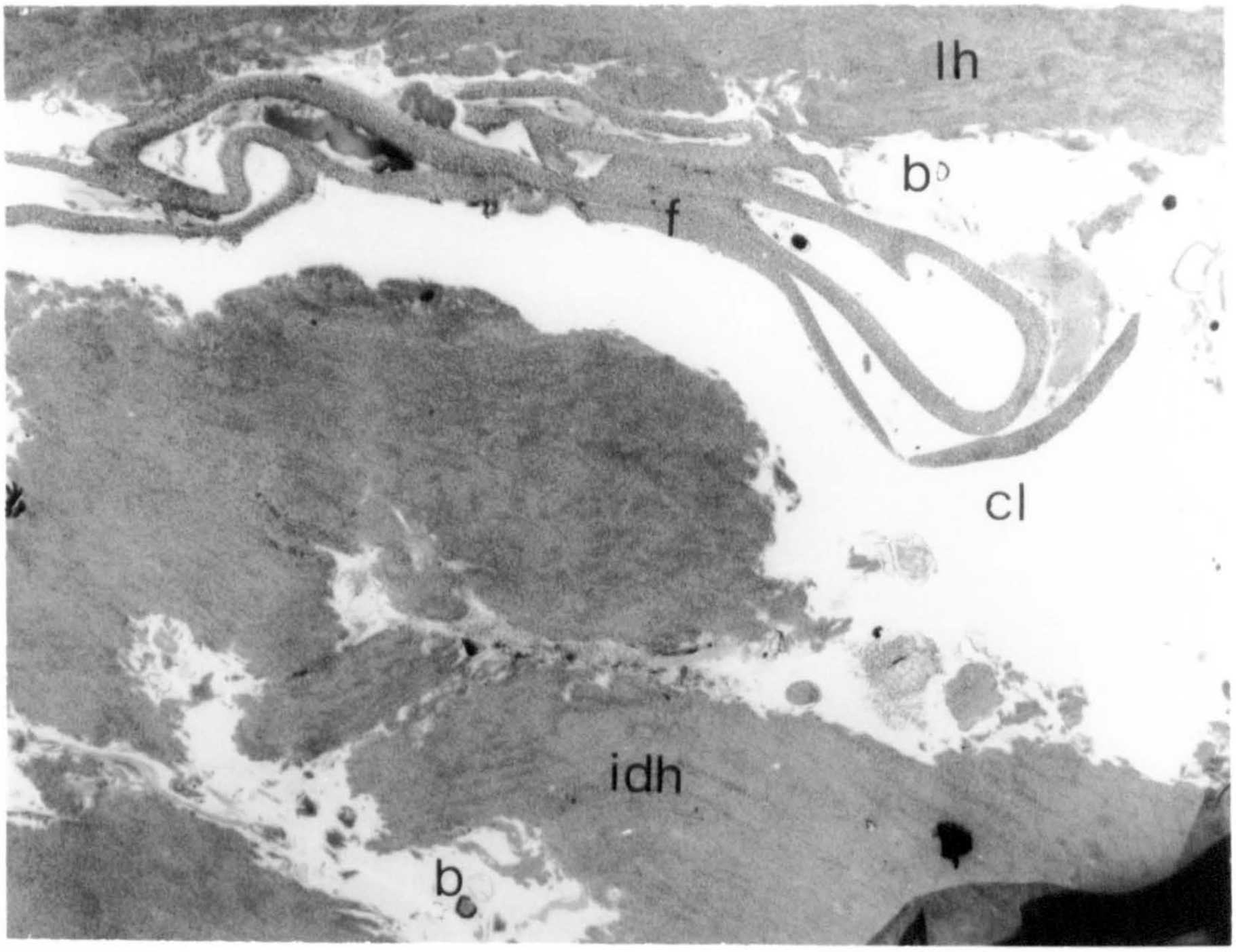
lh
b
f
cl
idh
b


lh
f
dh
lh
b
b

Figure 7.24
Transmission electron micrograph of laminar horn from a claw with a severe sole ulcer

The shape of squames is very unusual for the laminar horn. Electron lucent regions occur within the squames (*). Their electron density is similar to that of the intercellular material (i) present in the widened intercellular spaces. Some of the intercellular material has a reticulate pattern.

x 27,100

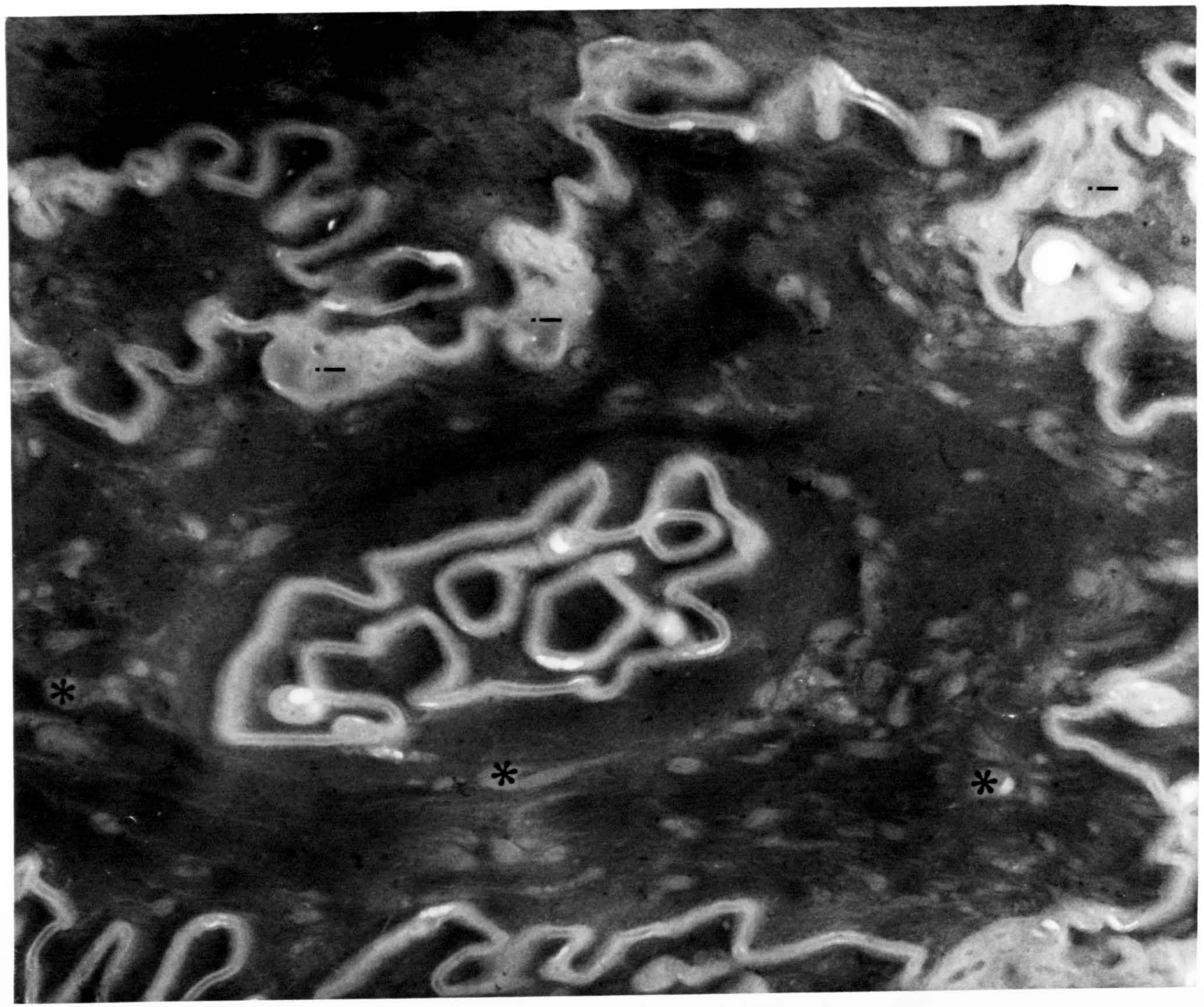

Figure 7.25
The variation in the volume fraction of intercellular material in the laminar horn at two different positions within samples of horn from the white line of the bovine claw

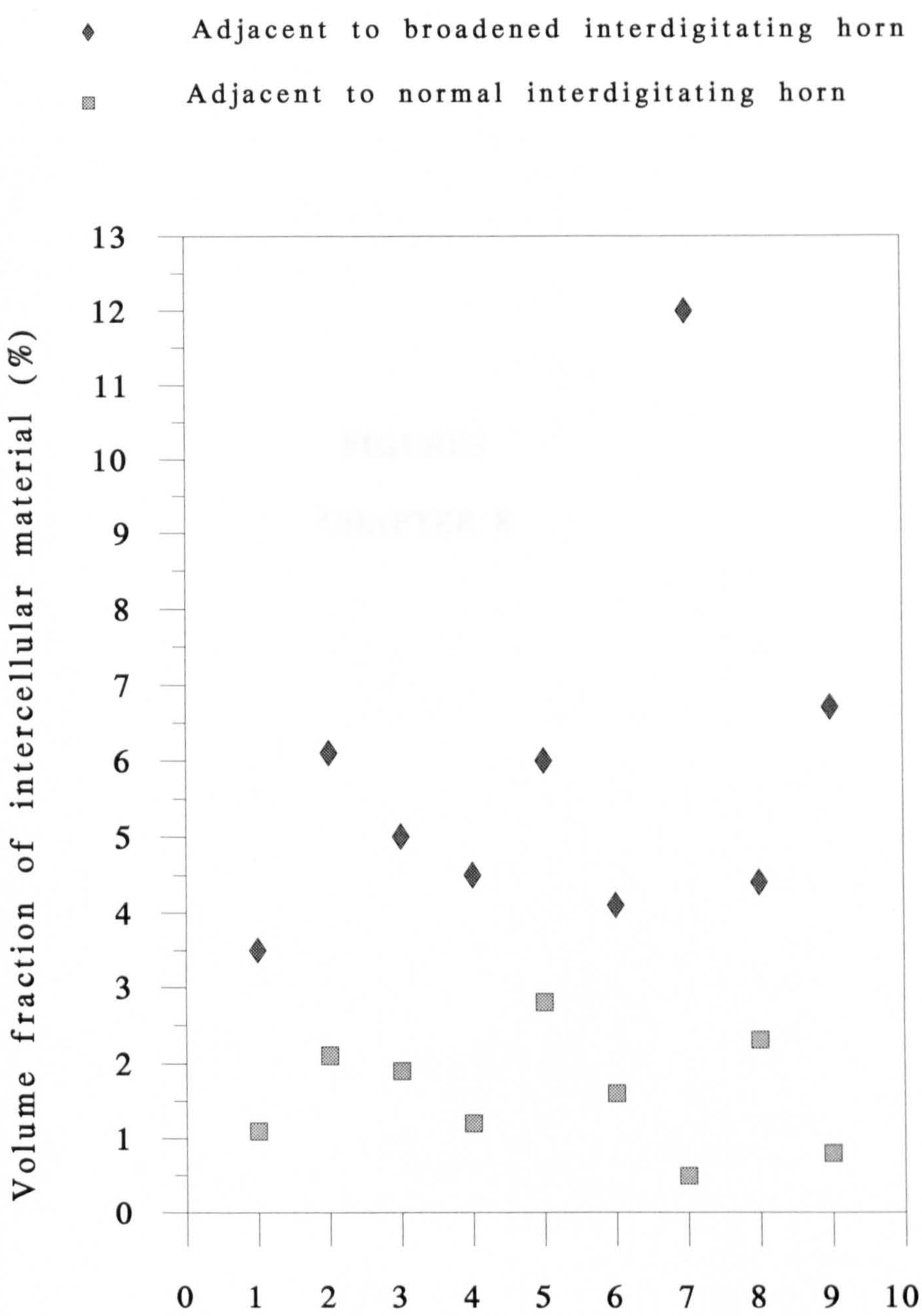
♦ Adjacent to broadened interdigitating horn
▩ Adjacent to normal interdigitating horn
Volume fraction of intercellular material (%)
13
12
11
10
9
8
7
6
5
4
3
2
1
0
0 1 2 3 4 5 6 7 8 9 10
Sample number

FIGURES

CHAPTER 8

Figure 8.1
Position of samples taken for histological and ultrastructural examination from claws suffering sole ulcers

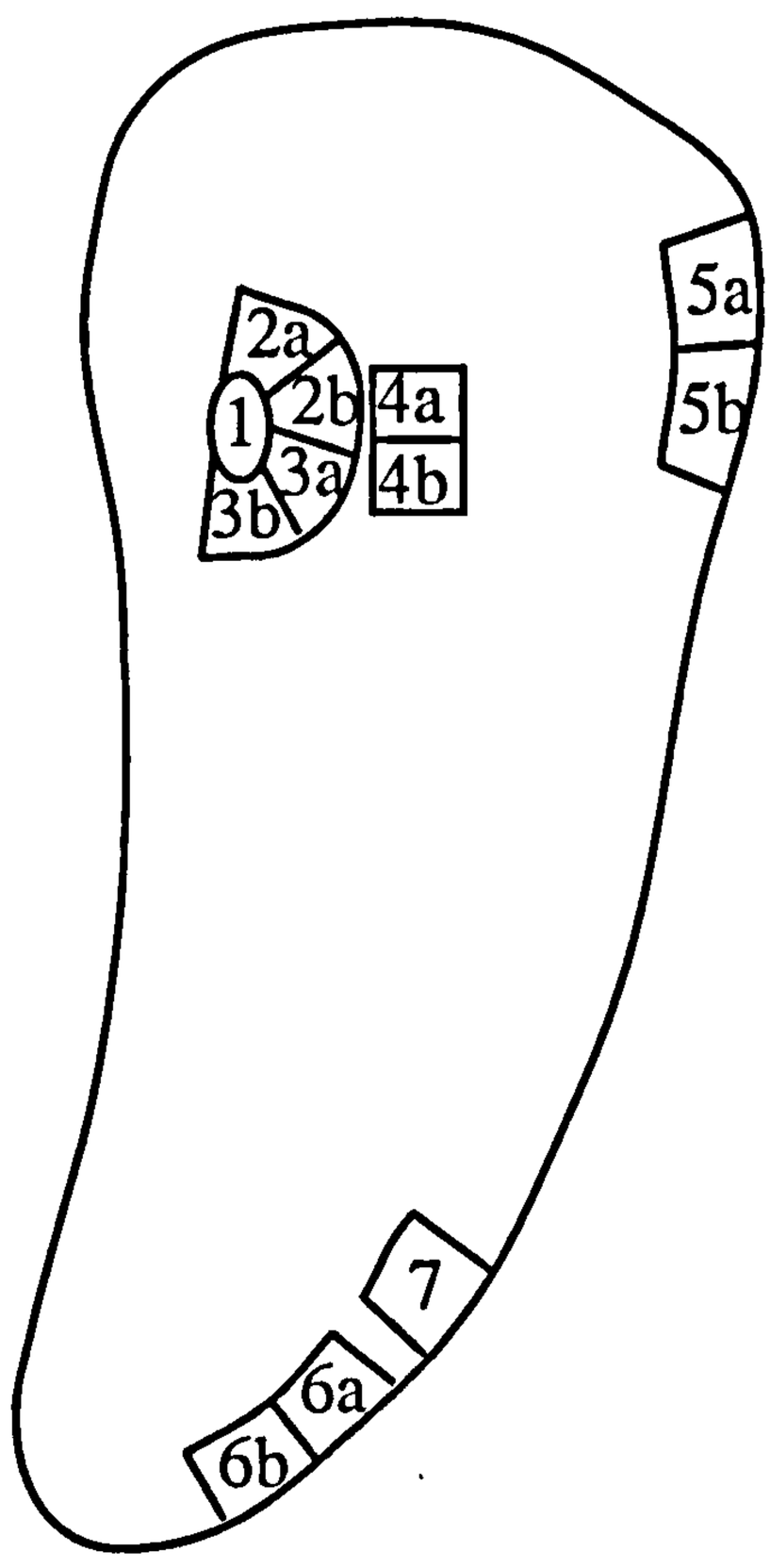

1. Plug of tissue filling ulcer cavity (right foot only)
2. and 3. Tissue adjacent to ulcer cavity
4. Tissue from the sole approximately 2 cm from the centre of the ulcer cavity
5. Distal block of a series from the wall adjacent to the abaxial groove
6. Distal block of a series from the dorsal wall
7. Sliver of horn for transmission electron microscopy from the standard sample site on the abaxial white line

Blocks marked "a" were processed for histology
Blocks marked "b" were processed for scanning electron microscopy

Figure 8.2
Weighted severity scores for sole lesions (Gs claw) in the outer hind claws of a cow suffering recurrent severe sole ulcers

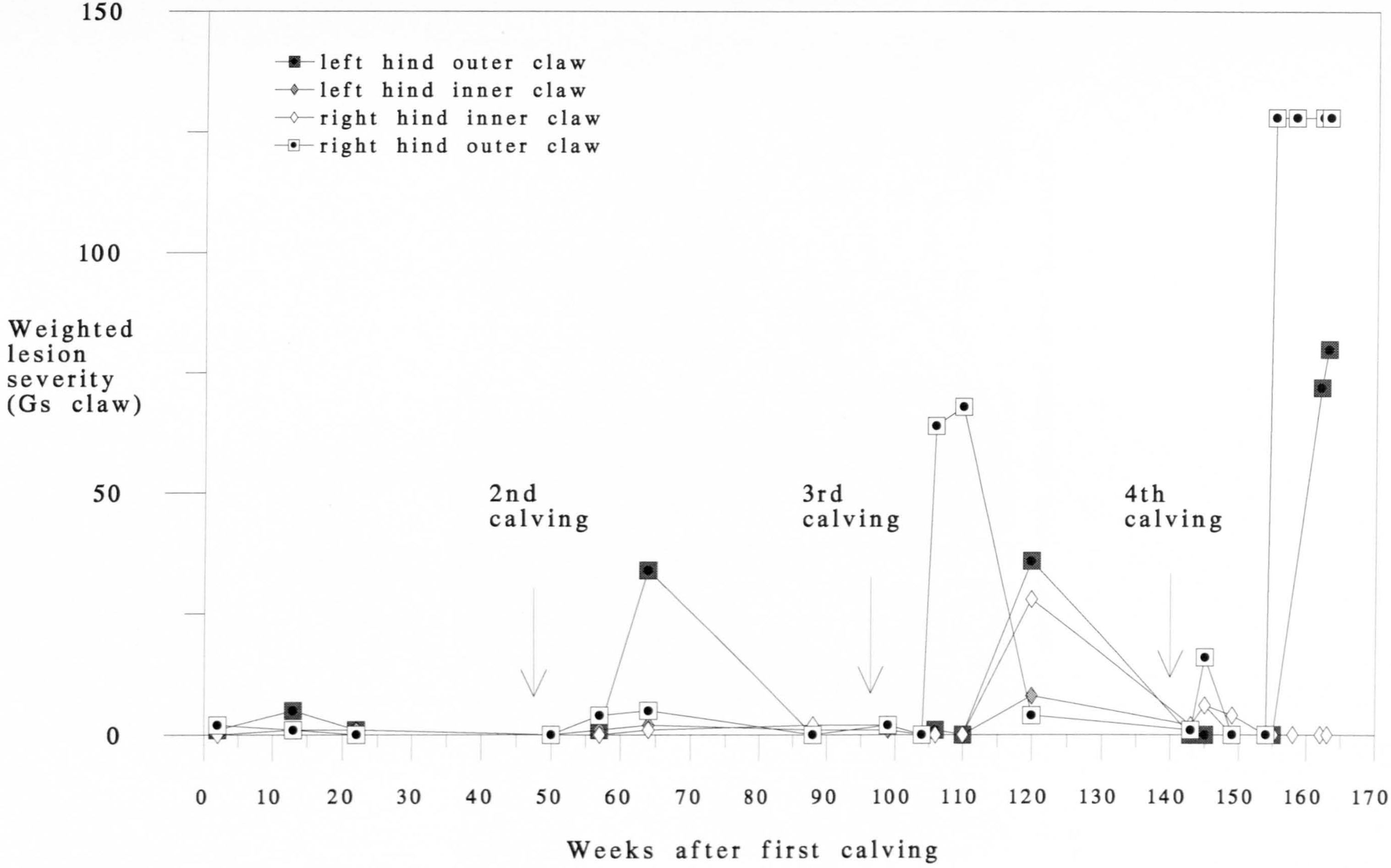
150
100
50
0
left hind outer claw
left hind inner claw
right hind inner claw
right hind outer claw
Weighted lesion severity (Gs claw)
2nd calving
3rd calving
4th calving
0 10 20 30 40 50 60 70 80 90 100 110 120 130 140 150 160 170
Weeks after first calving

Figure 8.3
Lateral view of the right hind outer claw photographed *post mortem*

The toe of the medial claw (M) is longer than that of the lateral claw (L) which has been trimmed. A considerable amount of bulb horn has been lost through heel erosion (the normal extent of the bulb is marked (↑)). Ridges (r↑) in the coronary horn of the wall indicate that there have been variations in horn growth rate. These ridges are closer together on the dorsal aspect of the wall and diverge towards the heel. This occurs because growth has been restricted in the dorsal part of the wall. The dorsal border of the lateral claw is slightly concave as a result.

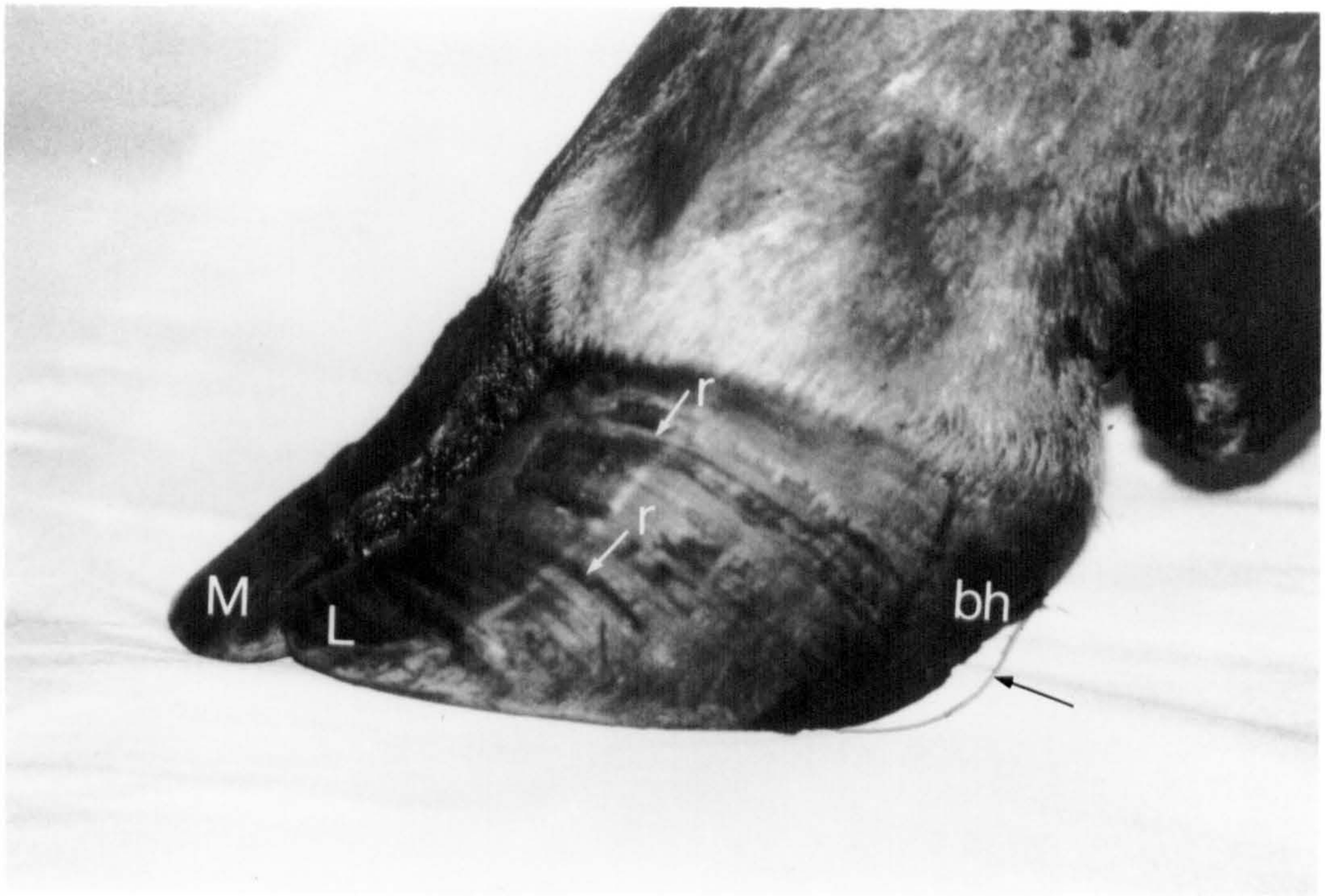
r
r
M
L
bh

Figure 8.4
The plantar surfaces of the hind feet of a cow suffering from severe sole ulcers, photographed *post-mortem*

Ulcers (U) have developed at the typical site at the sole - bulb junction on both outer hind claws. At the centre of the ulcer on the left hind foot the corium is exposed. The ulcer cavity on the right hind foot is filled by a plug of white fibrous tissue (↑). All claws show erosion of the bulb horn (bh), widening of the white line (wl) and thickening of the distal wall (w) at the toe. The inner claw of the right hind foot has been fitted with a rubber block (b) to relieve the affected claw from bearing weight. The right distal interphalangeal joint (j) is infected and swollen. The sole of the left foot shows under-running of horn (ur) and the sole of the right foot extensive haemorrhage (ha).

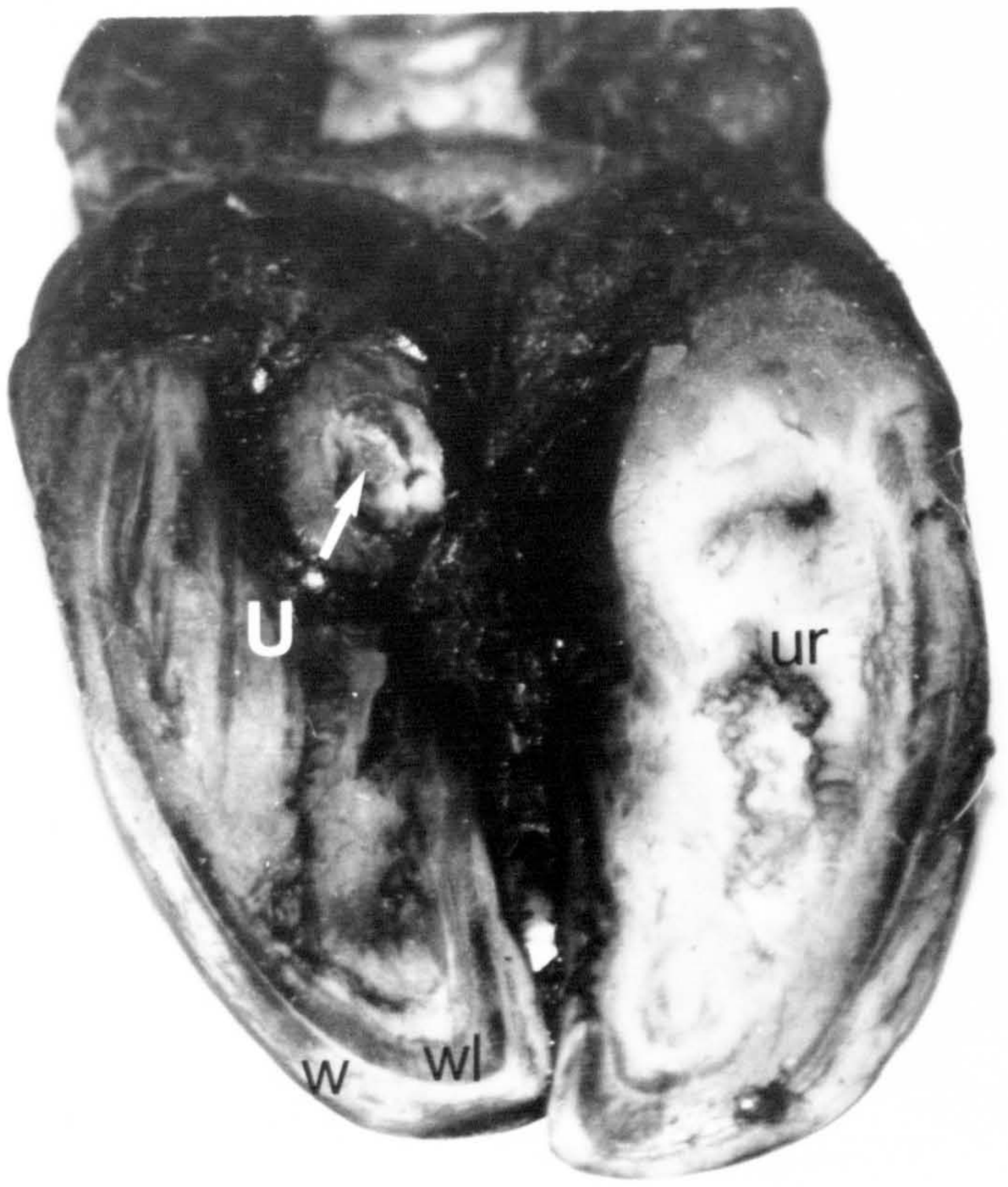
U
ur
w
wl

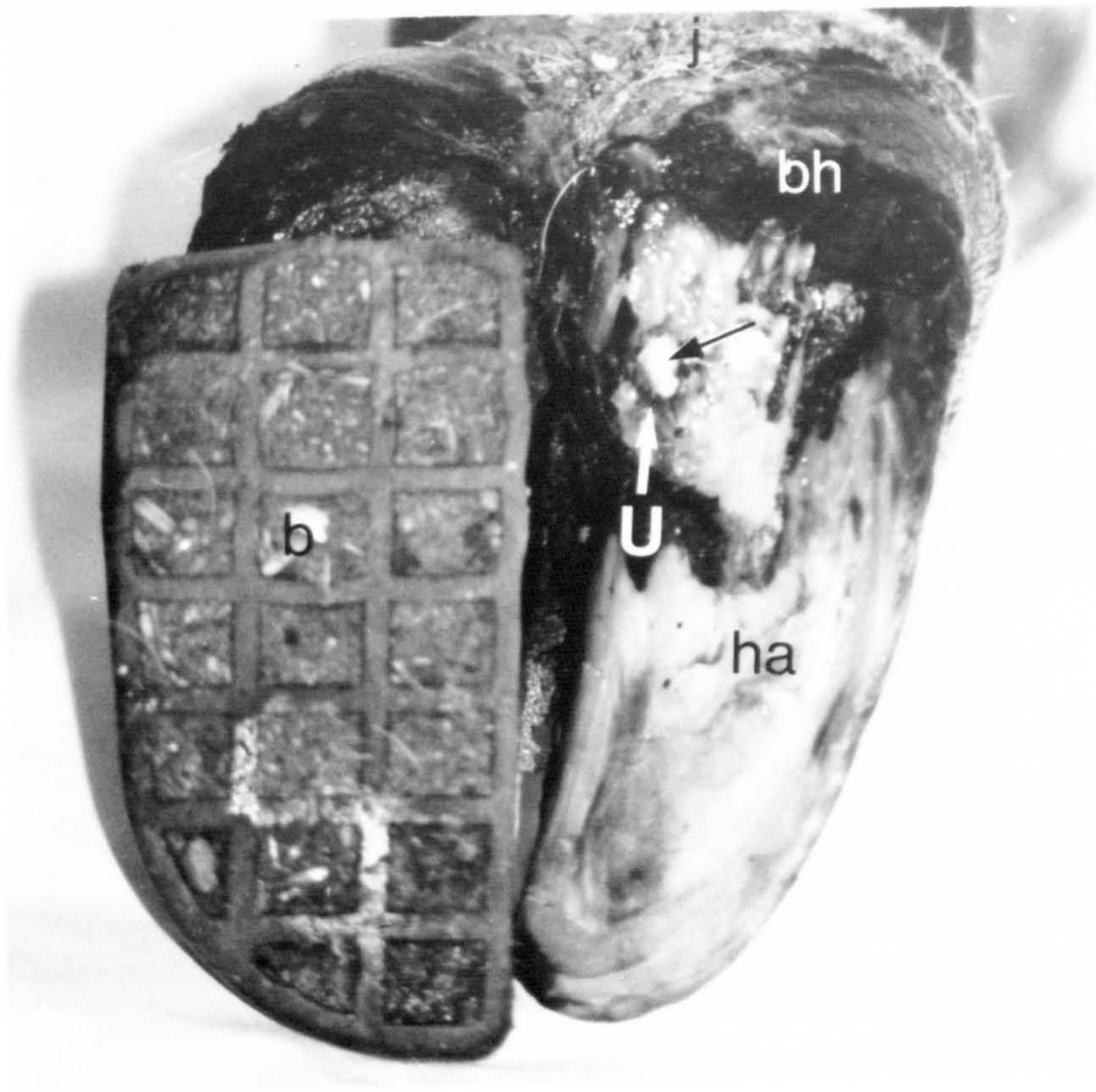
bh
b
U
ha

Figure 8.5a Dissection of the deep digital flexor tendon in a normal claw

The bulb horn and much of the digital torus have been dissected away, revealing the lateral branch of the deep digital flexor tendon (df). The digital torus (dt) is visible where it underlies the sole corium (sc). The digital torus is composed of bundles of collagen fibres (cf) which form a highly organised network enclosing regions of adipose tissue (a). Some fibres of the digital torus are continuous with those of the distal interdigital ligament.

Figure 8.5b Dissection of the deep digital flexor tendon in the infected right hind outer claw

The bulb horn and digital torus have been removed, exposing the lateral branch of the deep digital flexor tendon (df). The distal portion of the deep digital flexor tendon approaching its insertion on the distal phalanx is infected and highly necrotic (n). An exostosis (ex) is present on the plantar surface of the distal phalanx at the insertion of the deep digital flexor tendon. The approximate position of the opening of the ulcer cavity is marked (*). The organised structure of the digital torus (dt) is not apparent because of degeneration. The sole horn (sh) is relatively thick and the sole corium (sc) is compressed.

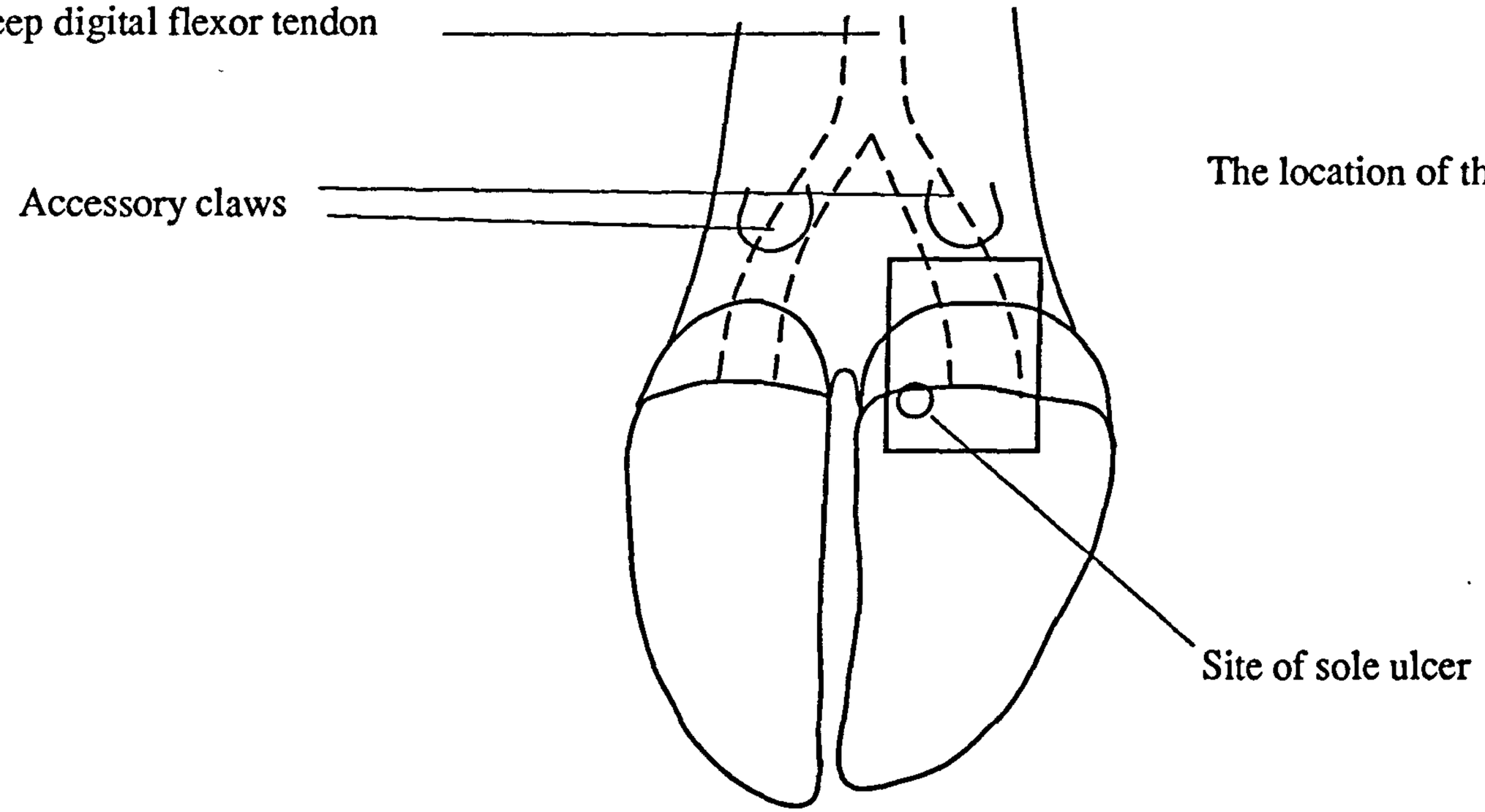

The location of the photographs is shown by the box

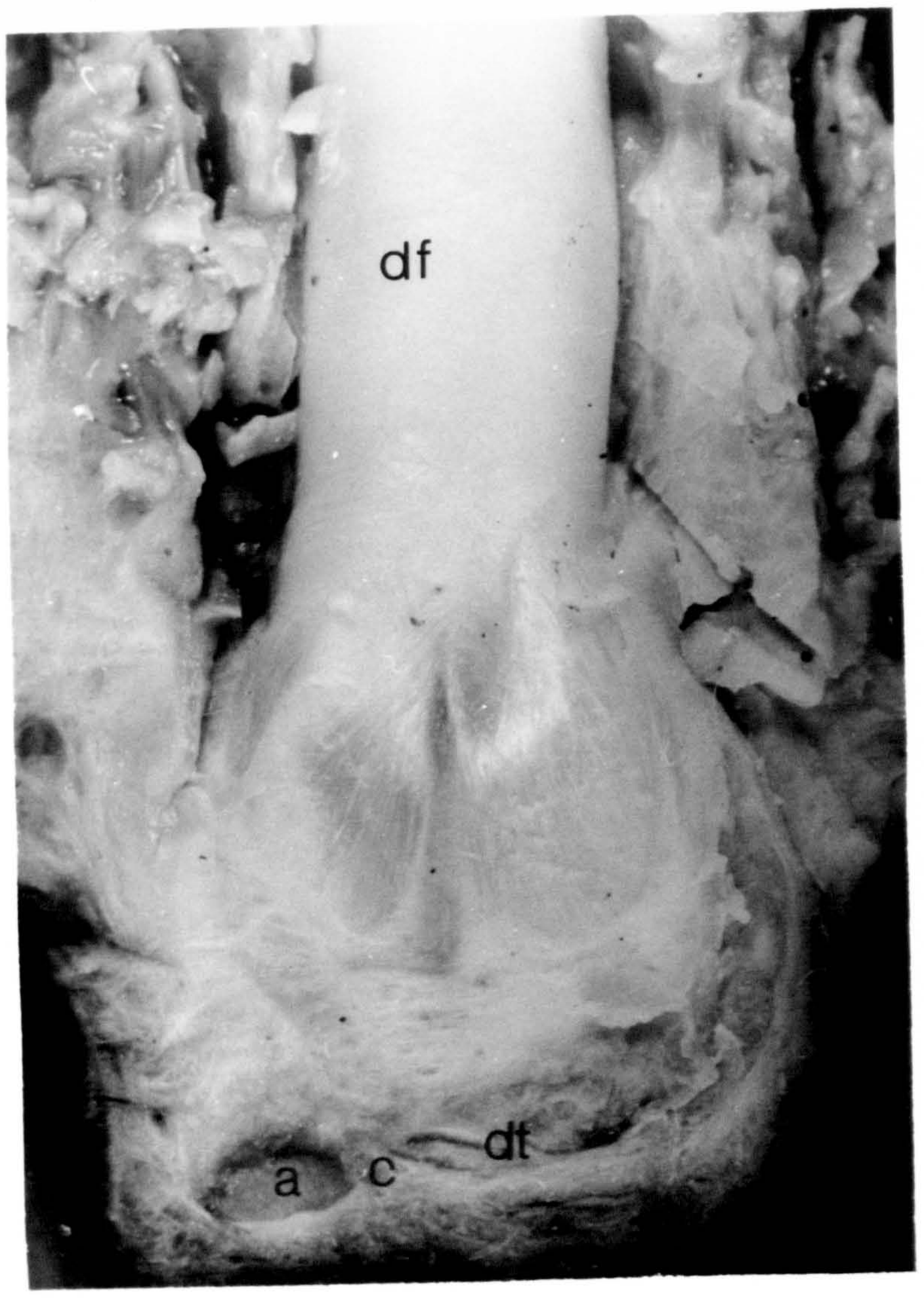
df
a
c
dt

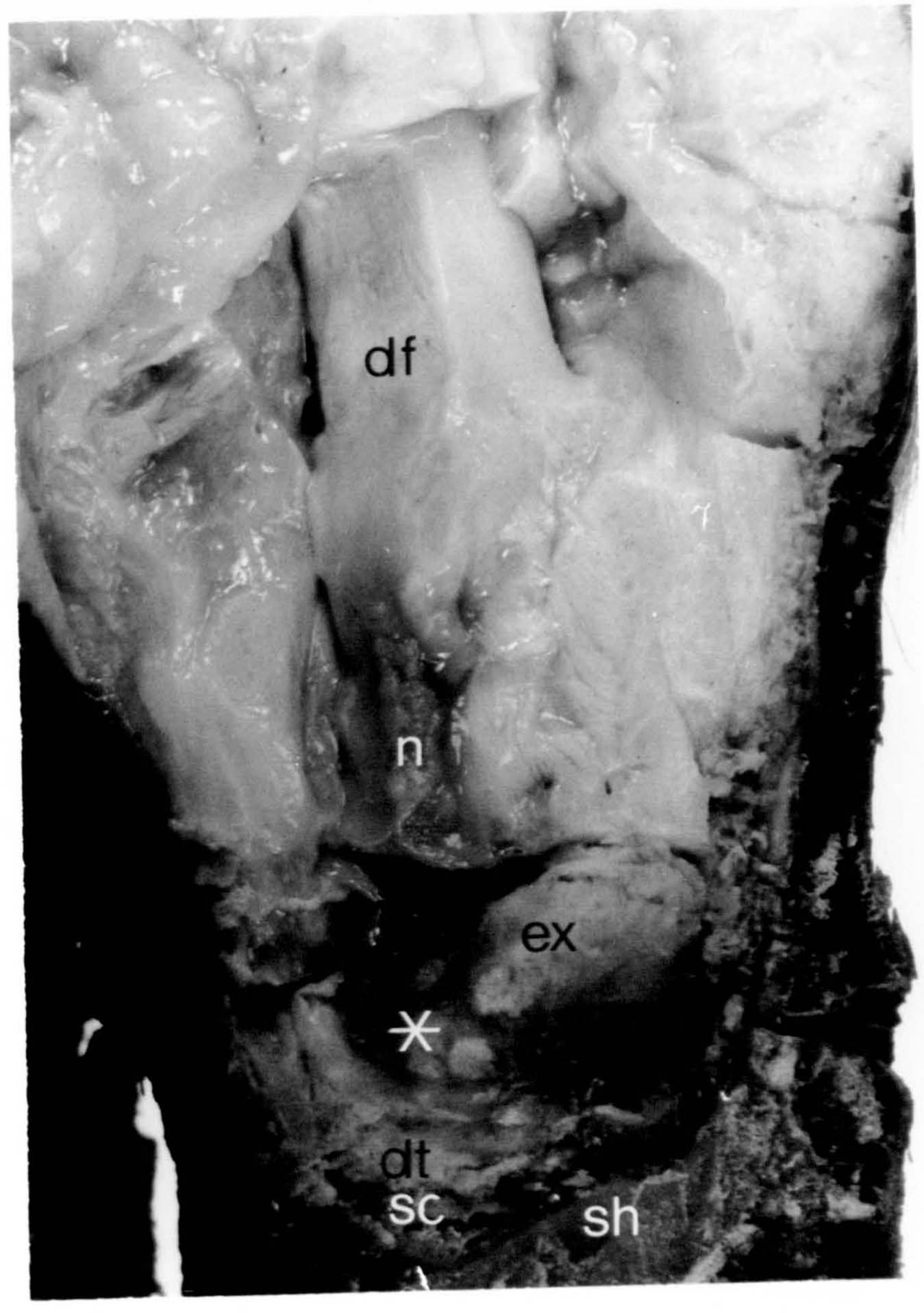
df
n
ex
dt
sc
sh

Figure 8.6a
Longitudinal section through the infected right hind outer claw after dissection of the deep digital flexor tendon and removal of the claw capsule

The deep digital flexor tendon (df) and the distal interphalangeal joint (j ↑) between the middle phalanx (PII), the distal phalanx (PIII) and the distal sesamoid or navicular bone (s) are uninfected. The claw capsule has been removed.

Figure 8.6b
Longitudinal section through the infected right hind outer claw after dissection of the deep digital flexor tendon

The distal extremity of the deep digital flexor tendon (df) is infected and necrotic (n). The infection had also entered the joint capsule of the distal interphalangeal joint (j↑) between the middle phalanx (PII), the distal phalanx (PIII) and the distal sesamoid or navicular bone (s). An extensive exostosis (ex) of the distal phalanx had developed distal to the point of insertion of the deep digital flexor tendon. The extensor process of the distal phalanx was exerting pressure on the coronary corium (←). This is thought to be the cause of the decreased thickness of the wall in the coronary region (w_1) in comparison with the laminar region (w_2). Streaks of haemorrhage (ha ↑) are visible in the thickened horn of the sole (sh).
(Some blocks of horn have been removed for microscopy)

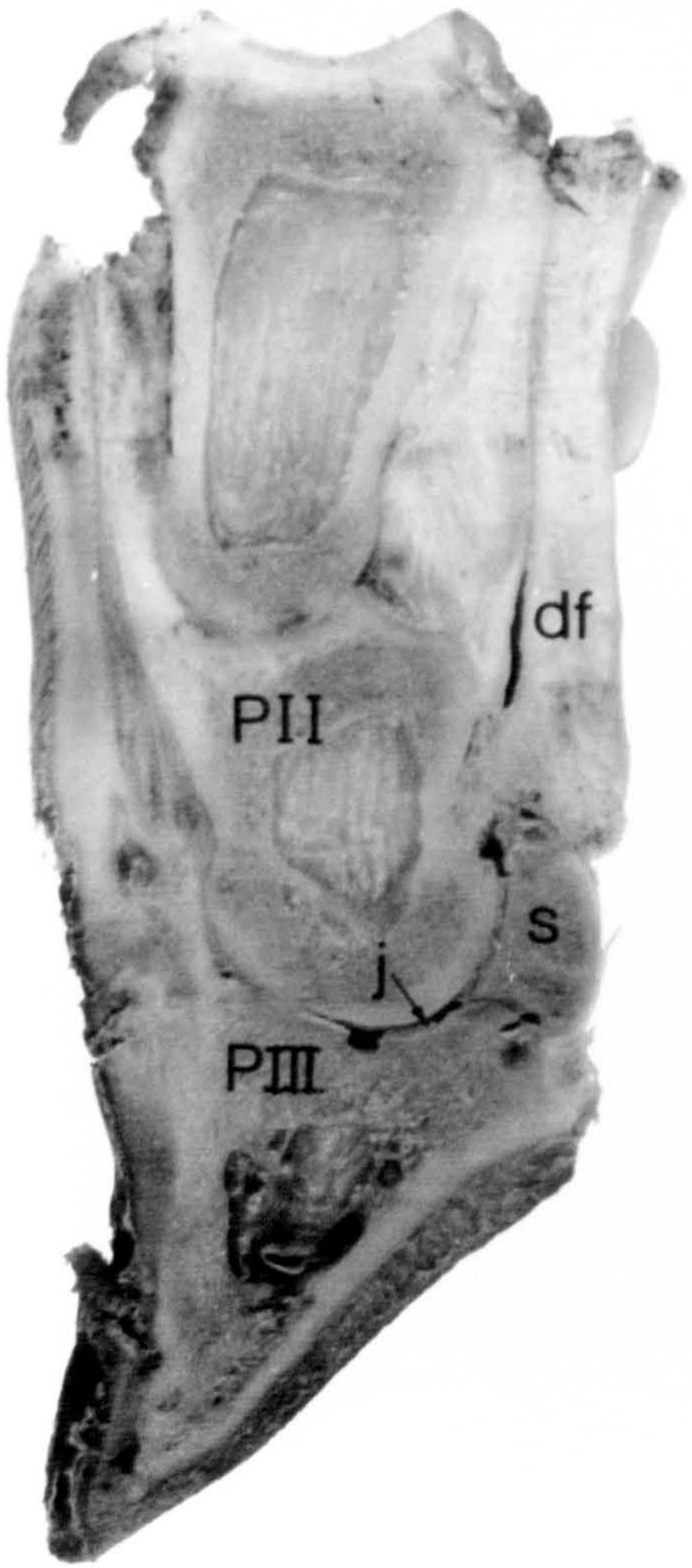
df
PII
s
j
PIII

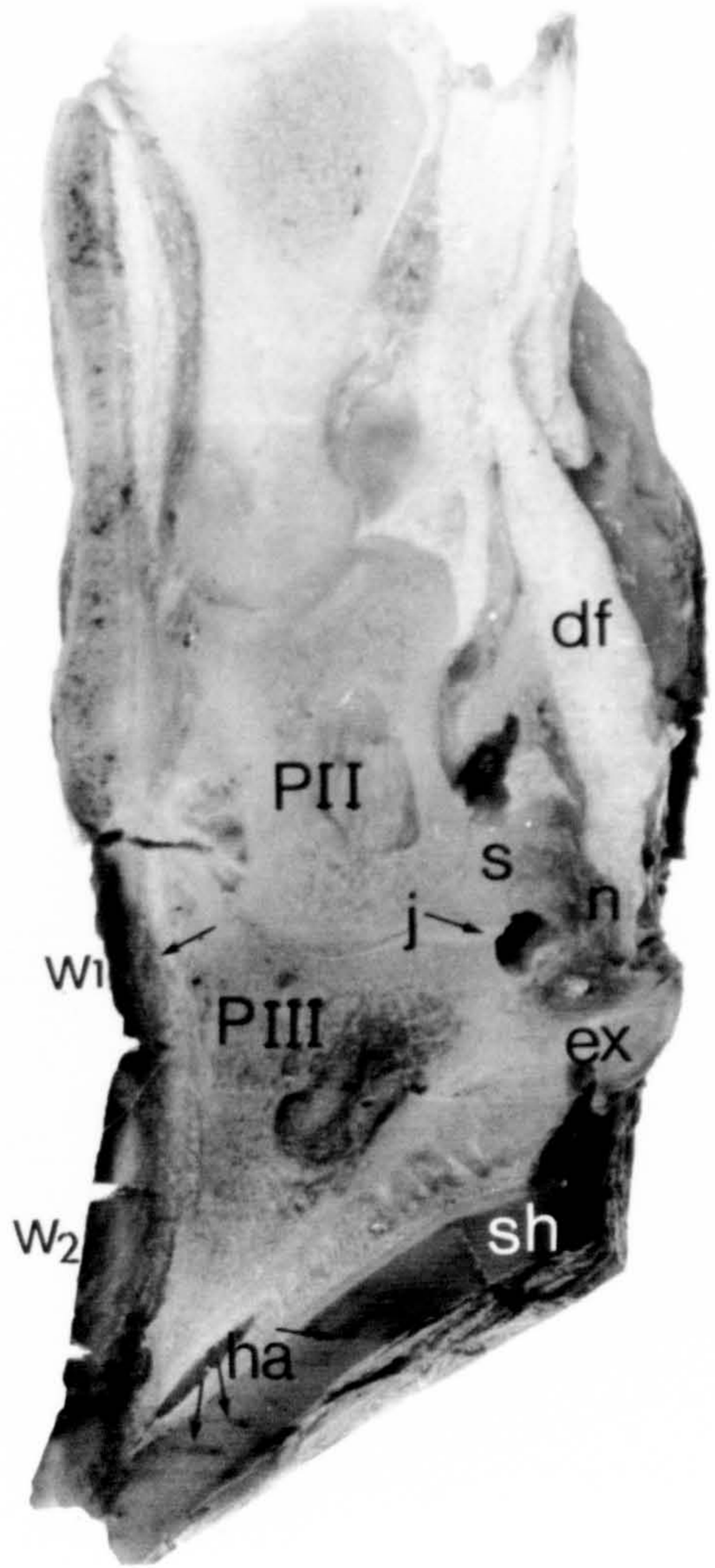
df
PII
s
n
j
W1
PIII
ex
W2
sh
ha

Figure 8.7
The plug of tissue from the centre of the ulcer on the right hind outer claw photographed in a dissection microscope

After drying, and prior to mounting and coating for the SEM, the plug of tissue filling the ulcer cavity in the right hind outer claw was photographed in a dissection microscope. The outer (distal) part is flared (↑↑). This part filled the cavity in the epidermis but was not fused to the surrounding epidermal tissues. The tapered end (↑) of the plug was attached to the deeper tissues of the digital torus.

x 7

Figure 8.8
Scanning electron micrograph of a cross sectional profile of the plug of tissue from the ulcer on the right hind outer claw

In cross section at higher power, the structure of the plug of tissue was seen to be well organised. Dense bundles of collagen fibres (c) are interspersed with looser connective tissue (↑). The dense bundles of collagen fibres are orientated parallel to the long axis of the plug and are continuous along its length.

x 38

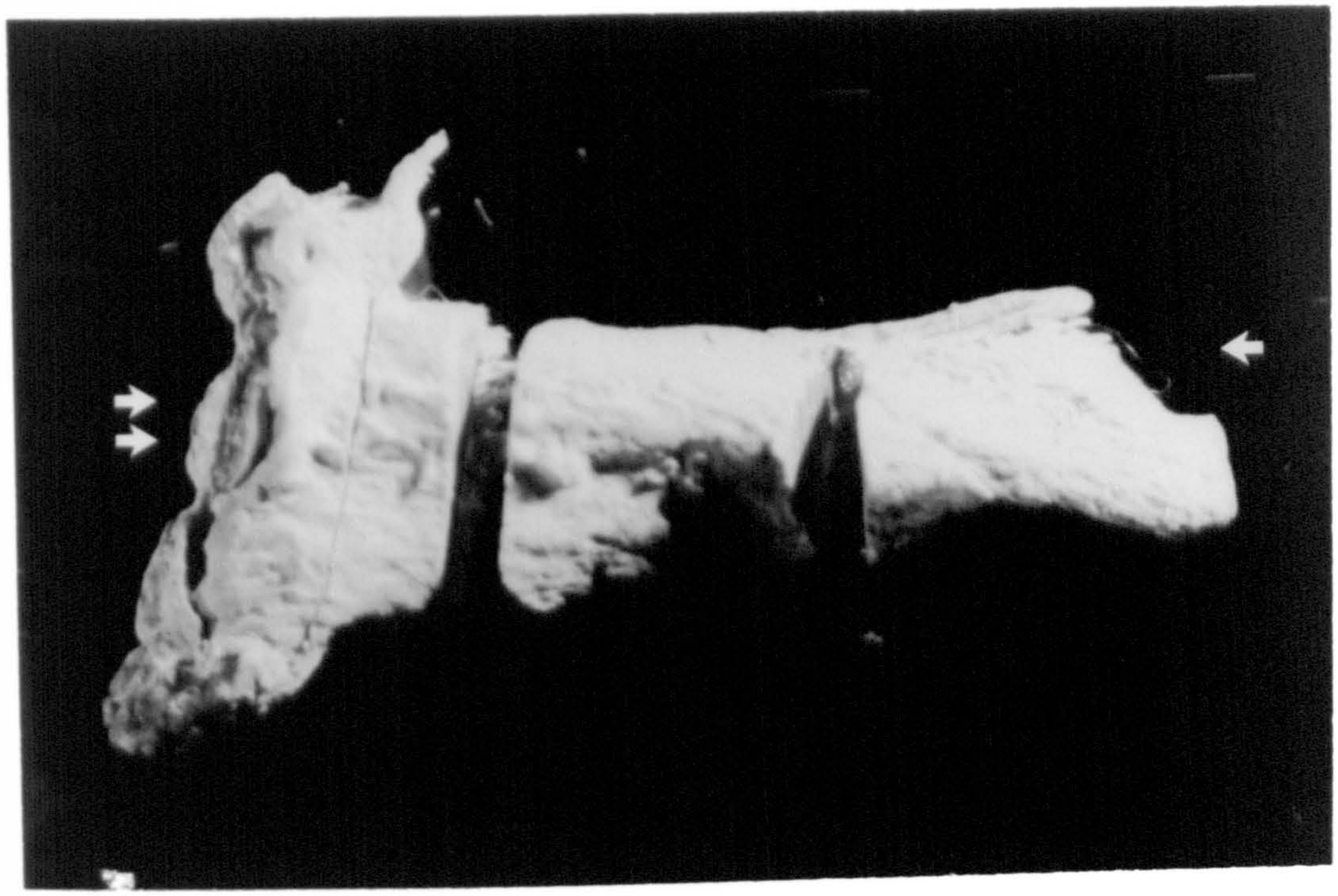

C

Figure 8.9
Scanning electron micrograph of the sole adjacent to the cavity of the ulcer in the right hind outer claw

The dermis (d) contains much fibrous tissue and few identifiable blood vessels (bv↑). Close to the cavity (Ca) of the ulcer the maturation zone (mz1) is more than twice as thick as that approximately 6 mm from the cavity (mz2). The maturation zone at the edge of the cavity (mz1) shows separation in the layers juxtaposed to the horn. At the point of separation the structure of the maturation zone is loose and disorganised compared with that further from the ulcer. Horn (↑) overlying the separated epidermis shows no normal structure and is relatively thin. In the adjacent horn some tubules (t↑) are present but their arrangement and course are irregular. Some areas (↑↑) of general disruption in normal horn structure can be seen.

x 13

Figure 8.10
Low power light micrograph of tissue adjacent to the ulcer cavity

Separation has occurred at the junction between the maturation zone (mz) and the horn (h). Further areas of weakness are apparent within the maturation zone (↑). Areas of damaged horn (↑↑) are interspersed with more compact horn. The horn has a variable staining reaction. The outermost layers of horn and those closest to the ulcer cavity (*) are particularly densely stained. Pockets of lymphocyte infiltration (l↑) are present in the dermis (d). The lymphocytes are concentrated close to the dermal-epidermal junction.

x 17

Stain: Haemotoxylin and Eosin

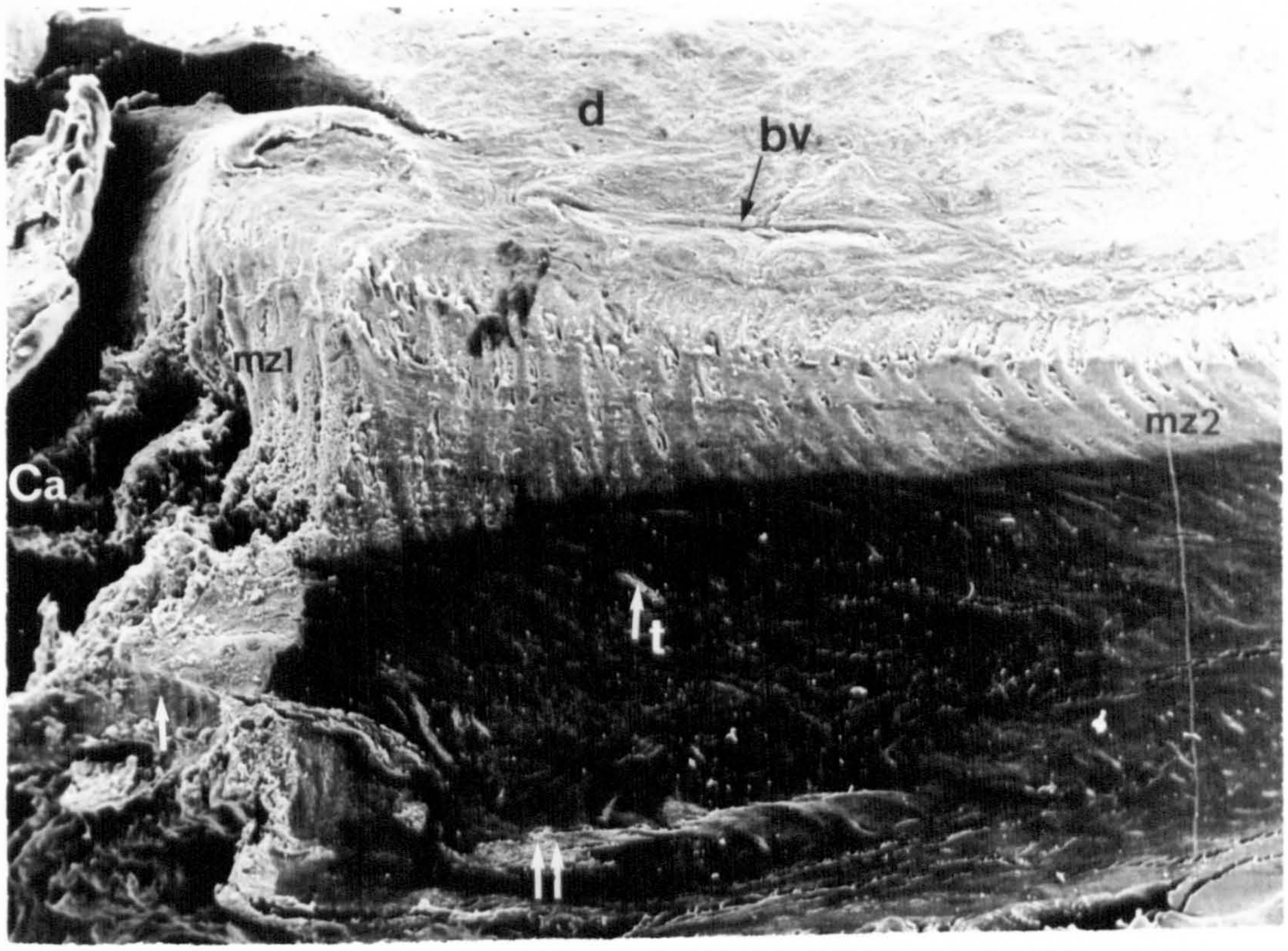
d
bv
mz1
mz2
Ca
t

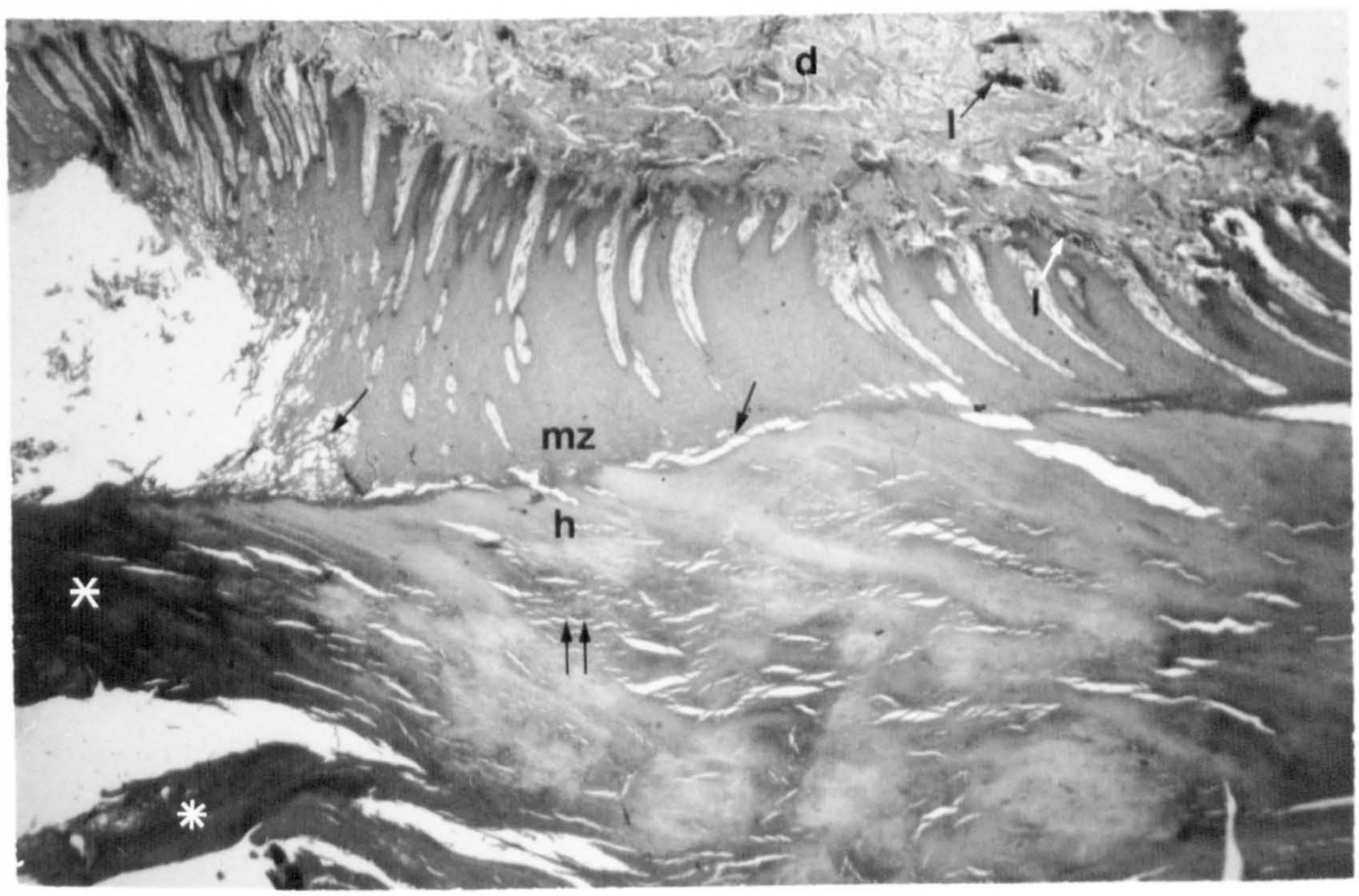
d
l
l
mz
h
*
*

Figure 8.11
Scanning electron micrograph of the sole horn close to the ulcer site

In the horn from the distal surface close to the ulcer site, the majority of the horn shows extensive disruption of normal structure (↑↑). The damage to the horn had resulted in the formation of deep penetrating clefts (cl). Areas of relatively tightly packed squames (↑) were uncommon. No tubular structures were identified.

x 60

Figure 8.12
Scanning electron micrograph of sole horn close to the ulcer site at higher power

At higher power the individual squames (Sq↑) are easily identified. The functional integrity of the horn is dependent on good squame to squame attachment. In some areas the squames are closely associated, forming a cohesive structure (↑). However, in other areas squames are loosely packed (↑↑) with wide intercellular spaces (Sp↑). In these regions the squames are poorly attached to one another and easily become separated.

x 210

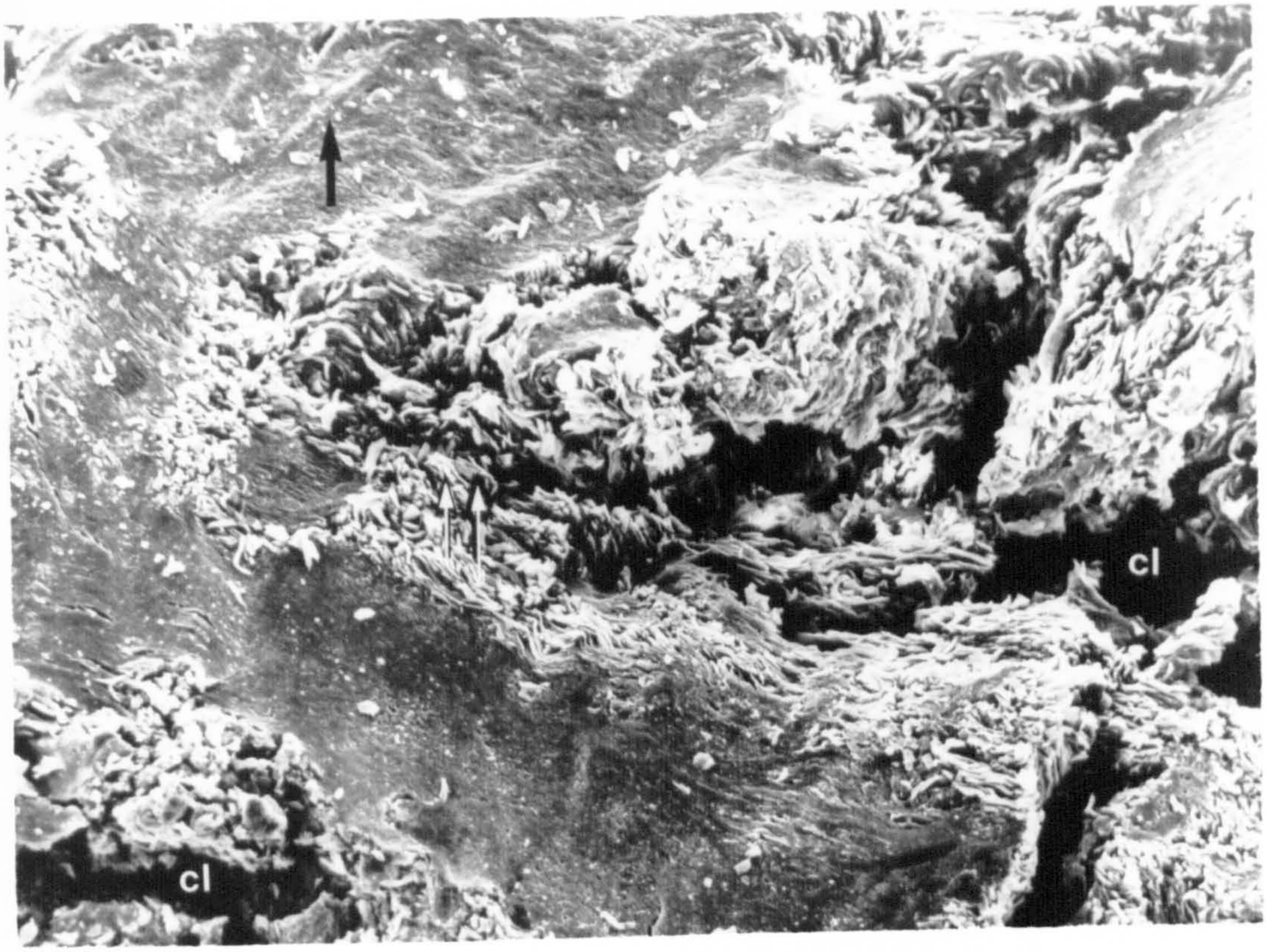
cl
cl

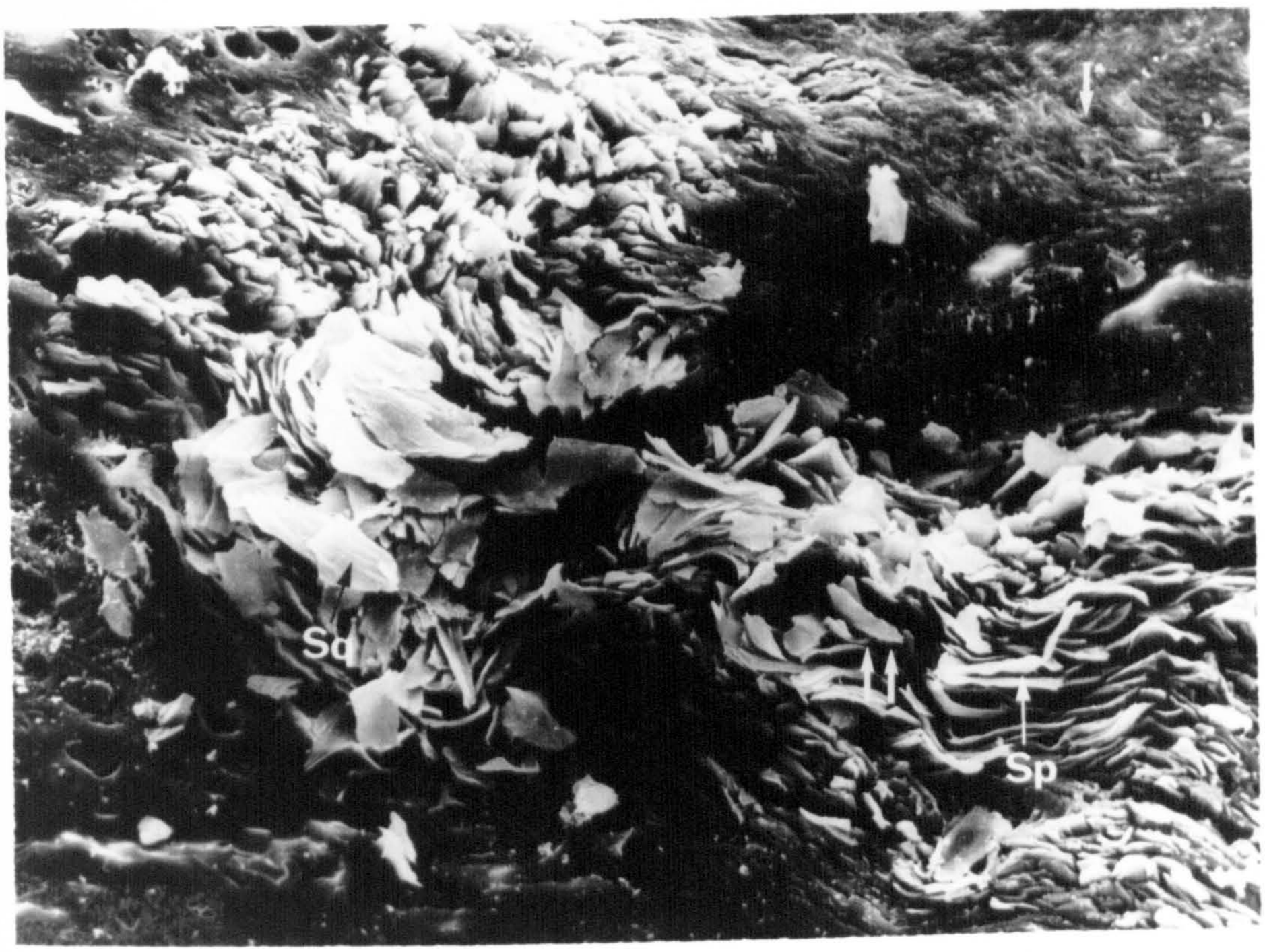
Sd
Sp

Figure 8.13
Block of tissue from the edge of the ulcer photographed in the dissection microscope

Adjacent to the cavity (Ca) of the ulcer the edge (↑) of the dermis (d) had become rounded and contained. Leading from the cavity is a large cleft (Cl) causing separation within the maturation zone (mz). The horn (h) surrounding the cavity of the ulcer is much thinner than normal and of abnormal structure.

x 9

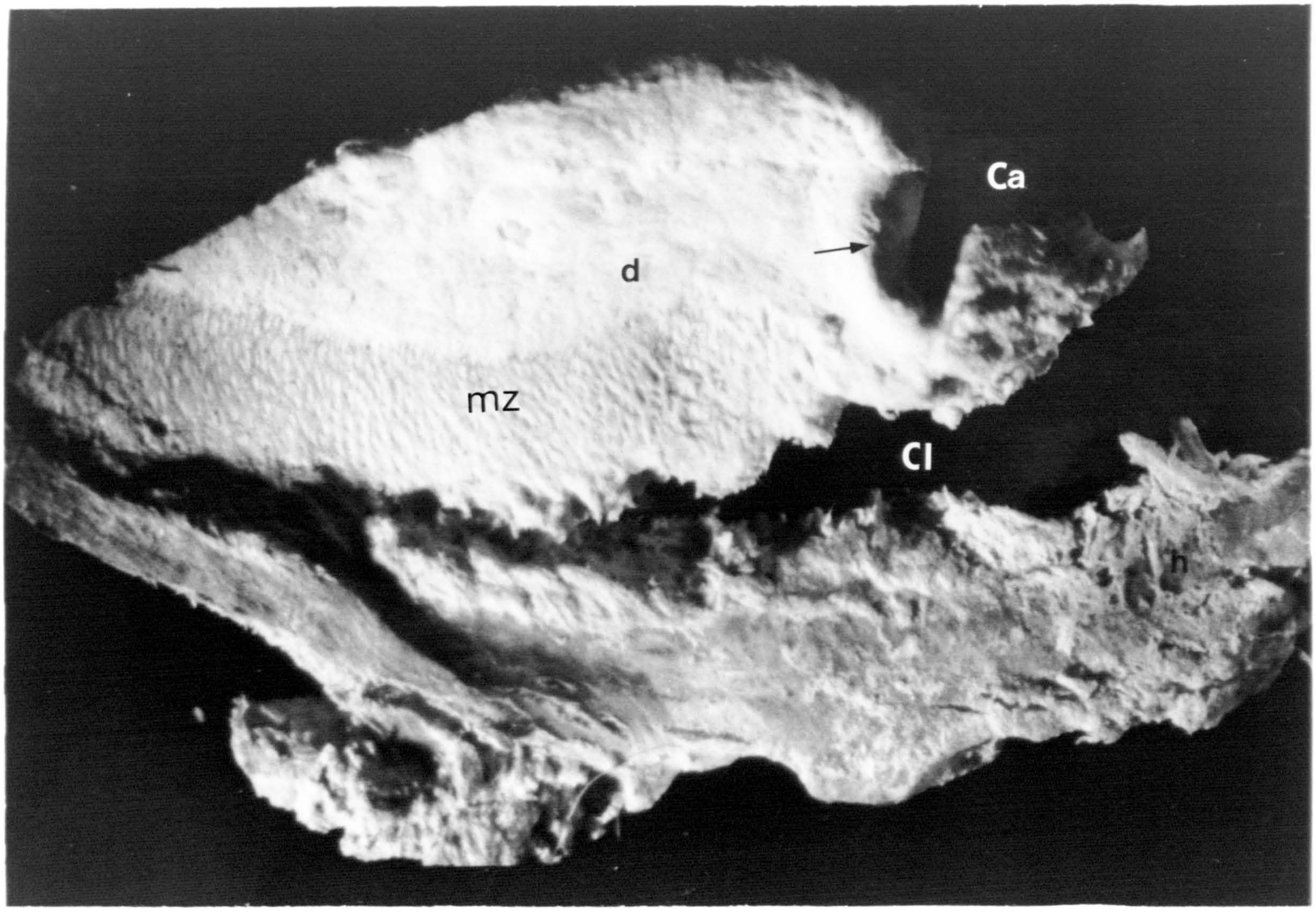
Ca
d
mz
CI
h

Figure 8.14
Light micrograph of the maturation zone adjacent to the ulcer site

The thickness of the maturation zone (mz) was greatly increased adjacent to the ulcer site. The basal cells (bc↑) showed a normal uniform staining reaction but in the middle and outer layers of the maturation zone clear, unstained areas within and between the keratinocytes produced a mottled effect. In the outermost layer of the maturation zone, adjacent to the horn (h), there was much destruction of the keratinocytes giving a lace-like appearance. Some of the resultant spaces contained filamentous material (↑).

x 60

Stain : Phloxine-Tartrazine

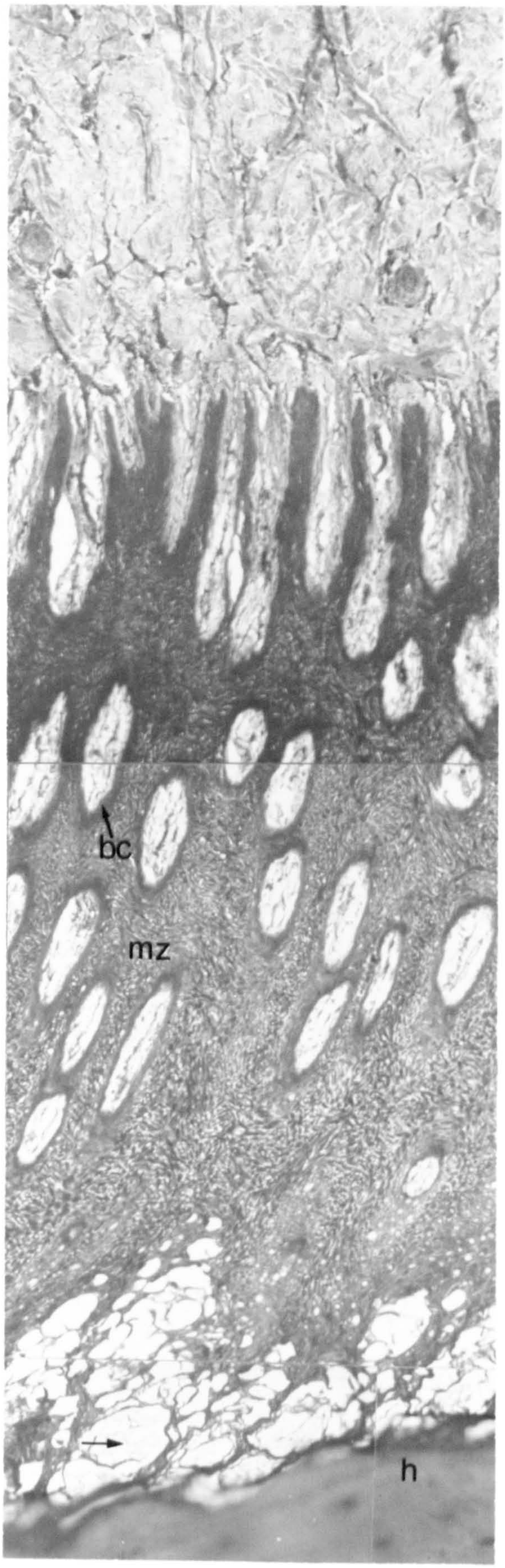
bc
mz
h

Figure 8.15
Low power light micrograph of the dermal-epidermal junction from the edge of the ulcer cavity

The horn and outer layer of the maturation zone had separated completely from the inner maturation zone (mz). The dermis (d) is packed with dense bundles of collagen fibres (cf). The lumena (↑) of dermal blood vessels (bv) are conspicuously constricted. It was difficult to indentify smaller blood vessels and capillaries.

x 20

Stain : Phloxine-Tartrazine

Figure 8.16
IIigh power light micrograph of the dermal-epidermal junction at the ulcer site

The dermis (d) contains a high density of fibrous tissue. The bundles of collagen fibres (cf) are orientated parallel to the epidermis. The few blood vessels (bv↑) seen within the dense fibrous tissue are collapsed and occluded. Normal blood capillaries are absent from the dermal papillae (dp), in which the normal connective tissue structure is disrupted. The basal cells (bc↑) are flattened and smaller than normal. In the maturation zone (mz) the intercellular spaces (↑↑) are enlarged and the keratinocytes (k↑) frequently reduced in size.

x 78

Stain : Phloxine-Tartrazine

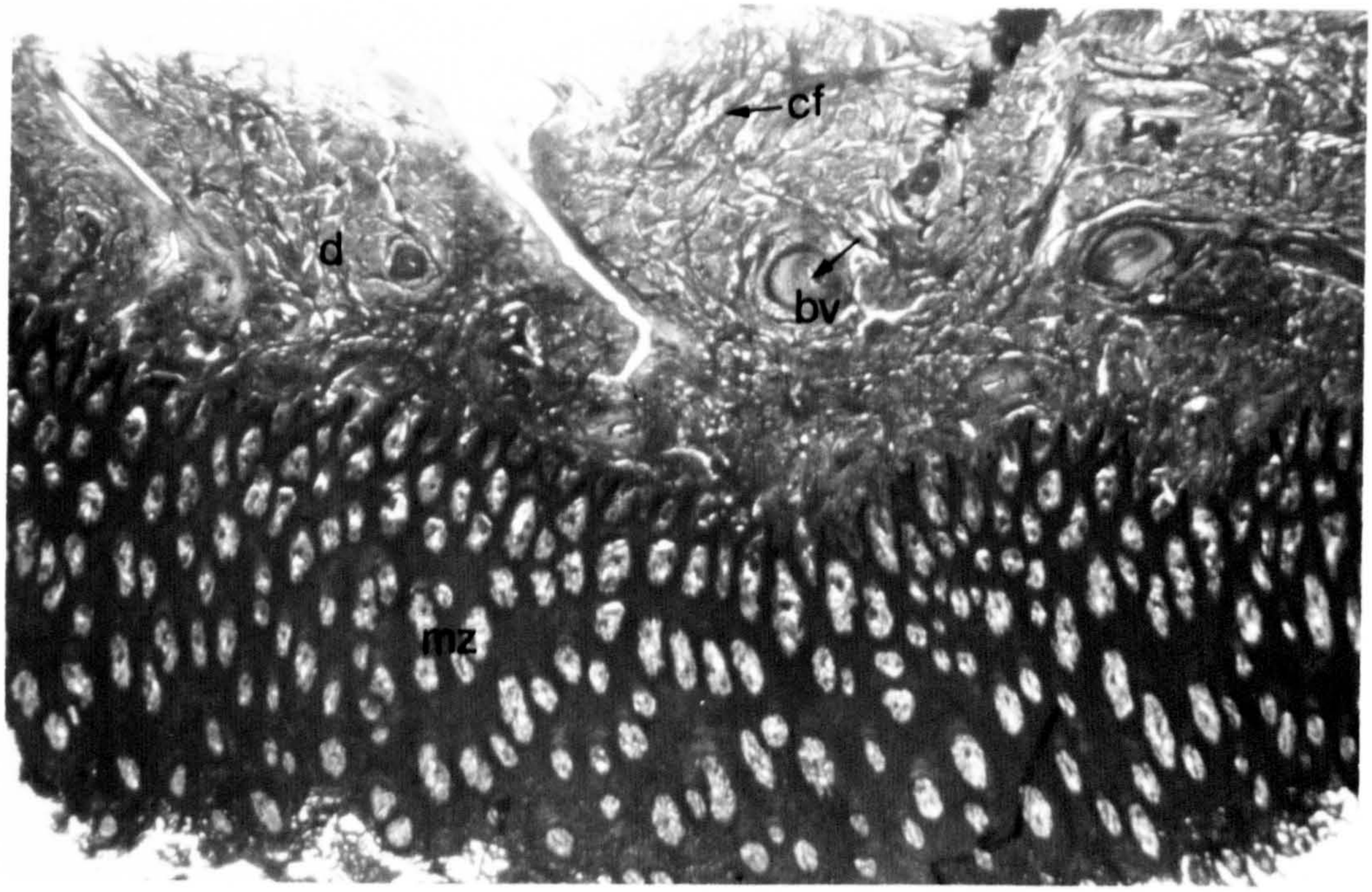
cf
d
bv
mz

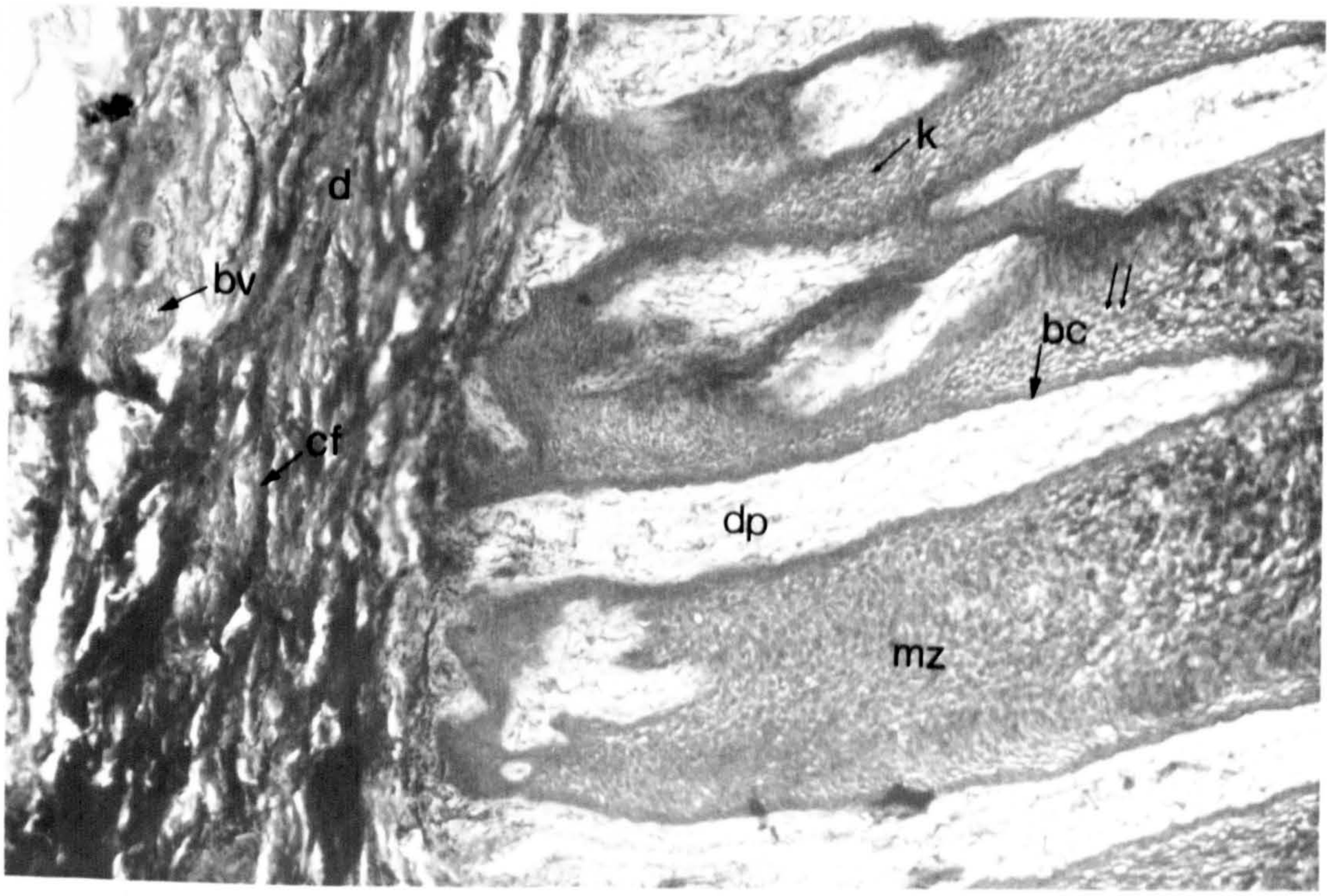
k
d
bv
bc
cf
dp
mz

Figure 8.17
Light micrograph of the dermal-epidermal junction at high power to show lymphocyte infiltration

Concentrations of lymphocytes (l↑) are interspersed between bundles of collagen fibres (c) in the dermis and scattered lymphocytes (↑) are present in the dermal papillae (dp). The basal cells (bc ↑) and cells in the three to four overlying layers are small and flattened.

x 210

Stain : Haemotoxylin and Eosin

Figure 8.18
Light micrograph showing the epidermis approximately 1 cm from the edge of the ulcer

Approximately 1 cm from the rim of the ulcer the maturation zone (mz) is of normal thickness although it still shows abnormal mottled staining properties. The basement membrane has increased in length with the formation of finger-like extensions (f ↑) of the epidermis that penetrate into the dermis (d). This response to the trauma increases the area of attachment of the epidermis to the underlying structures. The nuclei of basal cells (↑ bc) are conspicuous. Connective tissue in the dermal papillae (dp) has a normal appearance.

x 140

Stain : Phloxine-Tartrazine

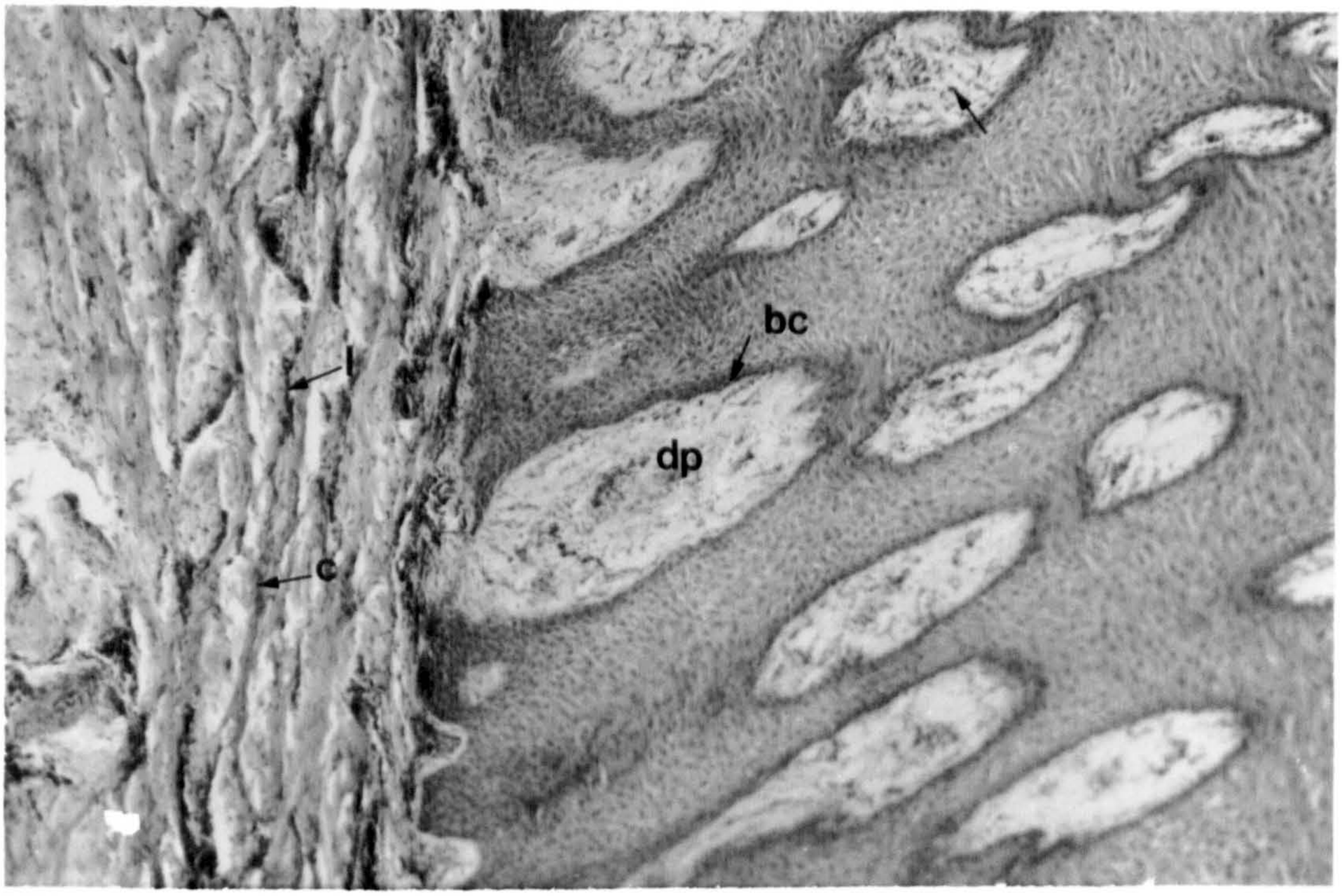
l
c
bc
dp

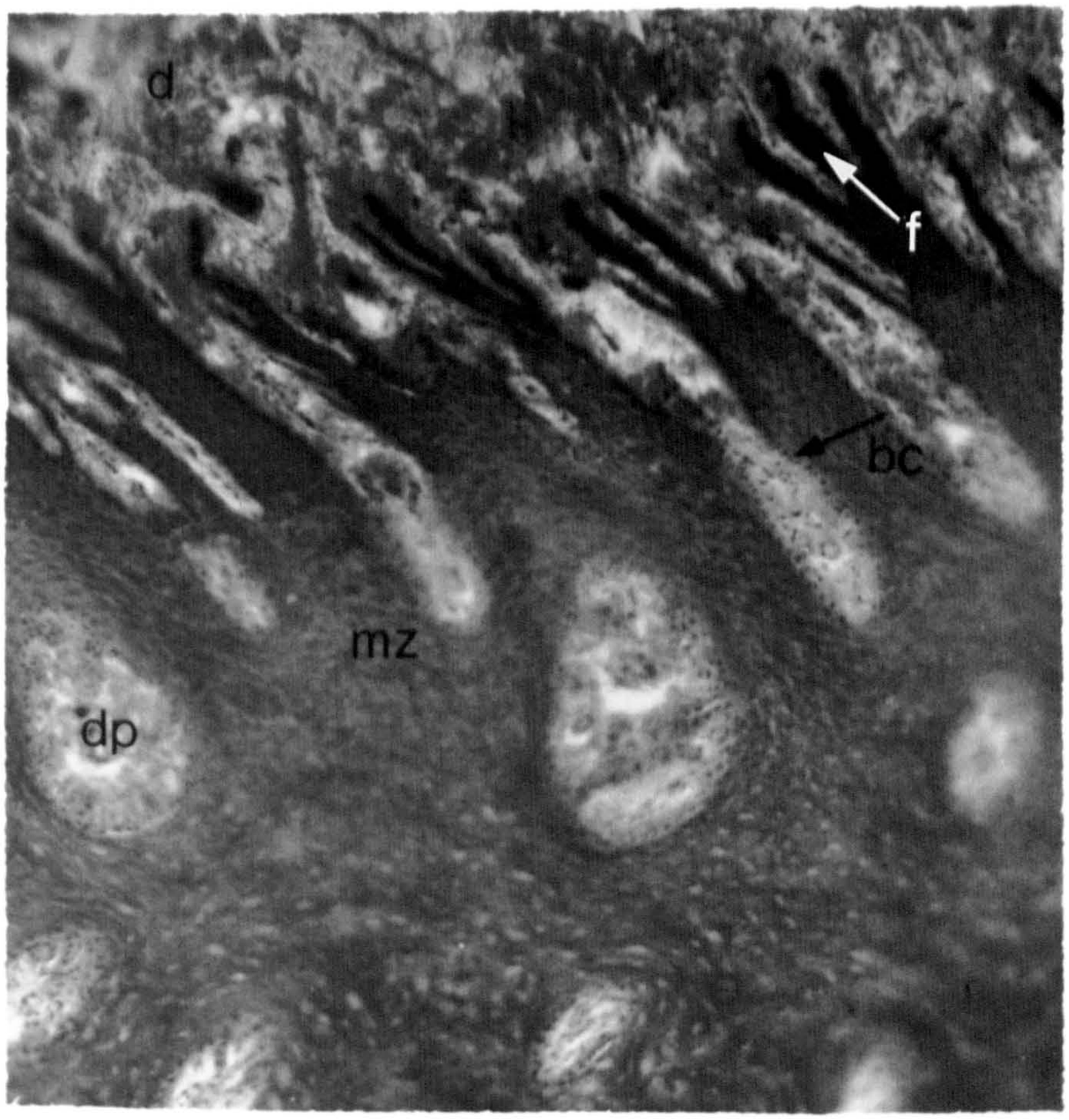
d
f
bc
mz
dp

Figure 8.19
Light micrograph of the laminar region of the right hind outer claw in longitudinal section

The micrograph covers the junction between the dermis (d) and the horn (h). The dermal laminae (dl) and epidermal laminae (el) are highly distorted. They have become separated from one another in places (↑).

x 28

Stain : Phloxine-Tartrazine

Figure 8.20
Light micrograph of the distal part of the laminar region of the right hind outer claw in transverse section

This section is taken at the level of the transition to the white line (equivalent to section 4 in Figure 6.2). The connective tissue within the dermal laminae (dl) was easily damaged during sectioning. Several dermal laminae are broadened (*) and have given rise to broadened sheets of interdigitating horn (idh ↑). Both dermal (dl) and epidermal laminae (el) show some distortion.

x 28

Stain : Phloxine-Tartrazine

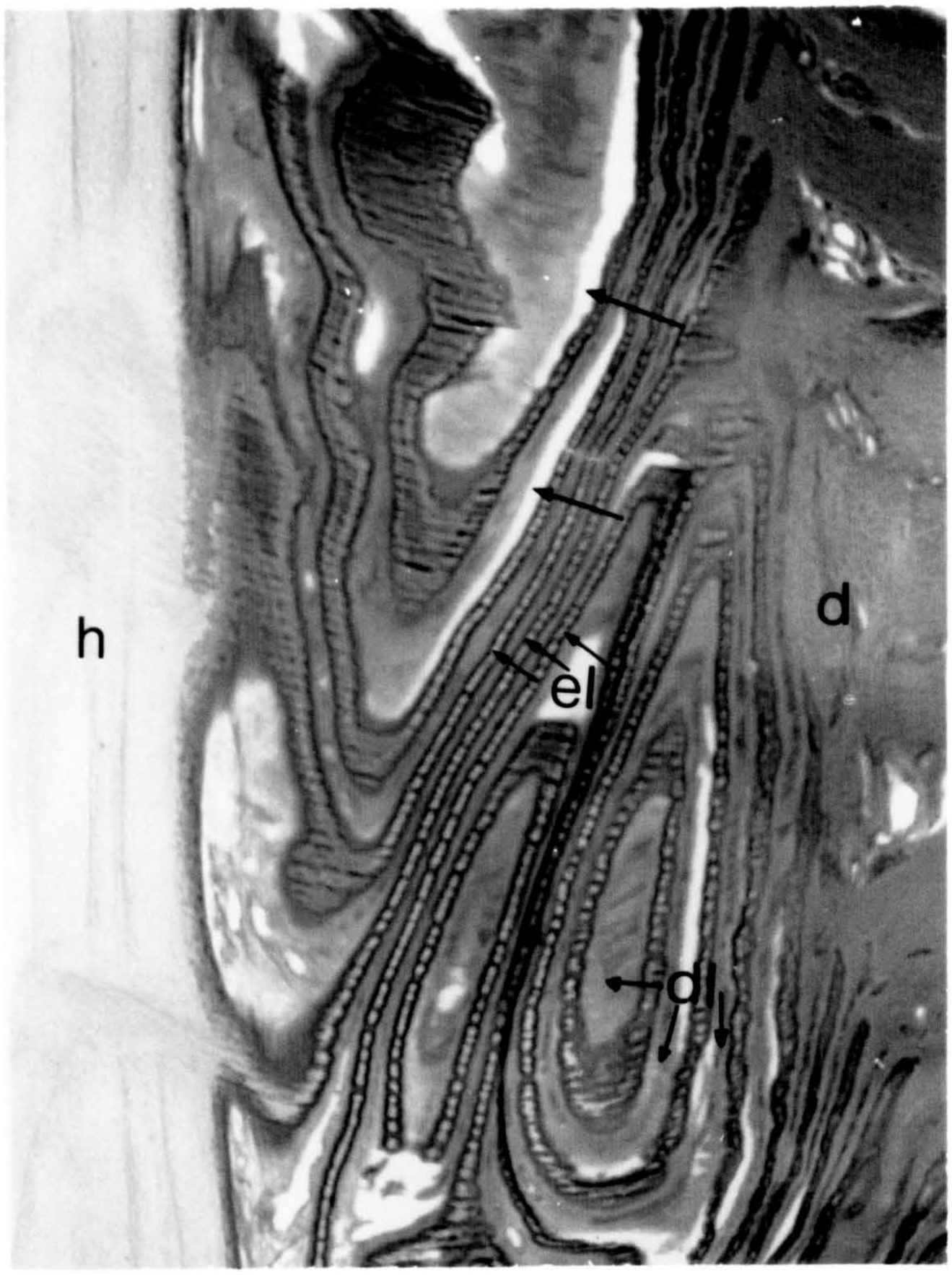
h
d
el
dl

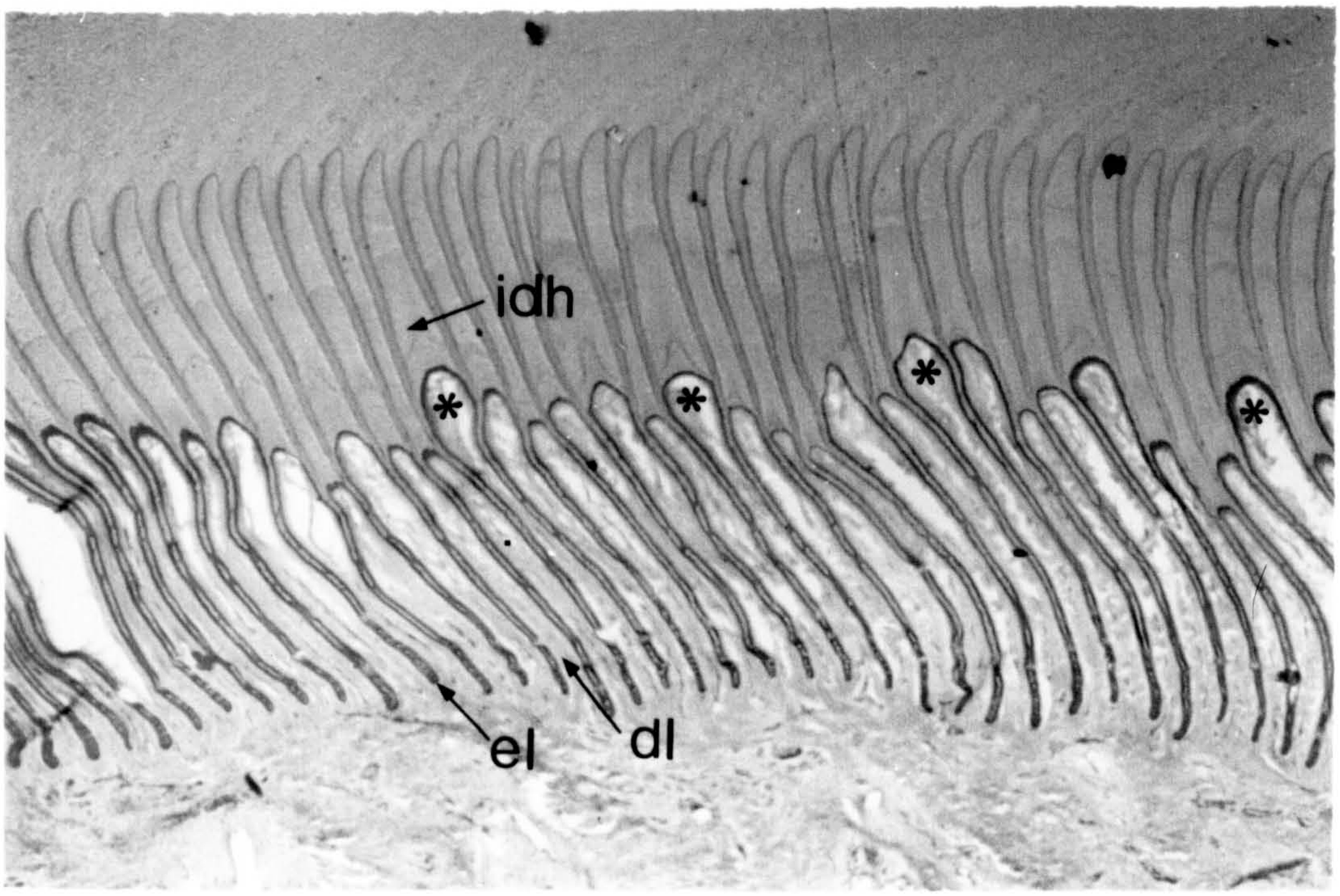
idh
el
dl

Figure 8.21
Light micrograph of the abaxial wall and white line of the right hind outer claw in longitudinal-oblique section

Tubules (t↑) in the wall are distorted in their course, forming undulating shapes. Sheets of interdigitating horn (idh) of the white line are also distorted and many contain discrete round regions of densely stained horn (↑).

x 28

Stain : Phloxine-Tartrazine

Figure 8.22
Light micrograph of the abaxial white line in the right hind outer claw in transverse section

The interdigitating horn (idh) is distorted in outline and the breadth of individual sheets of interdigitating horn is very irregular. The interdigitating horn and laminar horn leaflets (lh) are not always clearly distinguishable. Many sheets of interdigitating horn contain discrete round densely stained regions (↑). Rows of similar densely stained structures extend beyond the tips of the interdigitating horn into the caphorn (ch). Arches (ar) of densely staining horn are visible over the tips of some sheets of interdigitating horn, at the junction with the caphorn.

x 28

Stain : Phloxine-Tartrazine

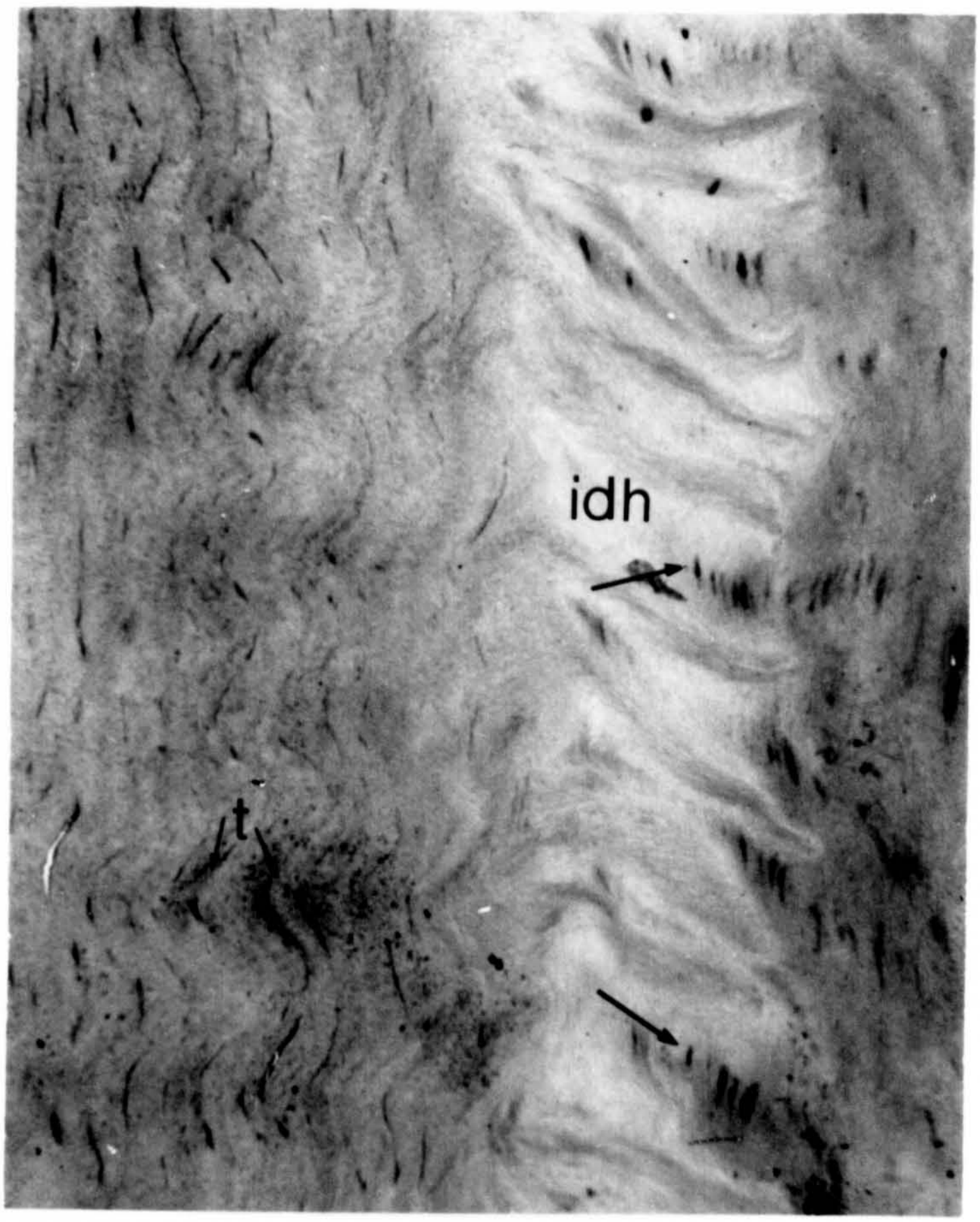
idh
t

ch
ar
ar
idh
lh

Figure 8.23
Transmission electron micrograph of the sole horn close to the ulcer on the right hind outer claw

The contents of squames (sq) have a marbled appearance due to failure of the normal association between keratin fibres and matrix. Intracellular electron-dense lipid deposits (l) are present. There are considerable amounts of intercellular material (i) in the widened intercellular spaces.

x 9,200

Figure 8.24
Higher power transmission electron micrograph of the sole horn close to the ulcer on the right hind outer claw

In these squames discrete electron lucent bodies (*) and regions of electron dense material (ed) are visible. However, despite this abnormal intracellular structure, strong desmosomal atachments (d) are maintained between the squames in this micrograph.

x 25,000

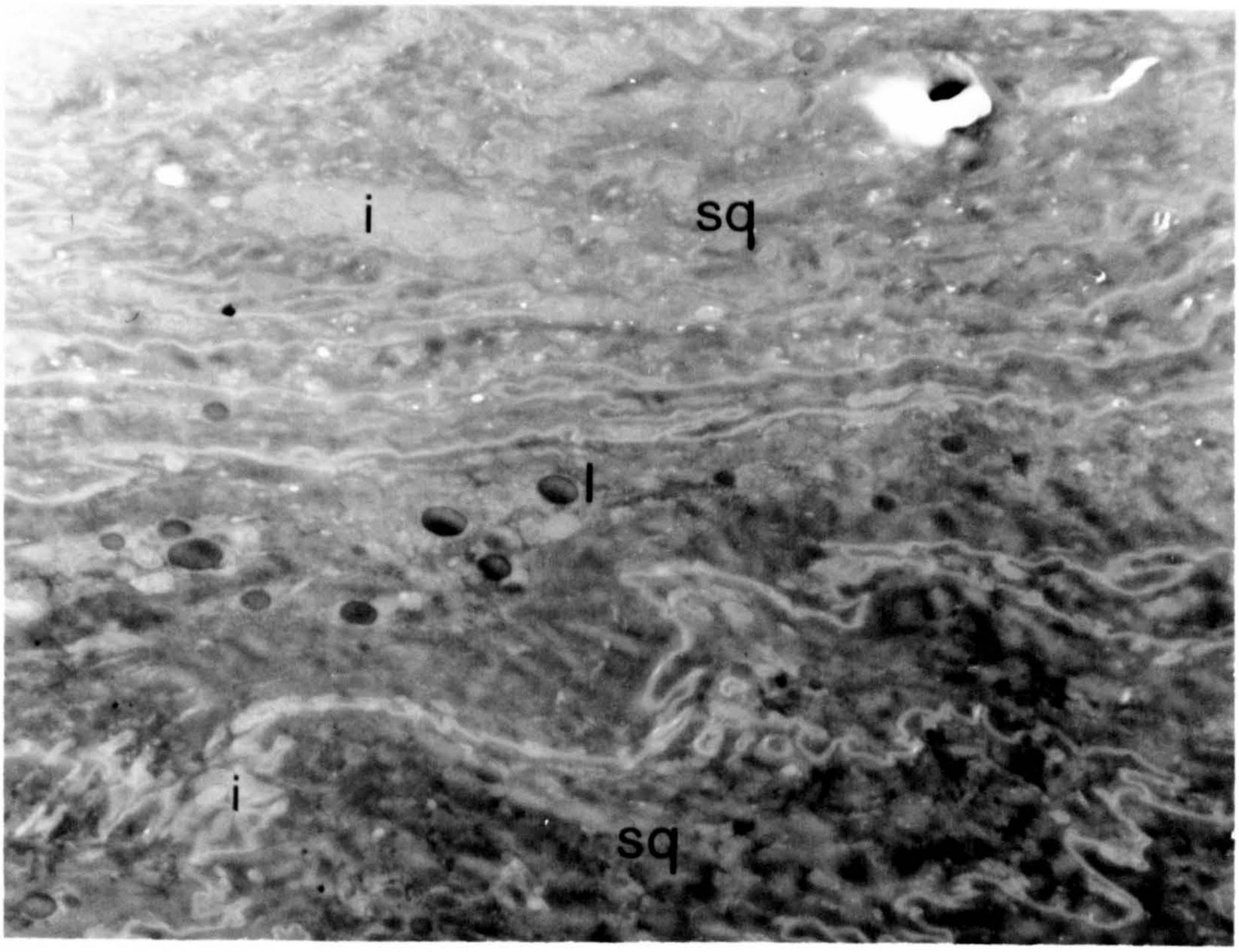
i
sq
l
i
sq

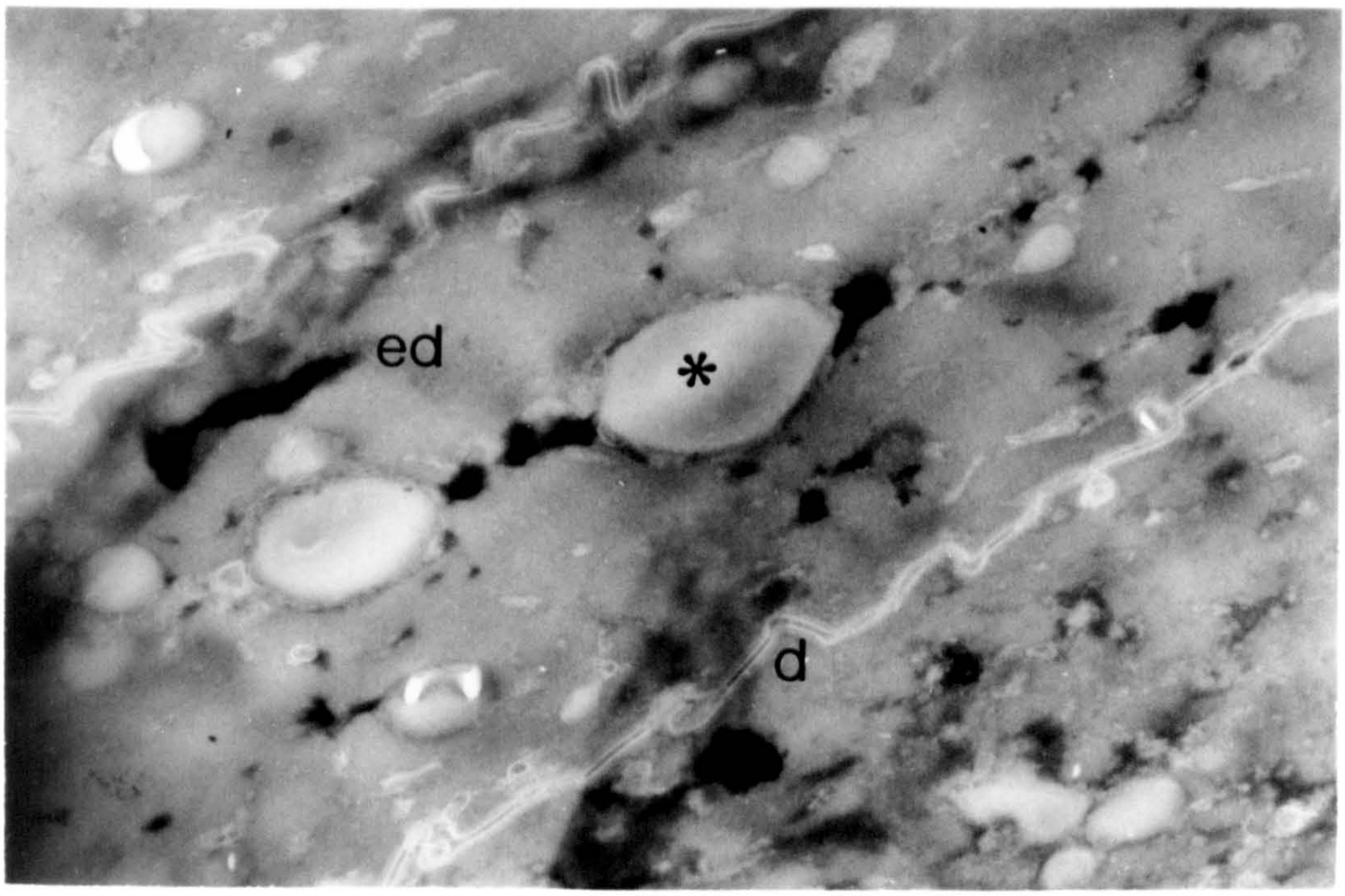
ed
*
d

Figure 8.25
Low power light micrograph of the exostosis on the distal surface of the distal phalanx

The normal bone of the distal phalanx (dp) is more densely stained and homogeneous than the calcified tissue of the exostosis (ex). The approximate position of the ulcer cavity is marked (Ca), distal to the caudal part of the exostosis. The sole horn (sh) in the section shows irregular staining, particularly in the distal layers.

x 10

Stain : Haemotoxylin and Eosin

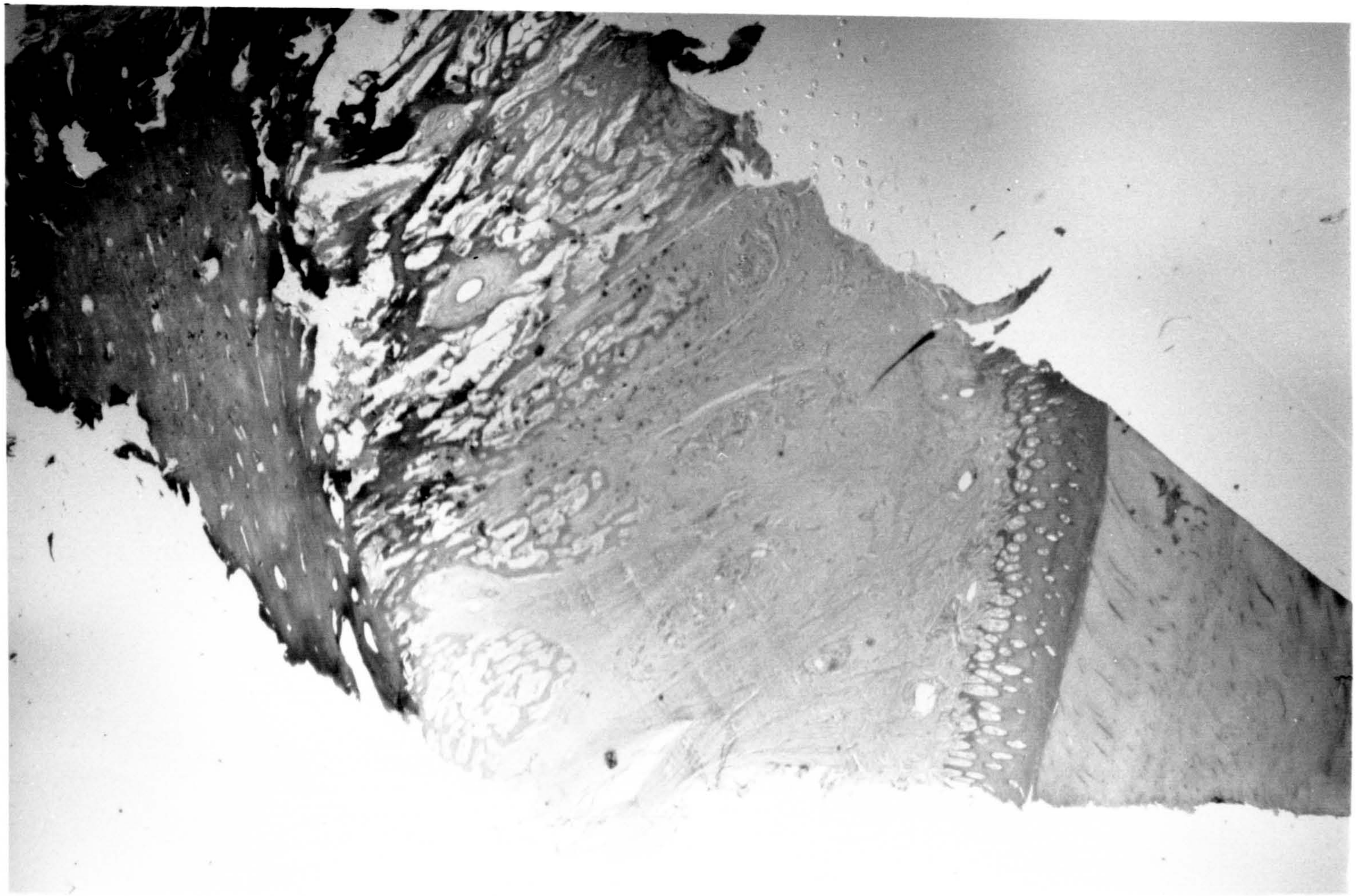

Figure 8.26
Light micrograph of the calcified tissue forming the exostosis on the plantar surface of the distal phalanx in the right hind outer claw

The bone of the distal phlanax (PIII) is stained more evenly and densely than the tissue of the exostosis (ex). Within the exostosis a blood vessel (bv) with thickened walls and a decreased lumen (l) is visible.

x 22

Stain : Haemotoxylin and Eosin

Figure 8.27
High power light micrograph of the posterior part of the exostosis

In the posterior part of the exostosis, the presence of osteoclasts (oc) and osteoblasts (ob) indicated that remodelling of bone was still taking place at the time of death. The appearance of clusters of blood capillaries (bv) was typical of a former chronic inflammatory reaction.

x 230

Stain : Haemotoxylin and Eosin

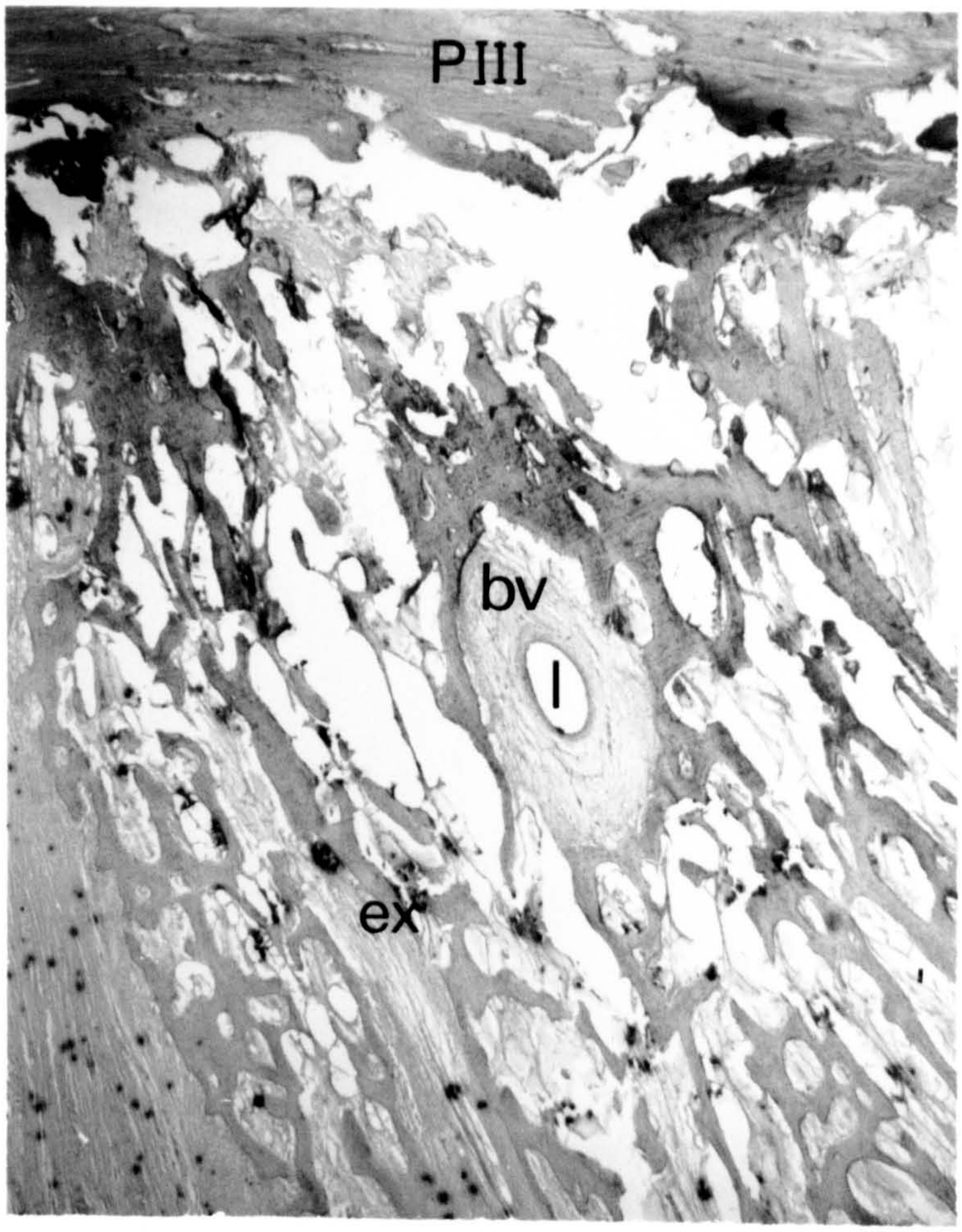
PIII
bv
l
ex

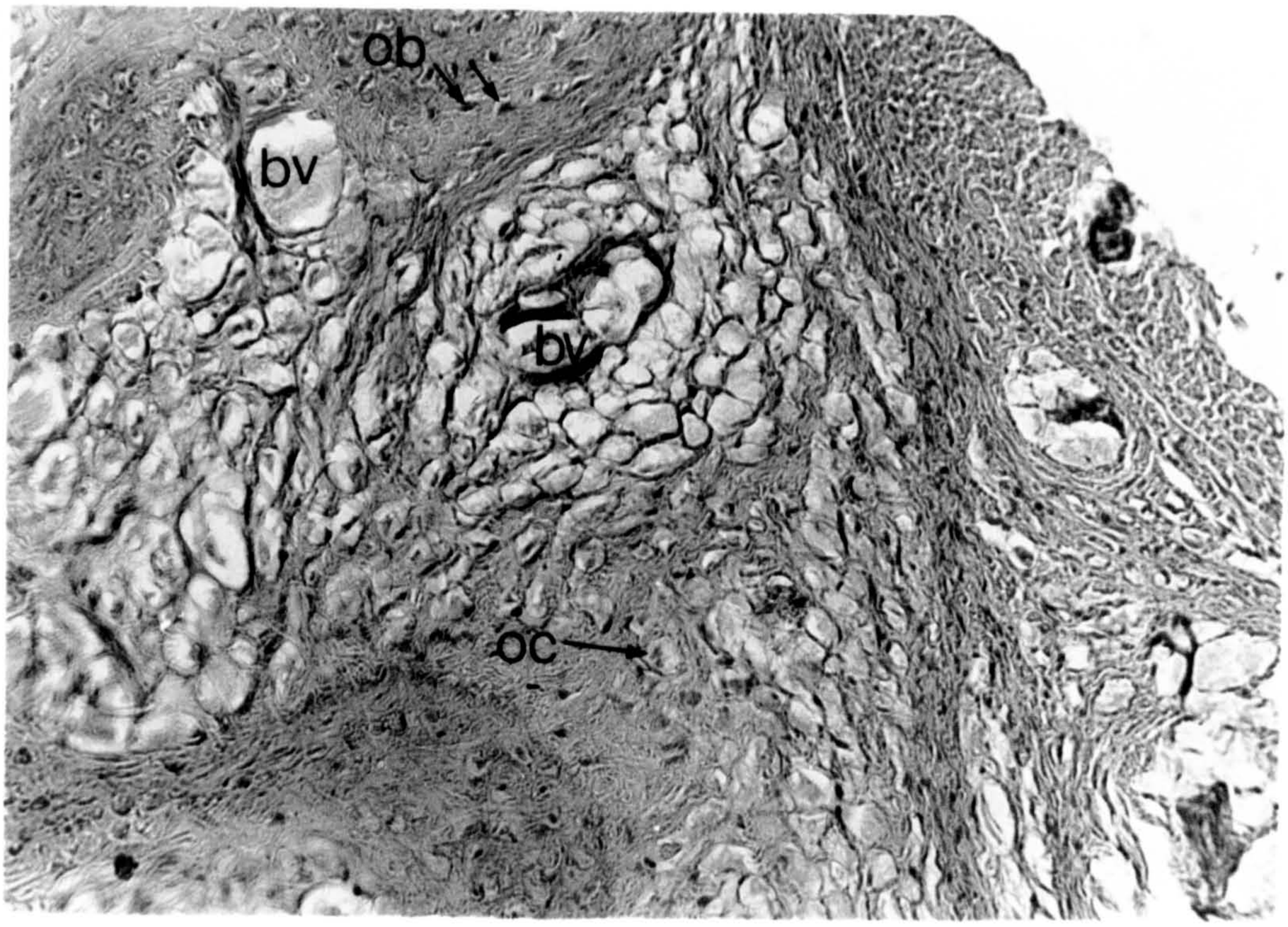
ob
bv
bv
oc

Figure 8.28
Scanning electron micrograph of horn from the heel bulb affected by heel erosion

The outer surface of the horn is rough and the loosely packed squames (sq↑) are flaking away from the surface. A large cleft (cl) extends deep into the horn. Horn tubules (t) are visible in transverse section. These are intact and degradation is progressing through the intertubular horn (it).

x 180

Figure 8.29
Higher power scanning electron micrograph of horn from the heel bulb affected by heel erosion

The porous structure of the intertubular horn resulting from loose packing of squames is more evident at higher power. The outer surface of the sample is rough and horn appears to have been worn away in layers, leaving a series of overlapping ridges and grooves (↑). Tissue in the tubule medullae (tm) has disintegrated during preparation of the sample.

x 900

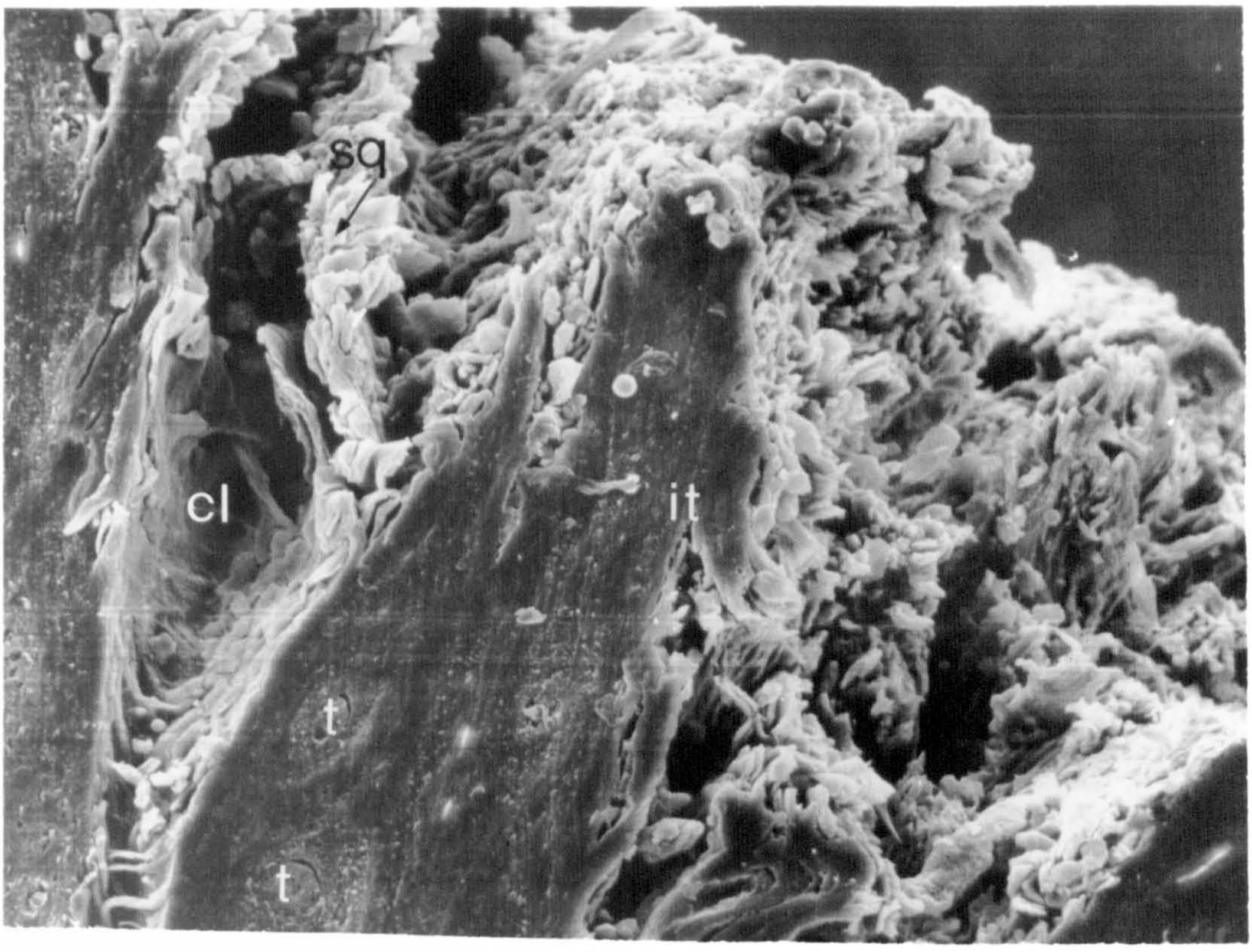
sq
cl
it
t
t

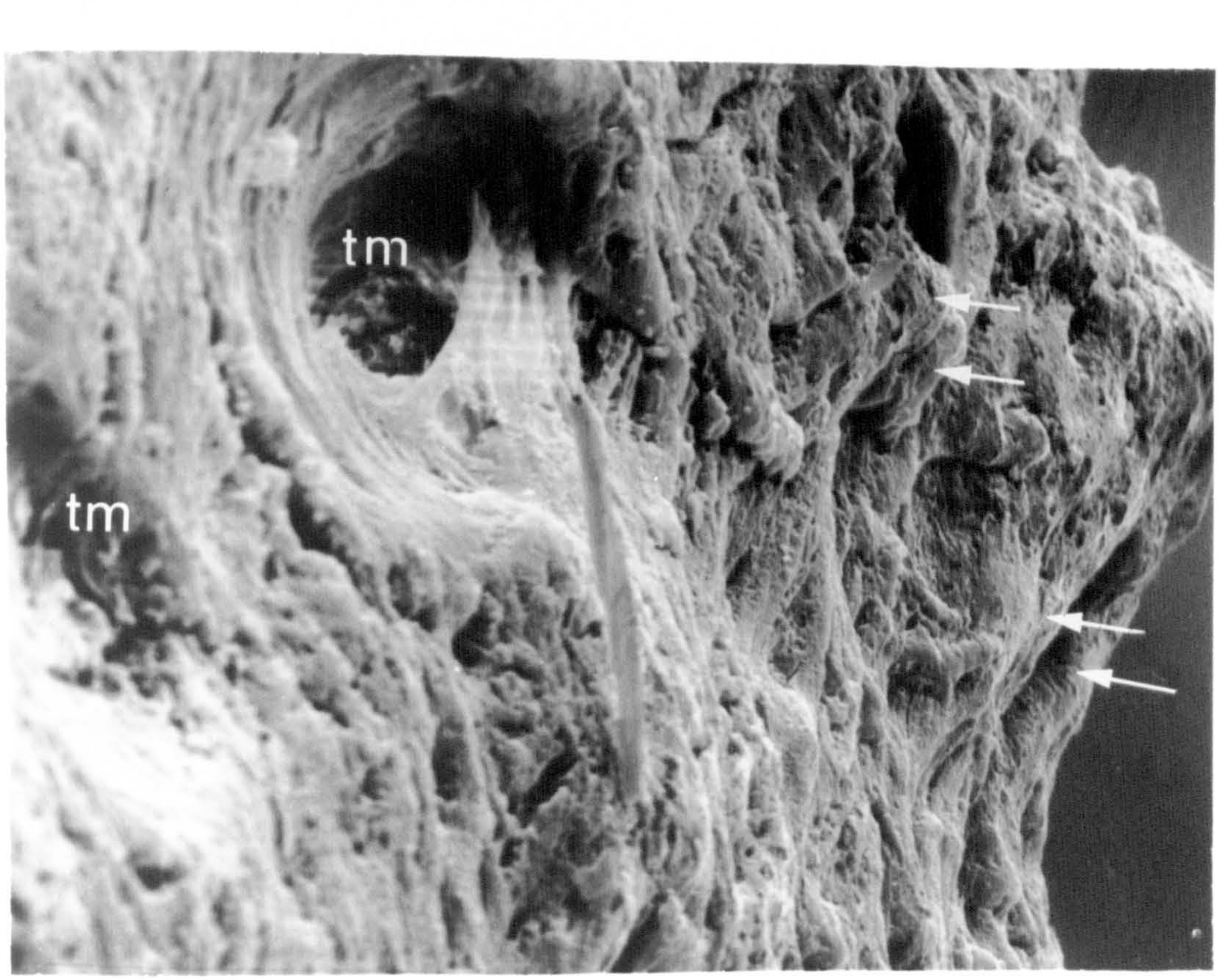
tm
tm